AD_____

Award Number: DAMD17-98-1-8260

TITLE: A Novel Apoptotic Protease Activated in Human Breast Cancer Cells after Poisoning Topoisomerase I

PRINCIPAL INVESTIGATOR: David A. Boothman, Ph.D.

CONTRACTING ORGANIZATION: Case Western Reserve University
Cleveland, Ohio 44106-7006

REPORT DATE: October 2000

TYPE OF REPORT: Annual

PREPARED FOR: U.S. Army Medical Research and Materiel Command
Fort Detrick, Maryland 21702-5012

REPORT DOCUMENTATION PAGE

Form Approved
OMB No. 074-0188

1. AGENCY USE ONLY (Leave blank)	2. REPORT DATE	3. REPORT TYPE AND DATES COVERED
	October 2000	Annual (15 Sep 99 - 14 Sep 00)

4. TITLE AND SUBTITLE
A Novel Apoptotic Protease Activated in Human Breast Cancer Cells after Poisoning Topoisomerase I

5. FUNDING NUMBERS
DAMD17-98-1-8260

6. AUTHOR(S)
David A. Boothman, Ph.D. 10/4/00

7. PERFORMING ORGANIZATION NAME(S) AND ADDRESS(ES)
Case Western Reserve University
Cleveland, Ohio 44106-7006
E-MAIL:
dab30@po.cwru.edu

8. PERFORMING ORGANIZATION REPORT NUMBER

9. SPONSORING / MONITORING AGENCY NAME(S) AND ADDRESS(ES)
U.S. Army Medical Research and Materiel Command
Fort Detrick, Maryland 21702-5012

10. SPONSORING / MONITORING AGENCY REPORT NUMBER

11. SUPPLEMENTARY NOTES

12a. DISTRIBUTION / AVAILABILITY STATEMENT
Approved for public release; distribution unlimited

12b. DISTRIBUTION CODE

13. ABSTRACT ***(Maximum 200 Words)***

The goal of this grant is to clone the unknown protease activated by the active anti-breast cancer agent, ß-lapachone (ß-lap). The research team showed for the first time that ß-lap requires NQ01, a two-electron reduction enzyme elevated in many human breast cancers, for activation. The team then characterized the unknown apoptotic protease activated in human breast cancer cells by ß-lap, defining endpoints which will be essential for the ultimate isolation of this novel apoptotic protease. The unknown protease: (a) is a non-caspase cytsteine protease; (b) cleaves p53, lamin B, and PARP (atypically) in an NQ01-dependent manner at a time co-incident with calpain activation (appearance of an 18 kDa active form and its movement into the nucleus by confocal microscopy); and (c) is calcium-dependent, where BAPTA-AM and EDTA blocked cell death caused by ß-lap. Cloning the unknown protease activated by ß-lap is ongoing by this research team using standard biochemical methodology and p53 and/or PARP cleavage site identification.

14. SUBJECT TERMS
Breast Cancer, Apoptosis, Calpain, NQO1, x-ray-inducible transript #3 (xip3), calcium.

15. NUMBER OF PAGES
134

16. PRICE CODE

17. SECURITY CLASSIFICATION OF REPORT	18. SECURITY CLASSIFICATION OF THIS PAGE	19. SECURITY CLASSIFICATION OF ABSTRACT	20. LIMITATION OF ABSTRACT
Unclassified	Unclassified	Unclassified	Unlimited

Table of Contents

A. INTRODUCTION:

Understanding and exploiting cell death processes in various human breast cancer cells following clinically useful anti-tumor drugs is a major focus in breast cancer research. The promise is that a better understanding of apoptotic and anti-apoptotic processes will allow improved anti-breast cancer efficacy of existing chemotherapeutic agents, as well as the development of additional efficacious drugs which elicit programmed cell suicide during treatment, without causing complicating inflammation reactions in normal tissue.

Apoptotic processes occurring in human breast cancer cells, particularly noncaspase-mediated cell death pathways, are poorly understood. Since many human cancers are thought to form, in part, because of deficient caspase pathway expression or activation, novel pathways of activating non-caspase-mediated pathways may be important for treating human breast cancers. We discovered that a previously used drug for anti-trypanosomal therapies, ß-lapachone (ß-lap), is an active agent for the initiation and execution of apoptosis in a variety of human breast cancer cells in a p53-independent fashion. In the course of defining the ability of ß-lapachone to cause cell death, we accomplished the following objectives, and defined the following mechanism of action of the drug: (a) the primary intracellular target for ß-lap was NQ01, a two-electron reductase that was ionizing radiation (IR)-inducible; NQ01-containing cells were sensitive, NQ01-deficient cells were resistant; (b) interaction of the drug with NQ01 caused a futile cycling of the compound in which calcium homeostasis was altered within 9-16 mins, and intracellular ATP levels decreased to <1% within 30 mins; (c) no evidence of caspase activation was detected in NQ01-containing breast cancer cells during ß-lap-mediated apoptosis; (d) an intracellular activation of a non-caspase cysteine protease was activated within 4-8 h, concomitant with the appearance of DNA fragmentation, measured by TUNEL assays; (e) protease activation was concurrent with atypical cleavage of PARP, and cleavages of lamin B, p53 and degradation of pRb; (f) administration of dicoumarol (an NQ01 inhibitor) or calcium chelators (intracellular: EGTA or EDTA and extra-cellular: BAPTA-AM) was (were) able to prevent ß-lap-mediated apoptosis, and in the case of dicoumarol, cell lethality.

The hypothesis being investigated is that ß-lap activates calpain, a non-caspase cysteine protease, or a calpain-like protease. The objective of the grant is to clone this unknown cyteine protease using a variety of strategies, including **(1)** substrate (PARP, p53 or lamin B) affinity chromatography; **(2)** previously published calpain isolation techniques; and **(3)** identification of specific ß-lap-mediated PARP and/or p53 cleavage sites, followed by use of these sites for the isolation of this ß-lap-activated, noncaspase cysteine protease. A complete understanding of the initiation and execution phases of ß-lap-mediated apoptosis should lead to improved therapy using this compound or more effective derivatives.

B. GRANT BODY:

Grant Objective: ***To test the hypothesis that expression of a novel apoptotic protease in human breast cancer cells directly correlates with the efficacy of ß-lap. The objectives of this grant are being accomplished as follows:***

Specific Aim #1: Clone the unknown apoptotic protease, which is activated by ß-lap and whose activity correlates with toxicity after acute drug exposures *(Years 0-2).*

ß-Lap activates a non-caspase, cysteine protease during apoptotic cell death. In order to determine the key enzymatic target for ß-lap, we first established a number of intracellular proteolytic reactions that occur in a temporal sense during ß-lap-mediated apoptosis in MCF-7:WS8 breast cancer cells. Since activation of pre-existing zymogens is common-place during apoptosis and specific apoptotic substrates are known [e.g., poly(ADP-ribosyl) polymerase (PARP), lamin B, the retinoblastoma protein (pRb)], we examined proteolytic cleavage reactions occurring *in vivo* in four human breast cancer cell lines at various times after ß-lap (4-8 μM) treatment (Pink et. al., *Exp. Cell Research,* Appendix). Typical cleavage of pRb and lamin B (Fig. 1) were observed at 8 h post-treatment with 4-8 μM ß-lap (Pink et. al., *Exp. Cell Research,* Appendix). In contrast, an atypical cleavage of PARP (appearance of a ~60 kDa PARP polypeptide) was observed in ß-lap-treated MCF-7 cells (Fig. 2, Pink et. al., *Exp. Cell Research,* Appendix), co-incident with lamin B and pRb cleavage (Fig. 1). Furthermore, cleavage of p53 in T47D human breast cancer cells was also found (Pink et. al., *Exp. Cell Research,* Appendix). The cleavage events described above occurred in ß-lap-treated MCF-7 or T47D cells regardless of cell cycle or p53 status, even when previously suggested targets, such as Topoisomerase II-alpha (Topo II-alpha), were not expressed. Furthermore, cells deficient in Topo II-alpha were still killed following ß-lap exposures. These data strongly suggesting that DNA Topoisomerase II-alpha (which is cell cycle regulated, present in G_2/M and S-phases and absent in G_0/G_1 cells) was not a determinant in ß-lap-mediated toxicity. Also, we noted that MDA-MB-468 and MDA-MB-231 cells were fairly resistant to ß-lap treatment found (Pink et. al., *Exp. Cell Research,* Appendix).

We next examined the effects of various specific and nonspecific enzyme inhibitors on ß-lap-mediated toxicity using the specific protein cleavage events *in vivo* described above. We discovered that iodoacetamide (I) and N-ethylmaleimide (N), global inhibitors of cysteine proteases, prevented PARP cleavage in ß-lap-treated MCF-7:WS8 cells (see Fig. 7, Pink et. al., *Exp. Cell Research,* Appendix). In contrast, global inhibitors of caspases (i.e., zVAD-fmk, zAAD-fmk, and zFA-fmk) did not block atypical ß-lap-mediated PARP cleavage in MCF-7:WS8 cells. In addition, inhibitors of granzyme B, cathepsins D and L, trypsin and chymotrypsin-like proteases did not prevent ß-lap-mediated atypical PARP cleavage. Furthermore, calpeptin, calpain inhibitor III, and leupeptin (Figs. 2 and 3) also did not block ß-lap-mediated apoptosis

and concomitant proteolyses *in vivo*. We concluded from these data that ß-lap treatment of certain sensitive human breast cancer cells caused the activation of a non-caspase cysteine protease during apoptosis; cells were demonstrated to be apoptotic by DNA fragmentation TUNEL assays (Pink et. al., *Exp. Cell Research,* Appendix).

NQ01 is the major intracellular determinant of ß-lap-mediated apoptosis, cell death and lethality. We then extended our studies to further define the intracellular determinants of ß-lap-mediated apoptosis and cell death. The structural similarities between ß-lap, menadione, and 1,2-naphthoquinones suggested that either one-electron reduction enzymes (p450 or b5R) or two-electron reductases (e.g., NQ01) may be involved in the toxification or detoxification of ß-lap. Administration of dicoumarol, a fairly specific inhibitor of NQ01, prevented ß-lap-mediated apoptosis, ß-lap-mediated proteolysis (e.g., atypical PARP cleavage), and ß-lap-induced cell death (see Figs. 1,2 and 4, Pink et. al., *J. Biol. Chem.,* Appendix). Furthermore, NQ01 levels appeared to correlate well with overall sensitivity to ß-lap: MCF-7:WS8>T47D>>>MDA-MB-468 cells. MCF-7 cells contained the greatest levels of NQ01, with T47D cells containing significantly lower levels and NQ01 level absent in MDA-MB-468 cells (see Fig. 3, Pink et. al., *J. Biol. Chem.,* Appendix). Furthermore, we noticed that MDA-MB-468 cells were fairly resistant to ß-lap and co-administration of dicoumarol with ß-lap did not affect the minimal toxicity caused by this drug in these cells.

To further demonstrate that MDA-MB-468 cells were resistant to ß-lap due to their lack of expression of NQ01, we then transfected these cells with CMV-controlled NQ01. Stable NQ01-expressing human MDA-MB-468 breast cancer transfectants were compared to cells containing pcDNA vector alone to their sensitivity to ß-lap with or without dicoumarol co-administration. As expected, NQ01-containing MDA-MB-468 transfectants were sensitive to ß-lap and this sensitivity was completely prevented by co-administration of dicoumarol. ß-Lap-mediated apoptosis and it's associated proteolyses (e.g., p53 and PARP cleavage events) *in vivo* in MDA-MB-468 transfectants were also prevent by dicoumarol. Surprisingly, the responses of NQ01-containing compared to NQ01-deficient MDA-MB-468 cells to menadione exposures were opposite those of ß-lap. NQ01-expressing MDA-MB-468 cells were extremely resistant to menadione-induced apoptosis, PARP cleavage and lethality due to the known detoxification of this drug by NQ01. Dicoumarol co-administration with menadione increased the sensitivity of NQ01-expressing MDA-MB-468 cells to this drug, in direct opposition to the protective effects of dicoumarol on ß-lap-mediated cell death. These data showed that ß-lap targets NQ01 for its lethal effects in human breast cancer cells. Furthermore, NQ01 detoxifies menadione, but enhances ß-lap toxicity (*J. Biol. Chem.,* Appendix).

ß-Lap undergoes NQ01-dependent futile cycling to initiate cell death. The opposing lethality data using co-administration of dicoumarol with menadione or ß-lap in NQ01-containing MCF-

7:WS8, T47D or transfected MDA-MB-468 cells strongly suggested that NQ01 detoxified menadione, but strongly enhanced ß-lap-mediated apoptosis and lethality. In NQ01 enzyme assays without the addition of cytochrome C, we noticed the continual cycling of ß-lap, as measured by the loss of NAD(P)H over time. Addition of menadione to S100 cell extracts or in purified NQ01 enzymatic assays led to one reaction cycling detoxification of menadione with the utilization of one mole NAD(P)H per one mole of menadione added. In contrast, one mole of ß-lap stimulated the loss of 5-8 moles of NAD(P)H in enzyme assays without the addition of cytochrome C. The activities above were completely prevented by administration of dicoumarol. These data strongly suggest that ß-lap undergoes futile cycling depleting cells of NAD(P)H, causing dramatic loss of energy in ß-lap-treated cells (*J. Biol. Chem.*, Appendix).

ß-Lap-activated proteolyses *in vivo* is calcium-dependent. Cleavage of p53 in ß-lap-treated, NQ01-containing human breast cancer cells strongly suggested that calpain was activated during apoptosis stimulated by this drug (Figs. Refer to Pink et. al., *J. Biol. Chem.*, Appendix). Ionomycin treatment, which causes massive influx of calcium from the outside of the cell, of human breast cancer cells also induced an identical atypical PARP cleavage independent of NQ01 expression (Fig. 3). These data suggested to us that ß-lap-mediated apoptosis was calcium-dependent. Exposure of ß-lap-treated NQ01-expressing MDA-MB-468 or MCF-7 cells with EGTA or EDTA caused a suppression of ß-lap-mediated atypical PARP cleavage (Figs. 4-6). In addition EDTA or EGTA co-administration also suppressed ß-lap-mediated p53 cleavage (Fig. 7 and 8) and lamin B (Fig. 8) in MCF-7 cells. In contrast, treatment of MCF-7 cells with thapsigargin, an inhibitor of the intracellular membrane-bound calcium pump and stimulator of calcium release from ER and mitochondrial stores, caused typical caspase-mediated apoptosis as seen by the typical cleavage of PARP to its 89 kDa cleavage fragment from its full-length 113 kDa peptide. Finally, administration of BAPTA, an intracellular calcium chelator also prevented ß-lap-mediated p53 and atypical PARP cleavage events in MCF-7 (Tagliarino et al., *J. Biol. Chem.*, submitted, Appendix) or NQ01-expressing MDA-MB-468 cells. EDTA or EGTA treatments of ß-lap-exposed NQ01-expressing cells also prevented the generation of ß-lap-mediated apoptosis (measured as TUNEL positive cells) (Pink et. al., *Exp Cell Res.*, Appendix). Administration of EDTA also prevented ionomycin-induced apoptosis, but not apoptosis induced by staurosporin (STS) or topotecan (TPT). Thus, the atypical PARP cleavage, as well as p53 cleavage in ß-lap-treated NQ01-expressing human breast cancer cells was mediated by a calcium-dependent noncaspase cysteine protease, which we high suspect is calpain.

Accomplishment of Stated Tasks: Using the above data, we are now in a better position to complete the stated tasks of our grant. Although we were delayed a bit with the move of our laboratory to Case Western Reserve from the University of Wisconsin almost 14 months ago, we have completed a majority of the stated tasks of Specific Aim #1. Furthermore, we now have

genetic models with which to isolate the calcium-dependent, NQ01-dependent, noncaspase cysteine protease, which we now strongly suspect is calpain.

Task 1: Generation of PARP cDNA bacterial and mammalian expression vectors, and ^{35}S-methionine-labeled PARP protein, plus or minus histidine Tags.

We have generated his- as well as flag-tagged PARP cDNA mammalian expression vectors that can be propagated in bacterial cells. Using either wheat germ or rabbit reticulocyte *in vitro* transcription-translation systems, we have demonstrated that calpain treated in vitro synthesized 35S-methionine PARP protein leads to an identical atypical PARP cleavage fragment, which is prevented by co-administration of calpastatin, addition of EDTA or EGTA, or calpain inhibitors.

Task 2: Initiate ß-lap-activated apoptotic protease isolation using two simultaneous procedures and ß-lap-treated MCF-7:WS8 human breast cancer cells.

We then established stably transfected MCF-7 cells over-expressing his-tagged PARP. Treatment of these cells with ß-lap caused the expected appearance of a 60 kDa atypical PARP cleavage fragment from endogenous sources of protein and a slightly larger his-tagged PARP fragment from exogenous sources. These cells will now be used in Specific Aim #2 as described below. The following Aims will be completed in Years 2 and 3.:

2A. Standard Protein Purification Procedure

1. Treat roller bottle-generated MCF-7:WS8 cells with ß-lap.
2. Confirm protease activation via endogenous PARP cleavage
3. Ammonium Sulfate Cuts Performed, active fractions pooled.
4. Mono-Q 16/10 FPLC
5. Mono-S 5/5 FPLC
6. Hydroxylapatite column chromatography
7. Superdex 200 26/60 gel filtration

*8. Active fractions pooled, analyzed by SDS-PAGE for atypical ^{35}S-PARP cleavage

9. In-gel PARP cleavage assay using cleavage site tetrapeptide fluorescent substrate generated from "Procedure B".

Progress: We have run pilot experiments to test each of the above listed procedures. We have been able to identify activity in steps 1-3 using radioactively labeled PARP substrates using in vitro activity assays.

2B. Affinity Chromatographic Purification Procedure

1. PARP cleavage point determination and tetrapeptide syntheses

1a. Immunoprecipitation of PARP fragments using C-2-10 Antibody.

1b. *In vitro* ^{35}S-PARP cleavage±His tag, immunoprecipitation.

1c. PARP fragment purification and microsequencing.

1d. Cleavage site determined by computer analyses.

1e. Fluoromethylketone and fluorescent-tetrapeptide cleavage site-specific peptides made by CWRU. Several will be made as positive and negative controls for subsequent enzyme inhibition or activity assays.

1f. Confirmation of tetrapeptide-fmk blockage of atypical PARP cleavage and apoptotic protease activity using the

tetrapeptide-fluorescent substrate.

1g. Mutagenization of PARP cDNA at cleavage site, *in vitro* translate, demonstrate no atypical PARP cleavage.

2. Construction of biotin-(streptavidin)-[X]-tetrapeptide-aldehyde.

4. DEAE Chromatographic Separation of ß-lap-treated MCF-7 cell extract, analyses of atypical cleavage activity using ^{35}S-methionine PARP.

5. Active fractions from "**Task #2B. 3**" are incubated with

6. biotin-[X]-tetrapeptide-aldehyde and bound to streptavidin-agarose beads and washed.

6. Apoptotic protease binding proteins are eluted with biotin.

*7. Eluted proteins are analyzed by SDS-PAGE, silver stained and assayed for ^{35}S-PARP cleavage.

The following Tasks may not be needed. The Specific Aims below may not be required should calpain be implicated. Calpain-negative cells, either deficient in calpain expression (mouse knock-out) or cells over-expressing dominant-negative calpain, will be used to explore the specific role of this one protease in ß-lap-sensitivity. Furthermore, using the cell models developed above we will also explore the signaling pathways between ß-la futile cycling and activation of the activation of calpain.:

Task 3: Production of polyclonal antisera using protein from (2A. *7) or (2B. *6) above.

Task 4: Microsequence purified apoptotic protease polypeptides from (2A. *7) or (2B. *6) above.

Task 5: Production of degenerative PCR probes corresponding to apoptotic protease amino acid sequences.

Task 6: Screen for ß-lap-activated apoptotic protease using antibodies from **Task #3** and PCR probes from **Task #5** in a sequential expression and cDNA hybridization approach.

Task 7: Screen for full-length ß-lap-activated apoptotic protease cDNA.

Task 8: Sequence and analyze the apoptotic protease DNA sequence.

Task 9: Subclone the apoptotic protease into the Tet-on response vector for **Aim #2.**

Task 10: Examine human breast cancer cells and patient tissue samples for ß-lap-activated apoptotic protease message, protein, and enzymatic activities.

Progress: Tasks 2B through Task 10 are being explored during this next year. Our focus is currently on (1) determining p53 and PARP cleavage sites in ß-lap-treated MCF-7 cells. The cleavage site will then be used to determine a cleavage site inhibitor, for use in affinity site column chromatography purification of the protease, as well as using the site for activity assays and standard biochemical purification assays to purify the activated protease.

Specific Aim #2: **Transfect sensitive (i.e., MCF-7) and resistant (i.e., MDA-MB-231) human breast cancer cells with sense and antisense expression vectors encoding the unknown protease to elucidate the role of this apoptotic death enzyme in drug resistance/sensitivities to ß-lap, or other Topo I poisons and DNA damaging agents (Years 2-3).**

Task 1: Transfect MCF-7:WS8 and MDA-MB-231 cells with Tet-on repressor cDNA and isolate doxycycline-responsive, low basal level subclones.

Task 2: Transfect Tet-on repressor-expressing subclones with doxycycline-responsive, sense- and antisense-oriented ß-lap-activated apoptotic protease expression vectors and double select (hygromycin and neomycin) clones.

Task 3: Examine cells generated in **Tasks #1-3** for apoptotic and survival responses to ß-lap, TPT, and other DNA damaging agents (such as ionizing radiation or Topo II-alpha poisons.

Task 4: Examine treated cells in **Task #3** for apoptotic cell death substrate cleavage and Caspase activities, as well as for the, now known, ß-lap (CPT + PDTC)-activated apoptotic protease.

Progress: Tasks 1-4, Specific Aim #2, will be completed when the cleavage site has been determined in Task #1, above.

Evidence for ß-lap-activated apoptosis mediated by calpain. We reasoned that if ß-lap stimulates NQ01-dependent calpain-mediated apoptosis, then the drug must cause significant alterations in calcium homeostasis. In collaboration with Drs. George Dubyak (Dept. Biophysics, CWRU) and Clark Distelhorst (Hem//Onc., CWRU) we demonstrated that ß-lap treatment of NQ01-containing MCF-7:WS8 or MDA-MB-468 transfectants caused dramatic calcium influx within 3 mins as measured by FURA-2 binding. Appropriate controls for the release of extracellular (ATP treatment) or intracellular (Thapsigargin) calcium were included. In contrast, calcium release was not evident in NQ01-deficient MDA-MD-468 parental or vector alone cells. Furthermore, treatment of MCF-7:WS8 or NQ01-expressing MDA-MB-468 transfectants with ß-lap caused the cleavage of p53 and atypical cleavage of PARP at the same time as the cleavage-dependent activation of calcium, as monitored by Western blot analyses of the appearance of the 18 kDa active subunit of calpain beginning at 8 hours. Furthermore, the appearance of these cleavage events at 8 hours coincides with the initial appearance of TUNEL-positive, condensed-nuclei-containing apoptotic cells (not shown) at 8 hours post-ß-lap-treatment of NQ01 contain (MCF-7 or MDA-MB-468 transfectants) as opposed to parental or vector alone-containing MDA-MB-468 cells. The appearance of all the cleavage fragments described above in NQ01-containing cells was prevented by co-administration of dicoumarol, the NQ01 inhibitor. Furthermore using confocal microscopy, we noted the dramatic movement of cytosolic calpain into the nuclei of ß-lap-treated NQ01-expressing, but not NQ01-deficient, cells. This movement of calpain into the nuclei of ß-lap-treated NQ01-expressing cells was prevented by dicoumoral co-administration, it coincided with the appearance at 4-8 hours posttreatment of atypical PARP cleavage, p53 cleavage and the appearance of the 18 kDa small subunit (active) form of calpain, and was not a result of massive breakdown of the nuclear membrane since NQ01 (which is entirely cytosolic) remained cytosolic and the Ku70/Ku80 heterodimer (which is nuclear, not cleaved during apoptosis and was detected by Ab #162) remained nuclear. Furthermore, the movement of calpain from the cytoplasm to the nucleus was blocked by co-administration of dicoumarol (*not shown*).

ß-Lap exposure to NQ01-containing cells causes dramatic ATP depletion, which is not prevented by EDTA or EGTA. The loss of NAD(P)H in enzyme assays using NQ01-containing S100 cellular extracts or in purified NQ01 reactions, suggested that dramatic and

rapid energy loss was occurring in NQ01-containing human breast cancer cells. We suspected that NQ01-mediated ß-lap futile cycling would lead to a dramatic loss of ATP within cells. Furthermore, we anticipated that such loss would be prevented by dicoumarol, but possibly not by EGTA or EDTA, since these would prevent calpain and apoptosis induction downstream but not affect the NQ01 enzyme. Using a luciferase assay, we demonstrated that NQ01-containing human breast cancer cells exhibited a dramatic loss in ATP within 30 mins post-treatment. We estimate that less than 1% of the total ATP in control cells remain within 30 mins after a 4 hour pulse of 4-8 μM ß-lap. Administration of EDTA or EGTA had little affect of ATP loss mediated by ß-lap in MCF-7 cells. Interestingly, neither ionomycin or staurosporin (STS) caused ATP loss. These data are consistent with an NQ01-dependent futile cycling of ß-lap in that treated cells run out of energy. We are interested in the relationship between this futile cycling of the drug and release of calcium (Tagliarino et al., *J. Biol. Chem.,* submitted)

C. KEY RESEARCH ACCOMPLISHMENTS:

-NQO1 determined as key intracellular determinant of ß-lap-mediated apoptosis and cell death. (*J. Biol. Chem.*, Appendix)

-Cell death by ß-lap-exposure was found to be due to futile cycling of the compound. (*J. Biol. Chem.,* Appendix)

-Atypical PARP cleavage, as well as p53 cleavage, in ß-lap-treated MCF-7 cells determined. (*Exp. Cell Res.,* Appendix)

-Calpain translocation in ß-lap-treated MCF-7 cells found at a time concomitant with atypical PARP and p53 cleavage events. (Tagliarino et. al., *J. Biol. Chem.,* Appendix)

-His-tagged PARP made and transfected into cells; HA-tagged p53 vector obtained.

-Calcium alterations detected following ß-lap-treated MCF-7 cells, wherein BAPTA-AM, EGTA, and EDTA all prevented atypical PARP and p53 cleavage events, as well as ß-lap-mediated apoptosis. (*Exp. Cell Res.,* Appendix).

-Calpain and radioactively-labeled PARP in vitro assays perfected.

-Pilot biochemical purification procedures performed.

-Bcl-2 protects NQO1-deficient HL60 cells from high dose ß-lap exposures (Planchon et. al., *Oncology Reports,* Appendix).

-NF-κB activation following camptothecin exposures, NF-κB inhibition after ß-lap exposures. (Miyamoto et al., *NY Natl. Acad. Scs.,* and Huang et al., *J. Biol. Chem.*)

D. REPORTABLE OUTCOMES *(Manuscripts, Abstracts, presentations,and patents and licenses applied for and/or used).*:

1. Manuscripts and Papers Published, In Press, and Submitted (See Appendix):

Planchon, S., Wuerzberger, S., Pink, J.J., Robertson, K., Bornmann, W. and **Boothman, D.A.** bcl-2 protects against caspase 3-mediated apoptosis induced by ß-lapachone. 1999; Oncology Reports 6: 485-492.

Pink, J.J., Planchon, S.M., Tagliarino, C., Wuerzberger-Davis, S.M., Varnes, M.E., Siegel, D., and **Boothman, D.A.** NAD(P)H:quinone oxidoreductase (NQO1) activity is the principal determinant of ß-lapachone cytotoxicity. 2000; J. Biol. Chem., 275 (8): 5416-5422.

Pink, J.J., Wuerzberger-Davis, S.M., Tagliarino C., Planchon, S.M., Yang, X-H., Froelich, C.J., and **Boothman, D.A.** A novel non-caspase-mediated proteolytic pathway activated in breast cancer cells during ß-lapachone-mediated apoptosis. 2000; Exp. Cell. Res., 255 (2): 144-155.

Huang, T.T., Wuerzberger-Davis, S.M., Seufer, B.J., Shumway, S.D., Kurama, T., Boothman, D.A., and Miyamoto, S. NF-κB activation by camptothecin: A linkage between nuclear DNA damage and cytoplasmic signaling events. 2000; J. Biol. Chem., 275 (13): 9501-9509.

Miyamoto, S., Huang, T., Wuerzberger-Davis, S., Pink, J.J., Tagliarino, C., Kinsella, T.J., and **Boothman, D.A.** Cellular and Molecular Responses to Topoisomerase I Poisons: Exploiting Synergy For Improved Radiotherapy. 2000; Annals of the New York Academy of Sciences, In Press.

Planchon, S.M., Pink, J.J., Tagliarino,, C., Bornmann, W.G., Varnes, M.E., and **Boothman, D.A**. ß-Lapachone-induced apoptosis in human prostate cancer cells: involvement of NQO1/xip3. 2000; Exp. Cell Res., submitted.

2. Abstracts:

-DOD Breast Cancer Initiative Symposium, Atlanta, GA "NQO1 is the principal determinant of ß-lap-mediated lethality". June, 2000.

-DOD Breast Cancer Initiative Symposium, Atlanta, GA "Calcium alterations following ß-lap exposures". June 2000.

-Keystone Symposium Meeting, Keystone, CO. "Involvement of calpain in ß-lap-mediated apoptosis" March. 2000.

-Gordon Research Conference on Apoptosis and Cell Cycle Regulation, New Hampshire "NQO1 is the key determinant of ß-lap-mediate lethality", June, 2000.

3. Patents:

None.

4. Presentations:

Invited Speaker, "Exploiting X-ray-inducible responses for improved therapy" Northern Illinois University, Dr. John Mitchell, host; Student's Choice Lecturer. *Feb. 4-6, 1999.*

Invited Speaker, Exploiting IR-inducible Proteins For Therapy Against Breast Cancer, Midwest DNA Repair Conference, Ann Arbor, Michigan, *June 13, 1999.*

Invited Speaker, "Exploiting X-ray-inducible proteins for apoptotic chemotherapy" Essen, Germany (C. Streffer, host) *July 14-17, 1999.*

Invited Speaker, "A novel noncaspase-mediated apoptotic pathway induced by ß-lapachone: involvement of NQ01", Department of Radiation Oncology, University of Maryland, (W.F. Morgan, host) *October 23, 1999.*

Invited Speaker, "Exploiting novel apoptotic pathways", Cleveland Clinic Lerner Research Institute. (A. Almasan, host) *November, 1999.*

Invited Speaker, New York Academy of Sciences Symposium, entitled "The camptothecins: unfolding their anticancer potential", Arlington, Virginia, *March 17-20, 2000.*

5. Degrees:

Ph.D.: Sarah Planchon, "ß-Lap stimulates apoptosis via NAD(P)H:oxidoreductase, an x-ray-inducible transcript, xip3" December, 1999, University of Wisconsin-Madison.

6. Cell Lines Developed:

-NQO1 expressing MDA-MB-231 and MDA-MB-468 cell lines, with corresponding vector alone, neo^R cell lines.

7. Funding Applied for (and received) based, in part, on the support for this award:

-Department of Defense (DOD), Breast Cancer Research Initiative, Pre-doctoral Fellowship, Student: Colleen Tagliarino, $60,000 for 3 years, started 04/01/00 to 03/31/03. Funded

-DOD Prostate Cancer Initiative, "Exploiting NQO1, a radiation-inducible enzyme, using ß-lapachone for improved radiotherapy of prostate cancer". $103,000/yr for 3 years. Submitted May 1, 2000. Additional information requested, funding pending.

NCI, NIH R01, "Exploiting NQO1 for enhanced radiotherapy using ß-lapachone" PI: D. A. Boothman. $200,000/yr for 5 years. Submitted October 1, 2000. Funding pending.

E. Conclusions:

The research ongoing and proposed in this proposal addresses a novel apoptotic agent, ß-lapachone, shown to be active against human breast and prostate cancer cells. Determination of the compound's intracellular target now makes the use of this compound for in vivo pre-clinical trials possible. ß-Lapachone's activity has been shown to be independent of p53 and pRb status and involves an exclusive apoptotic mechanism of cell death. Cell death mediated by this compound appears also to be independent of caspase activation, making the compound and a series of related derivatives, potentially important for treatment of numerous cancers of the breast and prostate. Since many cancers form due to the result of alterations in p53 or caspases, development of this compound for breast cancer therapy alone or in combination with ionizing radiation (IR) (Miyamoto et. al., In press) could grately improve therapy of these diseases. Cloning of the unknown protease that appears to be stimulated by ß-lap exposures should reveal a novel non-caspase-mediated apoptotic pathway.

REFERENCES (*In alphabetical order*):

Huang, T.T., Wuerzberger-Davis, S.M., Seufer, B.J., Shumway, S.D., Kurama, T., Boothman, D.A., and Miyamoto, S. NF-κB activation by camptothecin: A linkage between nuclear DNA damage and cytoplasmic signaling events. 2000; J. Biol. Chem., 275 (13): 9501-9509.

Miyamoto, S., Huang, T., Wuerzberger-Davis, S., Pink, J.J., Tagliarino, C., Kinsella, T.J., and **Boothman, D.A.** Cellular and Molecular Responses to Topoisomerase I Poisons: Exploiting Synergy For Improved Radiotherapy. 2000; Annals of the New York Academy of Sciences, In Press.

Pink, J.J., Planchon, S.M., Tagliarino, C., Wuerzberger-Davis, S.M., Varnes, M.E., Siegel, D., and **Boothman, D.A.** NAD(P)H:quinone oxidoreductase (NQO1) activity is the principal determinant of ß-lapachone cytotoxicity. 2000; J. Biol. Chem., 275 (8): 5416-5422.

Pink, J.J., Wuerzberger-Davis, S.M., Tagliarino C., Planchon, S.M., Yang, X-H., Froelich, C.J., and **Boothman, D.A.** A novel non-caspase-mediated proteolytic pathway activated in breast cancer cells during ß-lapachone-mediated apoptosis. 2000; Exp. Cell. Res., 255 (2): 144-155.

Planchon, S., Wuerzberger, S., Pink, J.J., Robertson, K., Bornmann, W. and **Boothman, D.A.** bcl-2 protects against caspase 3-mediated apoptosis induced by ß-lapachone. 1999; Oncology Reports 6: 485-492.

Planchon, S.M., Pink, J.J., Tagliarino,, C., Bornmann, W.G., Varnes, M.E., and **Boothman, D.A.** ß-Lapachone-induced apoptosis in human prostate cancer cells: involvement of NQO1/xip3. 2000; Exp. Cell Res., submitted.

APPENDIX ITEMS

Pink, J.J., Planchon, S.M., Tagliarino, C., Wuerzberger-Davis, S.M., Varnes, M.E., Siegel, D., and **Boothman, D.A.** NAD(P)H:quinone oxidoreductase (NQO1) activity is the principal determinant of ß-lapachone cytotoxicity. 2000; J. Biol. Chem., 275 (8): 5416-5422.

Pink, J.J., Wuerzberger-Davis, S.M., Tagliarino C., Planchon, S.M., Yang, X-H., Froelich, C.J., and **Boothman, D.A.** A novel non-caspase-mediated proteolytic pathway activated in breast cancer cells during ß-lapachone-mediated apoptosis. 2000; Exp. Cell. Res., 255 (2): 144-155.

Planchon, S., Wuerzberger, S., Pink, J.J., Robertson, K., Bornmann, W. and **Boothman, D.A.** bcl-2 protects against caspase 3-mediated apoptosis induced by ß-lapachone. 1999; Oncology Reports 6: 485-492.

Tagliarino,, C., Planchon, S.M., Pink, J.J., Bornmann, W.G., Varnes, M.E., and **Boothman, D.A.** ß-Lapachone-induced apoptosis in human prostate cancer cells: involvement of NQO1/xip3. 2000; Exp. Cell Res., submitted.

Huang, T.T., Wuerzberger-Davis, S.M., Seufer, B.J., Shumway, S.D., Kurama, T., Boothman, D.A., and Miyamoto, S. NF-κB activation by camptothecin: A linkage between nuclear DNA damage and cytoplasmic signaling events. 2000; J. Biol. Chem., 275 (13): 9501-9509.

Miyamoto, S., Huang, T., Wuerzberger-Davis, S., Pink, J.J., Tagliarino, C., Kinsella, T.J., and **Boothman, D.A.** Cellular and Molecular Responses to Topoisomerase I Poisons: Exploiting Synergy For Improved Radiotherapy. 2000; Annals of the New York Academy of Sciences, In Press.

THE JOURNAL OF BIOLOGICAL CHEMISTRY

Vol. 275, No. 8, Issue of February 25, pp. 5416–5424, 2000
Printed in U.S.A.

NAD(P)H:Quinone Oxidoreductase Activity Is the Principal Determinant of β-Lapachone Cytotoxicity*

(Received for publication, October 13, 1999, and in revised form, December 7, 1999)

John J. Pink‡, Sarah M. Planchon‡, Colleen Tagliarino‡, Marie E. Varnes‡, David Siegel§, and David A. Boothman‡¶

From the ‡Department of Radiation Oncology, Laboratory of Molecular Stress Responses, Ireland Comprehensive Cancer Center, Case Western Reserve University, Cleveland, Ohio 44106-4942 and the §Department of Pharmaceutical Sciences, School of Pharmacy and Cancer Center, University of Colorado Health Sciences Center, Denver, Colorado 80262

β-Lapachone activates a novel apoptotic response in a number of cell lines. We demonstrate that the enzyme NAD(P)H:quinone oxidoreductase (NQO1) substantially enhances the toxicity of β-lapachone. NQO1 expression directly correlated with sensitivity to a 4-h pulse of β-lapachone in a panel of breast cancer cell lines, and the NQO1 inhibitor, dicoumarol, significantly protected NQO1-expressing cells from all aspects of β-lapachone toxicity. Stable transfection of the NQO1-deficient cell line, MDA-MB-468, with an NQO1 expression plasmid increased apoptotic responses and lethality after β-lapachone exposure. Dicoumarol blocked both the apoptotic responses and lethality. Biochemical studies suggest that reduction of β-lapachone by NQO1 leads to a futile cycling between the quinone and hydroquinone forms, with a concomitant loss of reduced NAD(P)H. In addition, the activation of a cysteine protease, which has characteristics consistent with the neutral calcium-dependent protease, calpain, is observed after β-lapachone treatment. This is the first definitive elucidation of an intracellular target for β-lapachone in tumor cells. NQO1 could be exploited for gene therapy, radiotherapy, and/or chemopreventive interventions, since the enzyme is elevated in a number of tumor types (*i.e.* breast and lung) and during neoplastic transformation.

β-lap,[1] a novel 1,2-naphthoquinone, is a potent cytotoxic agent that demonstrates activity against various cancer cell lines (1–3). At lower doses, it is a radiosensitizer of a number of human cancer cell lines (4). We previously demonstrated that the primary mode of β-lap cytotoxicity is through the induction of apoptosis (1, 2). However, the clinical efficacy of this drug remains to be explored, and such studies await elucidation of its mechanism of action.

While a number of *in vitro* effects of β-lap have been described, the key intracellular target of β-lap remains unknown. β-lap has many diverse effects *in vitro*, including (*a*) inhibition of DNA polymerase α (5), (*b*) enhanced lipid peroxidation and free radical accumulation (6), (*c*) inhibition of DNA replication and thymidylate synthase activity (7), (*d*) inhibition of DNA repair (4, 8), (*e*) inhibition or activation of DNA topoisomerase I (1, 3), (*f*) oxidation of dihydrolipoamide (9), (*g*) induction of topoisomerase IIα-mediated DNA breaks (10), (*h*) inhibition of poly(ADP-ribose) polymerase (11), and (*i*) inhibition of NF-κB activity (12). While these effects could be hypothetically linked to the cytotoxicity caused by β-lap administration, most have not been demonstrated *in vivo*, and none have led to elucidation of the drug's intracellular target.

Structural similarities between β-lap and other members of the naphthoquinone family, such as menadione (vitamin K_3; 2-methyl-1,4 naphthoquinone), suggested that the enzyme, DT-diaphorase, quinone oxidoreductase, EC 1.6.99.2 (NQO1), may be involved in the activation or detoxification of β-lap (13–17). The x-ray-inducible nature of NQO1 (*i.e.* it was cloned by our laboratory as x-ray inducible transcript-3 (xip-3)) was also consistent with this compound's ability to sensitize irradiated cells (18).

NQO1 is a ubiquitous flavoprotein found in most eukaryotes. The human NQO1 gene encodes a 30-kDa protein that is expressed in most tissues but does show variable tissue-dependent expression. NQO1 is abundant in the liver of most mammals, except humans, where it is less abundant than in most other tissues (16, 19, 20). NQO1 knock-out mice show no detectable phenotype other than an enhanced sensitivity to menadione, suggesting that the principal function of NQO1 is the detoxification of quinone xenobiotics (21). Importantly, NQO1 is overexpressed in a number of tumors, including breast, colon, and lung cancers, compared with surrounding normal tissue (22–25). This observation, more than any other, suggests that drugs that are activated by NQO1 (*e.g.* MMC, streptonigrin, and EO9; see below) should show significant tumor-specific activity.

NQO1 catalyzes a two-electron reduction of various quinones (*e.g.* menadione), utilizing either NADH or NADPH as electron donors. Unlike most other cellular reductases, NQO1 reduces quinones directly to the hydroquinone, bypassing the unstable and highly reactive semiquinone intermediate. Semiquinones are excellent free radical generators, initiating a redox cycle that results in the generation of superoxide. Superoxide can dismutate to hydrogen peroxide, and hydroxyl radicals can then be formed by the iron-catalyzed reduction of peroxide via the Fenton reaction (26). All of these highly reactive species may directly react with DNA or other cellular macromolecules, such as lipids and proteins, causing damage. NQO1-mediated production of the hydroquinone, which can be readily conjugated and excreted from the cell, constitutes a protective mech-

* This work was supported by United States Army Medical Research and Materiel Command Breast Cancer Initiative Grant DAMD17-98-1-8260 (to D. A. B.) and Postdoctoral Fellowship DAMD17-97-1-7221 (to J. J. P.) and National Institutes of Health Grant CA51210 (to D. S.). The costs of publication of this article were defrayed in part by the payment of page charges. This article must therefore be hereby marked "*advertisement*" in accordance with 18 U.S.C. Section 1734 solely to indicate this fact.

¶ To whom correspondence should be addressed: Tel.: 216-368-0840; Fax: 216-368-1142; E-mail: dab30@po.cwru.edu.

[1] The abbreviations used are: β-lap, β-lapachone (3,4-dihydro-2,2-dimethyl-2H-naphtho[1,2-*b*]pyran-5,6-dione); xip-3, x-ray-inducible transcript-3; NQO1, NAD(P)H:quinone oxidoreductase, DT-diaphorase, xip-3 (EC 1.6.99.2); PARP, poly(ADP-ribose) polymerase; MMC, mitomycin C; TUNEL, terminal deoxynucleotidyl transferase-mediated dUTP nick end labeling.

anism against these types of damage (27). It is thought that the reducing activity of NQO1 protects cells from the toxicity of naturally occurring xenobiotics containing quinone moieties (14).

In addition to its protective effects, NQO1 can also reduce certain quinones to more reactive forms. The most well described of these compounds is MMC. It is through a two-electron reduction by NQO1 or through two separate one electron reductions by other reductases (such as NADH:cytochrome b_5 reductase and NADPH:cytochrome P-450 reductase) that the alkylating activity of MMC is revealed (28–30). A correlation was observed between MMC sensitivity and NQO1 activity in a study using 69 cell lines from the NCI, National Institutes of Health, human tumor cell panel. These data suggested that NQO1 was a critical activator of MMC and probably other quinone-containing antitumor agents (31). Similarly, streptonigrin and EO9 can be activated by NQO1-catalyzed reduction (32).

Dicoumarol (3–3′-methylene-bis(4-hydroxycoumarin)) is a commonly used inhibitor of NQO1, which competes with NADH or NADPH for binding to the oxidized form of NQO1. Dicoumarol thereby prevents reduction of various target quinones (33, 34). Co-administration of dicoumarol significantly enhances the toxicity of a number of quinones, including menadione, presumably by increasing oxidative stress in the cell (35–37).

We demonstrate that NQO1 is an important activating enzyme for β-lap in breast cancer cells. β-lap cytotoxicity was significantly enhanced in breast cancer cells expressing NQO1. Conversely, cells that lacked this enzyme were more resistant to a short term exposure to the drug. Co-administration of dicoumarol protected NQO1-expressing cells from all downstream apoptotic responses and greatly enhanced survival. Stable transfection of NQO1-deficient, MDA-MB-468 cells, homozygous for a proline to serine substitution at amino acid 187, which leads to the synthesis of unstable protein (38), with human NQO1 cDNA sensitized these otherwise resistant cells and re-established apoptotic responses. As seen in other cells expressing endogenous NQO1, cytotoxicity was significantly inhibited by dicoumarol. Our data establish that NQO1 activity is an important determinant of β-lap cytotoxicity in breast cancer cells. A novel downstream apoptotic pathway induced by β-lapachone is also discussed.

EXPERIMENTAL PROCEDURES

Cell Culture—MCF-7:WS8 and T47D:A18 cells were obtained from V. Craig Jordan (Northwestern University, Chicago, IL). MDA-MB-468 cells were obtained from the American Type Culture Collection. All tissue culture components were purchased from Life Technologies, Inc. unless otherwise stated. Cells were grown in RPMI 1640 supplemented with 10% calf serum, 2 mM L-glutamine, 100 units/ml penicillin, and 100 mg/ml streptomycin. Cells were routinely passed at 1:5–1:20 dilutions once per week using 0.1% trypsin. All cells were grown in a 37 °C humidified incubator with 5% CO_2, 95% air atmosphere. Tests for mycoplasma, using the Gen-Probe™ Rapid Detection Kit (Fisher), were performed quarterly, and all cell lines were found to be negative.

Stable Transfection—Cells were seeded into six-well dishes at 2×10^5 cells/well and allowed to attach overnight. The following day, 1.0 μg of BE8 plasmid DNA containing the human NQO1 cDNA in the pCDNA3 constitutive expression vector (39) was transfected into each of three wells using standard calcium phosphate methodology (40). After 2 days, cells were selected for growth in 350 μg/ml Geneticin® (G418, Life Technologies, Inc.). A stable, pooled population was established after approximately 3 weeks, and subsequently clones were isolated by limiting dilution cloning, as described (41).

Cell Growth Assays—Cells were seeded into each well of a 96-well plate (1500 cells/well) in 0.2 ml of media on day 0. The following day (day 1), media were removed, and 0.2 ml of medium containing the appropriate compound(s) was added for 4 h. Drugs were then removed, control growth medium was added, and cells were allowed to grow for an additional 7 days. Stock solutions of β-lap (a generous gift from William Bornmann, Sloan-Kettering Cancer Center, New York, NY) and menadione (Sigma) were dissolved in Me_2SO and stored at −80 °C. Drugs were added to medium at a 1:1000 dilution immediately before administration to cells. Dicoumarol (Sigma) was suspended in water and solubilized using a minimal amount of NaOH. Dicoumarol was added at a 1:100 dilution to the appropriate medium. DNA content (a measure of cell growth) was determined by fluorescence of the DNA dye Hoescht 33258 (Sigma), using an adaptation of the method of Labarca and Paigen (42), and read in a Cytofluor fluorescence plate reader. Data were expressed as relative growth, *T/C* (treated/control) from three or more wells per treatment. Each experiment was repeated at least three times, and data were expressed as mean ± S.E. Comparisons were performed using a two-tailed Student's *t* test for paired samples.

Colony-forming Assays—LD_{50} survival determinations were calculated by clonogenic assays (4). Briefly, cells were seeded at various densities on 35-cm^2 tissue culture dishes and allowed 48 h to attach and initiate log phase growth. Drugs were added for 4 h at various concentrations and removed, as described above. Colonies from control or treated conditions were allowed to grow for 10 days. Colonies with 50 or more normal appearing cells were counted, and data were graphed as mean ± S.E. Shown is a compilation of two independent experiments. Comparisons were performed using a two-tailed Student's *t* test for paired samples.

Western Blot Analyses—Whole cell extracts were prepared by direct lysis of scraped, PBS-washed cells (both floating and attached cells were pooled) in buffer composed of 6 M urea, 2% SDS, 10% glycerol, 62.5 mM Tris-HCl, pH 6.8, 5% β-mercaptoethanol, and 5 μg/ml bromphenol blue followed by sonication. Equal amounts of protein were heated at 65 °C for 10 min and loaded into each lane of a 10% polyacrylamide gel with a 5% stacking gel. Following electrophoresis, proteins were transferred to Immobilon-P (Millipore Corp., Bedford, MA) using Multiphor II semi-dry electroblotting (Amersham Pharmacia Biotech) according to the manufacturer's directions. Loading equivalence and transfer efficiency were monitored by Ponceau S staining of the membrane. Standard Western blotting techniques were used, and the proteins of interest were visualized by incubation with Super Signal (Pierce) at 20 °C for 5 min. Membranes were then exposed to x-ray film for an appropriate time and developed. The C-2-10 anti-PARP antibody was purchased from Enzyme Systems Products (Dublin, CA). The anti-p53 antibody (DO-1) was purchased from Santa Cruz Biotechnology, Inc. (Santa Cruz, CA). NQO1 antibody was contained in medium from a mouse hybridoma clone A180 (43) and was used at a 1:4 dilution in 10% serum, 1× PBS, 0.2% Tween 20 for Western blot analysis.

Preparation of S9 Supernatants—Cellular extracts for enzyme assays were prepared from cells in mid-log to late log phase growth. Cells were harvested by trypsinization (0.25% trypsin and 1 mM EDTA), washed twice in ice-cold, phenol red-free Hank's balanced salt solution, and then resuspended in a small volume of PBS, pH 7.2, containing 10 μg/μl aprotinin. The cell suspensions were sonicated on ice four times, using 10-s pulses, and then centrifuged at 14,000 × *g* for 20 min. The S9 supernatants were aliquoted into microcentrifuge tubes and stored at −80 °C until used.

Enzyme Assays—Three enzymes were assayed as described by Fitzsimmons *et al.* (31) and Gustafson *et al.* (39). Reaction medium contained 77 μM cytochrome *c* (practical grade; Sigma) and 0.14% bovine serum albumin in Tris-HCl buffer (50 mM, pH 7.5). NQO1 activity was measured using NADH (200 μM) as the immediate electron donor and menadione (10 μM) as the intermediate electron acceptor. Each assay was repeated in the presence of 10 μM dicoumarol, and activity attributed to NQO1 was that inhibited by dicoumarol (44). NADH: cytochrome b_5 reductase was measured using NADH (200 μM) as the electron donor, and NADH:cytochrome P-450 reductase was measured using NADPH (200 μM) as electron donor (45) in a Beckman DU 640 spectrophotometer (Beckman Coulter, Fullerton, CA). Reactions were carried out at 37 °C and were initiated by the addition of S9 supernatants. Varying amounts of supernatants, from 10 to 40 μl, were used to ensure linearity of rates with protein concentration. Enzyme activities were calculated as nmol of cytochrome *c* reduced/min/mg of protein, based on the initial rate of change in OD at 550 nm and an extinction coefficient for cytochrome *c* of 21.1 mM/cm. Results shown are the average enzyme activity for three separate cell extractions ± S.D. or both values from duplicate experiments.

NADH Recycling Assays—Assays were performed with either purified NQO1 (46) or S9 extracts from MCF-7:WS8 cells. For the assay using purified NQO1, 1.5 μg of recombinant human NQO1 was mixed with 200–500 μM NADH in 50 mM potassium phosphate buffer, pH 7.0. Reactions were initiated by the addition of 2–20 μM β-lap or menadione, and the change in absorbance at 340 nM was measured over time. For

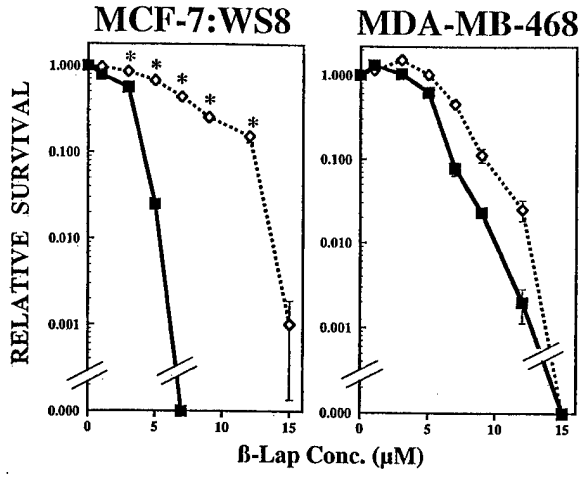

FIG. 1. **Co-administration of dicoumarol protects MCF-7:WS8, but not MDA-MB-468, cells from β-lap-mediated cytotoxicity.** Cells were seeded into 60-mm dishes (10,000 and 1000 cells/dish, in triplicate) and allowed to attach overnight. Cells were then exposed to a 4-h pulse of β-lap either alone (■) or with 50 μM dicoumarol (◇). Media were removed, fresh drug-free media were added, and cells were allowed to grow for 10 days. Plates were then washed and stained with crystal violet in 50% methanol. Colonies of greater than 50 normal-appearing cells were then counted and plotted *versus* β-lap concentration. Shown is the mean ± S.E. of triplicate plates from two independent experiments .

assays using MCF-7:WS8 S9 extracts, 5 μl of extracts containing approximately 2000 units of NQO1/mg of protein were mixed with 200–500 μM NADH in 50 mM Tris-HCl, pH 7.5, containing 0.14% bovine serum albumin. Reactions were initiated by the addition of 5–200 μM β-lap or menadione, and change in absorbance at 340 nM was measured for 10 min. All reactions were also performed in the presence of 10 μM dicoumarol, which inhibited all measurable NQO1 activity.

Flow Cytometry and Apoptotic Measurements—Flow cytometric analyses were performed as described (1, 2). TUNEL assays, to measure DNA fragmentation during apoptosis, were performed using APO-DIRECT™ as described by the manufacturer (Phoenix Flow Systems, Inc., San Diego, CA). Samples were read in an EPICS Elite ESP flow cytometer using an air-cooled argon laser at 488 nm, 15 milliwatts (Beckman Coulter Electronics, Miami, FL). Propidium iodide was read at 640 nm using a long pass optical filter, and fluorescein isothiocyanate was read at 525 nm using a band pass filter. Analysis was performed using the Elite acquisition software provided with the instrument. All experiments were performed a minimum of three times.

RESULTS

We previously showed that the naturally occurring 1,2-naphthoquinone, β-lap, induced apoptosis in a number of breast cancer cell lines (1, 2). We hypothesized that β-lap, as a member of the naphthoquinone family, may be a substrate for NQO1 and that its toxicity may be influenced by NQO1 expression. We therefore tested the effects of dicoumarol on β-lap-mediated cytotoxicity in MCF-7:WS8 or MDA-MB-468 breast cancer cell lines after a 4-h pulse of drug. Co-administration of 50 μM dicoumarol during a 4-h pulse of β-lap caused a significant survival enhancement in MCF-7:WS8 cells (Fig. 1). While this protection was dramatic at β-lap doses of 4–12 μM, the protective effects of dicoumarol were overcome by >14 μM β-lap. In contrast, MDA-MB-468 cells were relatively resistant (LD_{50} ~ 8 μM, compared with MCF-7:WS8, LD_{50} ~ 4 μM) to β-lap alone and were not significantly protected by dicoumarol (Fig. 1). Since MDA-MB-468 cells do not express NQO1 (Table I and Fig. 3) and dicoumarol significantly protected NQO1-expressing MCF-7:WS8 cells (Table I and Fig. 3), these data suggested that NQO1 expression was a critical determining factor in β-lap-mediated cytotoxicity.

We then extended these studies to compare the relative toxicity of menadione (2-methyl-1,4-naphthoquinone) to β-lap, either alone or in the presence of dicoumarol. Three breast

TABLE I
Endogenous reductase levels in breast cancer cell lines

Values represent averages for three or more separate S9 preparations ± S.D. except as noted in Footnote *c*.

Cell line	Enzyme activities[a]		
	NQO1	NADH:cytochrome b_5 reductase	NADPH:cytochrome P-450 reductase
	nmol/min/mg		
MCF-7:WS8	2641 ± 555	81 ± 18	27 ± 5.0
T47D:A18	82 ± 17	131 ± 35	31 ± 1.0
MDA-MB-468	<10.0[b]	93/108[c]	26/36[c]

[a] Units are nanomoles of cytochrome *c* reduced per min per mg of protein.

[b] <10.0**, NQO1 activity not detected. The difference in the rate of cytochrome *c* reduction with and without dicoumarol was not statistically significant, based on Student's *t* test.

[c] Both values from separate S9 preparations are shown.

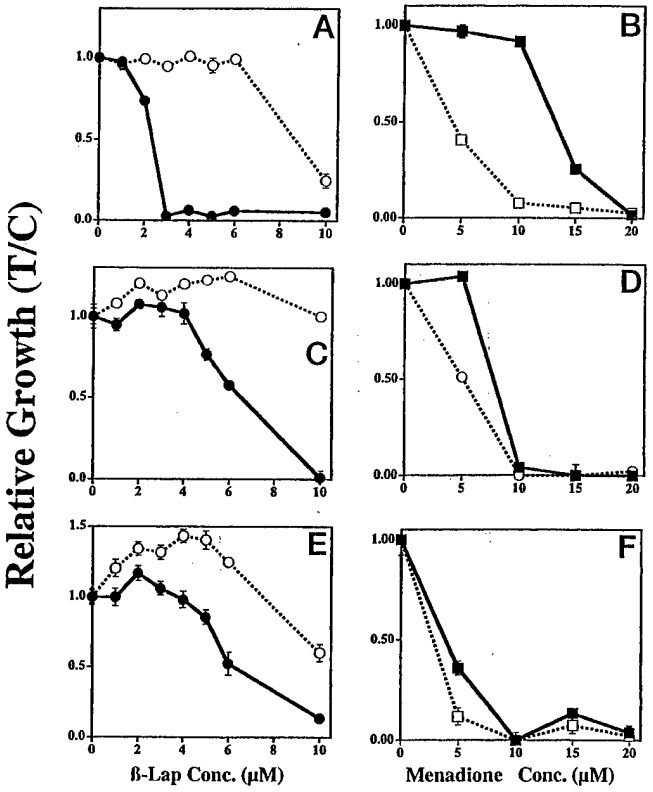

FIG. 2. **Relative growth inhibition of various breast cancer cell lines by β-lap or menadione.** Cells (MCF-7:WS8 (*A* and *B*), T47D:A18 (*C* and *D*) and MDA-MB-468 (*E* and *F*) were seeded into 96-well plates (1500 cells/well) and allowed to attach overnight. Media containing drugs (β-lap in *A*, *C*, and *E*; menadione in *B*, *D*, and *F*), either alone (β-lap (●) or menadione (■)) or in the presence of 50 μM dicoumarol (β-lap (○) or menadione (□)), were then added for 4 h. Media were then removed, fresh drug-free media were added, and the cells were allowed to grow for an additional 7 days. Relative DNA per well was then determined by Hoescht 33258 fluorescence, and relative growth (treated/control DNA) was plotted. Each point represents the mean of four independent wells ± S.E.

cancer cell lines (T47D:A18, MDA-MB-468, and MCF-7:WS8) were treated with a 4-h pulse of drugs, and relative growth was measured 7 days later (Fig. 2). Dicoumarol significantly inhibited β-lap toxicity in MCF-7:WS8 and T47D:A18 cells. In contrast, dicoumarol showed little or no protective effect in MDA-MB-468 cells (compare *graphs A, C,* and *E* in Fig. 2).

In a parallel experiment using menadione, alone or with dicoumarol, the relative sensitivities of the cell lines to menadione were opposite those found with β-lap; MCF-7:WS8 cells were the most resistant to menadione, and MDA-MB-468 cells

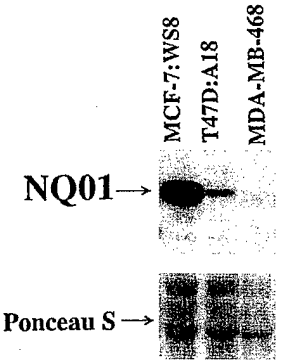

FIG. 3. **NQO1 expression in various breast cancer cell lines.** Whole cell extracts were prepared from exponentially growing cell lines. Equal protein was loaded into each lane and confirmed by Ponceau S staining. Proteins were separated by standard 10% SDS-polyacrylamide gel electrophoresis, transferred to Immobilon P, and probed with medium from an anti-NQO1 hybridoma followed by horseradish peroxidase-conjugated anti-mouse secondary antibody. Signals were visualized using Super Signal reagent as described under "Experimental Procedures." Shown is a representative blot from experiments performed at least three times.

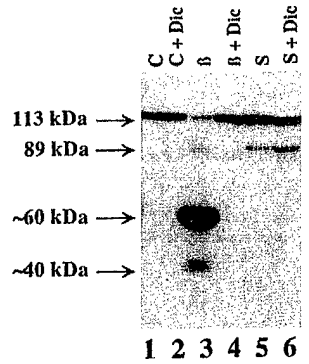

FIG. 4. **Dicoumarol inhibition of β-lap-induced atypical PARP cleavage.** MCF-7:WS8 cells were treated with a 4-h pulse of 8 μM β-lap (*β, lanes 3* and *4*) or a 24-h pulse of 1 μM staurosporine (*S, lanes 5* and *6*) either alone or with 50 μM dicoumarol during the time of drug exposure. Untreated cells (*C, lane 1*) or cells treated only with 50 μM dicoumarol (*C + Dic, lane 2*) were included as controls. Whole cell extracts were prepared at 24 h and analyzed using standard Western blot techniques as described for Fig. 3. The blot was probed with the C-2-10 anti-PARP monoclonal antibody followed by horseradish peroxidase-conjugated anti-mouse secondary antibody and visualized with Super Signal reagent. Shown is a representative blot from experiments performed at least three times.

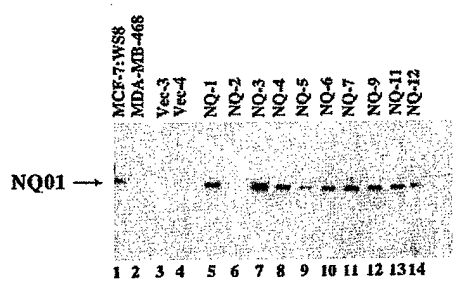

FIG. 5. **NQO1 protein expression in MDA-MB-468 transfectants.** Whole cell extracts were prepared from exponentially growing parental MCF-7:WS8 and MDA-MB-468 cells, two control vector alone MDA-MB-468 transfectants, and 10 NQO1 expression vector MDA-MB-468 transfectants. Equal amounts of protein were analyzed by standard Western blot techniques as described above using anti-NQO1 as described for Fig. 4. Shown is a representative blot from experiments performed at least three times.

were the most sensitive. Co-administration of dicoumarol caused a significant sensitization of MCF-7:WS8 cells to menadione toxicity, with a decrease in the relative IC_{50} from 12 to 3 μM. MDA-MB-468 cells, which were inherently more sensitive to menadione, were unaffected by dicoumarol co-administration. T47D:A18 cells were only minimally sensitized to menadione exposure when dicoumarol was co-administered (compare *graphs B, D,* and *F*; Fig. 2). These data were consistent with NQO1 expression (Fig. 3), where NQO1 protein levels were high in MCF-7:WS8 cells, moderate in T47D:A18 cells, and undetectable in MDA-MB-468 cells. NQO1 enzyme activities were consistent with protein levels (compare Fig. 3 and Table I). Using these cell extracts, we showed that β-lap could substitute for menadione in this *in vitro* assay, demonstrating that the compound was a suitable NQO1 substrate in intact cells (Fig. 9 and data not shown). These data demonstrated that both menadione and β-lap could serve as substrates for NQO1-mediated reduction and suggested that the end results of these reductions were opposite (*i.e.* menadione was inactivated by reduction, and β-lap was activated by reduction).

We previously showed that apoptosis in various human breast cancer cell lines induced by β-lap administration was unique, in that it caused a pattern of PARP and p53 cleavages distinct from that induced by other caspase-activating agents. After β-lap treatment, we observed a 60-kDa PARP fragment, which was probably due to the activation of a neutral, calcium-dependent protease with similar properties as calpain.[2] To investigate the effect of dicoumarol on this cleavage pattern in MCF-7:WS8 cells, we treated cells with a 4-h pulse of 8 μM β-lap alone or in the presence of 50 μM dicoumarol. Cells were lysed 20 h later, and PARP cleavage was monitored. We also investigated the effects of 1 μM staurosporine treatment, in order to determine if dicoumarol could block classic apoptotic proteolysis or if it was specific for β-lap-induced apoptosis. As seen in Fig. 4, dicoumarol completely abrogated atypical PARP cleavage after β-lap exposure but had no effect on staurosporine-induced classic PARP cleavage (*i.e.* formation of an 89-kDa PARP fragment (47)) in MCF-7:WS8 cells. The fact that dicoumarol significantly protected NQO1-expressing cells from β-lap-mediated apoptosis strongly suggested a role for NQO1 in β-lap toxicity. However, previous studies indicated that dicoumarol may also inhibit other cellular enzymes (48).

In order to definitively demonstrate the role of NQO1 in β-lap toxicity, we utilized the NQO1-negative, β-lap-resistant, MDA-MB-468 cell line to determine if exogenous expression of NQO1 could sensitize these cells to β-lap. We stably transfected MDA-MB-468 cells with a constitutive NQO1 expression vector under the control of a cytomegalovirus promoter. We also performed a parallel transfection using the empty vector, pcDNA3. Following selection of a pooled population of G418-resistant cells, we isolated a number of clones by limiting dilution subcloning, as described under "Experimental Procedures." NQO1 expression in isolated clones was then determined by Western blot analyses (Fig. 5) and enzyme assays (Table II). In all cases, enzyme activity correlated with protein expression. As shown in Fig. 5 and Table II, the empty vector-containing clones did not demonstrate measurable NQO1 expression, as observed with parental, nontransfected cells (see *lanes 2, 3,* and *4*). Of the 10 clones isolated from the NQO1 transfections, nine exhibited NQO1 expression. Clone NQ-2 (*lane 6*) showed no measurable NQO1 expression.

We tested a number of the clones for β-lap and menadione sensitivity. Growth inhibition was measured after a 4-h pulse of drugs, either alone or in the presence of 50 μM dicoumarol. Relative growth of β-lap-treated compared with control cells (*T/C*) was determined 7 days after drug exposures, using DNA

[2] J. J. Pink, S. Wuerzberger-Davis, C. Tagliarino, S. M. Planchon, X. Yang, C. J. Froelich, and D. A. Boothman (2000) *Exp. Cell Res.*, in press.

TABLE II
NQO1 expression in MDA-MB-468 transfectants

Clone	NQO1 activity[a]
	nmol/min/mg
Vec-3	<10[b]
NQ-1	6555/8264[c]
NQ-2	<10[b]
NQ-3	9276 ± 491[d]
NQ-6	14,684/18,511[c]
NQ-7	11,341/12,332[c]

[a] Units are nmol of cytochrome *c* reduced per min per mg of protein.
[b] $<10_1$, NQO1 not detected. The difference in the rate of cytochrome *c* reduction with and without dicoumarol was not statistically significant, based on Student's *t* test.
[c] Both values from two separate S9 preparations.
[d] Average for three separate S9 preparations ± S.D.

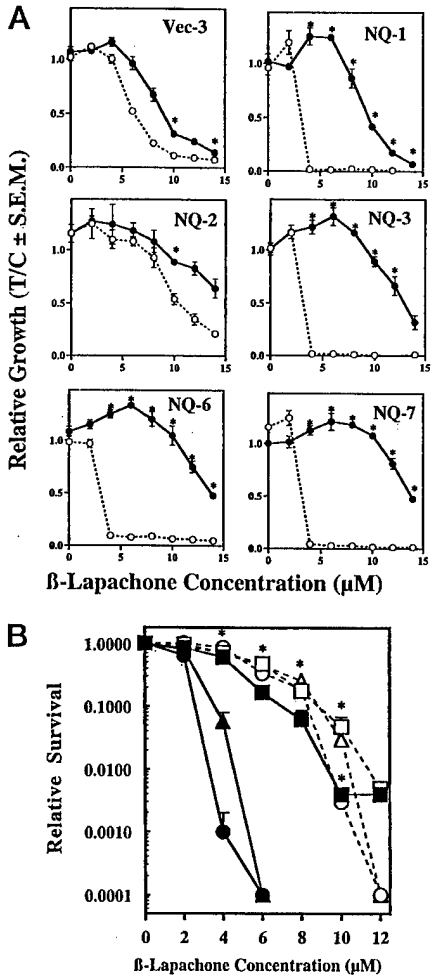

FIG. 6. **NQO1 expression sensitizes cells to acute β-lap cytotoxicity.** *A*, acute β-lap toxicity was determined using the control vector MDA-MB-468 transfectant (clone Vec-3) and five NQO1 vector-containing MDA-MB-468 transfectants, as described in Fig. 2. Note that clone NQ-2 showed no measurable NQO1 expression (Fig. 5 and Table II). Cells were exposed to a 4-h pulse of a range of β-lap doses either alone (●) or with 50 μM dicoumarol (○) and then allowed to grow for an additional 7 days, at which time DNA content for treated (*T*) cells was measured and plotted relative to control (*C*) cells. *B*, Vec-3 (■, □), NQ-1 (▲, △), and NQ-3 (●, ○) cells were treated with a 4-h pulse of a range of β-lap doses alone (■, ▲, ●) or with 50 μM dicoumarol (□, △, ○). Overall survival, as assessed by colony-forming ability, was measured after 10 days growth in control media. Shown is a representative graph from experiments performed at least three times with each group consisting of at least triplicate determinations. Differences between treatments were compared using a two-tailed Student's *t* test for paired samples and groups having $p < 0.01$ compared with β-lap or dicoumarol alone are indicated by an *asterisk*.

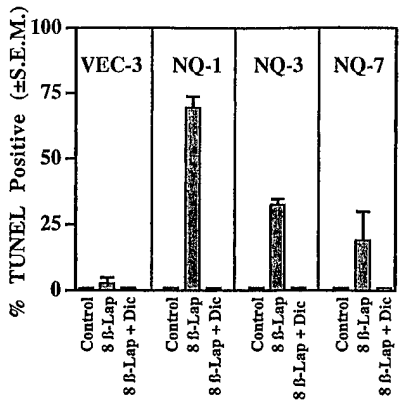

FIG. 7. **Acute β-lap-mediated apoptosis requires NQO1 activity.** DNA fragmentation was assessed using the TUNEL assay, as described under "Experimental Procedures." Cells were exposed to a 4-h pulse of β-lap alone or in combination with 50 μM dicoumarol, and TUNEL assays were performed to monitor apoptosis 44 h later using the APO-DIRECT™ kit. Data were analyzed using an EPICS Elite ESP flow cytometer. Shown are the results of one experiment representative of at least three independent assays.

amount per well as an indicator of cell growth. In all cases, expression of NQO1 led to a marked increase in sensitivity to β-lap (see Fig. 6*A*). Co-administration of 50 μM dicoumarol selectively inhibited β-lap toxicity in all clones that expressed NQO1. Dicoumarol did not affect the relatively more β-lap-resistant Vec-3 or NQ-2 clones, which did not express NQO1.

Opposite results were observed after menadione treatments. Cells expressing NQO1 were more resistant to menadione than NQO1-negative clones, and resistance could be ameliorated by dicoumarol co-administration (data not shown). To demonstrate that this effect was not due simply to transient growth inhibition, we also measured clonogenic survival of the Vec-3, NQ-3, and NQ-7 clones after a 4-h treatment with β-lap alone or in the presence of 50 μM dicoumarol (Fig. 6*B*). Relative survival closely mimicked growth inhibition, demonstrating the sensitizing effect of NQO1 expression on β-lap cytotoxicity. These data clearly established that NQO1 activity was critical for the acute toxicity of β-lap.

To confirm that cell death occurred due to the induction of apoptosis in the NQO1 transfectants, we used TUNEL assays to measure DNA fragmentation due to apoptosis after β-lap treatment. Cells were treated with a 4-h pulse of 8 μM β-lap alone or in combination with 50 μM dicoumarol, harvested 48 h later, and monitored for apoptosis using TUNEL assays, where terminal deoxynucleotide transferase-mediated FITC-dUTP incorporation was measured. As shown in Fig. 7, Vec-3 cells showed less than 2% TUNEL-positive (apoptotic) cells after β-lap treatment. All NQO1-expressing clones showed between 30 and 70% TUNEL-positive cells. Dicoumarol co-administration completely blocked apoptosis-related DNA fragmentation in all of the NQO1-expressing MDA-MB-468 clones. These findings further demonstrated that while certain aspects of β-lap cytotoxicity were unique (*e.g.* atypical PARP cleavage), other aspects conform to the classic apoptotic pathway (*e.g.* DNA fragmentation, as measured by TUNEL assays and the presence of a sub-G_0/G_1 cell population (2)).

We next utilized a number of the NQO1-expressing MDA-MB-468 clones to determine if cytotoxicity equated with corresponding increases in atypical apoptotic proteolysis, as measured by PARP and p53 cleavage. NQO1-expressing clones were exposed to 8 μM β-lap for 4 h, and cell lysates were prepared 48 h later. As observed in Fig. 8*A*, clones with NQO1 expression (*i.e.* NQ-1, NQ-3, NQ-6, and NQ-7) demonstrated a prevalent 60-kDa PARP cleavage fragment after exposure to 8 μM β-lap. The NQO1-negative clone, Vec-3, exhibited no PARP cleavage

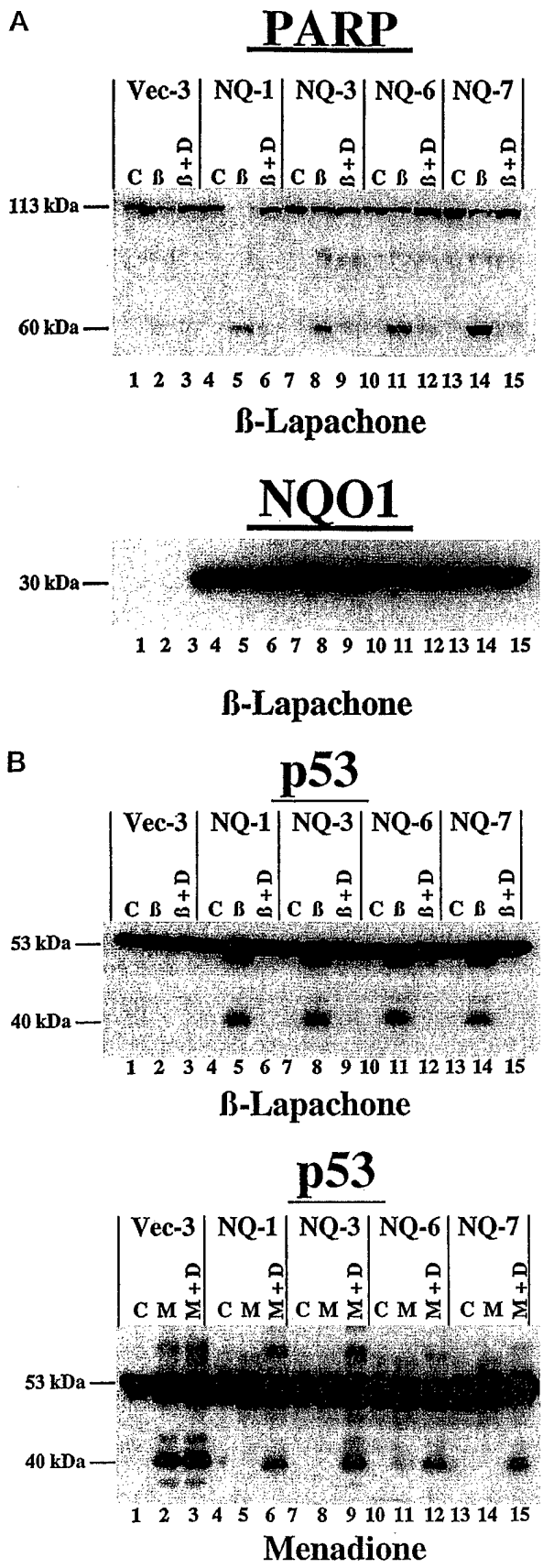

FIG. 8. **NQO1 expression sensitizes cells to β-lap-mediated apoptotic proteolysis and inhibits menadione-mediated apoptotic proteolysis.** Apoptotic proteolysis was measured in cells exposed to a 4-h pulse of 8 μM β-lap alone (*β*) or 8 μM menadione alone (*M*) or in combination with 50 μM dicoumarol (*β* + *D* and *M* + *D*, respectively). Whole cell extracts were prepared 44 h after drug treatment and analyzed using standard Western blot techniques. *A*, PARP cleavage was assessed using the C-2-10 monoclonal antibody, the blots were then stripped and reprobed with the anti-NQO1 antibody. *B*, cells were treated with either β-lap or menadione for 4 h and then probed with a p53 antibody (DO-1). Equal protein loading was assessed by Ponceau S staining as described under "Experimental Procedures." Shown is a representative blot from experiments performed at least three times.

at this β-lap dose. We noted cleavage of p53 (resulting in an ~40-kDa fragment) at the same β-lap dose that gave rise to the 60-kDa PARP fragment. Cells exposed to 10 μM menadione with or without dicoumarol showed an opposite pattern, as monitored by p53 and PARP cleavage (Fig. 8*B* and data not shown). Dicoumarol enhanced p53 cleavage after menadione exposure. Importantly, NQO1 expression also led to resistance to menadione-induced p53 cleavage, which could be reversed by co-administration of dicoumarol. Previous studies from our laboratory suggested that both the PARP and p53 cleavage events were the result of activation of the calcium-dependent protease, calpain.[2]

To further characterize the nature by which β-lap could serve as a substrate for NQO1, we measured NADH oxidation using a modified *in vitro* assay. Using purified recombinant human NQO1 or cell extracts containing NQO1, we measured the oxidation of NADH in the presence of either menadione or β-lap. This assay was different from that used to measure NQO1 activity in cell lysates (described in Tables I and II), in that a terminal electron acceptor (*i.e.* cytochrome *c*) was not included in the reaction. If the substrates (menadione or β-lap) were utilized once in the enzyme reaction, the compounds could not reduce a terminal electron acceptor and would thereby presumably accumulate in their respective hydroquinone forms. This would result in oxidation of 1 mol of NADH/mol of quinone reduced. As expected, menadione reduction resulted in the oxidation of 1–3 mol of NADH/mol of menadione in 2 min and 3–4 mol of NADH/mol of menadione in 3 min using S9 extracts from MCF-7:WS8 or NQ-3 cells (Fig. 9 and data not shown). β-lap resulted in the oxidation of 10–20 mol of NADH/mol of β-lap in 2 min and 50–60 mol of NADH/mol of β-lap in 3 min (Fig. 9). The relative NADH oxidation with β-lap may be an underestimate of β-lap-mediated NADH oxidation, due to exhaustion of reduced NADH at later time points. Using purified NQO1, this effect was even more pronounced, giving rise to oxidation of 10 mol of NADH/mol of β-lap in 10 s and 100 mol of NADH/mol of β-lap in 10 min (data not shown). These results strongly suggest that the hydroquinone form of β-lap is unstable and rapidly undergoes autoxidation to the parent quinone, which can again serve as substrate for reduction by NQO1.

DISCUSSION

We demonstrated that β-lap cytotoxicity is dependent upon the expression of the obligate two-electron reductase, NQO1. Dicoumarol, an NQO1 inhibitor, significantly protected NQO1-expressing breast cancer cell lines against all tested aspects of β-lap toxicity, including cell death. Overall, NQO1 expression correlated well with sensitivity of various breast cancer cell lines to the effects of β-lap. Use of the redox cycling compound menadione, which is detoxified by NQO1, demonstrated that the protection offered by dicoumarol is not the result of a global apoptotic inhibition, since dicoumarol significantly enhanced the cytotoxicity of menadione, in cells that expressed NQO1 (Fig. 2). Dicoumarol also did not protect against staurosporine-induced apoptosis, instead demonstrating a very modest enhancement of PARP cleavage. The nature of this response is unknown but may involve signaling through the MEKK1 pathway, as recently described by Cross *et al.* (49). In addition, the relative sensitivities of the cell lines to menadione were oppo-

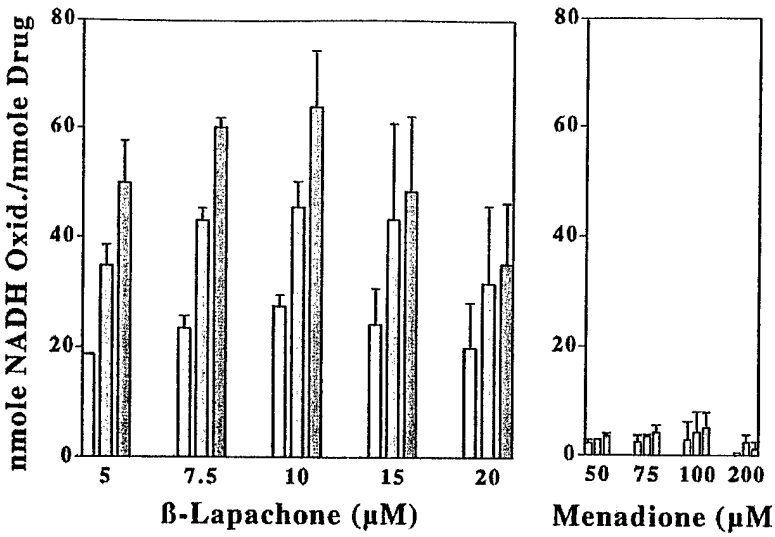

FIG. 9. **β-lap-mediated NADH oxidation and futile cycling by NQO1-containing cell extracts.** S9 extracts prepared from MCF-7:WS8 cells served as a source for NQO1 and were mixed with 500 μM NADH in 50 mM Tris-HCl, pH 7.5, as described under "Experimental Procedures." Reactions were initiated by adding β-lap or menadione, and changes in absorbance at 340 nm (NADH absorbs at 340; NAD+ does not) were measured over time for 3 min. Total loss of NADH was then calculated and divided by the concentration of β-lap or menadione used. This ratio was then plotted as a function of β-lap or menadione concentration after 1 (*light bars*), 2 (*darker bars*), and 3 (*darkest bars*) min. Shown is a representative graph from experiments repeated at least two times.

site those of β-lap, demonstrating that the β-lap-sensitive cells were not merely sensitive to unrelated cytotoxic compounds. Exogenous expression of NQO1, in NQO1-deficient MDA-MB-468 cells, shifted the LD_{99} from >10 μM to less than 4 μM. While this shift may appear modest, the dose-response curves for both growth inhibition and survival after β-lap treatment were extremely steep. At 4 μM β-lap, 60% of the NQO1-negative cells survived, whereas less than 0.05% survival was noted in cells transfected with NQO1. A similarly steep curve was noted with growth inhibition, where treatment with 4 μM β-lap led to greater than 90% growth in the NQO1-negative cells and undetectable growth in the NQO1-expressing cells. In both survival and growth measurements, addition of 50 μM dicoumarol protected NQO1-expressing cells completely and resulted in values nearly equal to that observed in untreated cells. While these findings suggest that β-lap should show considerable activity against NQO1 expressing tumors, the dose-response curves indicate that the overall drug exposure will undoubtedly need to be closely monitored if this drug is to prove clinically useful.

β-lap may be activated by NQO1 in a manner analogous to that of MMC or EO9 (50, 51). However, unlike MMC (52), there is no indication of direct DNA damage by β-lap as assessed by p53 induction, alkaline or neutral filter elution, or covalent complex protein-DNA formation (2, 53, 54). Most specific demonstrations of β-lap activity have come from *in vitro* assays. For example, topoisomerase IIα-mediated DNA damage has been observed *in vitro* after treatment with either β-lap or menadione (10). However, the expected downstream effects of this damage (*e.g.* p53 induction, DNA-topoisomerase IIα complexes, etc.) have not been observed (1, 2). In addition, we previously showed that topoisomerase I could be inhibited or activated *in vitro* in a manner distinct from that of the classic topoisomerase I inhibitor, camptothecin (1). Neither "cleavable complex" formation (8) nor increases in the steady state levels of wild-type p53 were observed following β-lap treatment. In contrast, camptothecin or topoisomerase IIα inhibitors caused a dramatic increase in p53, as previously reported (1, 55). The observations reported here suggest that β-lap must either be activated (reduced) to inhibit topoisomerases I or IIα or that topoisomerase inhibition is not a necessary component of β-lap-mediated cytotoxicity.

One particularly unique aspect of β-lap toxicity is the apparent activation of a novel protease, which we first discerned by observation of an atypical cleavage pattern of the DNA repair protein and apoptotic substrate, PARP.[2] This pattern (giving rise to an ~60-kDa fragment instead of the classic 89-kDa fragment) was unique to β-lap-mediated apoptosis and correlated well with lethality. In addition, investigation of p53 proteolysis after β-lap treatment showed a fragment of ~40 kDa (Fig. 7*B*), which was similar to that previously attributed to calpain activation (56). Calpain has been implicated in apoptosis in a number of systems (57–59), and we hypothesize that calpain is the primary protease activated in β-lap-mediated cell death.[2] The data regarding the role of calpain as an inducer of apoptosis or simply a component of the execution phase of apoptosis appear to depend upon the cell type and method of apoptosis induction. The demonstration of menadione-induced p53 cleavage (Fig. 8) suggests that this proteolytic pathway is not unique to β-lap. Enhancement of menadione-mediated proteolysis by dicoumarol suggests that the hydroquinone form of menadione is a nontoxic species or is rapidly conjugated and excreted from the cell and does not activate this cell death pathway (60). However, when menadione is reduced to the semiquinone, in the absence of NQO1 activity, it can also undergo a futile cycle, leading to the loss of reduced NAD(P)H (61). This futile cycle is less potent than the β-lap futile cycling but can be activated by high concentrations of menadione in NQO1 expressing cells and lower menadione concentrations in cells lacking NQO1 activity.

While reduction of β-lap appears to be important for its cytotoxic effects against breast cancer cells, the mechanism by which reduction of β-lap leads to toxicity is still unresolved. Our findings regarding the futile cycling of β-lap suggest a possible component of the cytotoxic mechanism. β-lap-mediated exhaustion of NADH in the *in vitro* studies (Fig. 8) suggests that the hydroquinone form of β-lap is unstable and autoxidizes back to the parent compound. In an intact cell, this futile cycle would be expected to continue until one of the critical components of the reaction is exhausted (Fig. 10). Since NQO1 can utilize either NADH or NADPH as electron donors, this futile cycle could lead to a substantial loss of NADH and NADPH with a concomitant rise in NAD+ and NADP+ levels. This would have a dramatic effect on any cellular process

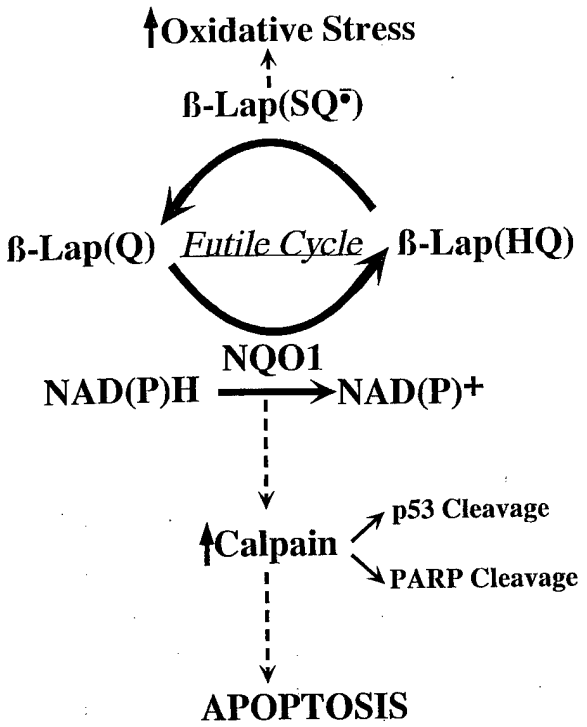

FIG. 10. **Proposed model for β-lapachone-mediated cytotoxicity in cells expressing NQO1.** In cells that express NQO1, the 1,2-naphthoquinone β-lap(Q) is reduced to the hydroquinone form (β-lap(HQ)) using one molecule of NADH per reaction. The hydroquinone form of β-lap is presumably unstable and spontaneously autoxidizes to its original parent form, probably through a semiquinone intermediate (β-lap (SQ^-), which can cause redox cycling and oxidative stress. The regenerated parent compound can then serve as substrate for another round of reduction. This futile cycle causes a rapid and severe loss in reduced NAD(P)H, which ultimately activates calpain by mechanisms that are not completely understood at present.

requiring NADH or NADPH. It is likely that this exhaustion of reduced enzyme co-factors may be a critical factor for the activation of the apoptotic pathway after β-lap treatment. The downstream consequences of this futile cycle are currently under investigation in our laboratory.

At higher doses of β-lap (>10 μM), NQO1-negative cells and NQO1-expressing cells treated with dicoumarol were killed by β-lap. This may be due to the production of oxidative stress, as a result of one electron reduction of β-lap by other enzymes, such as cytochrome b_5 reductase and/or cytochrome P-450 reductase (62). One electron reduction of β-lap to the semiquinone would be expected to cause extensive redox cycling with the formation of various reactive oxygen species, and previous studies showed that β-lap caused oxygen radical formation in trypanosomes (63, 64). We speculate that β-lap-mediated free radical formation can be lethal to NQO1-deficient cells, as we previously reported with HL60 cells. The result in these studies was stimulation of a caspase-mediated death pathway (1). This hypothesis is supported by a recent study that showed that β-lap can induce apoptosis in HL-60 cells through peroxide production (65). Alternatively, other members of the NQO1 family that are insensitive to dicoumarol, such as NQO2 (66, 67), may be present and reduce (*i.e.* activate) β-lap when administered at high doses. However, we hypothesize that the production of cytosolic free radicals is not a primary mode of cell death in NQO1-expressing cells, since free radical scavengers (*e.g.* α-tocopherol, *N*-acetyl-L-cysteine, or pyrrolidinedithiocarbamate) did not significantly affect lethality caused by β-lap exposure (data not shown). The free radical-driven pathways may predominate in NQO1-negative cells or in cells with inactivated NQO1. We propose that when active NQO1 is present, the pathway described in Fig. 10 is primarily responsible for cell death.

Our data identifying the intracellular target of β-lap as NQO1 may explain the myriad of *in vitro* and *in vivo* responses reported for this compound. β-lap exposure synergizes with MMS, ionizing radiation, and ultraviolet light irradiation damage (68). We speculate that the synergy between this compound and these DNA damaging agents is related to the induction of NQO1 (cloned as xip-3, an x-ray-inducible protein by our laboratory (18) and that of Fornace *et al.* (69)). This is further supported by the fact that only posttreatments of 4–5 h, and not pretreatments, with β-lap caused synergistic cell killing. Induction of β-lap's target may have been required for synergy, and the induction kinetics of NQO1/XIP3 after ultraviolet light or ionizing radiation exposures (*i.e.* ~2 h) appear to fit this mechanism (18). β-lap exposure also prevented the formation of ionizing radiation-inducible secondary neoplastic transformants in Chinese hamster embryo fibroblasts (53). Since NQO1 expression is thought to increase during early stages of neoplastic initiation (possibly due to the permanent induction of a normal stress response, *i.e.* induction of NQO1) (70, 71), it is possible that β-lap administration selectively eliminates genetically damaged cells that constitutively overexpress this preneoplasic marker (*i.e.* NQO1). These data suggest that it may be possible to exploit this IR-inducible NQO1 target protein for improved radiochemotherapy, which would also result in a significantly lower level of IR-induced secondary carcinogenesis, as previously reported (53).

Thus, our data strongly suggest that NQO1 expression is an important determinant of β-lap-mediated apoptosis and lethality. The connection between the futile cycle of oxidation and reduction of β-lap by NQO1 and the activation of calpain-mediated apoptosis (Fig. 10) is currently under investigation in our laboratory. Investigation of this drug should shed light on calpain-mediated cell death processes and yield clinical regimens using β-lap or more efficient drugs in combination with DNA-damaging agents (*e.g.* radiotherapy). Use of this drug against tumors that overexpress NQO1, such as breast, colon, or lung cancers, is indicated. Identification of NQO1 as the intracellular target of β-lap also suggests the use of this compound for chemoprevention, since NQO1 is commonly elevated during neoplastic progression (43).

Acknowledgments—We thank Dr. Dan Gustafson and Dr. Charles Waldren for the NQO1 cDNA expression vector. We also thank Dr. Jill Kolesar and Peter Allen for helpful discussions and Dr. David Ross for critical reading of the manuscript.

REFERENCES

1. Planchon, S. M., Wuerzberger, S., Frydman, B., Witiak, D. T., Hutson, P., Church, D. R., Wilding, G., and Boothman, D. A. (1995) *Cancer Res.* **55,** 3706–3711
2. Wuerzberger, S. M., Pink, J. J., Planchon, S. M., Byers, K. L., Bornmann, W. G., and Boothman, D. A. (1998) *Cancer Res.* **58,** 1876–1885
3. Li, C. J., Averboukh, L., and Pardee, A. B. (1993) *J. Biol. Chem.* **268,** 22463–22468
4. Boothman, D. A., Greer, S., and Pardee, A. B. (1987) *Cancer Res.* **47,** 5361–5366
5. Schuerch, A. R., and Wehrli, W. (1978) *Eur. J. Biochem.* **84,** 197–205
6. Docampo, R., Cruz, F. S., Boveris, A., Muniz, R. P., and Esquivel, D. M. (1979) *Biochem. Pharmacol.* **28,** 723–728
7. Boorstein, R. J., and Pardee, A. B. (1983) *Biochem. Biophys. Res. Commun.* **117,** 30–36
8. Boothman, D. A., Trask, D. K., and Pardee, A. B. (1989) *Cancer Res.* **49,** 605–612
9. Molina Portela, M. P., and Stoppani, A. O. (1996) *Biochem. Pharmacol.* **51,** 275–283
10. Frydman, B., Marton, L. J., Sun, J. S., Neder, K., Witiak, D. T., Liu, A. A., Wang, H. M., Mao, Y., Wu, H. Y., Sanders, M. M., and Liu, L. F. (1997) *Cancer Res.* **57,** 620–627
11. Vanni, A., Fiore, M., De Salvia, R., Cundari, E., Ricordy, R., Ceccarelli, R., and Degrassi, F. (1998) *Mutat. Res.* **401,** 55–63
12. Manna, S. K., Gad, Y. P., Mukhopadhyay, A., and Aggarwal, B. B. (1999)

Biochem. Pharmacol. **57,** 763–774
13. Robertson, N., Haigh, A., Adams, G. E., and Stratford, I. J. (1994) *Eur. J. Cancer* **30A,** 1013–1019
14. Cadenas, E. (1995) *Biochem. Pharmacol.* **49,** 127–140
15. Ross, D., Beall, H., Traver, R. D., Siegel, D., Phillips, R. M., and Gibson, N. W. (1994) *Oncol. Res.* **6,** 493–500
16. Rauth, A. M., Goldberg, Z., and Misra, V. (1997) *Oncol. Res.* **9,** 339–349
17. Ross, D., Siegel, D., Beall, H., Prakash, A. S., Mulcahy, R. T., and Gibson, N. W. (1993) *Cancer Metastasis Rev.* **12,** 83–101
18. Boothman, D. A., Meyers, M., Fukunaga, N., and Lee, S. W. (1993) *Proc. Natl. Acad. Sci. U. S. A.* **90,** 7200–7204
19. Chen, S., Knox, R., Lewis, A. D., Friedlos, F., Workman, P., Deng, P. S., Fung, M., Ebenstein, D., Wu, K., and Tsai, T. M. (1995) *Mol. Pharmacol.* **47,** 934–939
20. Jaiswal, A. K., McBride, O. W., Adesnik, M., and Nebert, D. W. (1988) *J. Biol. Chem.* **263,** 13572–13578
21. Radjendirane, V., Joseph, P., Lee, Y. H., Kimura, S., Klein-Szanto, A. J. P., Gonzalez, F. J., and Jaiswal, A. K. (1998) *J. Biol. Chem.* **273,** 7382–7389
22. Marin, A., Lopez de Cerain, A., Hamilton, E., Lewis, A. D., Martinez-Penuela, J. M., Idoate, M. A., and Bello, J. (1997) *Br. J. Cancer* **76,** 923–929
23. Malkinson, A. M., Siegel, D., Forrest, G. L., Gazdar, A. F., Oie, H. K., Chan, D. C., Bunn, P. A., Mabry, M., Dykes, D. J., Harrison, S. D., and Ross, D. (1992) *Cancer Res.* **52,** 4752–4757
24. Belinsky, M., and Jaiswal, A. K. (1993) *Cancer Metastasis Rev.* **12,** 103–117
25. Joseph, P., Xie, T., Xu, Y., and Jaiswal, A. K. (1994) *Oncol. Res.* **6,** 525–532
26. Buettner, G. R. (1993) *Arch. Biochem. Biophys.* **300,** 535–543
27. Ross, D., Thor, H., Orrenius, S., and Moldeus, P. (1985) *Chem. Biol. Interact.* **55,** 177–184
28. Riley, R. J., and Workman, P. (1992) *Biochem. Pharmacol.* **43,** 1657–1669
29. Siegel, D., Beall, H., Senekowitsch, C., Kasai, M., Arai, H., Gibson, N. W., and Ross, D. (1992) *Biochemistry* **31,** 7879–7885
30. Prakash, A. S., Beall, H., Ross, D., and Gibson, N. W. (1993) *Biochemistry* **32,** 5518–5525
31. Fitzsimmons, S. A., Workman, P., Grever, M., Paull, K., Camalier, R., and Lewis, A. D. (1996) *J. Natl. Cancer Inst.* **88,** 259–269
32. Beall, H. D., Murphy, A. M., Siegel, D., Hargreaves, R. H., Butler, J., and Ross, D. (1995) *Mol. Pharmacol.* **48,** 499–504
33. Hollander, P. M., and Ernster, L. (1975) *Arch. Biochem. Biophys.* **169,** 560–567
34. Hosoda, S., Nakamura, W., and Hayashi, K. (1974) *J. Biol. Chem.* **249,** 6416–6423
35. Duthie, S. J., and Grant, M. H. (1989) *Br. J. Cancer* **60,** 566–571
36. Akman, S. A., Doroshow, J. H., Dietrich, M. F., Chlebowski, R. T., and Block, J. S. (1987) *J. Pharmacol. Exp. Ther.* **240,** 486–491
37. Thor, H., Smith, M. T., Hartzell, P., Bellomo, G., Jewell, S. A., and Orrenius, S. (1982) *J. Biol. Chem.* **257,** 12419–12425
38. Siegel, D., McGuinness, S. M., Winski, S. L., and Ross, D. (1999) *Pharmacogenetics* **9,** 113–121
39. Gustafson, D. L., Beall, H. D., Bolton, E. M., Ross, D., and Waldren, C. A. (1996) *Mol. Pharmacol.* **50,** 728–735
40. Sambrook, J., Fritsch, E. F., and Maniatis, T. (1989) *Molecular Cloning: A Laboratory Manual,* pp. 16.33–16.36, Cold Spring Harbor Laboratory, Cold Spring Harbor, NY
41. Pink, J. J., Bilimoria, M. M., Assikis, J., and Jordan, V. C. (1996) *Br. J. Cancer* **74,** 1227–1236
42. Labarca, C., and Paigen, K. (1980) *Anal. Biochem.* **102,** 344–352
43. Siegel, D., Franklin, W. A., and Ross, D. (1998) *Clin. Cancer Res.* **4,** 2065–2070
44. Hollander, P. M., Bartfai, T., and Gatt, S. (1975) *Arch. Biochem. Biophys.* **169,** 568–576
45. Strobel, H. W., and Dignam, J. D. (1978) *Methods Enzymol.* **52,** 89–96
46. Beall, H. D., Mulcahy, R. T., Siegel, D., Traver, R. D., Gibson, N. W., and Ross, D. (1994) *Cancer Res.* **54,** 3196–3201
47. Kaufmann, S. H., Desnoyers, S., Ottaviano, Y., Davidson, N. E., and Poirier, G. G. (1993) *Cancer Res.* **53,** 3976–3985
48. Preusch, P. C., Siegel, D., Gibson, N. W., and Ross, D. (1991) *Free Radical Biol. Med.* **11,** 77–80
49. Cross, J. V., Deak, J. C., Rich, E. A., Qian, Y., Lewis, M., Parrott, L. A., Mochida, K., Gustafson, D., Vande Pol, S., and Templeton, D. J. (1999) *J. Biol. Chem.* **274,** 31150–31154
50. Siegel, D., Gibson, N. W., Preusch, P. C., and Ross, D. (1990) *Cancer Res.* **50,** 7483–7489
51. Keyes, S. R., Fracasso, P. M., Heimbrook, D. C., Rockwell, S., Sligar, S. G., and Sartorelli, A. C. (1984) *Cancer Res.* **44,** 5638–5643
52. Hess, R., Plaumann, B., Lutum, A. S., Haessler, C., Heinz, B., Fritsche, M., and Brandner, G. (1994) *Toxicol. Lett.* **72,** 43–52
53. Boothman, D. A., and Pardee, A. B. (1989) *Proc. Natl. Acad. Sci. U. S. A.* **86,** 4963–4967
54. Boothman, D. A., Wang, M., Schea, R. A., Burrows, H. L., Strickfaden, S., and Owens, J. K. (1992) *Int. J. Radiat. Oncol. Biol. Phys.* **24,** 939–948
55. Nelson, W. G., and Kastan, M. B. (1994) *Mol. Cell. Biol.* **14,** 1815–1823
56. Kubbutat, M. H., and Vousden, K. H. (1997) *Mol. Cell. Biol.* **17,** 460–468
57. Squier, M. K., and Cohen, J. J. (1997) *J. Immunol.* **158,** 3690–3697
58. Wood, D. E., and Newcomb, E. W. (1999) *J. Biol. Chem.* **274,** 8309–8315
59. Squier, M. K., Sehnert, A. J., Sellins, K. S., Malkinson, A. M., Takano, E., and Cohen, J. J. (1999) *J. Cell. Physiol.* **178,** 311–319
60. Wefers, H., and Sies, H. (1983) *Arch. Biochem. Biophys.* **224,** 568–578
61. Bellomo, G., Jewell, S. A., and Orrenius, S. (1982) *J. Biol. Chem.* **257,** 11558–11562
62. Iyanagi, T. (1990) *Free Radical Res. Commun.* **8,** 259–268
63. Molina Portela, M. P., Fernandez Villamil, S. H., Perissinotti, L. J., and Stoppani, A. O. (1996) *Biochem. Pharmacol.* **52,** 1875–1882
64. Docampo, R., Cruz, F. S., Boveris, A., Muniz, R. P., and Esquivel, D. M. (1978) *Arch. Biochem. Biophys.* **186,** 292–297
65. Chau, Y. P., Shiah, S. G., Don, M. J., and Kuo, M. L. (1998) *Free Radical Biol. Med.* **24,** 660–670
66. Zhao, Q., Yang, X. L., Holtzclaw, W. D., and Talalay, P. (1997) *Proc. Natl. Acad. Sci. U. S. A.* **94,** 1669–1674
67. Jaiswal, A. K. (1994) *J. Biol. Chem.* **269,** 14502–14508
68. Boorstein, R. J., and Pardee, A. B. (1984) *Biochem. Biophys. Res. Commun.* **118,** 828–834
69. Fornace, A. J., Jr., Alamo, I., Jr., and Hollander, M. C. (1988) *Proc. Natl. Acad. Sci. U. S. A.* **85,** 8800–8804
70. Williams, J. B., Wang, R., Lu, A. Y., and Pickett, C. B. (1984) *Arch. Biochem. Biophys.* **232,** 408–413
71. Farber, E. (1984) *Can. J. Biochem. Cell Biol.* **62,** 486–494

Experimental Cell Research 255, 144–155 (2000)
doi:10.1006/excr.1999.4790, available online at http://www.idealibrary.com on IDEAL®

Activation of a Cysteine Protease in MCF-7 and T47D Breast Cancer Cells during β-Lapachone-Mediated Apoptosis

John J. Pink,* Shelly Wuerzberger-Davis,*,[1] Colleen Tagliarino,* Sarah M. Planchon,* XiaoHe Yang,† Christopher J. Froelich,† and David A. Boothman*,[2]

*Laboratory of Molecular Stress Responses, Department of Radiation Oncology, Case Western Reserve University, Cleveland, Ohio 44106; and †Evanston Northwestern Healthcare Research Institute, Evanston, Illinois 60201

β-Lapachone (β-lap) effectively killed MCF-7 and T47D cell lines via apoptosis in a cell-cycle-independent manner. However, the mechanism by which this compound activated downstream proteolytic execution processes were studied. At low concentrations, β-lap activated the caspase-mediated pathway, similar to the topoisomerase I poison, topotecan; apoptotic reactions caused by both agents at these doses were inhibited by zVAD-fmk. However at higher doses of β-lap, a novel non-caspase-mediated "atypical" cleavage of PARP (i.e., an ~60-kDa cleavage fragment) was observed. Atypical PARP cleavage directly correlated with apoptosis in MCF-7 cells and was inhibited by the global cysteine protease inhibitors iodoacetamide and *N*-ethylmaleimide. This cleavage was insensitive to inhibitors of caspases, granzyme B, cathepsins B and L, trypsin, and chymotrypsin-like proteases. The protease responsible appears to be calcium-dependent and the concomitant cleavage of PARP and p53 was consistent with a β-lap-mediated activation of calpain. β-Lap exposure also stimulated the cleavage of lamin B, a putative caspase 6 substrate. Reexpression of procaspase-3 into caspase-3-null MCF-7 cells did not affect this atypical PARP proteolytic pathway. These findings demonstrate that β-lap kills cells through the cell-cycle-independent activation of a noncaspase proteolytic pathway. © 2000 Academic Press

Key Words: **apoptosis; β-lapachone; caspase; breast cancer; poly(ADP)-ribose polymerase; PARP; calpain; topotecan.**

INTRODUCTION

The execution phase of apoptosis culminates in the activation of a cascade of specific cysteine proteases which cleave following aspartate residues in target proteins. These proteases, named caspases [1], comprise a family of zymogens that are converted to activated proteases by specific cleavage reactions. Substrate cleavage products include the 89-kDa fragment of poly(ADP-ribose) polymerase (PARP), the 46-kDa polypeptide of lamin B, the ~100-kDa C-terminally or ~68-kDa internally cleaved polypeptides of retinoblastoma protein (pRb), and the ~68-kDa fragment derived from Sp1 [2–5]. The cleavage sites within some apoptotic death substrates have been precisely mapped and used to design inhibitors of the caspases, such as zVAD-fmk and DEVD-fmk, which were developed using the recognition sites for caspases-1 and -3, respectively [6]. In contrast, the global cysteine protease inhibitors iodoacetamide and *N*-ethylmaleimide react directly with active site cysteines and thereby inhibit all cysteine proteases, as well as other enzymes that contain accessible –SH groups [7, 8].

While a great deal of information regarding the action of caspases during apoptosis has been generated, less is known about alternate apoptotic proteolytic pathways that are activated after treatment with various cytotoxic agents. A number of reports have shown that the neutral calcium-dependent protease calpain can be activated during apoptosis [9–11]; a key *in vivo* target of calpain appears to be p53. Other reports have demonstrated the activation of noncaspase proteases, such as the nuclear scaffold protease [12, 13] and unknown serine proteases during apoptosis [14, 15]. The serine protease(s) described in these studies appeared to be distinct from granzyme B, which induces apoptosis through caspase activation [16].

β-Lapachone (β-lap) is a naturally occurring 1,2-naphthoquinone initially isolated from the bark of the lapacho tree, native to South America. We previously demonstrated that this drug is a radiosensitizing agent against human laryngeal carcinoma and melanoma cell lines [17]. Using cell-free assays, β-lap inhibited topoisomerase I (Topo I) by a mechanism quite different from that of camptothecin (CPT) or the related compounds topotecan (TPT), 9-aminocamptothecin, or

[1] Current address: Department of Human Oncology, University of Wisconsin Comprehensive Cancer Center, Madison, WI 53792.
[2] To whom reprint requests should be directed at the Department of Radiation Oncology, Laboratory of Molecular Stress Responses, BRB-3 East, Case Western Reserve University School of Medicine, 10900 Euclid Avenue, Cleveland, OH 44106-4942. Fax: (216) 368-1142. E-mail: dab30@po.cwru.edu.

0014-4827/00 $35.00

irinotecan [18]. For example, β-lap administration did not stabilize Topo I–DNA cleavable complexes *in vivo* [19] or *in vitro* [20]. In contrast, the CPT family members stabilized cleavable complexes [19], resulting in the formation of DNA single-strand nicks [21] and induction of wild-type p53 [22]. The fact that β-lap did not produce DNA single-strand nicks in human or hamster cancer cells [21, 23] was indirectly confirmed by the absence of wild-type p53 induction in breast or prostate cancer cells [18, 24]. While *in vitro* assays indirectly suggested that Topo I may be an intracellular target of β-lap, it seemed likely that it was not the only mechanism through which this compound acted [24, 25]. We recently reported that the cytotoxicity caused by β-lap in MCF-7 breast cancer cells could be solely accounted for by apoptotic responses [24].

Recent results have suggested that β-lap can lead to Topo IIα-mediated DNA breaks [25]. In contrast to Topo I, topoisomerase IIα causes ATP-dependent, double-strand DNA unwinding [26]. Topo IIα also shares another important distinction from Topo I, in its cell cycle regulation. Topo I is consistently expressed throughout the cell cycle while Topo IIα is poorly expressed during G_0/G_1 and expression increases during S phase, reaching a peak during late S and G_2 [27]. Drugs which primarily target Topo IIα are, therefore, cell cycle specific [28], while Topo I-specific drugs can kill cells in all phases of the cell cycle [29]. Variation in sensitivity to either β-lap or TPT during different cell-cycle stages was measured to address the relative importance of Topo I and Topo IIα activity for the cytotoxicity of these drugs.

Interestingly, β-lap-mediated apoptosis in MCF-7 cells was accompanied by a dramatic decrease in p53 steady-state levels, prior to the appearance of apoptotic morphologic changes [24]. We were, therefore, interested to see if this relationship between loss of survival and apoptosis held true for other breast cancer cells. We describe the activation of a noncaspase, cysteine protease, which shares some characteristics with the neutral calcium-dependent protease, calpain, during β-lap-mediated apoptosis. β-Lap-mediated cell death and proteolysis are induced in all phases of the cell cycle, suggesting that topoisomerase IIα was not the critical target for this death pathway.

MATERIALS AND METHODS

Chemicals and tissue culture reagents. Estradiol (E_2), 4-hydroxytamoxifen (4-OHT) (Sigma Chemical Co., St. Louis, MO), or ICI 182,780 (a generous gift from Dr. V. Craig Jordan, Northwestern University) were dissolved in 100% ethanol as 1000× stocks and maintained at −20°C. β-Lap (MW 242, $\epsilon = 25790$), generously supplied by Dr. William G. Bornmann (Memorial Sloan Kettering, New York, NY), and TPT (Smith Kline Beecham, Philadelphia, PA) were dissolved in DMSO and concentrations confirmed by spectrophotometric analyses [24, 30]. Nocodazole was purchased from Sigma Chemical Co., and a 2 mg/ml stock solution was made in DMSO immediately before use. All tissue culture reagents were purchased from GIBCO Laboratories (Grand Island, NY), unless otherwise stated. Charcoal-stripped serum was prepared by treating fetal bovine serum (FBS) three times with dextran-coated charcoal as described [31].

TABLE 1

Characteristics of Breast Cancer Cell Lines

Cell line	ER	p53	pRb
MCF-7:WS8	++++	WT	+
T47D:A18	++	Mutant	+

Antibodies and protease inhibitors. The C-2-10 PARP monoclonal antibody was purchased from Enzyme Systems Products (Dublin, CA). An N-terminal PARP (clone N-20), an Sp1 polyclonal, a p53 monoclonal (clone DO-1), and all horseradish peroxidase-conjugated secondary antibodies were obtained from Santa Cruz Biotechnologies (Santa Cruz, CA). Monoclonal antibodies to pRb (clone G3-245) and underphosphorylated pRb (clone G99-549) were obtained from PharMingen (San Diego, CA). A polyclonal antibody specific to phosphorylated serine 780 of the pRb protein was obtained from Medical and Biological Laboratories Co. Ltd. (Boston, MA). Antibody to caspase-3 was obtained from Transduction Laboratories (Lexington, KY). Antibody to lamin B was obtained from Matritech, Inc. (Cambridge, MA). zVAD-fmk, DEVD-fmk, zFA-fmk, and zAAD-fmk were obtained from Enzyme Systems Products (Dublin, CA), diluted in DMSO, and used at 25 μM unless otherwise stated. TPCK, TLCK, iodoacetamide, and *N*-ethylmaleimide were purchased from Sigma Chemical Co. and diluted in DMSO (TPCK and TLCK), ethanol (*N*-ethylmaleimide), or water (iodoacetamide). The pBabe/puro vector was a generous gift from Dr. Todd Sladek.

Tissue culture and growth conditions. MCF-7:WS8, T47D:A18 (clones of the standard MCF-7 and T47D cell lines, selected by limiting dilution cloning of the parental cell lines in whole serum [31–33], referred to as MCF-7 and T47D in the text) were obtained from Dr. V. Craig Jordan (Northwestern University, Chicago, IL). The ER, p53, and pRb statuses of these cell lines are outlined in Table 1. Cells were grown in RPMI 1640 medium supplemented with 10% FBS, 6 ng/ml bovine insulin, 2 mM L-glutamine, 100 U/ml penicillin, and 100 mg/ml streptomycin. For estrogen-free tissue culture medium, phenol red-free RPMI and charcoal-stripped FBS were used as previously described [31]. Cells were routinely passed at 1:5 to 1:20 dilutions once per week using 0.1% trypsin. All cells were mycoplasma free and grown at 37°C in a humidified incubator with 5% CO_2–95% air atmosphere.

Growth assays and estrogen-deprivation studies. Forty-eight-hour or 6-day growth assays were used to assess the relative sensitivities of breast cancer cells to various drug treatments as previously described [31–33]. For estrogen-deprivation studies, cells were grown in estrogen-free medium for at least 4 days prior to the start of experiments. Cells were seeded into 96-well plates (1.5×10^3 or 1×10^4 cells/well) in 0.2 ml of medium on day 0 and allowed to attach for 24 h. On day 1, fresh medium containing the indicated drug(s) was added to the appropriate wells. E_2, 4-OHT, or ICI 182,780 (ICI) were added to cells at 1:1000 dilutions from appropriate stock solutions. Estrogen-deprivation significantly retarded cell growth and dramatically increased the proportion of MCF-7 and T47D cells in G_1. For MCF-7, 83% G_1 cells were observed after 6 days of growth in estrogen-free medium compared to 53% in log-phase cultures. Changes in cell number, measured as DNA content, were then determined in untreated or drug-treated cells by an adaptation of the method of Labarca and Paigen [34] and analyzed using a Molecular Dynamics Biolumin 960 plate reader with an excitation wavelength of 360 and emission wavelength of 450 nm. Data were expressed as relative growth (*T/C*) by dividing the DNA content of treated cells

(*T*) by that of untreated cells (*C*) at identical times. Data points represent the means ± SEM of at least four replicate wells. All experiments were performed at least three times.

Western immunoblot analyses. Whole-cell extracts were prepared by direct lysis of PBS-washed cells (both floating and attached cells were pooled) in PARP extraction buffer [6 M urea, 2% SDS, 10% glycerol, 62.5 mM Tris–HCl (pH 6.8), 5% β-mercaptoethanol, and 5 mg/ml bromphenol blue]. Samples were then sonicated with a 15-s burst using a Fisher 550 sonic dismembrator. Equal amounts of protein were heated at 65°C for 10 min and separated by 10% SDS–PAGE. Separated proteins were transferred to Immobilon-P (Millipore Corp., Bedford, MA) membranes using a Multiphor II semidry electroblotting device (Pharmacia Biotech Inc., Piscataway, NJ) according to the manufacturer's instructions. Loading equivalence and transfer efficiency were monitored by Ponceau S staining of transferred membranes. Standard Western immunoblotting techniques were used to probe for various steady-state protein levels as indicated and previously described [18, 24]. Proteins of interest were visualized with ECL using the Super Signal chemiluminescence reagent (Pierce Chemical Co., Rockford, IL) at 20°C for 5 min. Membranes were exposed to X-ray film and developed. Gels shown represent results of experiments repeated at least three times.

Flow cytometry. Flow cytometric analyses of breast cancer cell lines before and after β-lap or TPT treatments were performed as previously described [18, 24]. TUNEL assays were performed using the APO-DIRECT kit (Phoenix Flow Systems, Inc., San Diego, CA). The samples were read in a EPICS Elite ESP flow cytometer using an air-cooled argon laser at 488 nm, 15 mW (Beckman Coulter Electronics, Miami, FL). Propidium iodide was read at 640 nm using a long-pass optical filter and FITC was read at 525 nm using a band-pass filter. Analyses were performed using the Elite acquisition software provided with the instrument.

Retroviral-mediated stable expression of caspase 3 in MCF-7 cells. The pBabe/puro/cpp32 plasmid was constructed by treating the *Bam*HI/*Pst*I cpp32 cDNA insert from the pBS/cpp32 plasmid (a generous gift from Dr. Vishva Dixit, Genentech, Inc.) with T4 DNA polymerase and then subcloning into the blunt-ended pBabe/puro vector.

MCF-7 cells (3×10^5 cells/plate) were seeded and allowed to grow overnight. The pBabe/puro retroviral vector (a generous gift from Dr. T. Sladek, Chicago Medical School) (2 μg/plate) encoding cpp32 (caspase-3) cDNA or empty vector was mixed with 10 μl of LipofectAMINE (Life Technologies, Gaithersburg, MD) and transfected into cells according to the manufacturer's instructions. After transfection (24 h), cells were split, diluted, and inoculated into 96-well plates. Transfected cells were selected with 2 μg/ml puromycin. Individual clones were screened by immunoblot analysis of caspase-3 expression and positive clones (5 of 12) were pooled for further characterization. A single caspase-3-expressing clone was selected for investigation.

RESULTS

Relative drug sensitivities. Log-phase MCF-7 and T47D breast cancer cells were exposed to a range of β-lap or TPT doses for 48 h and cell numbers were compared (using DNA content measurements) to untreated, log-phase growing control cells as described under Materials and Methods (Fig. 1). At higher doses, MCF-7 cells were more sensitive to β-lap (IC_{75} = 3.5 μM) than were T47D cells (IC_{75} = 7.0 μM); however, the IC_{50} dose was very similar in both cell lines. In contrast, T47D cells were more sensitive to TPT at all doses tested, with IC_{50} and IC_{75} values of 20 and 500

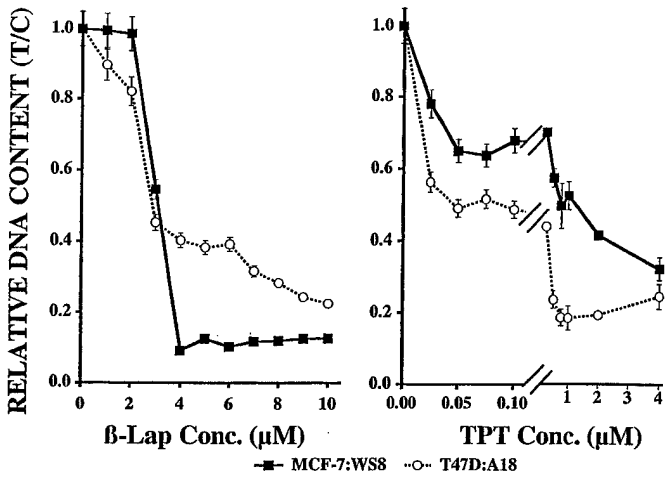

FIG. 1. Sensitivities of breast cancer cells to β-lap or TPT. Cells were seeded into 96-well tissue culture plates (1.5×10^3 cells/well) and allowed to attach overnight. Drugs were then added and cells were allowed to grow for an additional 48 h, as described under Materials and Methods. Cell number was assessed using Hoechst 33258 fluorescence, and relative growth inhibition (Relative DNA Content T/C) was calculated. Shown are toxicities for MCF-7 (■) and T47D (○) cell lines exposed to various concentrations of β-lap or TPT. Data shown are representative of at least two experiments expressed as means ± SEM of at least four replicate wells.

nM, respectively, compared with MCF-7 cells IC_{50} and IC_{75} values of 350 nM and 4.0 μM, respectively. Differences in relative sensitivities to TPT compared to β-lap suggested a disparate mechanism(s) of growth inhibition or cell death (possibly due to apoptosis).

Cell cycle-independent cytotoxicity. Since Topo I poisons are thought to kill cycling, but not arrested, cells (presumably due to DNA synthesis past Topo I–DNA "cleavable complexes"), we assessed the influence of cell cycle progression on β-lap compared to TPT cytotoxicity using DNA content assays. In addition, these studies would address the relative role of topoisomerase IIα inhibition in β-lap-mediated cytotoxicity, due to the cell-cycle-dependent expression of this protein. These studies utilized the estrogen-dependent MCF-7 and T47D breast cancer cell lines, since their growth in estrogen-deprived, phenol red-free culture medium has been well defined [33]. Cells were deprived of estrogen for 6 days, which caused a significant G_1 delay at a predetermined point in the cell cycle [33, 35, 36], prior to addition of either β-lap or TPT. Cells were then exposed to various concentrations of β-lap or TPT in estrogen-deprived (control) medium, control medium containing E_2 (10 nM), or medium containing whole serum alone or in the presence of inhibitory concentrations of the anti-estrogens 4-OHT or ICI for 48 h (Fig. 2). Both cell lines were stimulated to enter the cell cycle and begin log-phase growth after addition of medium containing 17β-estradiol or whole serum. Addition of anti-estrogens specifically inhibited

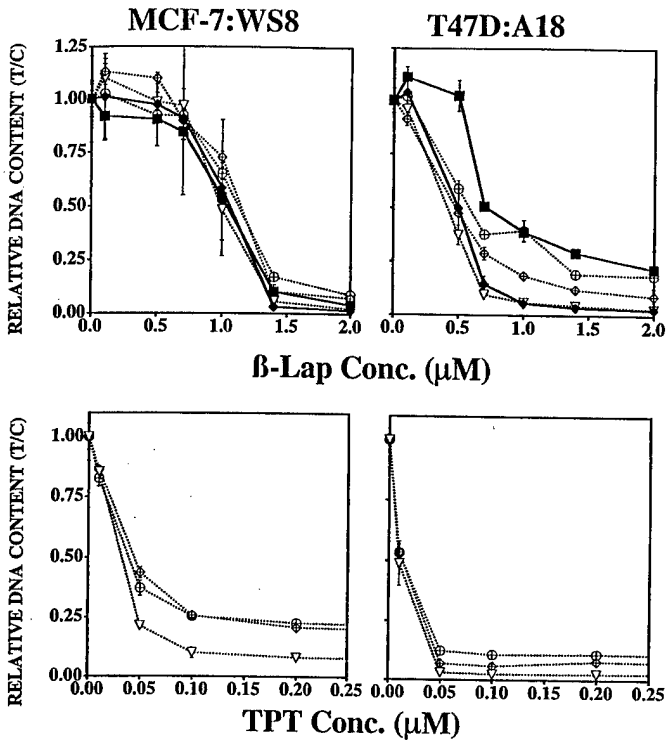

FIG. 2. β-Lap- or TPT-mediated cytotoxicity of G_1-arrested cells. MCF-7 and T47D estrogen-dependent cell lines were grown for 6 days in estrogen-depleted, phenol red-free medium and exposed to varying concentrations of β-lap or TPT for 6 days, as indicated. Drugs were included in RPMI 1640 medium containing estrogen-deprived calf serum (control, ■), estrogen-replenished, stripped calf serum (10 nM E_2, ◆), whole serum alone (▽), or whole serum treated with the anti-estrogens 4-hydroxytamoxifen (100 nM, ◇) or ICI 182,780 (100 nM, ○). Cell number was then assessed after 6 days using DNA content as in Fig. 1. Relative cell growth of treatment was determined using the DNA content of cells grown in comparable medium without β-lap or TPT. Data shown are representative of at least two experiments expressed as means ± SEM of at least four replicate wells.

estrogen-mediated cell growth. Estrogen deprivation and/or anti-estrogen administration led to a cytostatic growth inhibition of 75–85% compared with cells grown in medium containing E_2 or whole serum (data not shown and [32, 37]). Additional β-lap or TPT treatments led to a complete loss of cells, demonstrating a similar cytotoxic response in both log-phase ($+E_2$) and arrested ($-E_2$ or plus antiestrogens) cells (Fig. 2).

Apoptotic protease activation after β-lap or TPT treatment. To investigate caspase activation in MCF-7 and T47D breast cancer cells following TPT or β-lap exposures, we examined PARP cleavage using Western immunoblot analyses as described under Materials and Methods. Cells were treated continuously with 5 to 10 μM β-lap and PARP cleavage was assessed 48 h later. Treatment with 5 μM β-lap induced classic PARP cleavage, resulting in the appearance of an 89-kDa fragment in both cell lines (Fig. 3). In MCF-7 cells, a cross-reacting protein of ~80 kDa (indicated by an asterisk in Figs. 3, 4, and 5) was present even in untreated cells. The identity of this protein is unknown; however, it does appear to be degraded during apoptosis.

At higher doses of β-lap we observed an atypical ~60-kDa PARP fragment. This atypical cleavage of PARP was most apparent in MCF-7 cells (Fig. 3, lanes 4–6), which were more sensitive to β-lap (Figs. 1 and 2). In general, PARP cleavage reflected the relative sensitivity of each cell line to β-lap, by which MCF-7 cells demonstrated primarily the atypical cleavage pattern and T47D predominantly showed typical caspase-mediated PARP cleavage at lower doses and atypical PARP cleavage following treatment with 10 μM β-lap (see lane 12, Fig. 3). A minor PARP cleavage fragment of ~40 kDa was also observed in MCF-7 cells, which display maximal amounts of the 60-kDa PARP fragment (Fig. 3). It is currently unclear whether this is a unique fragment or the result of further cleavage of the original 60-kDa fragment. Interestingly, the apparent amount of the 60-kDa fragment was much greater than that of full-length PARP protein. Loading equivalence, as assessed by Ponceau S staining, showed that all lanes contained equal amounts of protein. This apparent incongruity may be the result of either more efficient extraction of the fragment from the nuclear matrix or increased accessibility of the epitope to the antibody, after β-lap-induced cleavage (Fig. 3).

MCF-7 and T47D cells were treated with a range of TPT doses (10 nM to 10 μM) for 48 h. We coadministered 25 μM zVAD-fmk, a caspase inhibitor, to deter-

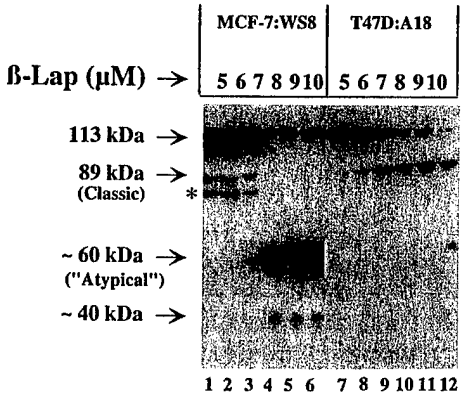

FIG. 3. Atypical and classic PARP cleavage in breast cancer cells following β-lap exposure. Breast cancer cell lines were treated with β-lap (5–10 μM) for 48 h and whole-cell lysates prepared at various times posttreatment from pooled (attached and floating) cells and assessed for cleavage of PARP using standard Western immunoblot procedures and the C-2-10 monoclonal PARP antibody, described under Materials and Methods. An unknown ~80-kDa cross-reacting protein was present in MCF-7 lysates as indicated by an asterisk. The Western blot shown is representative of at least three separate experiments.

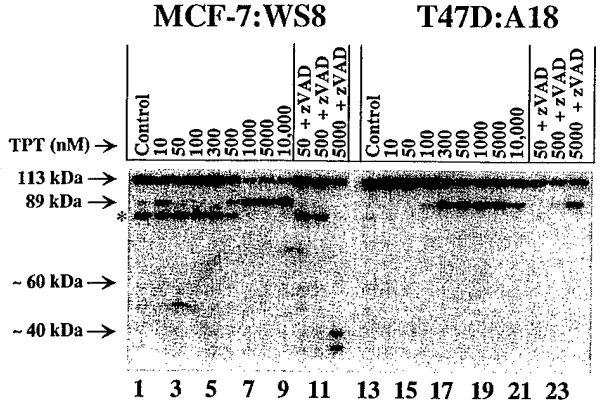

FIG. 4. Caspase-mediated, classical PARP cleavage in breast cancer cells following TPT treatment. Log-phase MCF-7 and T47D cells were treated with 10 nM to 10 μM TPT for 48 h. Three doses of TPT (50, 500, and 5000 nM, lanes 10–12 and 22–24, top and bottom) also included the caspase inhibitor zVAD-fmk (25 μM). An unknown ~80-kDa cross-reacting protein is present in MCF-7 lysates as indicated by an asterisk. Cells were then harvested and analyzed by Western immunoblotting using the C-2-10 monoclonal PARP antibody as described for Fig. 3.

mine if PARP cleavage was caused by caspase activation after three doses of TPT (50, 500, and 5000 nM) (Fig. 4). As observed following β-lap exposures, the relative sensitivity of MCF-7 and T47D cells to the growth inhibitory effects of TPT was reflected to some degree in PARP cleavage (Fig. 4). However, the doses of TPT required to elicit PARP cleavage *in vivo* were significantly above the apparent IC_{50} values for each cell line (see Fig. 1); this was not the case for cells exposed to β-lap. These data are consistent with previous data demonstrating that β-lap is a much more effective inducer of apoptosis than CPT or its derivatives [20]. Coadministration of zVAD-fmk inhibited TPT-mediated PARP cleavage in both MCF-7 (lanes 10–12) and T47D cells (lanes 22 and 23 with 50 and 500 nM, but not 5000 nM, TPT). These data suggested that TPT exposure led to the activation of the classic caspase pathway. Importantly, no dose of TPT gave rise to the atypical PARP cleavage fragment, even when 10 μM TPT was used (lanes 9 and 21, Fig. 4).

Evidence for two apoptotic proteolytic pathways activated by β-lap. In order to determine whether atypical PARP cleavage observed after β-lap treatment was the result of an activated caspase family member, or another class of cysteine proteases, cells were exposed for 48 h to 8 μM β-lap in the presence of a battery of known protease inhibitors (Fig. 5). Included were general chemical inhibitors and more specific cleavage site inhibitors [38]. Exposure of MCF-7 cells to 8 μM β-lap caused apoptotic responses (measured by PARP, pRb, and Sp1 cleavage) that were insensitive to any of the inhibitors, simultaneously administered at previously determined efficacious doses [38]. The modest level of 89-kDa PARP cleavage fragment observed in untreated MCF-7 cells was due to slight overgrowth of control cells, which activated a basal level of apoptosis and classic PARP cleavage. This basal, caspase-mediated PARP cleavage was completely inhibited by zVAD-fmk in both cell lines (compare the minor 89-kDa PARP cleavage fragment in lane 1 to the absence of this fragment in lane 2 for MCF-7 in Fig. 5).

As shown in Fig. 3, T47D cells exposed to 8 μM β-lap for 48 h showed classic PARP cleavage. As expected, this apoptotic cleavage reaction was completely blocked by coadministration of zVAD-fmk at 25 μM. β-Lap-treated T47D cells also showed cleavage of Sp1, giving rise to the previously described 68-kDa fragment [2]. In addition, T47D cells treated with β-lap showed a loss of phosphorylated pRb and appearance of an ~100-kDa cleavage fragment, previously described by Janicke *et al.* [4] (compare lanes 13 and 19, Fig. 5). All cleavage reactions observed in T47D cells after β-lap treatment were completely prevented by 25 μM zVAD-fmk. However, accumulation of hypophosphory-

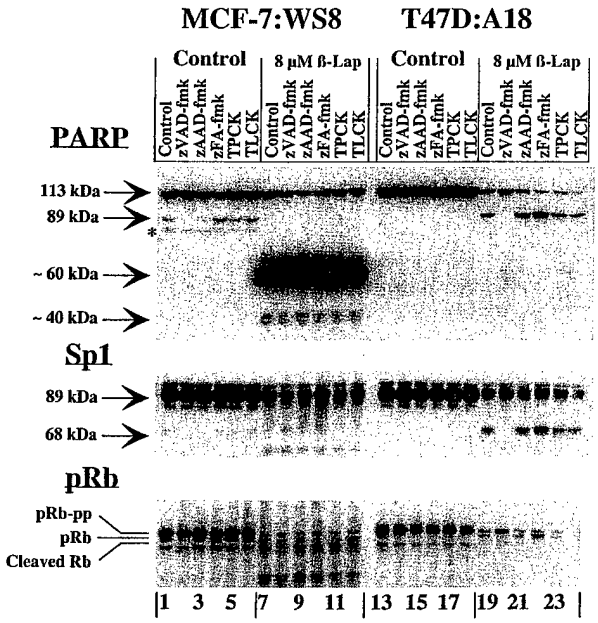

FIG. 5. Effect of global or specific cleavage site protease inhibitors on β-lap-mediated atypical PARP cleavage. Log-phase MCF-7 and T47D cells were grown for 48 h in RPMI medium alone or in medium containing 8 μM β-lap. Protease inhibitors were coadministered with β-lap. The protease inhibitors used were 25 μM zVAD-fmk (a caspase family inhibitor), 25 μM zAAD-fmk (an inhibitor of granzyme B), 25 μM zFA-fmk (an inhibitor of cathepsins B and L), 1.0 μM TPCK (a trypsin inhibitor), or 10 μM TLCK (a chymotrypsin inhibitor). Control cells received RPMI medium alone (lanes 1 and 13) or RPMI medium containing 8 μM β-lap (lanes 7 and 19). Whole-cell extracts were then analyzed by Western immunoblotting as described under Materials and Methods for PARP cleavage, pRb dephosphorylation and cleavage, and cleavage of the Sp1 transcription factor by repeated probing of the same blots. The Western blot shown is representative of at least three separate experiments.

lated pRb in T47D cells following β-lap treatment was unaffected by the administration of 25 μM zVAD (lanes 19 to 20, Fig. 5). These data are consistent with the activation of a caspase-mediated apoptotic pathway in T47D cells after β-lap treatment, which may be downstream of changes in pRb phosphorylation state.

MCF-7 cells, which showed only atypical PARP cleavage after 8 μM β-lap exposure, also demonstrated an overall decline in Sp1 steady-state levels. However, apoptotic cleavage fragments (as observed in T47D cells) were not observed after extended exposures of the Western blots in Fig. 5 (not shown). MCF-7 cells treated with β-lap showed an overall loss of pRb, with the presence of a modest amount of a 60-kDa pRb fragment (visible after extended exposure, data not shown), similar to that described by An and Dou [5]. pRb cleavage in MCF-7 cells caused by β-lap exposure was not affected by coadministered protease inhibitors (Fig. 5, lanes 8–12).

To confirm that β-lap cytotoxicity was primarily mediated by the induction of apoptosis and not necrosis, we utilized the TUNEL assay, which measures DNA breaks created by apoptotic endonucleases [39]. MCF-7 cells were exposed to a 4-h pulse of 8 μM β-lap and analyzed for terminal deoxynucleotide transferase-mediated incorporation of FITC-labeled dUTP, 20 h later. Greater than 90% of the β-lap-treated MCF-7 cells were TUNEL positive (Fig. 6). This finding, in addition to the dramatic nuclear condensation reported previously [24], confirms that cytotoxicity caused by β-lap is primarily apoptotic and not due to necrosis.

The global cysteine protease inhibitors iodoacetamide and *N*-ethylmaleimide [7, 40, 41] were used to determine if a cysteine protease was responsible for the formation of atypical PARP cleavage fragments in MCF-7 cells (Figs. 3 and 5). MCF-7 cells were treated with 5 μM β-lap in medium with or without 10 mM iodoacetamide or 10 mM *N*-ethylmaleimide (data not shown). Cleavage of PARP was prevented by both inhibitors, but was not inhibited by the caspase inhibitors zVAD-fmk or DEVD-fmk (Fig. 5 and data not shown), suggesting that a noncaspase, cysteine protease was primarily responsible for the atypical PARP cleavage observed after β-lap treatment. Administration of *N*-ethylmaleimide caused a mobility shift of the full-length PARP band, possibly due to methylation of cysteine and methionine groups in the protein [40]. Neither iodoacetamide nor *N*-ethylmaleimide prevented β-lap-mediated apoptosis in MCF-7 cells.

Simultaneous cleavage of PARP and p53. The inhibition of PARP cleavage by cysteine-alkylating agents suggested that a noncaspase cysteine protease may be responsible for the atypical PARP cleavage observed in cells after treatment with β-lap. One protease which may fit these data would be the neutral calcium-dependent protease calpain [9]. Calpain has a wide substrate specificity and has been shown to specifically cleave p53 during apoptosis [42, 43]. We treated MCF-7 cells with a 4-h pulse of 5 μM β-lap and isolated whole-cell extracts at various times, up to 28 h after drug exposure. Extracts were probed for PARP and subsequently stripped and reprobed for p53 steady-state expression (Fig. 7A). As expected, PARP cleavage was observed by 8 h after drug administration. Importantly, cleavage of p53, giving rise to an ~40-kDa fragment, accompanied this PARP cleavage. The p53 cleavage pattern resembled that observed by Pariat *et al.* [43] and Kubbutat *et al.* [42], which was the result of calpain activation.

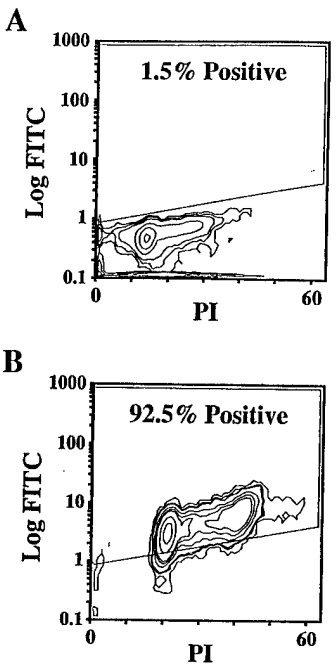

FIG. 6. β-Lapachone induced DNA fragmentation. MCF-7 cells were treated with 8 μM β-lap for 4 h and harvested 20 h later. Cells were analyzed for DNA fragmentation using the TUNEL assay. Cells which have significant DNA fragmentation incorporate FITC–dUTP and are shown above the line in both graphs. Shown are representative examples of experiments repeated at least three times.

Since calpain activity is dependent upon changes in Ca^{+2} homeostasis, we utilized the calcium chelators EDTA and EGTA to determine if removal of extracellular calcium influenced the appearance of atypical PARP cleavage in MCF-7 cells after β-lap treatment. MCF-7 cells were pretreated with 0.25, 1.0, or 3.0 mM EGTA or EDTA in complete medium for 30 min. After treatment, medium containing 5 μM β-lap or DMSO (control medium), including the corresponding concentration of EDTA or EGTA used in the pretreatment, was added for an additional 4 h. All cells were then treated with medium alone containing EGTA or EDTA for an additional 20 h. Whole-cell extracts were then prepared and analyzed for PARP and p53 cleavage

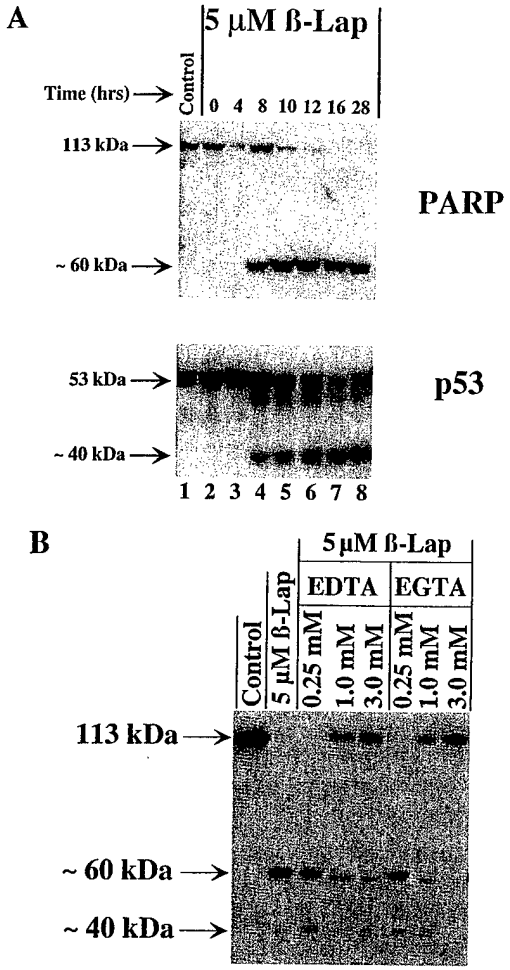

FIG. 7. Implication of calpain in atypical PARP cleavage. (A) MCF-7 cells were treated with 5 μM β-lap for 4 h and whole-cell extracts were prepared 20 h later. Western blots were probed with anti-PARP antibody, then stripped and reprobed with anti-p53 antibody. (B) MCF-7 cells were pretreated for 30 min with the designated concentrations of EDTA or EGTA in complete medium. Medium containing 5 μM β-lap was then added for 4 h in the continued presence of EDTA or EGTA. After β-lap exposure cells were treated with medium containing only the designated concentrations of EDTA or EGTA for an additional 20 h. Whole-cell extracts were prepared and probed for PARP as described above. The blots shown are representative of at least two independent experiments.

fragments. Both EDTA and EGTA showed a dose-dependent inhibition of β-lap-mediated atypical PARP cleavage and p53 cleavage in MCF-7 cells (Fig. 7B and data not shown). These data suggest that extracellular calcium is a necessary component for β-lap-mediated atypical PARP and p53 cleavage, an attribute consistent with activation of a calcium-dependent, noncaspase cysteine protease, such as calpain.

Loss of hypophosphorylated pRb and apoptosis induced by β-lap is independent of cell cycle status. To investigate the effects of cell cycle position on β-lap-induced accumulation of hypophosphorylated pRb and apoptosis, estrogen-dependent MCF-7 cells were cultured in estrogen-free medium for 6 days as described under Materials and Methods. To ensure a complete estrogen block, the pure anti-estrogen ICI 182,780 (1 nM) [44, 45] was added to cells growing in estrogen-free medium 2 days prior to the beginning of each experiment. Increases in G_1 cells (up to 85%) were noted, as described [46]. Arrested cells were compared to MCF-7 cells that were subsequently restimulated to enter the cell cycle by addition of 10 nM E_2 at the time of β-lap or TPT exposure (i.e., a 4-h pulse of either 8 μM β-lap or 5 μM TPT). Drugs were administered as short pulse treatments in order to determine if the rapid accumulation of hypophosphorylated pRb could be reversed after removal of β-lap or TPT. When used, ICI or E_2 was maintained in the medium.

MCF-7 cells treated with β-lap showed a dramatic loss of phosphorylated pRb within 6 h (compare lanes 3 and 4, Fig. 8), followed by general loss of the protein by 18 h after treatment (see lanes 10 and 13, Fig. 8); these data are consistent with earlier findings [24]. A similar loss of phosphorylated pRb was noted in MCF-7 cells after 5 μM TPT; however, significant accumulation of hypophosphorylated pRb was not observed until 12 h after treatment (not shown), and complete loss was not noted until more than 18 h posttreatment (Fig. 8 and data not shown). In control cells, stimulation of arrested cells with estradiol led to an increase in the relative level of hyperphosphorylated pRb (by 6 to 18 h) compared to estrogen-deprived and/or ICI-treated cells (compare hypophosphorylated retinoblastoma protein (pRb) to hyperphosphorylated retinoblastoma protein (pRb-pp) levels in lanes 6, 9, and 12 to lane 3, Fig. 8). The change in phosphorylation status of pRb was accompanied by a dramatic increase in the proportion of cells in S phase by 18 h after E_2 stimulation (43% S phase with E_2, 10% S phase without E_2, compare lanes 12 and 9, Fig. 8). In both the E_2- and the ICI-treated groups, β-lap exposure led to a complete loss of hyperphosphorylated pRb followed by an overall loss of all forms of pRb. Since estrogen-deprivation can cause an arrest in the cell cycle ~6 h from the restriction point in MCF-7 cells [47–49], possibly past the first cyclin D1–cdk2-dependent phosphorylation of pRb, the levels of hyperphosphorylated pRb in estrogen-deprived, anti-estrogen-treated MCF-7 cells were rather high (Fig. 8). In MCF-7 cells treated with either β-lap or TPT, PARP cleavage (atypical for β-lap, classic for TPT) was not apparent until 12–18 h after treatment (Fig. 8 for 18 h, and data not shown). Addition of E_2, or maintenance of MCF-7 cells in estrogen-deprived medium (including ICI), had no effect on the appearance of PARP cleavage (see lanes 10 and 13, Fig. 8).

We performed a similar series of experiments using nocodazole to arrest cells during M phase. All MCF-7 groups examined showed a similar pattern of PARP

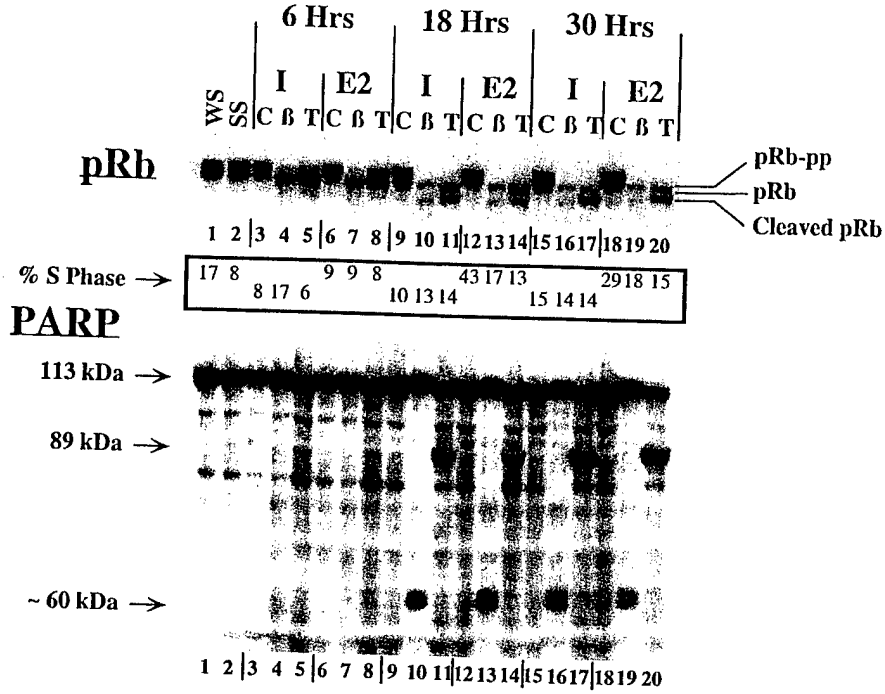

FIG. 8. Effect of β-lap or TPT on logarithmically growing or anti-estrogen-arrested MCF-7 cells. MCF-7 cells were estrogen-deprived for 6 days prior to seeding in estrogen-deprived medium containing 10 nM ICI 182,780 to ensure complete blockage of estrogen-stimulated growth. Cells were then treated with no drug (C), 5 μM β-lap (β), or 5 μM TPT (T), in estrogen-free RPMI media supplemented with either 100 nM ICI (I) or 10 nM E_2 (E_2). Whole-cell extracts were prepared at 6 and 18 h after treatment and changes in cell cycle distribution were monitored by flow cytometry, as described under Materials and Methods. For Western analyses, immunoblots were first probed with the C-2-10 anti-PARP monoclonal antibody, then stripped and reprobed with an anti-pRb monoclonal antibody which detected all forms of pRb. For controls, log-phase MCF-7 cells were grown continuously in medium containing whole serum (WS) or in medium containing estrogen-deprived serum (SS, for stripped serum) as described under Materials and Methods. Shown are three separate forms of the pRb protein: (a) pRb-pp, hyperphosphorylated pRb; (b) pRb, hypophosphorylated (nonphosphorylated) pRb; and (c) the cleaved form of pRb, in which 4 kDa of the C-terminus has been removed (Cleaved pRb). PARP protein forms included (a) the full-length PARP polypeptide of 113 kDa, (b) a caspase-mediated 89-kDa PARP fragment, and (c) an ~60-kDa atypical PARP cleavage polypeptide, which sometimes appears as a doublet at ~60 kDa. The Western blot shown is representative of at least three separate experiments.

cleavage after β-lap treatment (data not shown), supporting a cell-cycle-independent activation of apoptosis.

We [16], as well as others [50], showed that MCF-7 cells were devoid of caspase-3, due to a deletion in exon 3. To determine whether caspase-3 deficiency was responsible for atypical PARP cleavage, we isolated an MCF-7 clone that stably expressed full-length proform caspase-3 (Casp 3) (see Materials and Methods). A puromycin-resistant clone expressing empty vector (pBabe) was also analyzed. PARP, lamin B, and caspase-3 expression was monitored before or 24 h after β-lap treatment (2–10 μM). Cells were treated for 4 h with 2–10 μM β-lap and harvested 20 h later. As expected, Casp 3 cells expressed the 32-kDa proform of caspase-3, unlike MCF-7 cells transfected with the vector alone (Fig. 9, compare lanes 1 and 7). Atypical PARP cleavage was noted following β-lap treatment at similar levels in both transfected cell lines. Classic lamin B cleavage, presumably the result of caspase-6 activation [51, 52], was also observed. These data suggest that expression of caspase-3 had no effect on apoptotic cleavage events in MCF-7 cells following various doses of β-lap. Interestingly, loss of procaspase-3 protein, in Casp 3 cells, mirrored cleavage of both PARP and lamin B. Importantly, the active p12 and p20 fragments of caspase-3 were not observed due to the lower affinity of this antibody to the processed forms of caspase-3. In contrast to β-lap treatments, Casp 3 cells showed an increased rate of apoptosis after exposure to TNF-α or granzyme B compared to MCF-7 cells transfected with pBabe/puro alone [16].

DISCUSSION

We previously showed that β-lap killed a variety of cells by apoptosis. However, the mechanisms of specific proteolytic execution cascades that were activated by this compound remained unexplored. β-Lap induced apoptosis independent of p53 status and cell cycle distribution [18, 24]. In MCF-7 cells, the lethal effects of β-lap were accounted for solely by apoptosis. In this

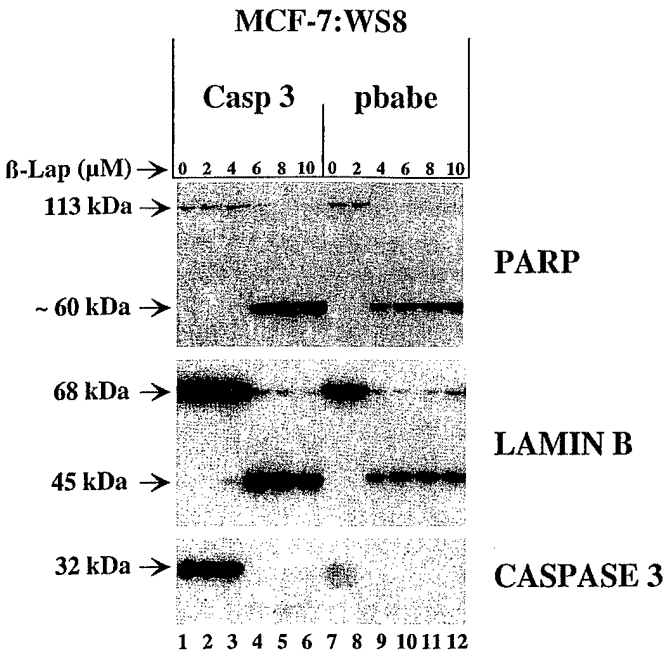

FIG. 9. Effect of caspase-3 expression on β-lap-mediated proteolysis. Caspase-3-negative MCF-7 cells were infected with a retroviral construct expressing full-length procaspase-3 (Casp 3) or vector alone (pbabe). Caspase 3 (full length is 32 kDa) expression is shown at the bottom. Cells were then treated with the designated concentrations of β-lap for 4 h, fresh medium was added, and whole-cell extracts were prepared 20 h later. Western immunoblots were then probed with the C-2-10 anti-PARP antibody, stripped, and reprobed with lamin B and later with caspase-3 antibodies. The Western blot shown is representative of at least three separate experiments.

study, we expanded our investigations to include the T47D cell line which has significant phenotypic and genotypic differences (Table 1). Using these cell lines (and others not shown here), we demonstrated that β-lap-mediated apoptosis did not require active ER and we confirmed that cell death was not dependent on wild-type p53 or cell-cycle status.

Our previous studies could not discern a cell cycle phase-specific apoptotic mechanism following β-lap exposure. In these studies, we utilized the estrogen-dependent G_1 arrest characteristics of MCF-7 and T47D cells (~80% growth inhibition in E_2-deprived, compared to log-phase cells) to show that both cell lines were equally sensitive to β-lap or TPT, irrespective of their progression through the cell cycle (Fig. 2). When arrested cells were treated with either β-lap or TPT, the relative cytotoxicity was identical to that of log-phase cells. This result is in apparent conflict with the current paradigm for the mechanism of action of Topo I poisons, which suggested that the primary lethal event was the creation of DNA double-strand breaks following movement of the replication fork through the "cleavable complex." This mechanism has been used to describe the S-phase-specific killing of cancer cells by TPT. Morris and Geller [53] also showed that CPT could induce apoptosis in postmitotic rat cortical neurons. Our data indicate that DNA synthesis may not be required for lethality or the stimulation of apoptosis in G_1-arrested breast cancer cells by β-lap or TPT. These data suggest that DNA–Topo I lesions caused by treatment may activate a nuclear signal (possibly originating from inhibited transcription) that triggers pRb dephosphorylation (see below) and downstream apoptotic reactions. Taken together, these results demonstrate that while actively growing cells may be killed more efficiently in some systems, arrested cells may also be sensitive to the toxic (i.e., apoptotic) effects of Topo I poisons. In comparison with β-lap, TPT was a less effective inducer of apoptosis, stimulating apoptotic reactions only at concentrations 20- to 100-fold over its IC_{50}. β-Lap killed cells by apoptosis at concentrations near its IC_{50}, as previously reported [24].

Using two methods of cell cycle arrest, estrogen deprivation (Figs. 2 and 9) and nocodazole administration (data not shown), we demonstrated that β-lap kills MCF-7 cells equally in all phases of the cell cycle. This would suggest that Topo IIα does not play a central role in β-lap toxicity. Unlike Topo I, the expression of Topo IIα is clearly cell cycle dependent ([26] and data not shown), and stages of the cell cycle in which Topo IIα was not expressed (i.e., G_0/G_1) would be expected to be protected from β-lap toxicity, if Topo IIα was a critical target. Conversely, stages of the cell cycle with highest Topo IIα expression (i.e., G_2/M) would be expected to be more sensitive to β-lap. It is important to note that the β-lap/Topo IIα-mediated cleavage has been observed using only *in vitro* assays, and β-lap/Topo IIα-mediated DNA breaks have not been demonstrated in intact cells. Importantly, downstream consequences of DNA damage, such as p53 induction, have not been observed after β-lap treatment [24]. These data are in apparent conflict with the suggested role of Topo IIα in β-lap-mediated toxicity as proposed by Frydman *et al.* [25].

β-Lap induces a novel apoptotic protease. Exposure to β-lap gave rise to a unique pattern of proteolysis. At lower doses, β-lap treatment caused classic PARP cleavage. At higher doses, an ~60-kDa atypical PARP fragment was observed. The dose range over which this novel fragment appeared was quite sharp and correlated well with the notably sharp growth inhibition responses noted in Figs. 1 and 2 and previously described cytotoxicity [24]. Atypical PARP fragmentation was not simply the result of supralethal drug exposure, since cells treated with TPT at doses 200-fold greater than the IC_{50} of the drug did not show the same atypical cleavage pattern. Doses of β-lap necessary to induce atypical PARP cleavage were generally less than 5-fold over the IC_{50} for β-lap, depending upon the cell line examined and the method of treatment (i.e., continuous exposure or 4-h pulse). The lack of

observable atypical PARP cleavage at the IC_{50} dose was likely due to a relatively modest, but constant, loss of cells through apoptosis that does not result in the accumulation of enough cells containing cleaved PARP to be observed in Western analyses.

Previous reports have shown cleavage of PARP during necrosis, giving rise to a 50-kDa fragment [54]. However, the atypical PARP fragment observed in β-lap treated cells was ~60 kDa (Fig. 4). The demonstration of nuclear condensation, appearance of sub-G_0/G_1 cells [24], >90% TUNEL-positive cells (Fig. 6), and inhibition of apoptosis by EDTA and EGTA (Fig. 7B) leave little doubt that this response was apoptotic. Interestingly, in β-lap-treated cells, we have noted some unique characteristics that do not fit the "classic" definition of apoptosis. Further study of the action of this novel apoptosis-inducing agent may allow for elucidation of cell death processes which contain characteristics of apoptotic as well as necrotic proteolytic cascades. This agent may induce a heretofore uncharacterized apoptotic pathway that may be exploited for improved treatment of breast cancer. For example, this agent may be useful for treatment of breast cancer which has lost classic caspase-mediated apoptotic responses.

Atypical PARP cleavage observed in MCF-7 cells was not likely the result of caspase, granzyme B, cathepsins B or L, trypsin, or chymotrypsin-like proteases (see Fig. 5) [38]. However, the classic cleavage pattern observed in T47D cells after low-level β-lap exposures was prevented by 25 μM zVAD-fmk, a general caspase inhibitor. Classic PARP cleavage induced by low-dose β-lap exposure was unaffected by other protease inhibitors, suggesting that a different member of the caspase family was responsible for apoptotic proteolysis in T47D cells. At higher doses of β-lap, T47D cells responded like MCF-7 cells, undergoing apoptosis and atypical PARP cleavage. Lack of inhibition of atypical PARP cleavage by zVAD-fmk in MCF-7 cells treated with β-lap strongly suggests that activation of the caspase pathway was not necessary for atypical PARP cleavage.

In β-lap-treated MCF-7 cells, atypical PARP fragmentation was blocked by iodoacetamide or *N*-ethylmaleimide, both cysteine-alkylating agents (data not shown). Additionally, atypical PARP cleavage was not inhibited by a battery of inhibitors (Fig. 5), each used at previously determined effective doses. These data suggest that atypical fragmentation of PARP *in vivo* was due to the activation of a cysteine protease which is apparently not a member of the caspase family of proteases. However, the nonspecific reactivity of iodoacetamide and *N*-ethylmaleimide does allow the possibility that the unknown protease may be indirectly activated after β-lap treatment by a factor which contains critical –SH groups. One protease which fits the available data could be the neutral calcium-dependent protease calpain. This possibility is further supported by the fact that p53 was cleaved in β-lap-treated MCF-7 cells, giving rise to fragments (Fig. 7A) which match those previously described as being the result of calpain activity [42, 43]. Furthermore, the time course of p53 cleavage was concomitant with the appearance of atypically cleaved PARP. Additionally, we provide evidence showing that the cysteine protease is Ca^{+2} dependent, since its activity (as measured by atypical PARP or p53 cleavage) was prevented by coadministration of EDTA or EGTA (Fig. 8B and data not shown). While these findings do not conclusively prove that calpain is responsible for this cleavage, they are suggestive. Our laboratory is currently in the process of definitively identifying the protease responsible for this cleavage of PARP. The use of caspase-3-expressing MCF-7 cells demonstrated that reexpression of caspase-3 did not lead to enhanced apoptosis or appearance of the caspase-mediated 89-kDa PARP fragmentation after β-lap exposure. In contrast, other studies have demonstrated enhanced apoptotic reactions in caspase-3-expressing MCF-7 cells after granzyme B or TNF-α treatments, compared to cells infected with the empty vector [16].

While β-lap treatment of MCF-7 cells appeared to activate a novel apoptotic pathway, classic lamin B cleavage (primarily due to the activation of caspase-6) was also observed ([24, 51] and Fig. 9). While caspase-6 is thought to be activated directly by caspase-3 [55, 56], our data suggest that either a distinct upstream protease can activate caspase-6 after β-lap treatment or an unknown, β-lap-activated protease can directly cleave lamin B, giving rise to fragments of size similar to those observed after caspase-6 cleavage. Our data suggest that once the apoptotic protease is activated, it dominates proteolysis in β-lap-treated MCF-7 cells, since visible classic PARP cleavage fragments were not observed. Interestingly, overexpression of caspase-3 in MCF-7 cells did not affect β-lap cytotoxicity, while increasing sensitivity to granzyme B or TNF-α [16].

Our studies demonstrate that β-lap can induce at least two independent apoptotic pathways in breast cancer cells. The apoptotic response seems to be independent of the *in vitro* observed β-lap/Topo IIα-mediated DNA cleavage [25], since G_1-arrested cells (which contain very low Topo IIα enzyme activity) were as effectively killed by β-lap as log-phase or G_2/M-arrested cells (which express high levels of Topo IIα enzyme activity). Furthermore, the *in vivo* pathway activated by β-lap leading to apoptosis may also be independent of the Topo I inhibition observed *in vitro*. In some cells, β-lap mediates typical caspase activation, leading to the formation of the classic 89 kDa PARP cleavage fragment *in vivo* [57]. In other cells (specifically, MCF-7), β-lap activates a calcium-dependent, noncaspase cysteine protease. Interestingly, activation of this pathway of apoptosis (which may also result in midprotein cleavage of pRb) eventually occurred in MCF-7 and T47D breast cancer cells. An interesting profile of sensitivity of breast cancer cells to

β-lap was observed. Sensitivity to this agent was very different from the cytotoxic responses observed following TPT treatment. In MCF-7 cells, the primary proteolytic events, which correlate directly with apoptosis induction and loss of survival, appear to be the result of this novel calcium-dependent noncaspase protease. Activation of this protease was not affected by inhibitors of a variety of proteases, most importantly the caspase inhibitors zVAD-fmk and DEVD-fmk. We hypothesize that this calcium-dependent, noncaspase cysteine protease is calpain. When this protease is activated, its novel apoptotic pathway may be a specific target for manipulation in the clinical treatment of breast cancer.

Funding for this work was provided to us by a grant from the United States Army Medical Research and Materiel Command Breast Cancer Initiative (DAMD17-98-1-8260 to D.A.B.) and by a Postdoctoral Fellowship from the U.S. Army (DAMD17-97-1-7221 to J.J.P.). We thank Dr. V. Craig Jordan for supplying us with the breast cancer cell lines and the anti-estrogen ICI 182,780 and Dr. Vishva Dixit for the caspase 3 cDNA. We thank Dr. William Bornmann for supplying us with β-lap and Dr. Nancy Oleinick for critically reviewing the manuscript. We are also grateful for support through the efforts of Mrs. Sara Hildebrand through the Breast Cancer Inspiration Fund and the Breast Cancer Research Fund. This work was also supported by the Arthritis Foundation–Illinois chapter (to C.J.F.). Finally, we are grateful to our many colleagues at the University of Wisconsin Comprehensive Cancer Center for their help in initiating these studies.

REFERENCES

1. Alnemri, E. S., Livingston, D. J., Nicholson, D. W., Salvesen, G., Thornberry, N. A., Wong, W. W., and Yuan, J. Y. (1996). Human Ice/Ced-3 protease nomenclature. *Cell* **87,** 171.
2. Piedrafita, F. J., and Pfahl, M. (1997). Retinoid-induced apoptosis and Sp1 cleavage occur independently of transcription and require caspase activation. *Mol. Cell. Biol.* **17,** 6348–6358.
3. Patel, T., Gores, G. J., and Kaufmann, S. H. (1996). The role of proteases during apoptosis. *FASEB J.* **10,** 587–597.
4. Janicke, R. U., Walker, P. A., Lin, X. Y., and Porter, A. G. (1996). Specific cleavage of the retinoblastoma protein by an ICE-like protease in apoptosis. *EMBO J.* **15,** 6969–6978.
5. An, B., and Dou, Q. P. (1996). Cleavage of retinoblastoma protein during apoptosis: An interleukin 1 beta-converting enzyme-like protease as candidate. *Cancer Res.* **56,** 438–442.
6. Talanian, R. V., Quinlan, C., Trautz, S., Hackett, M. C., Mankovich, J. A., Banach, D., Ghayur, T., Brady, K. D., and Wong, W. W. (1997). Substrate specificities of caspase family proteases. *J. Biol. Chem.* **272,** 9677–9682.
7. Kaufmann, S. H., Desnoyers, S., Ottaviano, Y., Davidson, N. E., and Poirier, G. G. (1993). Specific proteolytic cleavage of poly(ADP-ribose) polymerase: An early marker of chemotherapy-induced apoptosis. *Cancer Res.* **53,** 3976–3985.
8. Wang, X., Pai, J. T., Wiedenfeld, E. A., Medina, J. C., Slaughter, C. A., Goldstein, J. L., and Brown, M. S. (1995). Purification of an interleukin-1 beta converting enzyme-related cysteine protease that cleaves sterol regulatory element-binding proteins between the leucine zipper and transmembrane domains. *J. Biol. Chem.* **270,** 18044–18050.
9. Squier, M. K., Miller, A. C., Malkinson, A. M., and Cohen, J. J. (1994). Calpain activation in apoptosis. *J. Cell. Physiol.* **159,** 229–237.
10. Wood, D. E., Thomas, A., Devi, L. A., Berman, Y., Beavis, R. C., Reed, J. C., and Newcomb, E. W. (1998). Bax cleavage is mediated by calpain during drug-induced apoptosis. *Oncogene* **17,** 1069–1078.
11. Porn-Ares, M. I., Samali, A., and Orrenius, S. (1998). Cleavage of the calpain inhibitor, calpastatin, during apoptosis. *Cell Death Differ.* **5,** 1028–1033.
12. Chandra, J., Niemer, I., Gilbreath, J., Kliche, K. O., Andreeff, M., Freireich, E. J., Keating, M., and McConkey, D. J. (1998). Proteasome inhibitors induce apoptosis in glucocorticoid-resistant chronic lymphocytic leukemic lymphocytes. *Blood* **92,** 4220–4229.
13. McConkey, D. J. (1996). Calcium-dependent, interleukin 1-converting enzyme inhibitor-insensitive degradation of lamin B1 and DNA fragmentation in isolated thymocyte nuclei. *J. Biol. Chem.* **271,** 22398–22406.
14. Shimizu, T., and Pommier, Y. (1997). Camptothecin-induced apoptosis in p53-null human leukemia HL60 cells and their isolated nuclei: Effects of the protease inhibitors Z-VAD-fmk and dichloroisocoumarin suggest an involvement of both caspases and serine proteases. *Leukemia* **11,** 1238–1244.
15. Marthinuss, J., Andrade-Gordon, P., and Seiberg, M. (1995). A secreted serine protease can induce apoptosis in Pam212 keratinocytes. *Cell Growth Differ.* **6,** 807–816.
16. Yang, X., Stennicke, H. R., Wang, B., Green, D. R., Janicke, R. U., Srinivasan, A., Seth, P., Salvesen, G. S., and Froelich, C. J. (1998). Granzyme B mimics apical caspases. Description of a unified pathway for trans-activation of executioner caspase-3 and -7. *J. Biol. Chem.* **273,** 34278–34283.
17. Boothman, D. A., Trask, D. K., and Pardee, A. B. (1989). Inhibition of potentially lethal DNA damage repair in human tumor cells by beta-lapachone, an activator of topoisomerase I. *Cancer Res.* **49,** 605–612.
18. Planchon, S. M., Wuerzberger, S., Frydman, B., Witiak, D. T., Hutson, P., Church, D. R., Wilding, G., and Boothman, D. A. (1995). Beta-lapachone-mediated apoptosis in human promyelocytic leukemia (HL-60) and human prostate cancer cells: A p53-independent response. *Cancer Res.* **55,** 3706–3711.
19. Boothman, D. A., Wang, M., Schea, R. A., Burrows, H. L., Strickfaden, S., and Owens, J. K. (1992). Posttreatment exposure to camptothecin enhances the lethal effects of x-rays on radioresistant human malignant melanoma cells. *Int. J. Radiat. Oncol. Biol. Phys.* **24,** 939–948.
20. Li, C. J., Averboukh, L., and Pardee, A. B. (1993). beta-Lapachone, a novel DNA topoisomerase I inhibitor with a mode of action different from camptothecin. *J. Biol. Chem.* **268,** 22463–22468.
21. Boothman, D. A., and Pardee, A. B. (1989). Inhibition of radiation-induced neoplastic transformation by beta-lapachone. *Proc. Natl. Acad. Sci. USA* **86,** 4963–4967.
22. Nelson, W. G., and Kastan, M. B. (1994). DNA strand breaks: The DNA template alterations that trigger p53-dependent DNA damage response pathways. *Mol. Cell. Biol.* **14,** 1815–1823.
23. Boothman, D. A. (1994). Enhanced malignant transformation is accompanied by increased survival recovery after ionizing radiation in Chinese hamster embryo fibroblasts. *Radiat. Res.* **138,** S121–S125.
24. Wuerzberger, S. M., Pink, J. J., Planchon, S. M., Byers, K. L., Bornmann, W. G., and Boothman, D. A. (1998). Induction of apoptosis in MCF-7:WS8 breast cancer cells by beta-lapachone. *Cancer Res.* **58,** 1876–1885.
25. Frydman, B., Marton, L. J., Sun, J. S., Neder, K., Witiak, D. T., Liu, A. A., Wang, H. M., Mao, Y., Wu, H. Y., Sanders, M. M., and Liu, L. F. (1997). Induction of DNA topoisomerase II-mediated

DNA cleavage by beta-lapachone and related naphthoquinones. *Cancer Res.* **57,** 620–627.

26. Larsen, A. K., Skladanowski, A., and Bojanowski, K. (1996). The roles of DNA topoisomerase II during the cell cycle. *Prog. Cell. Cycle. Res.* **2,** 229–239.
27. D'Arpa, P., and Liu, L. F. (1989). Topoisomerase-targeting antitumor drugs. *Biochim. Biophys. Acta* **989,** 163–177.
28. Slevin, M. L. (1991). The clinical pharmacology of etoposide. *Cancer* **67,** 319–329.
29. Jonsson, E., Fridborg, H., Csoka, K., Dhar, S., Sundstrom, C., Nygren, P., and Larsson, R. (1997). Cytotoxic activity of topotecan in human tumour cell lines and primary cultures of human tumour cells from patients. *Br. J. Cancer* **76,** 211–219.
30. Lamond, J. P., Wang, M., Kinsella, T. J., and Boothman, D. A. (1996). Radiation lethality enhancement with 9-aminocamptothecin: Comparison to other topoisomerase I inhibitors. *Int. J. Radiat. Oncol. Biol. Phys.* **36,** 369–376.
31. Pink, J. J., Bilimoria, M. M., Assikis, J., and Jordan, V. C. (1996). Irreversible loss of the oestrogen receptor in T47D breast cancer cells following prolonged oestrogen deprivation. *Br. J. Cancer* **74,** 1227–1236.
32. Pink, J. J., Jiang, S. Y., Fritsch, M., and Jordan, V. C. (1995). An estrogen-independent MCF-7 breast cancer cell line which contains a novel 80-kilodalton estrogen receptor-related protein. *Cancer Res.* **55,** 2583–2590.
33. Pink, J. J., and Jordan, V. C. (1996). Models of estrogen receptor regulation by estrogens and antiestrogens in breast cancer cell lines. *Cancer Res.* **56,** 2321–2330.
34. Labarca, C., and Paigen, K. (1980). A simple, rapid, and sensitive DNA assay procedure. *Anal. Biochem.* **102,** 344–352.
35. Musgrove, E. A., and Sutherland, R. L. (1993). Acute effects of growth factors on T-47D breast cancer cell cycle progression. *Eur. J. Cancer* **29A,** 2273–2279.
36. Musgrove, E. A., and Sutherland, R. L. (1991). Steroids, growth factors, and cell cycle controls in breast cancer. *Cancer Treat. Res.* **53,** 305–331.
37. Pink, J. J., Fritsch, M., Bilimoria, M. M., Assikis, V. J., and Jordan, V. C. (1997). Cloning and characterization of a 77-kDa oestrogen receptor isolated from a human breast cancer cell line. *Br. J. Cancer* **75,** 17–27.
38. Lotem, J., and Sachs, L. (1996). Differential suppression by protease inhibitors and cytokines of apoptosis induced by wild-type p53 and cytotoxic agents. *Proc. Natl. Acad. Sci. USA* **93,** 12507–12512.
39. Li, X., Traganos, F., Melamed, M. R., and Darzynkiewicz, Z. (1995). Single-step procedure for labeling DNA strand breaks with fluorescein- or BODIPY-conjugated deoxynucleotides: Detection of apoptosis and bromodeoxyuridine incorporation. *Cytometry* **20,** 172–180.
40. Zollner, H. (1993). "Handbook of Enzyme Inhibitors," pp. 728–730, VCH, Weinheim/New York.
41. Waxman, L. (1981). Calcium-activated proteases in mammalian tissues. *Methods Enzymol.* **80,** 664–680.
42. Kubbutat, M. H., and Vousden, K. H. (1997). Proteolytic cleavage of human p53 by calpain: A potential regulator of protein stability. *Mol. Cell. Biol.* **17,** 460–468.
43. Pariat, M., Carillo, S., Molinari, M., Salvat, C., Debussche, L., Bracco, L., Milner, J., and Piechaczyk, M. (1997). Proteolysis by calpains: A possible contribution to degradation of p53. *Mol. Cell. Biol.* **17,** 2806–2815.
44. Wakeling, A. E., and Bowler, J. (1992). ICI 182,780, a new antioestrogen with clinical potential. *J. Steroid Biochem. Mol. Biol.* **43,** 173–177.
45. Pink, J. J., and Jordan, V. C. (1995). Molecular mechanisms of antiestrogen resistance. *In* "Drug and Hormonal Resistance in Breast Cancer: Cellular and Molecular Mechanisms" (R. B. Dickson and M. E. Lippman, Eds.), Ellis Horwood, Hemel Hempstead, UK.
46. Musgrove, E. A., Sarcevic, B., and Sutherland, R. L. (1996). Inducible expression of cyclin D1 in T-47D human breast cancer cells is sufficient for Cdk2 activation and pRB hyperphosphorylation. *J. Cell. Biochem.* **60,** 363–378.
47. Musgrove, E. A., and Sutherland, R. L. (1994). Cell cycle control by steroid hormones. *Semin. Cancer Biol.* **5,** 381–389.
48. Musgrove, E. A., Wakeling, A. E., and Sutherland, R. L. (1989). Points of action of estrogen antagonists and a calmodulin antagonist within the MCF-7 human breast cancer cell cycle. *Cancer Res.* **49,** 2398–2404.
49. Foster, J. S., and Wimalasena, J. (1996). Estrogen regulates activity of cyclin-dependent kinases and retinoblastoma protein phosphorylation in breast cancer cells. *Mol. Endocrinol.* **10,** 488–498.
50. Li, F., Srinivasan, A., Wang, Y., Armstrong, R. C., Tomaselli, K. J., and Fritz, L. C. (1997). Cell-specific induction of apoptosis by microinjection of cytochrome c. Bcl-xL has activity independent of cytochrome c release. *J. Biol. Chem.* **272,** 30299–30305.
51. Orth, K., Chinnaiyan, A. M., Garg, M., Froelich, C. J., and Dixit, V. M. (1996). The CED-3/ICE-like protease Mch2 is activated during apoptosis and cleaves the death substrate lamin A. *J. Biol. Chem.* **271,** 16443–16446.
52. Takahashi, A., Alnemri, E. S., Lazebnik, Y. A., Fernandes-Alnemri, T., Litwack, G., Moir, R. D., Goldman, R. D., Poirier, G. G., Kaufmann, S. H., and Earnshaw, W. C. (1996). Cleavage of lamin A by Mch2 alpha but not CPP32: Multiple interleukin 1 beta-converting enzyme-related proteases with distinct substrate recognition properties are active in apoptosis. *Proc. Natl. Acad. Sci. USA* **93,** 8395–8400.
53. Morris, E. J., and Geller, H. M. (1996). Induction of neuronal apoptosis by camptothecin, an inhibitor of DNA topoisomerase-I: Evidence for cell cycle-independent toxicity. *J. Cell Biol.* **134,** 757–770.
54. Shah, G. M., Shah, R. G., and Poirier, G. G. (1996). Different cleavage pattern for poly(ADP-ribose) polymerase during necrosis and apoptosis in HL-60 cells. *Biochem. Biophys. Res. Commun.* **229,** 838–844.
55. Faleiro, L., Kobayashi, R., Fearnhead, H., and Lazebnik, Y. (1997). Multiple species of CPP32 and Mch2 are the major active caspases present in apoptotic cells. *EMBO J.* **16,** 2271–2281.
56. Hirata, H., Takahashi, A., Kobayashi, S., Yonehara, S., Sawai, H., Okazaki, T., Yamamoto, K., and Sasada, M. (1998). Caspases are activated in a branched protease cascade and control distinct downstream processes in Fas-induced apoptosis. *J. Exp. Med.* **187,** 587–600.
57. Planchon, S. M., Wuerzberger-Davis, S. M., Pink, J. J., Robertson, K. A., Bornmann, W. G., and Boothman, D. A. (1999). Bcl-2 protects against β-lapachone-mediated caspase 3 activation and apoptosis in human myeloid leukemia (HL-60) cells. *Oncol. Rep.* **6,** 485–492.

Received August 11, 1999
Revised version received December 10, 1999

Bcl-2 protects against ß-lapachone-mediated caspase 3 activation and apoptosis in human myeloid leukemia (HL-60) cells

SARAH M. PLANCHON[1], SHELLY M. WUERZBERGER-DAVIS[1], JOHN J. PINK[1], KENT A. ROBERTSON[2], WILLIAM G. BORNMANN[3] and DAVID A. BOOTHMAN[1]

[1]Department of Radiation Oncology, Laboratory of Molecular Stress Responses, Case Western Reserve University, Cleveland, OH 44106; [2]Herman B. Wells Center for Pediatric Research, Indiana University Medical Center, Indianapolis, IN 46202; [3]Preparative Synthesis Core Facility, Memorial Sloan-Kettering Cancer Center, New York, NY 10021, USA

Received February 5, 1999; Accepted February 10, 1999

Abstract. We previously demonstrated that ß-lapachone (ß-lap) killed cancer cells solely by apoptosis. ß-Lap induced apoptosis in HL-60 cells in a dose-dependent manner as measured by flow cytometry and DNA ladder formation. Cell cycle changes, such as accumulations in S and G_2-phases, were not observed. Apoptosis was accompanied by activation of caspase 3 and concomitant cleavage of poly(ADP-ribose) polymerase (PARP) to an 89 kDa polypeptide. PARP cleavage was blocked by zDEVD-fmk or zVAD-fmk, caspase-specific cleavage site inhibitors. Retrovirally introduced *bcl*-2 prevented ß-lap-mediated caspase 3 activation and PARP cleavage and increased the viability of Bcl-2-expressing HL-60 cells compared to cells with vector alone. Various ß-lap-related analogs (e.g., dunnione and naphthoquinone derivatives) induced equivalent apoptosis in HL-60 cells, but no compound was more effective than ß-lap. These data provide further evidence that the primary mode of cell killing by ß-lap is by the initiation and execution of apoptosis in human cancer cells.

Introduction

Myeloid leukemia (HL-60) cells, as well as a variety of other human cancer cells, undergo dramatic apoptotic responses after ß-lapachone (ß-lap, 3,4-dihydro-2,2-dimethyl-2H-naphtho [1,2-b]pyran-5,6-dione) exposure (1,2). ß-Lap is an *o*-naphthoquinone, originally derived from the bark of the South American Lapacho tree. It can be synthesized directly from 1,2-naphthoquinone (3). While ß-lap is reported to be an inhibitor of topoisomerases I and IIα (Topo I and Topo IIα, respectively) *in vitro* (1,2,4,5), its exact intracellular mechanism of action remains unknown. Recent data have indicated that, unlike known Topo I (6,7) or IIα poisons (7,8), the main mode of cytotoxicity by this compound is by the induction of apoptosis without significant cell cycle checkpoint delays in S or G_2/M (9). ß-Lap holds promise as a potential chemotherapeutic agent since its mechanism of action does not require functional p53 (1,9).

Apoptosis is a tightly regulated form of cell death (10). It is characterized by several classic morphologic and biochemical changes. In its execution phase, nuclear and chromatin condensation, DNA fragmentation, and formation of apoptotic bodies are observed (11,12). Certain cell-death stimuli may result in the cleavage and activation of apoptotic proteases, termed caspases (13). These, in turn, stimulate downstream caspases (14) and cleave specific apoptotic substrates (15) such as poly(ADP-ribose) polymerase (PARP), DNA-PK_{cs}, Lamin B, and U1-70 kDa. Cleavage of these cell death substrates may down-regulate essential homeostatic processes, structural components, and DNA repair.

Cleavage of PARP from its 113 kDa full-length form into 89 and 24 kDa fragments is often observed in apoptotic cells. This cleavage may represent the *in vivo* activation of caspase 3 (also known as CPP32, Apopain or YAMA), along with several other caspases (e.g., caspase 7). Caspase-mediated cleavage of PARP can be irreversibly blocked by the administration of specific cleavage-site-directed peptides (16). The activity of a particular caspase can be blocked by inhibiting upstream caspases (preventing processing and subsequent activation of the zymogen form), or by preventing downstream proteolysis (17).

Bcl-2 expression is also able to block the caspase cascade. Bcl-2 is the product of a proto-oncogene isolated from the t(14:18) translocation present in human B cell leukemias and lymphomas (18). It is a 26 kDa protein that is primarily localized to mitochondrial and perinuclear membranes (19). Bcl-2 acts upstream by directly preventing protease activation (20,21). Bcl-2 may integrate into the mitochondrial or endoplasmic reticulum membranes to prevent cytochrome c release or calcium changes, respectively (22,23). Cytochrome c release may then activate Apaf-1, which in turns activates caspase 9 and triggers apoptosis (24).

We demonstrate that the apoptotic execution pathway in HL-60 cells following ß-lap exposure includes the upstream

Correspondence to: Dr David A. Boothman, Department of Radiation Oncology, Laboratory of Molecular Stress Responses, Case Western Reserve University, School of Medicine, 326 Biomedical Research Building, 10900 Euclid Avenue, Cleveland, OH 44106-4942, USA

Key words: Bcl-2, apoptosis, caspase 3, ß-lapachone, HL-60

activation of caspase 1 or caspase 1-like proteases. Caspase 1-like proteases then initiate the apoptotic cascade by activating caspase 3, which results in PARP cleavage, DNA fragmentation and apoptosis. Exogenous Bcl-2 expression prevented caspase 3 activation, prevented PARP cleavage, and enhanced the viability of HL-60 cells after ß-lap exposure. These data suggest that in these cells a typical caspase-mediated apoptotic protease cascade is initiated.

Materials and methods

Cell lines and cell culture. HL-60 cells were obtained from the ATCC and were grown in RPMI media supplemented with 10% fetal bovine serum (FBS) in a humidified incubator containing 5% CO_2-95% air atmosphere at 37°C as described (1). HL-60 cells infected with the LXSN retroviral vector containing or not containing the *bcl*-2 cDNA were grown under neomycin (G418) selection (25). Lbcl-2SN cells express elevated levels of Bcl-2, which confers resistance to apoptosis initiated by various cytotoxic agents (25). Cell viability at 24 or 48 h posttreatments with DMSO or various ß-lap concentrations was monitored using trypan blue exclusion assays (25). Statistical analyses of data were performed using a paired t-test. Untreated HL-60 cells exhibited a basal level of apoptosis; however, it was negligible in comparison to levels observed following ß-lap treatment.

Chemicals and protease inhibitors. ß-Lap (MW: 242) was synthesized by us. SO_3-naphthoquinone was obtained from the Sigma Chemical Company (St. Louis, MO). ß-Lap, dunnione, and 1,2-naphthoquinone derivatives were a gift from Dr Donald Witiak (UW-Madison). All compounds were dissolved in DMSO and stored in aliquots at -20°C. A number of caspase or protease inhibitors were used as described (26): a) zVAD-fmk, which inhibits caspase 1 and caspase 1-like proteases; b) zDEVD-fmk, which inhibits caspase 3 and caspase 3-like proteases; c) zAAD-fmk, which inhibits Granzyme B; and d) zFA-fmk, which inhibits cathepsins B and L (Enzyme Systems Products, Dublin, CA). The chloromethylketone-containing protease inhibitors, TLCK, which inhibits trypsin-like serine and some cysteine proteases, and TPCK, which inhibits chymotrypsin-like serine and some cysteine proteases (Sigma, St. Louis, MO), were also used.

DNA laddering and cell cycle analyses. Cells (1-10x10^6/condition in 5 ml media) were treated with various doses of drug for 4 h, as indicated. Drugs were removed and replaced with fresh media. At various times posttreatment, samples were analyzed for G_0/G_1, S, G_2/M, and apoptotic (i.e., sub-G_0/G_1) cells as described (1). Treated and control cells were also analyzed for DNA fragmentation characteristic of apoptosis (1,2). The apoptotic-inducing potential of compounds was compared by the presence of DNA laddering by agarose gel electrophoresis using various concentrations in a 4-h period. Lack of DNA laddering was scored as a negative result. All experimental samples were compared to HL-60 control cells treated with an equal percentage of DMSO (the solvent in all drug treatments); DMSO did not affect HL-60 cell cycle distribution, but did stimulate a low level of apoptosis as indicated. All experiments were performed at least three times.

Western blot analyses. Control or treated HL-60 cells were examined for changes in PARP and caspase 3 cleavage. Briefly, using techniques previously described (9), equivalent amounts of protein were denatured (65°C, 15 min) and polypeptides separated by SDS-PAGE. Separated proteins were then transferred to Immobilon-P membranes (Millipore, Danvers, MA) and equivalent protein loading was confirmed by Ponceau S staining. Primary antibodies included the anti-PARP C-2-10 (1:10,000 dilution, Enzyme Systems Products, Dublin, CA) and anti-caspase 3 (1:2,000 dilution, Transduction Laboratories, Lexington, KY). Western blot membranes were then developed with enhanced chemiluminescence (ECL) substrate (Amersham, Arlington Heights, IL), and exposed to Fuji X-ray film as described (9). All experiments were performed at least three times.

Results

Kinetics of ß-lap-induced apoptosis. HL-60 cells were treated with 1.0, 5.0, or 10 µM ß-lap for 4 h and samples were analyzed for cell cycle changes and apoptotic DNA fragmentation (appearing as 180-200 bp oligonucleosome ladders) (Fig. 1), as described (1,2). Increases in DNA ladder formation were noted with increasing doses of ß-lap and with longer posttreatment time, consistent with earlier data (1,2). DNA fragmentation was not observed in control, DMSO-treated HL-60 cells.

Cell cycle analyses of control or ß-lap-treated HL-60 cells were also performed at 24 h posttreatment, when an optimal level of sub-G_0/G_1 apoptotic cells was detected (Fig. 1B) as described (1,27). Although basal levels of apoptosis were observed after 0.1% DMSO (drug vehicle control), apoptosis increased proportionally with increasing ß-lap concentrations. Over 50% of the total population consisted of apoptotic sub-G_0/G_1 cells after 10 µm ß-lap (Fig. 1B). Accumulation of cells at either S or G_2-phases was not observed.

Time-course experiments were also performed after various doses of ß-lap. Treatment conditions were identical to those described in Fig. 1A and the results were graphed as treated/control (T/C) (Fig. 2). HL-60 cells treated with 0.25 µM ß-lap showed little apoptosis for up to 72 h posttreatment. Treatment of HL-60 cells with 1.0 µM ß-lap induced a low level of apoptosis, which peaked at 24 h and decreased slightly by 72 h. In contrast, treatment of HL-60 cells with 5.0 or 10 µM ß-lap induced dramatic apoptotic responses, which increased with dose and time (Figs. 2 and 3A). No changes in cell cycle distribution occurred after 0.25 or 1.0 µM ß-lap; however, slight increases in G_0/G_1, with concomitant decreases in S and G_2/M, were observed following 5.0 or 10 µM ß-lap treatments.

Caspase 3 activation and PARP cleavage after ß-lap treatment. HL-60 cells were treated with various doses of ß-lap and monitored for apoptosis at various times (Fig. 3A), as described in Figs. 1 and 2. Background apoptosis was noted in control HL-60 cells treated with 0.1% DMSO alone; however, the percentage of apoptotic HL-60 cells substantially increased

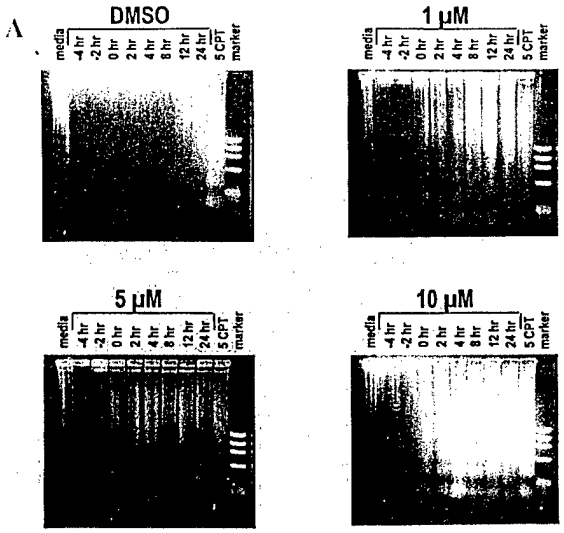

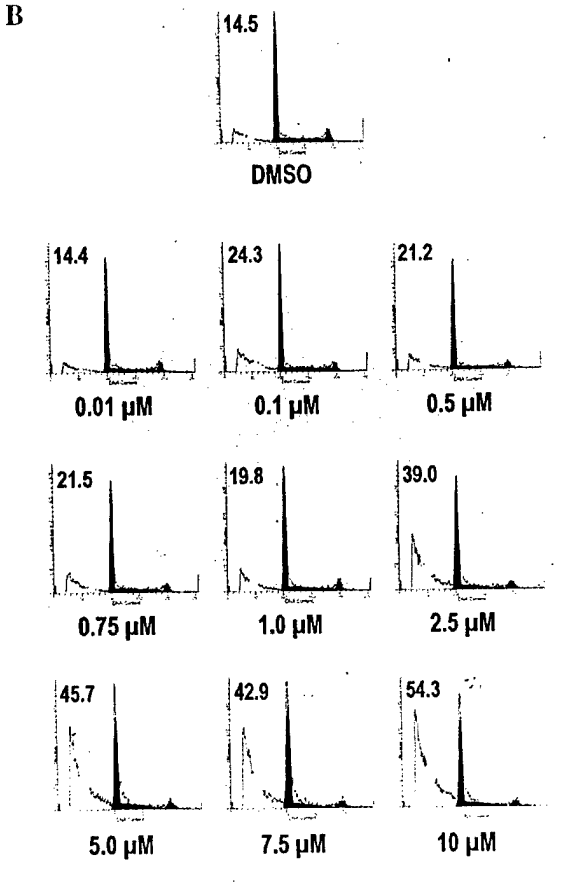

Figure 1. Apoptosis in HL-60 cells following ß-lap treatment. A, Dose-response and time-course of apoptosis; formation of 180-200 bp oligonucleosome DNA ladders in HL-60 cells following ß-lap or DMSO treatments (given as 4 h pulses) at indicated doses. The first sample taken after a 4-h drug exposure (t= -4 to 0 h) was designated as t=0. Samples were then analyzed after drug exposure (t=2 to 24 h) at the indicated doses of ß-lap. DNA molecular weight markers were ϕX174 DNA cut with the *Hae*III restriction enzyme (fragment sizes, in bp, are as follows: 1,353; 1,078; 872; 603; 310; 281; 234; 194; 118). B, Apoptotic responses at 24 h posttreatment following various doses of ß-lap as measured by the appearance of sub-G_0/G_1 (<2N DNA content) HL-60 cells by flow cytometry. Numbers in the upper left-hand corner of each DNA histogram indicate the percentage of apoptotic cells after each treatment.

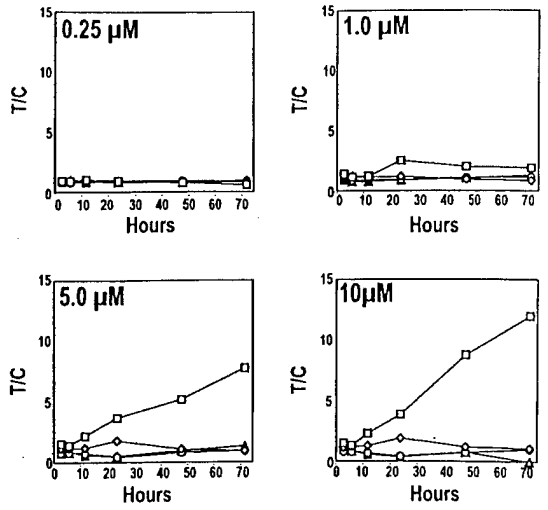

Figure 2. Apoptotic dose-response, time-course experiments, and changes in cell-cycle distribution in HL-60 cells treated with ß-lap. HL-60 cells were treated with ß-lap at the indicated doses for 4 h and analyzed for cells in G_0/G_1, (◇); S, (○); G_2/M, (△); and apoptosis, (□) at various times post-treatment, as described in Materials and methods. Data were graphed as treated over control (T/C) with respect to HL-60 cells treated with DMSO alone. The DMSO concentration in all groups was held constant at 0.1%, which did not affect cell cycle distribution or apoptosis when compared to HL-60 cells exposed to medium alone.

with ß-lap doses, ranging from 0.25 to 10 μM. Peak levels of apoptosis were routinely observed at 24 h posttreatment (Fig. 3A). Apoptosis declined between 48-72 h after 0.25 or 1.0 μM ß-lap, suggesting cell re-growth, recovery, or death due to differentiation, as previously noted (2). Following 5.0 or 10 μM ß-lap, however, HL-60 cells did not recover, and significant apoptosis was noted for up to 72 h.

We concomitantly analyzed ß-lap-treated cells (above) for apoptotic cell death substrate cleavage reactions *in vivo*. Cleavage of PARP from a 113 kDa full-length polypeptide to an 89 kDa fragment (Fig. 3B) directly correlated with changes in apoptosis (Fig. 3A) in HL-60 cells. Basal spontaneous levels of apoptosis observed after DMSO alone or after 0.25 μM ß-lap treatments (Figs. 2 and 3A) were indirectly confirmed by low level PARP cleavage (Fig. 3B). PARP cleavage increased in HL-60 cells treated with 1.0 μM ß-lap 3-12 h posttreatment; however, steady state full-length PARP levels re-appeared 24-72 h posttreatment (Fig. 3B). Re-appearance of full-length PARP correlated well with potential cell recovery, re-growth, or differentiation responses (Fig. 3A). Treatment of HL-60 cells with higher doses of ß-lap resulted in dramatically increased PARP cleavage and concomitant decreases in full-length PARP protein. Re-appearance of full-length PARP, as noted after 1.0 μM ß-lap, was much less obvious after 5.0 or 10 μM ß-lap, suggesting more complete apoptotic responses.

Activation of caspase 3 was also monitored via cleavage of its full-length inactive zymogen form. Loss of the pro-caspase 3 protein (Fig. 3C) correlated well with both PARP cleavage (Fig. 3B) and apoptosis (Fig. 3A). A close correlation between loss of the zymogen form of caspase 3 and PARP

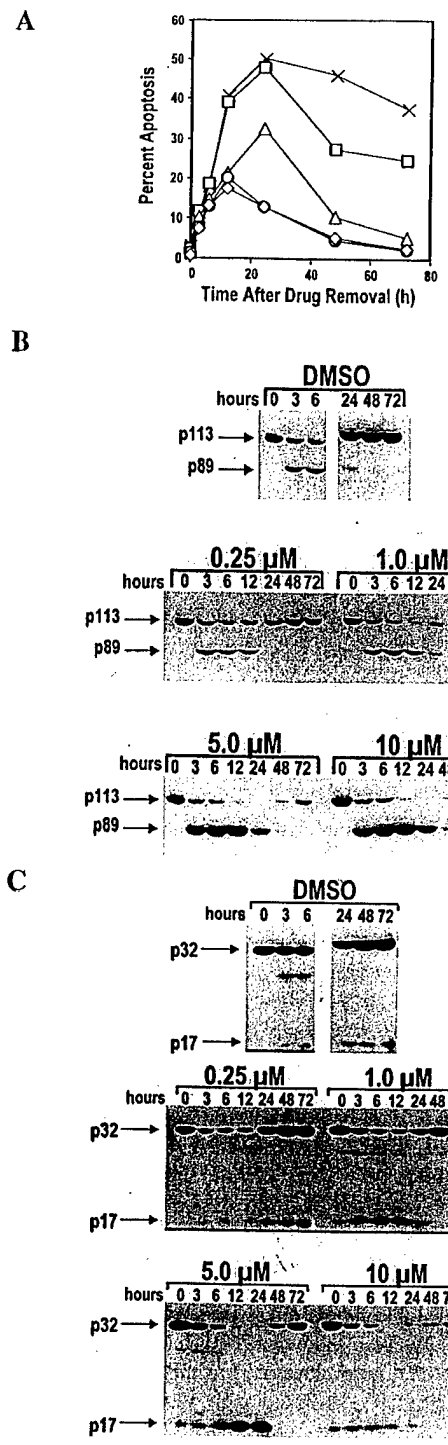

Figure 3. PARP cleavage and caspase 3 activation after ß-lap. HL-60 cells were treated with various doses of ß-lap for 4 h and whole cell protein extracts were analyzed for steady state levels of PARP (113 kDa) and its apoptotic cleavage fragment (89 kDa). Activation of caspase 3, indicated by the loss of the 32 kDa zymogen form and appearance of the 17 kDa 'active' protease form, was also assayed. A, Dose-response and time-course appearance of apoptosis in HL-60 cells treated with various concentrations of ß-lap, analyzed by flow cytometry. Conditions were, 0.1% DMSO alone, (◇); 0.25 µM ß-lap, (○); 1.0 µM ß-lap, (△); 5.0 µM ß-lap, (□); and 10 µM ß-lap, (×). B, Western immunoblot analyses of PARP cleavage. C, Western immunoblot analysis of caspase 3 activation. Protein extracts of HL-60 cells treated with DMSO alone were separated by SDS-PAGE along with the protein samples from ß-lap-treated cells. For clarity, DMSO alone control timepoints were grouped together.

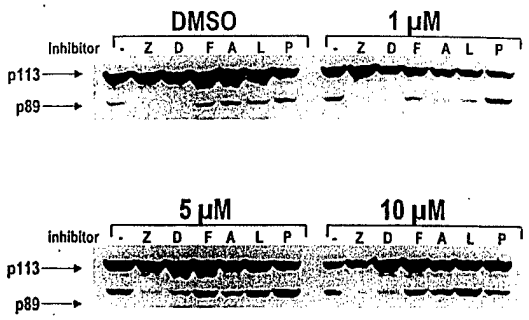

Figure 4. Abrogation of PARP cleavage by protease inhibitors. Steady state levels of PARP (113 kDa) and its apoptotic cleavage fragment (89 kDa) in ß-lap-treated HL-60 cells were monitored by Western immunoblot analyses as described in Materials and methods. HL-60 cells were treated with 5 µM ß-lap in the presence of protease inhibitors for 4 h, then for an additional 5 h with inhibitors alone. Conditions were: no inhibitor added, (-); 25 µM zVAD-fmk, (Z); 25 µM zDEVD-fmk, (D); 25 µM zFA-fmk, (F); 25 µM zAAD-fmk, (A); 25 µM TLCK, (L); and 25 µM TPCK, (P).

cleavage was noted. Loss of the 32 kDa pro-caspase 3 protein was, therefore, used in subsequent analyses as an indirect measure of activation. Alterations in caspase 3 levels after 0.25 µM ß-lap treatment were attributed to loading variations and did not correlate with apoptosis (Fig. 3A) or PARP cleavage (Fig. 3B).

Caspase pathway elucidation using protease inhibitors. HL-60 cells were treated with various doses of ß-lap in the presence or absence of general or caspase cleavage-site-specific inhibitors for 4 h as described in Figs. 1-3 and in Materials and methods. Cells were washed and incubated in media containing protease inhibitors for an additional 5 h. Cell extracts were then monitored for PARP cleavage (Fig. 4). All doses of ß-lap stimulated PARP cleavage above DMSO-basal levels (Fig. 4 lanes marked '-'). Addition of zVAD-fmk or zDEVD-fmk prevented PARP cleavage in HL-60 cells exposed to DMSO alone and 1 µM ß-lap, but were not as effective in HL-60 cells exposed to 5.0 and 10 µM ß-lap. Addition of zFA-fmk, zAAD-fmk, TLCK, and TPCK did not inhibit PARP cleavage in HL-60 cells exposed to any concentration of ß-lap, nor did these inhibitors prevent basal or DMSO-mediated apoptosis (Fig. 4). Consistent with data in Fig. 3B, a low level of PARP cleavage was apparent in DMSO-treated, HL-60 control cells (Fig. 4).

Bcl-2 protects against ß-lap-mediated apoptosis in HL-60 cells. To examine the effect of Bcl-2 on ß-lap-mediated apoptosis, HL-60 cells containing a retroviral *bcl-2* expression vector (Lbcl-2SN) or LXSN vector alone (25) were treated with ß-lap or DMSO for 4 h and examined for changes in viability and cleavage of PARP and caspase 3. Viability was measured by trypan blue exclusion at 24 and 48 h post-treatment (Fig. 5A), as described (25). Cells transduced with the LXSN empty vector exhibited a 30-60% decrease in viability, after various doses of ß-lap, in 24 or 48 h post-treatment. In contrast, HL-60 cells transduced with *bcl-2* (Lbcl-2SN cells) resulted in significantly higher viability after various doses of ß-lap at both 24 and 48 h. Differences

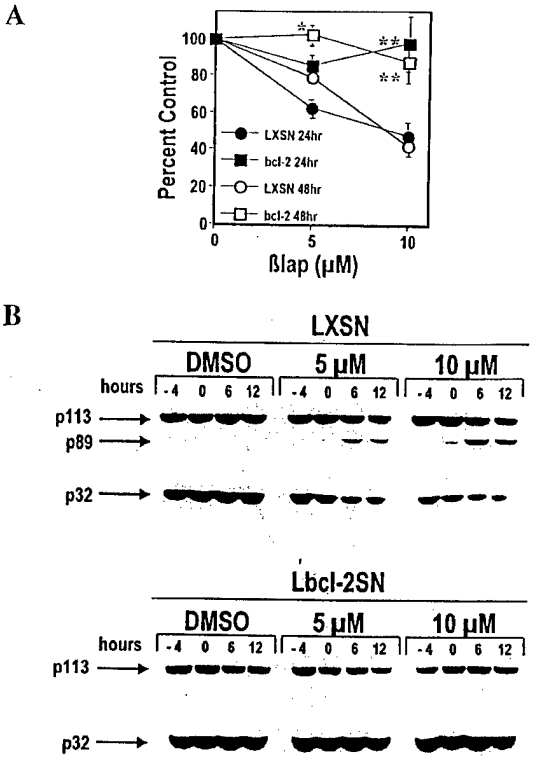

Figure 5. *bcl*-2 inhibition of PARP cleavage, caspase 3 activation and lethality induced by ß-lap. A, *bcl*-2 protected HL-60 cells against ß-lap-mediated cell death and lethality. The viability of HL-60 cells after DMSO or various concentrations of ß-lap was monitored by trypan blue exclusion at 24 and 48 h as described in the text and in Materials and methods. Cells were treated at $2x10^6$ cells/ml. Values for cell viability were expressed as percentage of control (DMSO-treated). Conditions were HL-60 cells expressing: LXSN empty vector, 24 h posttreatment, (●); LXSN empty vector, 48 h posttreatment, (○); *bcl*-2, 24 h posttreatment, (■); and *bcl*-2, 48 h posttreatment, (□). Conditions were compared using the paired t-test and values were indicated as follows: *p≤0.05; **p≤0.01. B, Western immunoblot analyses of PARP cleavage and caspase 3 activation (cleavage fragments identified are described in Figs. 3 and 4) in ß-lap-treated HL-60 cells containing retrovirally transduced *bcl*-2 (Lbcl-2SN cells) or its corresponding control containing the LXSN empty vector.

in cell viability were statistically significant for 5.0 µM ß-lap at 48 h (p≤0.05), and for 10 µM ß-lap treatments at 24 and 48 h (p≤0.01) each vs. DMSO. Extensive PARP cleavage and caspase 3 activation, with similar kinetics as observed in Fig. 3, were observed in HL-60 cells containing the LXSN empty vector following 5.0 or 10 µM ß-lap (Fig. 5B). In contrast, Lbcl-2SN cells, which overexpressed *bcl*-2, did not demonstrate visible PARP cleavage or caspase 3 activation; the steady state levels of their full-length polypeptides remained unchanged.

Apoptosis following ß-lap-related compounds. Limited structure/function analyses were performed with ß-lap, 1,2-naphthoquinone, dunnione, and α-lapachone analogs. HL-60 cells were treated with various drug doses for 4 h as indicated in Table I. Apoptosis was assessed immediately thereafter. All ß-lap analogs with chromane ring substitutions at the 3-position induced equivalent apoptosis at 1 µM except for 3-malonyl-ß-lapachone (Table I); drug concentrations between 0.5-1.0 µM represented minimal doses required for apoptosis in HL-60 cells, and no substantial differences between these related ß-lap compounds were noted (data not shown). Members of the α-lapachone family (including α-lapachone and nor-α-lapachone) induced apoptosis in HL-60 cells only after treatment with ≥100 µM.

Dunnione analogs, which are related to ß-lap but contain five-membered chromane rings, were equivalent inducers of apoptosis as ß-lap and its 3-position chromane ring-substituted analogs (Table I). Dunnione induced apoptosis at levels as low as 5 µM, while the related derivatives, dimethyl dunnione and monomethyl dunnione, induced these responses at 1 µM, equivalent to ß-lap or its 3-substituted ß-lap analogs (Table I).

In contrast, 1,2-naphthoquinone did not induce apoptosis in HL-60 cells, even after 100 µM. A sulfoxy derivative of 1,2-naphthoquinone (i.e., SO_3-naphthoquinone) induced apoptosis at 100 µM, but cell death responses were not noted at lower doses. The remaining naphthoquinone derivatives were able to induce apoptosis at concentrations similar to the most effective dunnione or ß-lap analogs tested in Table I. Apoptosis was apparent after treatment with 5 µM methoxy-, pentoxy-, and dimethylaminoethyl-1,2-naphthoquinones, but not after lower doses of these compounds. Apoptosis was also induced in HL-60 cells exposed to 1 µM isopropoxy-, isobutoxy-, isopentoxy-, allyloxy-, benzyloxy-, and cyclohexylmethoxy-1,2-naphthoquinone.

Discussion

We previously reported that ß-lapachone treatment induced p53-independent apoptosis, since cells lacking p53 expression (e.g., HL-60 cells), as well as those expressing mutant p53, were killed (1,2). The exact manner by which HL-60 cells performed the execution phase of apoptosis was, however, not defined.

A common theme arising from the study of apoptotic pathways is the activation of a cascade of proteases (e.g., caspases), which ultimately results in cleavage of substrates involved in homeostasis, repair, and the structural integrity of the cell. One commonly used marker for apoptosis is the cleavage of PARP, a DNA-repair protein thought to be involved in base excision and single and double strand break repair (28). Cleavage of PARP (113 kDa) to fragments of 89 kDa and 24 kDa has been linked to activation of caspase 3 (29). HL-60 cells treated with ß-lap demonstrated this cleavage pattern of PARP (Fig. 3A), implicating caspase 3 in this apoptotic pathway.

While suggestive of caspase activation, cleavage of apoptotic substrates is not proof that a particular protease is activated. Upon activation, the zymogen form of the caspase is cleaved into 3 fragments, two of which heterotetramerize to form the newly activated caspase (30). In HL-60 cells treated with ß-lap, cleavage of caspase 3 from its 32 kDa precursor zymogen form to a 17-kDa fragment was observed (Fig. 3B); this fragment is one of two components of the active caspase 3 protease. The dose and time-course activation data demonstrated in Figs. 3 and 4, respectively,

Table I. Induction of apoptosis by ß-lap derivatives and related compounds.

Compound	Drug treatments							
	DMSO	0.1 μM	1.0 μM	5.0 μM	10 μM	25 μM	50 μM	100 μM
ß-lapachones								
ß-lapachone	-	-	+	+	+	+	+	+
ß-nor lapachone	-	-	+	+	+	+	+	+
3-hydroxy ß-lapachone	-	-	+	+	+	+	+	+
3-allyl ß-lapachone	-	-	+	+	+	+	+	+
3-methyl ß-lapachone	-	-	+	+	+	+	+	+
3-bromo ß-lapachone	-	-	+	+	+	+	+	+
3-malonyl ß-lapachone	-	-	-	-	-	-	-	-
α-lapachones								
α-lapachone	-	-	-	-	-	-	-	+
α-nor lapachone	-	-	-	-	-	-	-	+
α-dehydro lapachone	-	-	-	-	-	-	-	-
Dunniones								
Dunnione	-	-	-	+	+	+	+	+
Dimethyl dunnione	-	-	+	+	+	+	+	+
Monomethyl dunnione	-	-	+	+	+	+	+	+
1,2-naphthoquinones								
1,2-naphthoquinone	-	-	-	-	-	-	-	-
SO_3-naphthoquinone	-	-	-	-	-	-	-	+
Methoxy naphthoquinone	-	-	-	+	+	+	+	+
Pentoxy naphthoquinone	-	-	-	+	+	+	+	+
Isopropoxy naphthoquinone		-	+	+	+	+	+	+
Isobutoxy naphthoquinone	-	-	+	+	+	+	+	+
Isopentoxy naphthoquinone	-	-	+	+	+	+	+	+
Allyloxy naphthoquinone	-	-	+	+	+	+	+	+
Benzyloxy naphthoquinone	-	-	+	+	+	+	+	+
Cyclohexylmethoxy naphthoquinone	-	-	+	+	+	+	+	+
Dimethylaminoethyl naphthoquinone	-	-	-	+	+	+	+	+

Log-phase HL-60 cells were treated with indicated compounds for 4 h. Apoptosis was monitored by the appearance of 180-200 bp oligonucleosome DNA ladders as described in Materials and methods and demonstrated for HL-60 cells treated with ß-lap (Fig. 1). The results were expressed as: (+), indicated visible apoptosis; and (-), indicated no visible DNA laddering.

strongly suggest that ß-lap treatment activates caspase 3, which subsequently gains access to the nucleus and cleaves PARP. Activation of caspase 3 following ß-lap exposure correlated well with apoptosis, in terms of time-course and dose-responses, as measured by flow cytometry and/or DNA fragmentation.

Further evidence supporting the role of caspase 3 in ß-lapachone-mediated apoptosis in HL-60 cells was obtained using specific and general protease inhibitors. ß-Lap-induced PARP cleavage in HL-60 cells was abrogated by zVAD-fmk, and partially blocked after zDEVD-fmk treatment (Fig. 4). These results support the hypothesis that caspase 3 is involved in ß-lap-induced apoptosis in HL-60 cells. However, stimulation of caspase 3 may not be the only apoptotic pathway activated in HL-60 cells following ß-lap treatment. If caspase 3 were the key component, either zVAD-fmk or

zDEVD-fmk would have prevented PARP cleavage in HL-60 cells following ß-lap. Since zDEVD-fmk only partially blocked PARP cleavage, another ß-lap-activated apoptotic protease may also cleave PARP. This is not without precedent, since caspases other than caspase 3 may cleave PARP (31). The remaining inhibitors were ineffective at preventing PARP cleavage, which suggest that the abrogation of PARP cleavage by zVAD-fmk and zDEVD-fmk was a specific phenomenon.

Bcl-2, an anti-apoptotic proto-oncogene, is an effective inhibitor of caspase 3-mediated apoptosis (20,21,32). HL-60 cells containing retrovirally-introduced *bcl*-2 did not activate caspase 3 nor cleave PARP after various doses of ß-lap. In contrast, treatment of the HL-60 cells containing the LXSN empty vector with ß-lap resulted in both caspase 3 activation and PARP cleavage (Fig. 5A), in a similar fashion as that observed in non-transduced HL-60 cells. These results suggest that Bcl-2 prevented activation of the caspase 3 apoptotic cascade, which is activated by ß-lap treatment. Although it was recently reported that *bcl*-2 expression would merely delay apoptosis after ß-lap (33), our data suggest that Bcl-2 overexpression may prevent caspase 3 activation and PARP cleavage in HL-60 cells. Bcl-2 overexpression thereby protects cells from ß-lap-induced cell death.

In an effort to find more effective drugs, we screened derivatives of ß-lap and several structurally related compounds for their ability to induce apoptosis in HL-60 cells. All 3-position-substituted ß-lap derivatives, with the exception of 3-malonyl-ß-lap, elicited equivalent apoptotic responses. The minimal concentrations required to induce apoptosis were identical to those induced by ß-lap. The lack of an apoptotic response in HL-60 cells treated with 3-malonyl-ß-lap could be attributed to the polarity of the sidegroup, which may have affected the ability of the compound to enter the cell. Interestingly, the α-lapachone isomer and its derivatives did not activate apoptosis in HL-60 cells, and a lack of activity of these compounds as radiosensitizers or as inhibitors of the Topo I enzyme *in vitro* was reported (34). These data indicate that either the lower chromane ring of ß-lap or the neighboring keto groups may be essential for apoptosis induced by ß-lap. Similar conclusions were reached for the radiosensitizing properties of ß-lap (34). None of the ß-lap-related compounds were more effective apoptosis-inducing agents than ß-lap.

Dunnione and its derivatives, which contain five-membered instead of six-membered chromane rings, were nearly as effective as ß-lap at inducing apoptosis in HL-60 cells. Loss of the lower chromane ring, but retention of the keto groups in 1,2-naphthoquinone and its sulfur-containing derivative, made the compound inactive. Unexpectedly, addition of various groups to the 1,2-naphthoquinone base compound restored apoptotic responses in HL-60 cells. 1,2-Naphthoquinone analogs containing methyl-, pentyl-, dimethyl amino-, or ethyl-side groups caused apoptosis in HL-60 cells similar to that (in terms of effective drug concentration) observed following ß-lap. These data indicate that a number of compounds related to ß-lap were able to induce apoptosis, but none were better than ß-lap. These compounds may be useful in future development of this class of apoptosis-inducing compounds.

Finally, it was recently reported that ß-lap, as well as 1,2-naphthoquinone and its derivatives, could inhibit Topo IIα and cause DNA double strand breaks, and that this may be the mechanism by which these compounds act (4). Our data do not appear to be consistent with this mechanism, since a) neither ß-lap nor 1,2-naphthoquinone treatment of HL-60 cells caused apparent cell cycle changes (i.e., G_1 or G_2 arrests), which are characteristic of many DNA damaging agents (35); and b) ß-lap and 1,2-naphthoquinone derivatives caused very different concentration-dependent apoptosis in HL-60 cells, with minimal cytotoxicity noted after 100 μM 1,2-naphthoquinone.

Thus, we show that the pathway through which HL-60 cells undergo ß-lap-mediated programmed cell death involves the activation of caspase 3, which subsequently leads to signature proteolytic substrate cleavage responses *in vivo* (e.g., formation of an 89 kDa fragment of PARP). These apoptotic responses were prevented by the peptide inhibitors, zVAD-fmk and zDEVD-fmk, and most importantly by the overexpression of the anti-apoptotic proto-oncogene, *bcl*-2. Therefore, Bcl-2 levels in tumor cells may be an important determinant of ß-lap efficacy in leukemic cells; however, even highly overexpressed bcl-2 protein levels did not completely protect cells, suggesting that additional unknown factors influence the cell death responses to ß-lap.

Acknowledgments

The authors are grateful to Ms. Lisa Mueller for her outstanding technical assistance. This work was initiated at the University of Wisconsin-Madison and completed at Case Western Reserve University. We are grateful to Drs Paul Friesen and Clark Distelhorst for their helpful discussions. This work was supported by a grant from the CaPCURE Foundation, grant #BC971431, from the US Army Medical Research and Material Command Breast Cancer Initiative to D.A.B., and by the efforts of Mrs. Sara Hildebrand and the Breast Cancer Inspiration and Breast Cancer Funds.

References

1. Planchon SM, Wuerzberger S, Frydman B, Witiak DT, Hutson P, Church DR, Wilding G and Boothman DA: Beta-lapachone-mediated apoptosis in human promyelocytic leukemia (HL-60) and human prostate cancer cells: a p53-independent response. Cancer Res 55: 3706-3711, 1995.
2. Li CJ, Wang C and Pardee AB: Induction of apoptosis by beta-lapachone in human prostate cancer cells. Cancer Res 55: 3712-3715, 1995.
3. Amaral ACF and Barnes RA: The total synthesis of ß-lapachone. J Heterocycl Chem 29: 1457-1460, 1992.
4. Frydman B, Marton LJ, Sun JS, Neder K, Witiak DT, Liu AA, Wang HM, Mao Y, Wu HY, Sanders MM and Liu LF: Induction of DNA topoisomerase II-mediated DNA cleavage by beta-lapachone and related naphthoquinones. Cancer Res 57: 620-627, 1997.
5. Li CJ, Averboukh L and Pardee AB: beta-lapachone, a novel DNA topoisomerase I inhibitor with a mode of action different from camptothecin. J Biol Chem 268: 22463-22468, 1993.
6. Furuya Y, Ohta S and Ito H: Apoptosis of androgen-independent mammary and prostate cell lines induced by topoisomerase inhibitors: common pathway of gene regulation. Anticancer Res 17: 2089-2093, 1997.
7. Dubrez L, Goldwasser F, Genne P, Pommier Y and Solary E: The role of cell cycle regulation and apoptosis triggering in determining the sensitivity of leukemic cells to topoisomerase I and II inhibitors. Leukemia 9: 1013-1024, 1995.

8. Loughlin S, Gandhi V, Plunkett W and Zwelling LA: The effect of 9-beta-D-arabinofuranosyl-2-fluoroadenine and 1-beta-D-arabinofuranosylcytosine on the cell cycle phase distribution, topoisomerase II level, mitoxantrone cytotoxicity, and DNA strand break production in K562 human leukemia cells. Cancer Chemother Pharmacol 38: 261-268, 1996.
9. Wuerzberger SM, Pink JJ, Planchon SM, Byers KL, Bornmann WG and Boothman DA: Induction of apoptosis in MCF-7-WS8 breast cancer cells by beta-lapachone. Cancer Res 58: 1876-1885, 1998.
10. Kerr J, Wyllie AH and Currie AR: Apoptosis: a basic biological phenomenon with wide-ranging implications in tissue kinetics. Br J Cancer 26: 239-257, 1972.
11. Cohen JJ: Apoptosis. Immunol Today 14: 126-130, 1993.
12. Compton MM: A biochemical hallmark of apoptosis: internucleosomal degradation of the genome. Cancer Metastasis Rev 11: 105-119, 1992.
13. Alnemri ES, Livingston DJ, Nicholson DW, Salvesen G, Thornberry NA, Wong WW and Yuan J: Human ICE/CED-3 protease nomenclature (letter). Cell 87: 171, 1996.
14. Srinivasula SM, Fernandes-Alnemri T, Zangrilli J, Robertson N, Armstrong RC, Wang L, Trapani JA, Tomaselli KJ, Litwack G and Alnemri ES: The Ced-3/interleukin 1beta converting enzyme-like homolog Mch6 and the lamin-cleaving enzyme Mch2alpha are substrates for the apoptotic mediator CPP32. J Biol Chem 271: 27099-27106, 1996.
15. Casiano CA, Martin SJ, Green DR and Eng MT: Selective cleavage of nuclear autoantigens during CD95 (Fas/Apo-1)-mediated T cell apoptosis. J Exp Med 184: 765-770, 1996.
16. Talanian RV, Quinlan C, Trautz S, Hackett MC, Mankovich JA, Banach D, Ghayur T, Brady KD and Wong WW: Substrate specificities of caspase family proteases. J Biol Chem 272: 9677-9682, 1997.
17. Slee EA, Zhu H, Chow SC, MacFarlane M, Nicholson DW and Cohen GM: Benzyloxycarbonyl-Val-Ala-Asp (OMe) fluoromethylketone (Z-VAD.FMK) inhibits apoptosis by blocking the processing of CPP32. Biochem J 315: 21-24, 1996.
18. Bakhshi A, Jensen JP, Goldman P, Wright JJ, McBride OW, Epstein AL and Korsmeyer SJ: Cloning the chromosomal breakpoint of t(14;18) human lymphomas: clustering around JH on chromosome 14 and near a transcriptional unit on 18. Cell 41: 899-906, 1985.
19. Boise LH, Gottschalk AR, Quintans J and Thompson CB: Bcl-2 and Bcl-2-related proteins in apoptosis regulation. Curr Top Microbiol Immunol 200: 107-121, 1995.
20. Monney L, Otter I, Olivier R, Ravn U, Mirzasaleh H, Fellay I, Poirier GG and Borner C: Bcl-2 overexpression blocks activation of the death protease Cpp32/Yama/Apopain. Biochem Biophys Res Commun 221: 340-345, 1996.
21. Shimizu S, Eguchi Y, Kamiike W, Matsuda H and Tsujimoto Y: Bcl-2 expression prevents activation of the ice protease cascade. Oncogene 12: 2251-2257, 1996.
22. Distelhorst CW and McCormick TS: Bcl-2 acts subsequent to and independent of Ca^{2+} fluxes to inhibit apoptosis in thapsigargin- and glucocorticoid-treated mouse lymphoma cells. Cell Calcium 19: 473-483, 1996.
23. Kluck RM, Bossy-Wetzel E, Green DR and Newmeyer DD: The release of cytochrome c from mitochondria: a primary site for Bcl-2 regulation of apoptosis (see comments). Science 275: 1132-1136, 1997.
24. Li P, Nijhawan D, Budihardjo I, Srinivasula SM, Ahmad M, Alnemri ES and Wang XD: Cytochrome C and dATP-dependent formation of Apaf-1/caspase-9 complex initiates an apoptotic protease cascade. Cell 91: 479-489, 1997.
25. Park JR, Robertson K, Hickstein DD, Tsai S, Hockenbery DM and Collins SJ: Dysregulated *bcl*-2 expression inhibits apoptosis but not differentiation of retinoic acid-induced HL-60 granulocytes. Blood 84: 440-445, 1994.
26. Lotem J and Sachs L: Differential suppression by protease inhibitors and cytokines of apoptosis induced by wild-type p53 and cytotoxic agents (published erratum appears in Proc Natl Acad Sci USA 94: 1603, 1997). Proc Natl Acad Sci USA 93: 12507-12512, 1996.
27. Darzynkiewicz Z, Li X and Gong J: Assays of cell viability: discrimination of cells dying by apoptosis. Methods Cell Biol 41: 15-38, 1994.
28. Lindahl T, Satoh MS, Poirier GG and Klungland A: Post-translational modification of poly(ADP-ribose) polymerase induced by DNA strand breaks. Trends Biochem Sci 20: 405-411, 1995.
29. Tewari M, Quan LT, O'Rourke K, Desnoyers S, Zeng Z, Beidler DR, Poirier GG, Salvesen GS and Dixit VM: Yama/CPP32 beta, a mammalian homolog of CED-3, is a CrmA-inhibitable protease that cleaves the death substrate poly(ADP-ribose) polymerase. Cell 81: 801-809, 1995.
30. Hale AJ, Smith CA, Sutherland LC, Stoneman VE, Longthorne V, Culhane AC and Williams GT: Apoptosis: molecular regulation of cell death. Eur J Biochem 236: 1-26, 1996.
31. Gu Y, Sarnecki C, Aldape RA, Livingston DJ and Su MS: Cleavage of poly(ADP-ribose) polymerase by interleukin-1 beta converting enzyme and its homologs TX and Nedd-2. J Biol Chem 270: 18715-18718, 1995.
32. Cosulich SC, Green S and Clarke PR: Bcl-2 regulates activation of apoptotic proteases in a cell-free system. Curr Biol 6: 997-1005, 1996.
33. Chau Y-P, Shiah S-G, Don M-J and Kuo M-L: Involvement of hydrogen peroxide in topoisomerase inhibitor ß-lapachone-induced apoptosis and differentiation in human leukemia cells. Free Radic Biol Med 24: 660-670, 1998.
34. Boothman DA, Trask DK and Pardee AB: Inhibition of potentially lethal DNA damage repair in human tumor cells by beta-lapachone, an activator of topoisomerase I. Cancer Res 49: 605-612, 1989.
35. Paulovich AG, Toczyski DP and Hartwell LH: When checkpoints fail. Cell 88: 315-321, 1997.

ß-Lapachone-Induced Apoptosis in Human Prostate Cancer Cells: Involvement of NQO1/xip3

Colleen Tagliarino[1], Sarah M. Planchon[1], John J. Pink, William G. Bornmann, Marie E. Varnes, and David A. Boothman[3]

Departments of Radiation Oncology and Pharmacology, Ireland Comprehensive Cancer Center, Laboratory of Molecular Stress Responses, Case Western Reserve University, 10900 Euclid Avenue, Cleveland, Ohio 44106-4942 [C.T., S.M.P., J.J.P., M.E.V., and D.A.B.]; and Preparative Synthesis Core Facility, Memorial Sloan Kettering Cancer Center, New York, New York 10021 [W.G.B.]

Running Title: ***ß-Lap-mediated, NQO1-dependent apoptosis***

Key Words: ß-lapachone, apoptosis, NQO1, x-ray-inducible protein #3 (xip3), Prostate Cancer, atypical PARP cleavage, p53 cleavage.

Footnotes:

[1]These authors have contributed equally to the completion of this manuscript.

[2]Support for this research was provided by grants from the United States Army Medical Research and Materiel Command Breast Cancer Initiative: Idea Award #DAMD17-

98-1-8260 to D.A.B and a Post-doctoral Fellowship #DAMD17-97-1-7221 to J.J.P. We were also grateful for support for S.M.P. from the Human Oncology Training Grant, Department of Human Oncology, University of Wisconsin-Madison.

[3]To whom reprint requests and other inquiries should be addressed at: Departments of Radiation Oncology and Pharmacology, Ireland Comprehensive Cancer Center, Laboratory of Molecular Stress Responses, Case Western Reserve University, 10900 Euclid Avenue, Cleveland, Ohio 44106-4942, Tel.: (216) 368-0840, Fax: (216) 368-1142, e-mail: dab30@po.cwru.edu.

[4]Abbreviations: ß-lap, ß-lapachone; b5R, NADH:cytochrome b5 reductase; CFA, colony forming ability; CPT, camptothecin; DMEM, Dulbecco's minimal essential medium; NQO1, NAD(P)H:quinone oxidoreductase 1; PARP, poly(ADP-ribosyl) polymerase; P450, NADH:cytochrome P-450 reductase; SD, standard deviation; TUNEL, Terminal dUTP N-terminal End Labeling; zVAD-fmk, benzyloxycarbonyl-val-ala-asp (OMe) fluoromethylketone;.

Abstract

ß-Lapachone (ß-lap) induces apoptosis in various cancer cells and its intracellular target has just recently been elucidated in breast cancer cells. Here we show that NAD(P)H:quinone oxidoreductase (NQO1/xip3) expression in human prostate cancer cells is also a key determinant for apoptosis and lethality after ß-lap exposures, showing this is not specific to breast cancer cells, but is rather a general mechanism of activation for the drug. ß-Lap-treated, NQO1-deficient LNCaP cells were significantly more resistant to apoptosis and lethality as compared to NQO1-expressing DU-145 or PC-3 cells after equimolar drug exposures. Formation of an atypical 60 kDa poly (ADP-ribosyl) polymerase (PARP) cleavage fragment in DU-145 or PC-3 cells was induced after 10 μM ß-lap and correlated with apoptotic cells. In contrast, LNCaP cells required 25μM ß-lap to induce similar responses. Atypical PARP cleavage in ß-lap-treated cells was not affected by 100 μM zVAD-fmk, a global caspase inhibitor, that prevented apoptosis-related, 89 kDa PARP fragmentation after camptothecin. Co-administration of dicoumarol, a specific inhibitor of NQO1, reduced ß-lap-mediated cytotoxicity, apoptosis, and atypical PARP cleavage in NQO1-expressing cells. Dicoumarol did not affect the more ß-lap-resistant LNCaP cells. Dicoumarol did not affect apoptosis, lethality or typical PARP cleavage in any cell lines examined after camptothecin.

Stable transfection of LNCaP cells with NQO1 significantly increased their sensitivity to ß-lap, enhancing apoptotic DNA fragmentation, atypical PARP cleavage and lethality as compared to parental LNCaP cells or vector alone transfectants.

Dicoumarol abrogated these responses and increased survival of ß-lap-treated NQO1-expressing LNCaP transfectants. Dicoumarol did not affect ß-lap-resistant LNCaP vector alone or parental cells. Thus, NQO1 activity is a key determinant of ß-lap-mediated apoptosis and cytotoxicity. Identification of NQO1 as a key intracellular target for ß-lap in multiple cell lines should allow the drug's development as an antitumor agent and may explain its radiosensitizing capacity; NQO1 was identified by our laboratory as X-ray-inducible gene/protein #3 (xip3).

Introduction

ß-Lapachone (ß-lap, 3,4-dihydro-2,2-dimethyl-2*H*-naphtho[1,2-b]pyran-5,6-dione) is a naturally occurring *o*-naphthoquinone present in the bark of the Lapacho tree (*Tabebuia avellanedae*) native to South America. The purified drug has anti-trypanosomal, -fungal, -tumor, and -HIV properties, and induces apoptosis in a variety of cell types (1). The mechanism of action and intracellular target(s) of the compound have, however, remained elusive and have prevented the preclinical development of this drug for use as an antitumor or antiviral agent until recently. We have recently shown in breast cancer cell lines that the enzymatic activity of NQO1 is a key determinant for β-lap mediated cytotoxicity (2). Using a series of assays *in vitro*, proposed mechanisms of action for this drug have included: (a) activation of Topoisomerase (Topo) I (3); (b) induction of apoptosis (4) (c) inhibition of Topo I (1, 5, 6); (d) inhibition of Topo II-alpha (7); and (e) suppression of NF-κB activation (8). ß-Lap can induce apoptosis in several cell systems, including leukemic (HL-60), prostate, and breast cancer cell lines (1, 4, 5). The apoptotic response caused by ß-lap was independent of both p53 status and androgen dependence in human prostate cancer cell lines (1). Camptothecin (CPT), a Topo I poison, can also induce apoptosis but to a lesser degree than ß-lap (4).

Apoptosis is a genetically programmed form of cell death, whose initiation and execution is thought to be the basis of lethality caused by many chemotherapeutic agents (9-11). Cells undergoing apoptosis exhibit characteristic changes, including cell shrinkage, membrane blebbing, chromatin condensation, internucleosomal DNA cleavage, and cleavage of specific intracellular substrates involved in cell structure, DNA repair [e.g., poly(ADP-ribosyl) polymerase (PARP)], and general homeostasis. These

intracellular alterations are often the result of activation of a family of apoptotic proteases, including caspases (12-16) and/or calpains [Wolf, 1999 #140; Wood, 1999 #141; Squier, 1999 #142; Squier, 1994 #143].

Caspases are activated by multiple signaling pathways during apoptosis and typically result in the cleavage of PARP; the full-length 113 kDa polypeptide is cleaved to diagnostic 89kDa and 24 kDa proteins (17). CPT appears to induce an apoptotic pathway that includes activation of the caspases, leading to classical PARP cleavage (18). HL-60 cells treated with ß-lap also activated the caspases (19), however, a different cell death response appeared to be stimulated by the drug in various human breast cancer cells (4, 20). In many breast cancer (especially MCF-7:WS8) cells, an atypical PARP fragmentation *in vivo* was noted at times and doses correlating with apoptosis; apoptotic responses were monitored by DNA fragmentation (TUNEL positive cells), dephosphorylation of pRb, typical lamin B cleavage, atypical PARP cleavage, and cleavage of mutant or wild-type p53. ß-Lap-mediated apoptosis was proposed to involve the activation of calpain due to the specific calcium-dependent cleavage of both p53 and PARP (20). Interestingly, only global cysteine protease inhibitors and calcium chelators have been able to block apoptosis and proteolytic cleavage of downstream substrates following transient (4 h) ß-lap exposures in human epithelial cancer cell lines(20)and Tagliarino *et al* unpublished data).

NAD(P)H:quinone reductase (NQO1, DT Diaphorase, xip3, EC 1.6.99.2) is a flavoenzyme that catalyzes the two-electron reduction of quinones into their subsequent hydroquinone form, bypassing the often mutagenic semiquinone intermediate and the formation of free radicals (21, 22). NQO1 detoxifies many quinones, [e.g., menadione

(23, 24)], and bioactivates other compounds, such as Mitomycin C, Streptonigrin or E09 (25-28).

NQO1/xip3 gene expression is widespread, with detectable levels in human heart, brain, placenta, lung, skeletal muscle, kidney, and pancreatic tissue, and low or absent levels in human liver (21). More importantly, NQO1 levels were significantly up-regulated (5- to 20-fold above adjacent normal tissue) in several forms of cancer, including breast and non-small cell lung tumors (29-31). Such elevations in certain cancers make NQO1 a potential target for the development of tumor-directed therapies potentially involving ß-lap or its derivatives (19). Recently, our laboratory discovered that NQO1 was the key determinant of β-lap cytotoxicity in human breast cancer cell lines (2). In this report, we demonstrate that NQO1 is also a key determinant of ß-lap-induced apoptosis and lethality in human prostate cancer cell lines, suggesting a general mechanism of activation for the compound. Variations in NQO1 activity dramatically affected the sensitivity of human prostate cancer cell lines to ß-lap as determined by comparing various cell lines expressing different levels of the enzyme, transfection of NQO1 expression vectors into enzyme-deficient cells, and/or by the use of an NQO1 inhibitor, dicoumarol. Co-administration of the NQO1 inhibitor, dicoumarol, abrogated ß-lap-mediated cytotoxicity and downstream apoptotic endpoints in NQO1-expressing, but not in NQO1-deficient, human prostate cancer cell lines. Transfection of NQO1-deficient LNCaP cells with NQO1 significantly enhanced sensitivity (apoptosis, substrate proteolysis, and lethality) to ß-lap, which was subsequently blocked by dicoumarol co-administration.

Materials and Methods

Compounds and Drug Preparations. ß-Lap was synthesized and dissolved in DMSO as described (1). CPT and dicoumarol were obtained from Sigma Chemical Company (St. Louis, MO), prepared in DMSO or water respectively, and drug concentrations were determined spectrophotometrically (4). zVAD-fmk was obtained from Enzyme Systems Products (Dublin, CA). Control treatments containing an equivalent percentage of DMSO were included as described (1, 3, 4). The highest DMSO concentration used was 0.2%, which did not affect survival, cell growth or apoptosis in various human breast or prostate cancer cells examined (1, 3, 4).

Cell Culture Conditions. PC-3, DU-145, and LNCaP human prostate cancer cells were obtained from Dr. George Wilding (Univ. Wisconsin-Madison) and grown in Dulbecco's minimal essential medium (DMEM) with 5% FBS at 37 °C in an humidified 5% CO_2-95% air atmosphere as described (32-34). Tests for mycoplasma infection, using the Gen-Probe™ Rapid Detection Kit (Fisher Scientific, Pittsburgh, PA), were performed quarterly and all cell lines were negative.

Drug Treatments. For all experiments, cells were plated, allowed at least 24 h to initiate log-phase growth, and were then exposed to ß-lap or CPT at indicated doses for four hours (4-h). After exposure, drug-containing media were removed and replaced with complete media. Dicoumarol was administered (50 μM) concomitantly with ß-lap or CPT for 4-h as described above. For zVAD-fmk exposures, cells were pretreated with 100 μM zVAD-fmk for 30 mins or treated with media alone. ß-lap or CPT was then co-

administered in the presence or absence of zVAD-fmk for 4-h. All drug-containing media was then removed and replaced with media containing 100 μM zVAD-fmk alone or with fresh, non-drug-containing media.

Stable Transfection of LNCaP Cells With NQO1. Log-phase LNCaP cells were seeded onto 6-well dishes at 2 x 10^5 cells/well and allowed to attach overnight. The following day, 1.0 μg of BE8 plasmid DNA, containing human NQO1 cDNA under the control of the CMV promoter in the pcDNA3 constitutive expression vector (35), was added into each of three wells using standard calcium phosphate transfection methodology (36). After two days growth without selection, cells were exposed to 350 μg/ml Geneticin® (G418, Gibco BRL, Gaithersburg, MD). A stable, pooled population was established after approximately three weeks growth in media containing 350 μg/ml G418. Clonal transfectants were finally derived from the pooled population by limiting dilution cloning. Isolated transfectants were then analyzed for NQO1 expression and enzymatic activity as described below and in 'Results'.

Colony Forming Ability (CFA) Assays. Anchorage–dependent CFA assays were performed (3, 37). For CFA assays, cells were seeded at 1-2000 viable cells per dish in 35 mm^2 tissue culture plates (with grids) and incubated overnight. Plated cells were then treated with equal volumes of media containing ß–lap at various concentrations for 4-h. Control cells were treated with DMSO equivalent to the highest dose of ß-lap used. ß-Lap exposures in the presence or absence of 50 μM dicoumarol or other inhibitors were performed as indicated above, and in 'Results'. Colonies were allowed to grow for 10-14 days, with one change of medium at day seven. Plates were stained with 1.0 % crystal

violet in 20% EtOH, destained with water, and colonies of >50 normal-appearing cells were counted (3, 37).

TUNEL Assays. Flow cytometric analyses were performed in combination with TUNEL assays, to measure DNA fragmentation, sub-G_0/G_1 cell populations, and changes in cell cycle distribution following various drug treatments. TUNEL assays were performed using APO-DIRECT™, as described by the manufacturer (Phoenix Flow Systems, Inc. San Diego, CA). Samples were analyzed in an EPICS Elite ESP flow cytometer using an air-cooled argon laser at 488 nm, 15 mW (Beckman Coulter Electronics, Miami, FL). Propidium iodide was read with a 640 nm long pass optical filter. FITC was read with a 525 nm band pass filter. Sample analyses were performed using the Elite acquisition software provided with the instrument. Data were analyzed using ModFit (Verity Software House, Inc., Topsham, ME) (1, 4, 19). Results presented were mean $\pm$SD for at least three separate experiments, repeated in duplicate.

Western Immunoblot Analyses. Control or treated human prostate cancer cells were examined for changes in PARP, p53, and lamin B, and for levels of NQO1. Actin was used as a loading control. Briefly, control or treated cells were washed in ice-cold PBS and lysed in loading buffer [62.5 mM Tris, pH 6.8; 6M urea; 10% glycerol; 2% SDS; 0.003% bromophenol blue; 5% 2-mercaptoethanol (freshly added)]. Samples were sonicated with a Fisher Scientific Sonic Dismembrator (model 550) fitted with a microtip probe, and stored at -20 °C for later analyses as described (19). Equivalent amounts of protein were incubated at 65 °C for 15 mins and polypeptides were separated by SDS-PAGE. Separated proteins were then transferred to Immobilon-P membranes (Millipore,

Danvers, MA) and equivalent protein loading was confirmed by Ponceau S staining [0.2% Ponceau S (w/v) in 3% trichloroacetic acid (w/v) and 3% sulfosalicylic acid (w/v)] (Sigma Chemicals, St Louis, MO) using standard techniques. Western immunoblots were treated with PBS containing 0.2% Tween 20 and 10% FBS for 1 h to prevent nonspecific binding. Membranes were then incubated overnight with primary antibodies diluted in the same buffer at 4 °C. Primary antibodies included separate, and sometimes in combination, exposures to anti-PARP C2-10 (Enzyme Systems Products, Dublin, CA), anti-p53 DO-1 (Santa Cruz Biotechnology, Santa Cruz, CA), anti-lamin B (Calbiochem, San Diego, CA), and anti-actin (Amersham Pharmacia Biotech, Piscataway, NJ). An NQO1 antibody was contained in medium from a mouse hybridoma, Clone A180, and used according to previously published procedures (38). Membranes were washed in PBS containing 0.2% Tween and then incubated with horseradish peroxidase-conjugated secondary antibody (Santa Cruz Biotechnology, Santa Cruz, CA) for one hour. Western immunoblots were then washed in PBS containing 0.2% Tween, developed with enhanced chemiluminescence (ECL) substrate (Amersham, Arlington Heights, IL), and exposed to Fuji X-ray film. All Western immunoblots shown below are representative of experiments repeated at least three times.

Preparation of S9 supernatants. Cellular extracts for enzyme assays were prepared from cells in mid- to late-log phase growth. Cells were harvested by trypsinization (0.25% trypsin and 1 mM EDTA), washed twice in ice-cold, phenol red-free Hank's balanced salt solution, and resuspended in a small volume of PBS, pH 7.2, containing 10 μg/μl aprotinin. Cell suspensions were sonicated four times on ice using 10-sec. pulses,

then centrifuged at 14000 x *g* for 20 min. S9 supernatants were aliquoted into microfuge tubes and stored at -80 °C for later use as described below.

NQO1, Cytochrome b5 reductase (b5R), and Cytochrome P450 (P450) enzyme assays. Three general reductase enzyme assays were assayed as described (39, 40). Enzyme reactions contained 77 μM cytochrome c (practical grade, Sigma Chemical Co., St. Louis, MO) and 0.14% bovine serum albumin in Tris-HCl buffer (50 mM, pH 7.5). NQO1 activity was measured using NADH (200 μM) as the immediate electron donor and menadione (10 μM) as the intermediate electron acceptor. Each assay was repeated in the presence of 10 μM dicoumarol, and activity attributed to NQO1 was that inhibited by dicoumarol (41). NADH:cytochrome b5 reductase (b5R) was measured using NADH (200 μM) as the electron donor, and NADH:cytochrome P-450 reductase (P450) was measured using NADPH (200 μM) as the electron donor (42) in a Beckman DU 640 spectrophotometer (Beckman Coulter, Fullerton, CA). Reactions were performed at 37 °C, and were initiated by addition of S9 supernatants. Varying amounts (10 to 40 μl) of S9 supernatants were used to ensure linearity of enzyme rates with protein concentration. Enzyme activities were calculated as nmoles cytochrome c reduced/min/mg protein, based on the initial rate of change in OD at 550 nm. An extinction coefficient of 21.1 mM/cm was used for cytochrome c.

Results

Dicoumarol enhanced the survival of DU-145 or PC-3, but not LNCaP, cells following ß-lap exposure. While testing various chemical and peptide inhibitors for their abilities to protect against ß-lap-induced cytotoxicity, we noted that co-administration of dicoumarol conferred significant resistance to DU-145 or PC-3 cells. Dicoumarol significantly enhanced the survival of ß-lap-treated DU-145 or PC-3 cells (Fig. 1). The LD_{90} values for DU-145 and PC-3 cells were increased (i.e., the drug was less toxic) by 3- and 2-fold, respectively, as compared to β-lap alone. For example, over 95% lethality was noted in DU-145 cells treated with 4.0 μM ß-lap, whereas the same ß-lap exposure was ineffective (>95% survival) when 50 μM dicoumarol was co-administered. In contrast, dicoumarol had no influence on the survival of ß-lap-treated LNCaP cells, which also exhibited more intrinsic resistance to ß-lap-mediated lethality (LD_{90}= 7.0 μM) when compared to DU-145 (LD_{90}=3.5 μM) or PC-3 (LD_{90}=5.0 μM) cells. ß-Lap-treated LNCaP cells also exhibited 3-fold less apoptosis than either DU-145 or PC-3 cells when exposed to equitoxic concentrations (1). In contrast, dicoumarol co-administration did not affect the survival of LNCaP, DU-145 or PC-3 cells following CPT exposures (Fig. 1A).

Dicoumarol blocked morphologic changes and apoptosis of DU-145 cells after ß-lap treatment. In human breast cancer cells, ß-lap induced morphologic changes indicative of apoptosis (4). Similar alterations in morphology, such as chromatin condensation, cell shrinkage, and detachment, occurred in DU-145 or PC-3 cells following 4 h ß-lap exposures (shown are DU-145 cells, Fig. 2A). As with ß-lap-treated human breast cancer cells, no evidence of cell lysis during ß-lap-mediated apoptosis in DU-145 or PC-3 cells

was noted, suggesting that cell death was not necrotic in nature. Addition of 50 μM dicoumarol significantly blocked ß-lap-induced morphologic changes (Fig. 2A) and cells grew normally, consistent with enhanced survival as measured using CFA assays (Fig. 1).

We previously demonstrated the formation of an apoptotic sub-G_0/G_1 peak in human prostate or breast cancer cell lines following ß-lap treatment. DU-145 or PC-3 cells underwent apoptosis, in contrast, LNCaP cells showed significantly lower levels of cell death (1). To further characterize cell death responses in human prostate cancer cell lines after exposure to ß-lap or CPT, TUNEL assays were performed to monitor apoptotic-related DNA fragmentation, with or without dicoumarol (Fig. 2B). ß-Lap-treated DU-145 or PC-3 cells exhibited the formation of TUNEL positive cells (71.3% and 82.2%, respectively). ß-Lap-mediated apoptotic reactions were completely abrogated by dicoumarol co-treatments. In contrast, ß-lap-treated LNCaP cells showed a much lower percentage of cells staining positive with the TUNEL assay (28.1%), consistent with prior data (1) and co-administration of dicoumarol did not affect ß-lap-mediated responses in these cells. Treatment of each cell line with CPT resulted in only modest apoptosis (i.e., 22-43% TUNEL-positive cells), as previously described (4) and predictably, CPT-induced apoptosis was not affected by dicoumarol co-treatments (Fig 2B).

Apoptotic substrate cleavage events in human prostate cancer cells after ß-lap exposure. Human prostate cancer cell lines treated with ß-lap exhibited the formation of an atypical ~60 kDa PARP polypeptide, in contrast to classical, CPT-induced, and caspase-mediated, 89 kDa PARP cleavage (Fig. 3A, open arrow). Atypical 60 kDa PARP fragmentation was apparent in DU-145 and PC-3 cells treated with 10 μM ß-lap

(Fig. 3A, open arrow) and correlated well with apoptosis as monitored by TUNEL assays (Fig. 2), consistent with similar responses in human breast cancer cells (2, 20). Furthermore, formation of ß-lap-induced PARP cleavage was completely blocked by co-administration of 50 μM dicoumarol (Fig. 3A), consistent with this NQO1 inhibitor's ability to prevent ß-lap-mediated apoptosis (Fig. 2) and lethality (Fig. 1). The more ß-lap-resistant LNCaP cells required a greater concentration of ß-lap (25 μM) to induce an identical atypical PARP cleavage fragment. Co-administration of dicoumarol with ß-lap did not significantly affect the formation of the 60 kDa PARP cleavage fragment in ß-lap-treated LNCaP cells (Fig. 3A). In contrast, all three human prostate cancer cell lines exhibited the formation of an 89 kDa PARP cleavage fragment (Fig. 3A, closed arrow) after 10 μM CPT exposures, in direct proportion to the level of apoptosis observed (Fig. 2B). Dicoumarol co-administration had no effect on classical, caspase-mediated PARP cleavage after CPT exposures.

Global caspase inhibitors, such as zVAD-fmk, can prevent the activation of many of the caspases and their downstream events (i.e., substrate proteolysis and cell death) (43). As expected, addition of 100 μM zVAD-fmk completely abrogated the formation of CPT-induced, PARP fragmentation (89 kDa), occurring in direct response to apoptosis induced by this agent (Fig. 3B). In contrast, atypical PARP fragmentation noted in ß-lap-treated DU-145 cells (open arrow) was not affected by 100 μM zVAD-fmk, suggesting that either ß-lap induces a non-caspase-mediated pathway, or that zVAD-fmk cannot inhibit this particular caspase-mediated pathway (Fig. 3B).

Cleavage of lamin B (60 kDa full-length protein) to a characteristic 46 kDa polypeptide, typically by caspase 6, is believed to aid in the breakdown of the

architecture necessary for apoptosis-related nuclear condensation and membrane blebbing (44, 45). Cleavage of lamin B in ß-lap-treated MCF-7:WS8 cells was noted (4). In DU-145 cells, ß-lap- but not CPT-treatment resulted in lamin B cleavage, possibly due to the relatively poor apoptotic responses induced by CPT compared to ß-lap. Interestingly, 100 μM zVAD-fmk, the pan-caspase inhibitor, did not inhibit ß-lap-mediated cleavage of lamin B (Fig. 3B). These data are consistent with prior data from our laboratory that ß-lap can stimulate a non-caspase-mediated, cysteine protease-directed apoptotic pathway in certain human cancer cells (20).

We previously showed that p53 is not necessary for ß-lap-induced apoptosis (1). In fact, we reported that the basal level of p53 *decreased* following treatment of wild-type p53-expressing MCF-7 breast cancer cells following 4-10 μM ß-lap (4). In mutant p53-expressing DU-145 cells, ß-lap treatment resulted in the formation of two cleavage fragments (40 kDa and ~20 kDa) that were not inhibited by 100 μM zVAD-fmk co-administration (Fig. 3B). A similar cleavage of p53 has been described during calpain-mediated apoptosis, and this protease may be involved in ß-lap-mediated cell death responses (20). Treatment of DU-145 cells with CPT did not result in any changes in the level or cleavage of p53, even though 20% of the cells were apoptotic (i.e., TUNEL-positive); DU-145 cells express stable, high levels of mutant p53 protein whose levels are not stabilized by CPT-mediated damage.

Expression of NQO1 and p53 in Human Prostate Cancer Cells. The data presented in Fig. 1 suggested a selective protective affect of dicoumarol on PC-3 and DU-145, but not on LNCaP cells. Since dicoumarol is a relatively specific inhibitor of the two-electron reduction enzyme, NAD(P)H:quinone oxidoreductase-1 (NQO1) (46), we examined

LNCaP, PC-3 and DU-145 cells for their activities of this enzyme. ß-Lap-sensitive DU-145 and PC-3 cells expressed NQO1 protein (Fig. 4) and demonstrated dicoumarol-sensitive, enzyme activity (Table 1), measured by menadione-mediated, NQO1 reduction of cytochrome c as described in 'Materials and Methods' (39). In contrast, LNCaP cells did not express NQO1 protein or enzyme activity (Table 1).

Stable Transfection of LNCaP Cells with NQO1. LNCaP cells were transfected with either pcDNA3 empty vector or pcDNA3 containing full-length NQO1 cDNA, in which expression of this two-electron reductase was controlled by the CMV promoter. Five clonal cell lines containing NQO1 (LN-NQ Cl 1-4, 10) and one vector alone-control (LN-pcDNA3) were isolated. All five NQO1-containing cell lines demonstrated both enzyme activity (15- to 30-fold above nontransfected levels, Table 1) and protein expression (Fig. 7). LNCaP transfectants containing pcDNA3 vector alone exhibited neither NQO1 enzyme activity nor protein expression, similar to nontransfected LNCaP parental cells (Table 1, Fig. 7).

While NQO1 catalyzes a two-electron reduction of quinones to form hydroquinones, a similar intracellular quinone reduction can also be accomplished through reductases which perform one-electron reductions, such as the NADH:cytochrome P450 (P450) and NADH:cytochrome b5 reductase (b5R) family of enzymes. To determine whether LNCaP cells compensated for their NQO1 deficiency by increasing the activities of one-electron enzymes, levels of P450 and cytochrome b5R were determined in the three parental cell lines, as well as in six LNCaP transfectants. No significant differences in P450 or b5R enzyme activities were noted in any LNCaP clonal cell lines examined (Table 1).

Transfection of NQO1 sensitized human LNCaP prostate cancer cells to ß-lap. In clonogenic assays, NQO1-deficient parental LNCaP cells showed moderate resistance to ß-lap, relative to DU-145 and PC-3 cells, which express high levels of the enzyme (Fig. 1). Similarly, NQO1-containing LNCaP clones demonstrated significantly increased sensitivity to ß-lap relative to the NQO1-deficient, LNCaP transfectant cell line containing pcDNA3 vector alone (Fig. 5A). Co-administration of dicoumarol, to inhibit exogenously expressed NQO1, returned NQO1-expressing LNCaP cell clones to the relatively resistant phenotype of the NQO1-deficient, pcDNA3 vector alone, control line. As with parental LNCaP cells, dicoumarol co-administration had no effect on the sensitivity of NQO1-deficient, LNCaP cells (containing pcDNA3 vector alone) to ß-lap treatment (Fig. 5A). Menadione is a quinone that is detoxified by NQO1 and thus toxic to cells in the absence of the enzymatic activity of NQO1. Thus, in contrast to ß-lap-mediated toxicity, NQO1-deficient LNCaP parental or vector alone transfectants were more sensitive to menadione. NQO1-containing, LN-NQ Cl 10 cells were resistant to menadione toxicity compared to NQO1-deficient, LN-pcDNA3 cells (Fig. 5B). Thus, the toxicities of menadione and ß-lap appear to be reversed, wherein NQO1 expression conferred resistance to menadione, but enhanced sensitivity to ß-lap (compare results in Fig. 5A to Fig. 5B). Similar results were found with human NQO1-transfected (or vector alone-transfected) MDA-MB-468 breast cancer cells treated with ß-lap or menadione (2). Suggesting NQO1 is not merely sensitizing the cells, but is indeed activating β-lap.

Transfection of LNCaP cells with NQO1 enhanced ß-lap-induced apoptosis. Exposure of each NQO1-expressing LNCaP transfectant (LN-NQ Cl 1-4, 10) to 10 μM ß-lap resulted in significantly increased apoptosis (i.e., 80-90% of the cell population demonstrating positive TUNEL staining at 48 h posttreatment) compared to control LNCaP transfectants containing pcDNA3 empty vector alone (LN-pcDNA3 cells, which demonstrated less than 5% apoptotic cells in the same 48-h posttreatment period). As expected, NQO1-mediated, ß-lap-stimulated apoptosis in LN-NQ Cl 1-4, 10 cells lines was prevented by co-administering 50 μM dicoumarol. In contrast, dicoumarol did not affect ß-lap-induced apoptosis in LNCaP cells containing the pcDNA3 empty vector (LN-NQ pcDNA3 cells, Fig. 6) or in the parental nontransfected LNCaP cells (Fig. 2).

Expression of NQO1 In LNCaP cells enhanced atypical PARP cleavage in response to ß-lap exposure. Parental LNCaP cells produced an apoptosis-related, atypical cleavage of PARP (formation of a 60 kDa PARP polypeptide) following 25 μM ß-lap, nearly 5 times the drug's LD_{50} (see Figs. 2 and 3B). In contrast, atypical PARP cleavage was apparent in PC-3 or DU-145 cells after 5-10 μM ß-lap, at or near the drug's LD_{90} for these cells. In general, atypical PARP cleavage correlated well with the sensitivities (apoptosis) of each cell line after ß-lap exposures in NQO1-expressing cells (Figs. 1A and 3B) and that observed in breast cancer epithelial cells (20). Empty vector (LN-NQ pcDNA3)- or NQO1-transfected LNCaP (LN-NQ Cl1-4, 10) cells were examined for PARP cleavage following ß-lap treatments. Atypical 60 kDa PARP fragmentation in each NQO1-expressing clone only required 5-10 μM β-lap, whereas the parental and vector alone clones needed significantly greater ß-lap doses (>25 μM) for the same atypical PARP cleavage reactions (Fig. 7). Thus, PARP fragmentation in NQO1-

containing LNCaP cells, but not in LNCaP parental or empty vector transfectants, following ß-lap treatment strongly correlated with overall apoptosis (Fig. 6) and lethality (Fig. 5A). In contrast, altered expression of NQO1 did not influence apoptotic reactions induced by CPT in any of the LNCaP cell lines examined above.

Discussion

NQO1 may be a clinically exploitable target for therapy against certain tumors using ß-lap or its derivatives. Our results demonstrate that NQO1 as a key intracellular target for ß-lap in human prostate epithelial cancer cells, since dicoumarol prevented NQO1-directed, ß-lap-mediated apoptosis, and lethality in DU-145 and PC-3, and did not affect β-lap-induced apoptosis in NQO1-deficient LNCaP cells. This conclusion was further supported by our demonstration that re-expression of NQO1 in LNCaP cells increased their sensitivity to ß-lap-mediated apoptosis and lethality. Thus, our data suggests a specific target for ß-lap in prostate cancer cells, NQO1, that correlates with that seen in breast cancer cells (2). Although many laboratories (including our own) have published data supporting other potential targets *in vitro*, including Topo I and Topo II-alpha, none of these previous studies demonstrated convincing data for an intracellular target for this drug until recently.

We previously showed that ß-lap-induced a p53-independent apoptotic response in human prostate cancer cells (1). We now demonstrate that such p53-independent apoptotic responses caused by ß-lap are greatly enhanced by NQO1 expression (Fig. 7). Furthermore, we demonstrate that NQO1 expression-dependent lethality for ß-lap is opposite to that of menadione, wherein NQO1 over-expression increases ß-lap lethality

but decreases the cytotoxicity of menadione. Similar results were found in human MDA-MB-468 breast cancer cells, which also lack NQO1 expression (2). Collectively, our data suggest that ß-lap is bioactivated by some unknown mechanism(s) in cells expressing NQO1. The possibility of a bioactivated form of ß-lap interacting with previously suggested *in vitro* targets, such as Topo I (3), is possible and not yet known.

ß-Lap induces a unique apoptotic response in epithelial cancer cell lines, such as those of breast or prostate origin. In epithelial cancer cells, ß-lap stimulates a novel cell death pathway that appears to be caspase-independent (Fig. 4), calcium-dependent, and NQO1-mediated (Fig. 7) (2, 20); dicoumarol prevents its activation and cells lacking NQO1 do not demonstrate p53 or PARP proteolytic cleavage events after physiological ß-lap exposures (non-supralethal doses) (Fig. 3B) (2). Treatment of human prostate cancer cells with ß-lap induced the formation of an atypical PARP cleavage fragment, different from the classical 89 kDa fragment formed during caspase-mediated (via caspases 3,6 and 7) apoptosis (47). The production of this 60 kDa atypical PARP fragment correlated well with apoptosis and overall sensitivity of prostate or breast epithelial cancer cells to ß-lap (compare Figs. 5A and 7) (2). Addition of 100 μM zVAD-fmk, a widely used pan-caspase inhibitor, blocked caspase-induced typical PARP cleavage initiated in DU-145 cells by treatment with 10 μM CPT (Fig. 3B). However, the same concentration of zVAD-fmk had no effect on atypical PARP cleavage or cleavage of other ß-lap-induced apoptotic substrates, such as lamin B or p53, in NQO1-expressing human prostate cancer cell lines. These data are consistent with prior data using human breast cancer cells and strongly suggest that when NQO1 is expressed, ß-lap

predominantly stimulates a noncaspase-mediated apoptotic response, which we theorize is directed by the activation of the calcium-dependent cysteine protease, calpain (20).

LNCaP cells, while relatively resistant, did exhibit toxicity following ß-lap exposures, despite their deficiency in NQO1 expression at significantly higher doses of β–lap as compared to NQO1 expressing cells. The observed toxicity in LNCaP parental cells may be attributed to the lower affinity of one-electron reducing enzymes for ß-lap, such as the p450 enzyme family, as well as other nonrelated enzymes (e.g., cytochrome b5 reductase). These enzymes may catalyze two one-electron reductions of quinones in order to form the hydroquinone, whereas NQO1 mediates one higher affinity two electron reduction forming the same byproduct. As a result, a higher dose of ß-lap was required (compared to NQO1-containing PC-3, DU-145 or LNCaP transfectants) for a similar biological affect (i.e., lethality). Re-expression of NQO1 in LNCaP cells, via stable transfection with CMV-controlled mammalian NQO1 expression vectors *significantly* increased their sensitivity to ß-lap, a sensitivity ablated by dicoumarol co-administration. These data indicate that while NQO1 is not the only enzyme capable of activating or metabolizing ß-lap, its ability far surpasses the efficiency of other reductases (or other as yet unidentified enzymes) in the cell to bioactivate the drug. Furthermore, apoptotic responses (monitored by TUNEL-positive cells) in human prostate cancer epithelial cell lines elicited by ß-lap appear essentially dependent on NQO1, suggesting that NQO1-independent death may be via necrosis or 'interphase' cell death.

Current dogma states that all apoptotic pathways include caspase activation, and that all caspase-independent mechanisms lead exclusively to necrosis. Our data strongly suggest that other noncaspase-mediated apoptotic pathways (e.g., mediated by calpain)

exist after certain drug treatments. Furthermore, we suggest that there is a spectrum of cell death responses, ranging from clear caspase-mediated apoptosis to dramatic cell lysis during necrosis (i.e., cell plasma membrane rupture and lysis, as observed after sodium azide exposure). Cells treated with ß-lap exhibit many characteristics of cells undergoing apoptosis, including morphologic changes (Fig. 2A), chromatin condensation (4), DNA ladder formation (1, 5), generation of sub G_0/G_1 apoptotic cells (1), cells staining positive with the TUNEL assay, which monitors for endonuclease-specific DNA double strand breaks (Fig. 2B, 6), specific dephosphorylation of pRb (4), and specific intracellular cleavage of unique substrates (i.e., Topo I, Topo II, lamin B, and p53), while most other proteins (e.g., cyclins A, B, E and bcl-2) remained intact ((4), Fig. 3A, Fig. 3B, Fig. 7)(20). Yet, concrete evidence of caspase activation is lacking. It was previously reported that ß-lap induced apoptosis in some cell systems and necrosis in others, although specific endpoints for necrosis were not examined (48). ß-lap-treated breast or prostate cancer cells demonstrated extensive formation of apoptotic cells, as monitored by TUNEL assays, formation of sub-G_0/G_1 cells, morphology changes (i.e., condensed nuclei and rounded cells) and lamin B cleavage (Fig. 3B), as early as 4-8 h following ß-lap treatment (2, 20). Since some DNA fragmentation may occur during late stage necrosis (49), the early (4-8 h) appearance of TUNEL positive cells concomitant with specific protein cleavage events (e.g., PARP and p53) following ß-lap treatment strongly suggests that an apoptotic, rather than necrotic, cell death mechanism was triggered by ß-lap. ß-Lap-treated NQO1-expressing cells demonstrate extensive nuclear condensation, unique intracellular substrate cleavages and the cells detached in a rounded form (Fig. 2). Most importantly, ß-lap-treated cells show no visible morphologic hallmarks of necrosis,

such as extensive cell debris (Fig. 2). Few cells survive the treatment and the cytotoxic responses have a sharp dose-response curve in which apoptosis and loss of survival are directly correlated in NQO1-expressing cells. All NQO1-containing breast and prostate cancer cells examined thus far respond with identical apoptotic mechanisms to the drug. In contrast, all NQO1-deficient breast or prostate cancer cells appear to be more resistant to ß-lap, showing significantly less apoptosis (2).

We previously showed that ß-lap was a radiosensitizer (after IR exposure) of human cancer cells compared to normal cells (3). Furthermore, those normal cells that did survive the IR exposures plus ß-lap posttreatments demonstrate lower than basal levels of neoplastic transformants (50). Our laboratory also demonstrated that NQO1 was an X-ray-inducible transcript and protein (i.e., xip3) (22). The discovery that NQO1 is a major determinant in the sensitivity of human prostate and breast[4] epithelial cancer cells to ß-lap may explain the compound's ability to radiosensitize certain cancer cells which express low basal levels of NQO1, but in which the cell's enzyme levels can be dramatically induced by IR pretreatment. We previously found that posttreatments, and not pretreatments, of ß-lap sensitized cells to IR (3, 50-52). A five hour posttreatment of 4-5 μM ß-lap was required, in which IR-treated cells were killed and non-IR-treated cells were spared (<20% lethality). Since we also showed that NQO1 levels were induced 5- to 20-fold in three to four hours in the same cell line (22), we speculate that the compound's radiosensitizing capacity was due to the exploitation of this damage-inducible, bioactivating (for ß-lap) enzyme. Since NQO1 is commonly elevated during early stages of carcinogenesis (53, 54), normal cells which become genetically unstable following IR exposure and later induce stable expression of NQO1, would be rather

sensitive to cell death by ß-lap posttreatments. We previously demonstrated that post-IR-exposure to 4-5 μM ß-lap could dramatically reduce IR-mediated neoplastic transformants (52). We speculate, therefore, that this compound may not only be useful against NQO1-overexpressing cancer cells (e.g., breast, lung and possibly prostate cancers), but the compound could possess great potential as an anti-carcinogenic agent by eliminating genetically unstable, NQO1-overexpressing severely damaged normal cells, which would otherwise become neoplastically transformed.

References

1. Planchon, S. M., Wuerzberger, S., Frydman, B., Witiak, D. T., Hutson, P., Church, D. R., Wilding, G., and Boothman, D. A. Beta-lapachone-mediated apoptosis in human promyelocytic leukemia (HL-60) and human prostate cancer cells: a p53-independent response. Cancer Research, *55:* 3706-11, 1995.

2. Pink, J. J., Planchon, S. M., Tagliarino, C., Varnes, M. E., Siegel, D., and Boothman, D. A. NAD(P)H:Quinone oxidoreductase activity is the principal determinant of beta-lapachone cytotoxicity. J Biol Chem, *275:* 5416-24, 2000.

3. Boothman, D. A., Trask, D. K., and Pardee, A. B. Inhibition of potentially lethal DNA damage repair in human tumor cells by beta-lapachone, an activator of topoisomerase I. Cancer Research, *49:* 605-12, 1989.

4. Wuerzberger, S. M., Pink, J. J., Planchon, S. M., Byers, K. L., Bornmann, W. G., and Boothman, D. A. Induction of apoptosis in MCF-7-WS8 breast cancer cells by beta-lapachone. Cancer Research, *58:* 1876-1885, 1998.

5. Li, C. J., Wang, C., and Pardee, A. B. Induction of apoptosis by beta-lapachone in human prostate cancer cells. Cancer Research, *55:* 3712-5, 1995.

6. Li, C. J., Averboukh, L., and Pardee, A. B. beta-Lapachone, a novel DNA topoisomerase I inhibitor with a mode of action different from camptothecin. J Biol Chem, *268:* 22463-8, 1993.

7. Frydman, B., Marton, L. J., Sun, J. S., Neder, K., Witiak, D. T., Liu, A. A., Wang, H. M., Mao, Y., Wu, H. Y., Sanders, M. M., and Liu, L. F. Induction of DNA topoisomerase II-mediated DNA cleavage by beta- lapachone and related naphthoquinones. Cancer Res, *57:* 620-7, 1997.

8. Manna, S. K., Gad, Y. P., Mukhopadhyay, A., and Aggarwal, B. B. Suppression of tumor necrosis factor-activated nuclear transcription factor-kappaB, activator protein-1, c-Jun N-terminal kinase, and apoptosis by beta-lapachone. Biochem Pharmacol, *57:* 763-74, 1999.

9. da Silva, C. P., de Oliveira, C. R., da Conceicao, M., and de Lima, P. Apoptosis as a mechanism of cell death induced by different chemotherapeutic drugs in human leukemic T-lymphocytes. Biochemical Pharmacology, *51:* 1331-40, 1996.

10. Decaudin, D., Geley, S., Hirsch, T., Castedo, M., Marchetti, P., Macho, A., Kofler, R., and Kroemer, G. Bcl-2 and Bcl-XL antagonize the mitochondrial dysfunction preceding nuclear apoptosis induced by chemotherapeutic agents. Cancer Research, *57:* 62-7, 1997.

11. Cotter, T. G., Glynn, J. M., Echeverri, F., and Green, D. R. The induction of apoptosis by chemotherapeutic agents occurs in all phases of the cell cycle. Anticancer Research, *12:* 773-9, 1992.

12. Casiano, C. A., Martin, S. J., Green, D. R., and Eng, M. T. Selective Cleavage Of Nuclear Autoantigens During Cd95 (Fas/Apo-1)-Mediated T Cell Apoptosis. Journal of Experimental Medicine, *184:* 765-770, 1996.

13. Yuan, J. Transducing signals of life and death. Current Opinion in Cell Biology, *9:* 247-51, 1997.

14. Talanian, R. V., Quinlan, C., Trautz, S., Hackett, M. C., Mankovich, J. A., Banach, D., Ghayur, T., Brady, K. D., and Wong, W. W. Substrate specificities of caspase family proteases. Journal of Biological Chemistry, *272:* 9677-82, 1997.

15. Miller, D. K. The role of the Caspase family of cysteine proteases in apoptosis. Seminars in Immunology, *9:* 35-49, 1997.

16. Porter, A. G., Ng, P., and Janicke, R. U. Death substrates come alive. Bioessays, *19:* 501-7, 1997.

17. Lazebnik, Y. A., Kaufmann, S. H., Desnoyers, S., Poirier, G. G., and Earnshaw, W. C. Cleavage of poly(ADP-ribose) polymerase by a proteinase with properties like ICE. Nature, *371:* 346-7, 1994.

18. Datta, R., Banach, D., Kojima, H., Talanian, R. V., Alnemri, E. S., Wong, W. W., and Kufe, D. W. Activation Of the Cpp32 Protease In Apoptosis Induced By 1-Beta-D-Arabinofuranosylcytosine and Other Dna-Damaging Agents. Blood, *88:* 1936-1943, 1996.

19. Planchon, S. M., Wuerzberger-Davis, S. M., Pink, J. J., Robertson, K. A., Bornmann, W. G., and Boothman, D. A. Bcl-2 protects against beta-lapachone-mediated caspase 3 activation and apoptosis in human myeloid leukemia (HL-60) cells. Oncol Rep, *6:* 485-92, 1999.

20. Pink, J. J., Wuerzberger-Davis, S., Tagliarino, C., Planchon, S. M., Yang, X., Froelich, C. J., and Boothman, D. A. Activation of a cysteine protease in MCF-7 and T47D breast cancer cells during beta-lapachone-mediated apoptosis. Exp Cell Res, *255:* 144-55, 2000.

21. Joseph, P., Xie, T., Xu, Y., and Jaiswal, A. K. NAD(P)H:quinone oxidoreductase1 (DT-diaphorase): expression, regulation, and role in cancer. Oncol Res, *6:* 525-32, 1994.

22. Boothman, D. A., Meyers, M., Fukunaga, N., and Lee, S. W. Isolation of x-ray-inducible transcripts from radioresistant human melanoma cells. Proceedings of the National Academy of Sciences of the United States of America, *90:* 7200-4, 1993.

23. Tampo, Y. and Yonaha, M. Enzymatic and molecular aspects of the antioxidant effect of menadione in hepatic microsomes. Arch Biochem Biophys, *334:* 163-74, 1996.

24. Joseph, P. and Jaiswal, A. K. NAD(P)H:quinone oxidoreductase1 (DT diaphorase) specifically prevents the formation of benzo[a]pyrene quinone-DNA adducts generated by cytochrome P4501A1 and P450 reductase. Proc Natl Acad Sci U S A, *91:* 8413-7, 1994.

25. Ross, D., Siegel, D., Beall, H., Prakash, A. S., Mulcahy, R. T., and Gibson, N. W. DT-diaphorase in activation and detoxification of quinones. Bioreductive activation of mitomycin C. Cancer Metastasis Rev, *12:* 83-101, 1993.

26. Tedeschi, G., Chen, S., and Massey, V. DT-diaphorase. Redox potential, steady-state, and rapid reaction studies. J Biol Chem, *270:* 1198-204, 1995.

27. Smitskamp-Wilms, E., Hendriks, H. R., and Peters, G. J. Development, pharmacology, role of DT-diaphorase and prospects of the indoloquinone EO9. Gen Pharmacol, *27:* 421-9, 1996.

28. Ross, D., Beall, H., Traver, R. D., Siegel, D., Phillips, R. M., and Gibson, N. W. Bioactivation of quinones by DT-diaphorase, molecular, biochemical, and chemical studies. Oncol Res, *6:* 493-500, 1994.

29. Belinsky, M. and Jaiswal, A. K. NAD(P)H:quinone oxidoreductase1 (DT-diaphorase) expression in normal and tumor tissues. Cancer Metastasis Rev, *12:* 103-17, 1993.

30. Marin, A., Lopez de Cerain, A., Hamilton, E., Lewis, A. D., Martinez-Penuela, J. M., Idoate, M. A., and Bello, J. DT-diaphorase and cytochrome B5 reductase in human lung and breast tumours. Br J Cancer, *76:* 923-9, 1997.

31. Rauth, A. M., Goldberg, Z., and Misra, V. DT-diaphorase: possible roles in cancer chemotherapy and carcinogenesis. Oncol Res, *9:* 339-49, 1997.

32. Stone, K. R., Mickey, D. D., Wunderli, H., Mickey, G. H., and Paulson, D. F. Isolation of a human prostate carcinoma cell line (DU 145). Int J Cancer, *21:* 274-81, 1978.

33. Mickey, D. D., Stone, K. R., Wunderli, H., Mickey, G. H., and Paulson, D. F. Characterization of a human prostate adenocarcinoma cell line (DU 145) as a monolayer culture and as a solid tumor in athymic mice. Prog Clin Biol Res, *37:* 67-84, 1980.

34. Horoszewicz, J. S., Leong, S. S., Kawinski, E., Karr, J. P., Rosenthal, H., Chu, T. M., Mirand, E. A., and Murphy, G. P. LNCaP model of human prostatic carcinoma. Cancer Res, *43:* 1809-18, 1983.

35. Gustafson, D. L., Beall, H. D., Bolton, E. M., Ross, D., and Waldren, C. A. Expression of human NAD(P)H: quinone oxidoreductase (DT-diaphorase) in Chinese hamster ovary cells: effect on the toxicity of antitumor quinones. Mol Pharmacol, *50:* 728-35, 1996.

36. Sambrook, J., Fritsch, E. F., and Maniatis, T. Molecular Cloning-A Laboratory Manual. Cold Spring Harbor Press, Cold Spring Harbor, 1989.

37. Rago, R., Mitchen, J., and Wilding, G. DNA fluorometric assay in 96-well tissue culture plates using Hoechst 33258 after cell lysis by freezing in distilled water. Anal Biochem, *191:* 31-4, 1990.

38. Siegel, D., Franklin, W. A., and Ross, D. Immunohistochemical detection of NAD(P)H:quinone oxidoreductase in human lung and lung tumors. Clin Cancer Res, *4:* 2065-70, 1998.

39. Fitzsimmons, S. A., Workman, P., Grever, M., Paull, K., Camalier, R., and Lewis, A. D. Reductase enzyme expression across the National Cancer Institute Tumor cell line panel: correlation with sensitivity to mitomycin C and EO9 [see comments]. J Natl Cancer Inst, *88:* 259-69, 1996.

40. Thor, H., Smith, M. T., Hartzell, P., Bellomo, G., Jewell, S. A., and Orrenius, S. The metabolism of menadione (2-methyl-1,4-naphthoquinone) by isolated hepatocytes. A study of the implications of oxidative stress in intact cells. J Biol Chem, *257:* 12419-25, 1982.

41. Hollander, P. M., Bartfai, T., and Gatt, S. Studies on the reaction mechanism of DT diaphorase. Intermediary plateau and trough regions in the initial velocity vs substrate concentration curves. Arch Biochem Biophys, *169:* 568-76, 1975.

42. Strobel, H. W. and Dignam, J. D. Purification and properties of NADPH-cytochrome P-450 reductase. Methods Enzymol, *52:* 89-96, 1978.

43. Lotem, J. and Sachs, L. Differential suppression by protease inhibitors and cytokines of apoptosis induced by wild-type p53 and cytotoxic agents [published erratum appears in Proc Natl Acad Sci U S A 1997 Feb 18;94(4):1603]. Proceedings of the National Academy of Sciences of the United States of America, *93:* 12507-12, 1996.

44. Rao, L., Perez, D., and White, E. Lamin proteolysis facilitates nuclear events during apoptosis. Journal of Cell Biology, *135:* 1441-55, 1996.

45. Zhivotovsky, B., Gahm, A., and Orrenius, S. Two different proteases are involved in the proteolysis of lamin during apoptosis. Biochemical & Biophysical Research Communications, *233:* 96-101, 1997.

46. Preusch, P. C., Siegel, D., Gibson, N. W., and Ross, D. A note on the inhibition of DT-diaphorase by dicoumarol. Free Radic Biol Med, *11:* 77-80, 1991.

47. Margolin, N., Raybuck, S. A., Wilson, K. P., Chen, W., Fox, T., Gu, Y., and Livingston, D. J. Substrate and inhibitor specificity of interleukin-1 beta-converting enzyme and related caspases. Journal of Biological Chemistry, *272:* 7223-8, 1997.

48. Li, Y. Z., Li, C. J., Pinto, A. V., and Pardee, A. B. Release of mitochondrial cytochrome C in both apoptosis and necrosis induced by beta-lapachone in human carcinoma cells. Mol Med, *5:* 232-9, 1999.

49. Nishizaki, K., Yoshino, T., Orita, Y., Nomiya, S., and Masuda, Y. TUNEL staining of inner ear structures may reflect autolysis, not apoptosis. Hear Res, *130:* 131-6, 1999.

50. Boothman, D. A. and Pardee, A. B. Inhibition of radiation-induced neoplastic transformation by beta-lapachone. Proceedings of the National Academy of Sciences of the United States of America, *86:* 4963-7, 1989.

51. Boothman, D. A., Greer, S., and Pardee, A. B. Potentiation of halogenated pyrimidine radiosensitizers in human carcinoma cells by beta-lapachone (3,4-dihydro-2,2-dimethyl-2H- naphtho[1,2-b]pyran- 5,6-dione), a novel DNA repair inhibitor. Cancer Res, *47:* 5361-6, 1987.

52. Boothman, D. A. and Pardee, A. B. Inhibition of radiation-induced neoplastic transformation by beta- lapachone. Proc Natl Acad Sci U S A, *86:* 4963-7, 1989.

53. Segura-Aguilar, J., Cortes-Vizcaino, V., Llombart-Bosch, A., Ernster, L., Monsalve, E., and Romero, F. J. The levels of quinone reductases, superoxide dismutase and glutathione- related enzymatic activities in diethylstilbestrol-induced carcinogenesis in the kidney of male Syrian golden hamsters. Carcinogenesis, *11:* 1727-32, 1990.

54. Leonard, T. B., Dent, J. G., Graichen, M. E., Lyght, O., and Popp, J. A. Comparison of hepatic carcinogen initiation-promotion systems. Carcinogenesis, *3:* 851-6, 1982.

Figure Legends

Figure 1. Dicoumarol protects DU-145 and PC-3, but not LNCaP, human prostate cancer epithelial cell lines from ß-lapachone (ß-lap)-induced cytotoxicity. The survival of DU-145, PC-3, and LNCaP human prostate cancer cell lines following ß-lap treatment, with or without dicoumarol co-administration, was determined by colony forming ability assays as described in 'Materials and Methods'. ß-Lap or CPT, with or without 50 μM dicoumarol co-treatments, were given as 4-h pulse treatments as described in 'Materials and Methods'. Shown are the results (mean ±SD) of three experiments repeated in duplicate.

Figure 2A. Dicoumarol blocks morphologic changes in DU-145 cells after ß-lap treatment. DU-145 cells were treated with 5 μM or 10 μM ß-lap, with or without 50 μM dicoumarol, for 4 h. At 24 h post-treatment, phase-contrast photomicrographs were taken of treated or control cells. Shown are representative photos of experiments repeated three or more times. Magnification = 100X.

Figure 2B. Dicoumarol prevents apoptosis induced in human prostate cancer cells following ß-lap, but not CPT. TUNEL assays to monitor apoptosis in ß-lap- or CPT-treated human prostate cancer cells, with or without 50 μM dicoumarol co-administration, were performed 48 h following 4-h drug treatments. The percentage of cells which stained positive in the TUNEL assay, appears in the top right corner of each panel.

Figure 3A. PARP cleavage in human prostate cancer cells following ß-lap or CPT exposures. Human prostate cancer cell lines were treated for 4-h with ß-lap (10 or 25 μM) or CPT (15 μM), with or without 50 μM dicoumarol co-administration. Cells were harvested for analyses 24 h post-treatment and analyzed for specific changes in protein cleavage events by Western blot analyses. Closed arrow: typical 89 kDa PARP cleavage fragment,. Open arrow: atypical 60 kDa PARP cleavage fragment.

Figure 3B. zVAD-fmk blocks CPT- but not ß-lap-induced apoptotic proteolytic substrate cleavage in DU-145 cells. DU-145 human prostate cancer cells were treated with either 10 μM ß-lap or 10 μM CPT, with or without 100 μM zVAD-fmk, for 4 h and specific protein cleavage events were monitored by Western immunoblot analyses. zVAD-fmk treatment began one hour prior to ß-lap addition, treatment was continued throughout the ß-lap treatment, and cells were harvest as described in 'Materials and Methods'. PARP: full length polypeptide, 113 kDa; typical PARP cleavage fragment (closed arrow), 89 kDa; atypical PARP cleavage fragment (open arrow), ~60 kDa. p53: full length polypeptide, 53 kDa; p53 cleavage fragment, ~40 kDa. Lamin B: full length polypeptide, 68 kDa; lamin B cleavage fragment, 45 kDa.

Figure 4. NQO1 and p53 status of three human prostate cancer cell lines. Western immunoblot analyses of untreated lysates from three human prostate cancer cell lines, DU-145, PC-3, and LNCaP were performed as described in 'Materials and Methods'.

Figure 5A. Transfection of LNCaP cells with NQO1 enhances ß-lap-induced lethality. NQO1-containing (LN-NQ Cl1-4, 10) and -deficient (LN-pcDNA3) LNCaP clonal cell lines were treated with 4-h pulses of various doses of ß-lap, with or without concomitant 50 μM dicoumarol co-administration. Survival was then determined by colony forming ability (CFA) assays as described in 'Materials and Methods'. Experiments were performed three times, each in triplicate. Symbols represent mean ±SD. Open symbols: ß-lap alone. Closed symbols: ß-lap with 50 μM dicoumarol co-administration.

Figure 5B. Transfection of LNCaP cells with NQO1 decreases menadione-induced lethality. One NQ01-transfected LNCaP clonal cell line (LN-NQ Cl 10) and the LNCaP vector alone clonal isolate (LN-pcDNA3) were treated with 4-h pulses of various doses of menadione and survival was determined by CFA assays as described in 'Materials and Methods'. Experiments were performed three times, each in triplicate. Symbols represent mean ±SD.

Figure 6. Stable transfection of LNCaP cells with NQO1 enhances ß-lap-induced apoptosis. Stably transfected LNCaP clonal cell lines containing NQO1 or vector alone (from Fig. 5A) were treated for 4-h with various concentrations of ß-lap, with or without 50 μM dicoumarol, as described in 'Materials and Methods'. Forty-eight hours (48-h) posttreatment, cells were monitored for apoptosis-related DNA fragmentation using TUNEL assays. Symbols represent mean ±SD of experiments performed three or more times, each in triplicate. LNCaP isolated clonal cell lines examined were: pcDNA3,

LNCaP stably transfected with vector alone; LN-NQ Cl 1-4 and 10, five separate LNCaP cell lines stably transfected with CMV-controlled NQ01 cDNA, Clones 1-4, and 10.

Figure 7. ß-Lap-induced atypical PARP cleavage is enhanced by NQ01 overexpression. NQO1-containing and -deficient LNCaP clonal cell lines (described in Figs. 5A and 6), were exposed to 4-h treatments with various doses of ß-lap or 10 μM CPT. Cells were harvested for western immunoblot analyses 24 h following drug removal as previously described. Open arrow, atypical PARP cleavage fragment of ~60 kDa molecular weight by SDS-PAGE.

Acknowledgements

We would like to thank Shelly Wuerzberger-Davis for her outstanding assistance in the early stages of this study. Drs. Nancy Oleinick, Tom Davis, and Timothy Kinsella for their helpful discussions.

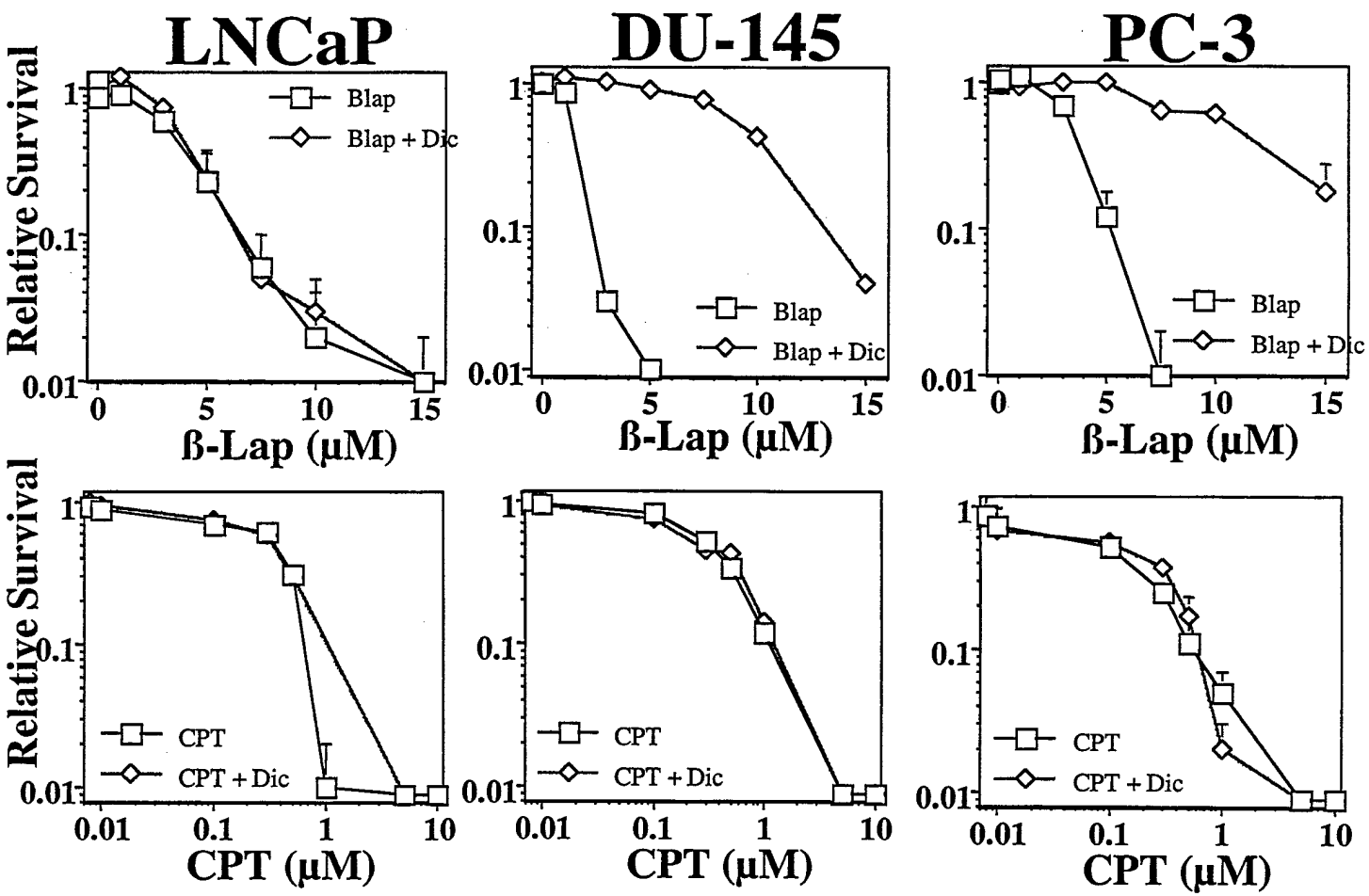
LNCaP
DU-145
PC-3
Relative Survival
1
0.1
0.01
Blap
Blap + Dic
0
5
10
15
ß-Lap (µM)
CPT
CPT + Dic
0.01
0.1
1
10
CPT (µM)

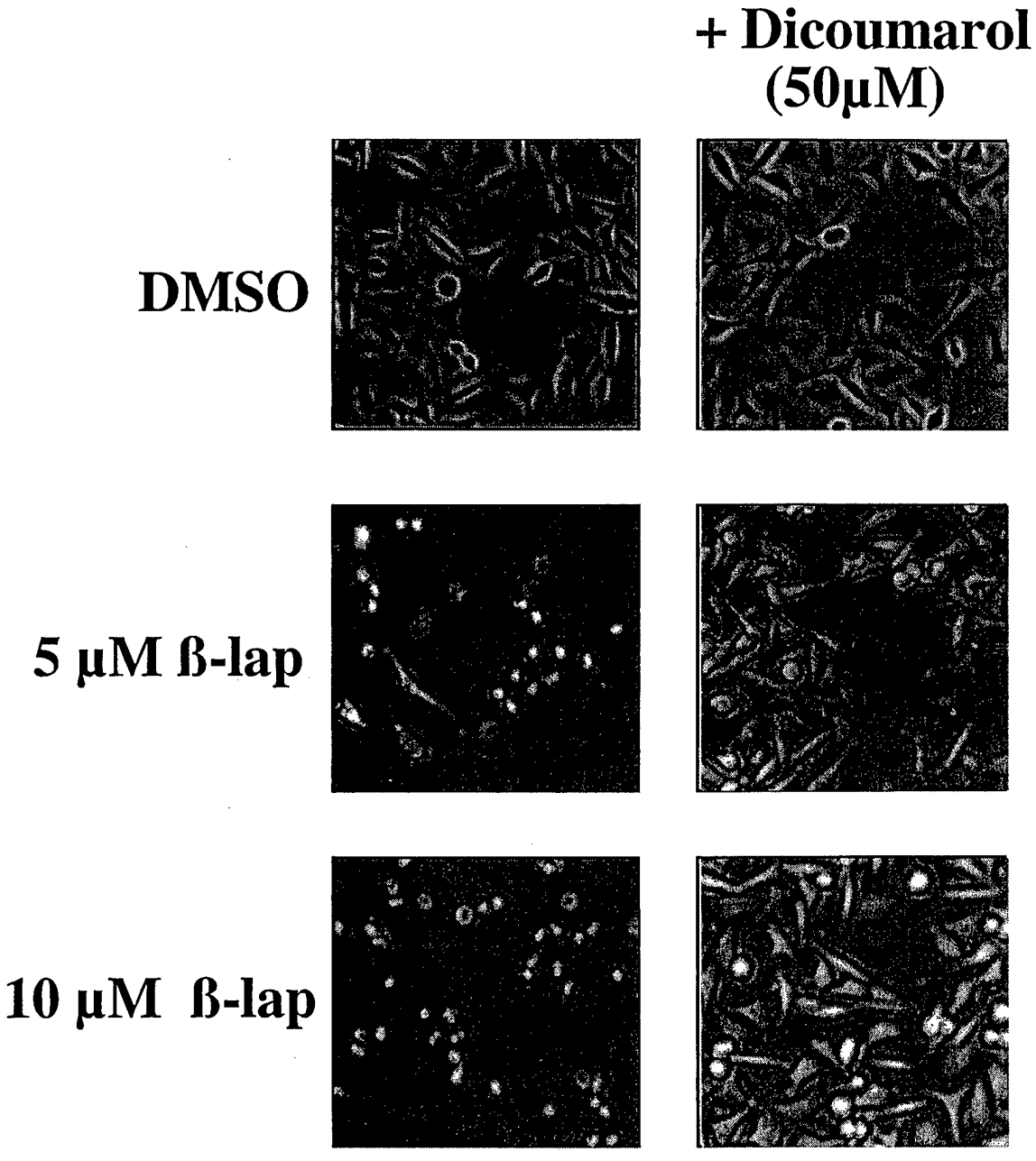
+ Dicoumarol
(50µM)
DMSO
5 µM ß-lap
10 µM ß-lap

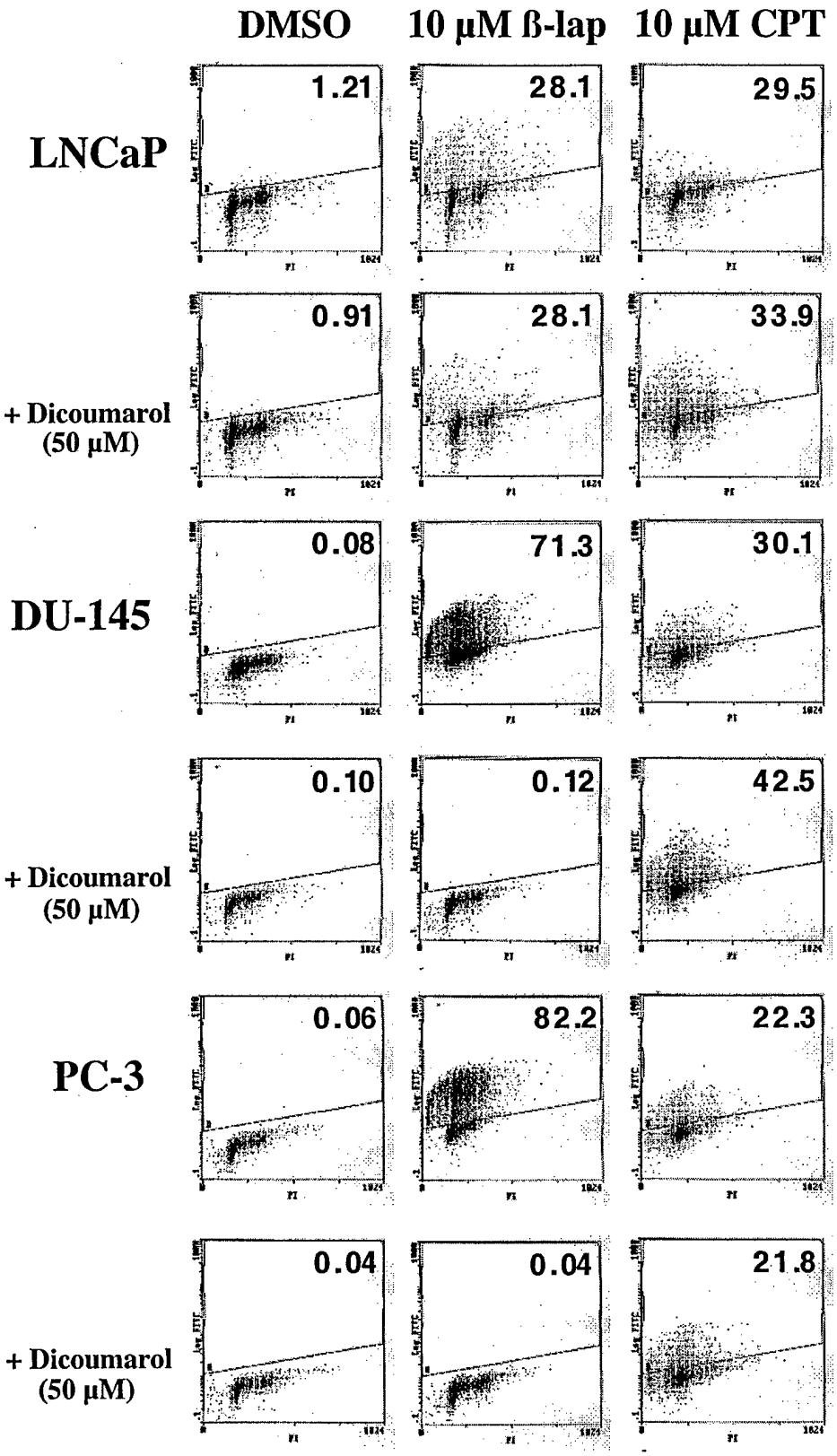
DMSO
10 µM ß-lap
10 µM CPT
LNCaP
1.21
28.1
29.5
+ Dicoumarol (50 µM)
0.91
28.1
33.9
DU-145
0.08
71.3
30.1
+ Dicoumarol (50 µM)
0.10
0.12
42.5
PC-3
0.06
82.2
22.3
+ Dicoumarol (50 µM)
0.04
0.04
21.8

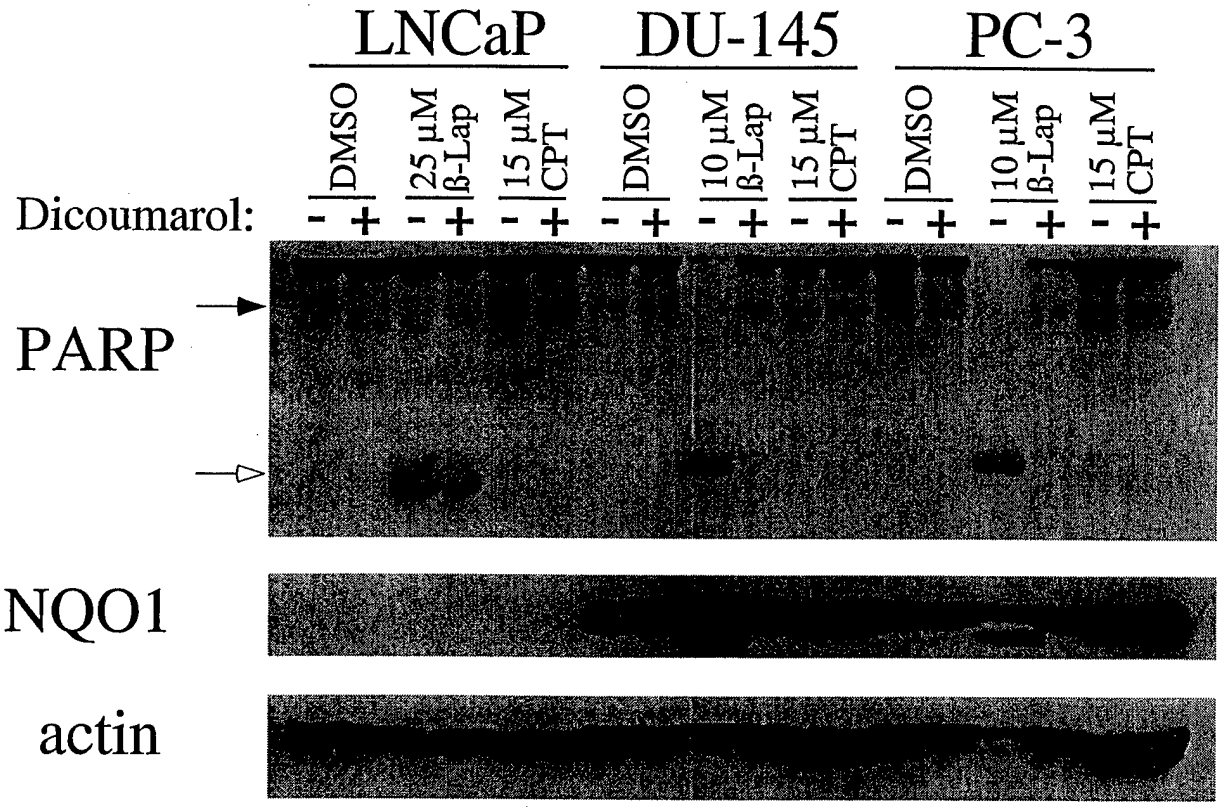
LNCaP
DU-145
PC-3
DMSO
25 µM β-Lap
15 µM CPT
10 µM β-Lap
Dicoumarol:
PARP
NQO1
actin

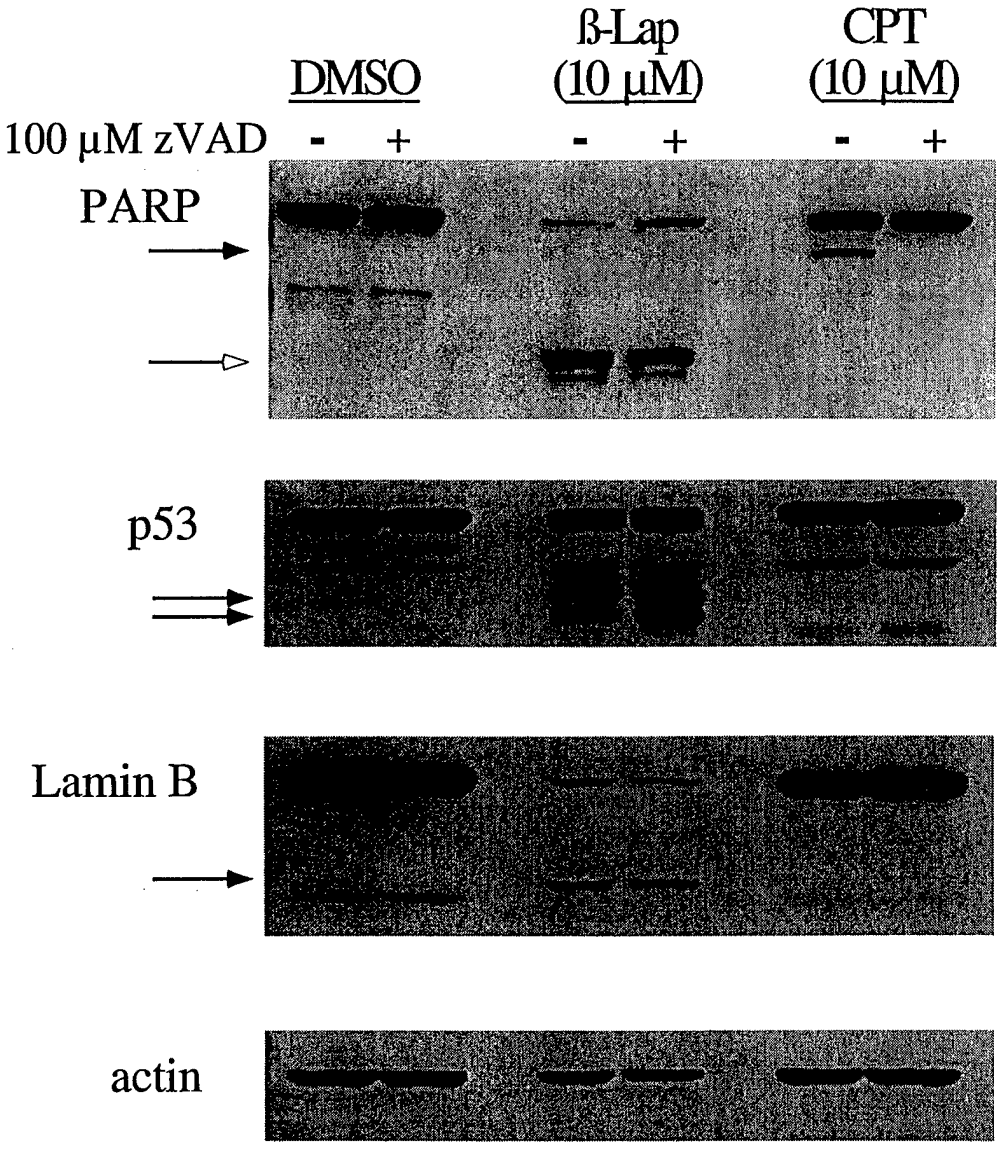
DMSO
ß-Lap (10 µM)
CPT (10 µM)
100 µM zVAD - + - + - +
PARP
p53
Lamin B
actin

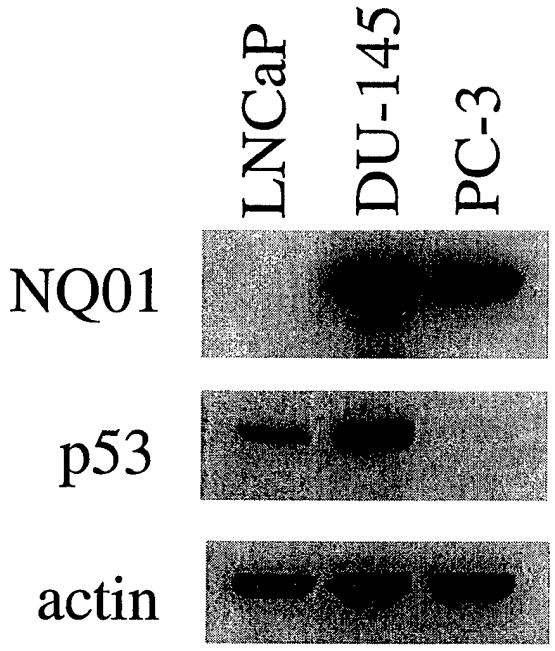
LNCaP
DU-145
PC-3
NQ01
p53
actin

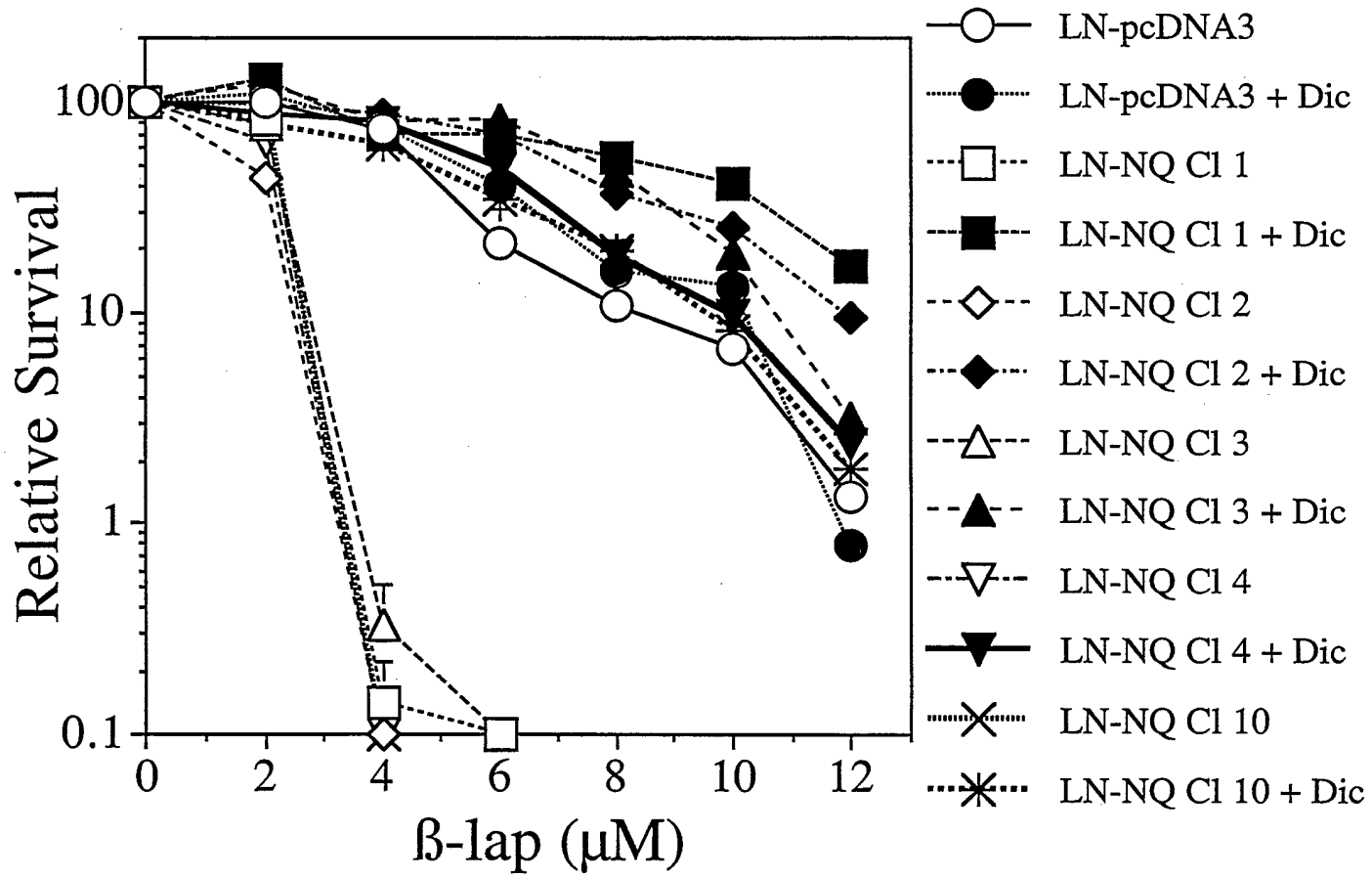
Relative Survival
100
10
1
0.1
0
2
4
6
8
10
12
ß-lap (μM)
LN-pcDNA3
LN-pcDNA3 + Dic
LN-NQ Cl 1
LN-NQ Cl 1 + Dic
LN-NQ Cl 2
LN-NQ Cl 2 + Dic
LN-NQ Cl 3
LN-NQ Cl 3 + Dic
LN-NQ Cl 4
LN-NQ Cl 4 + Dic
LN-NQ Cl 10
LN-NQ Cl 10 + Dic

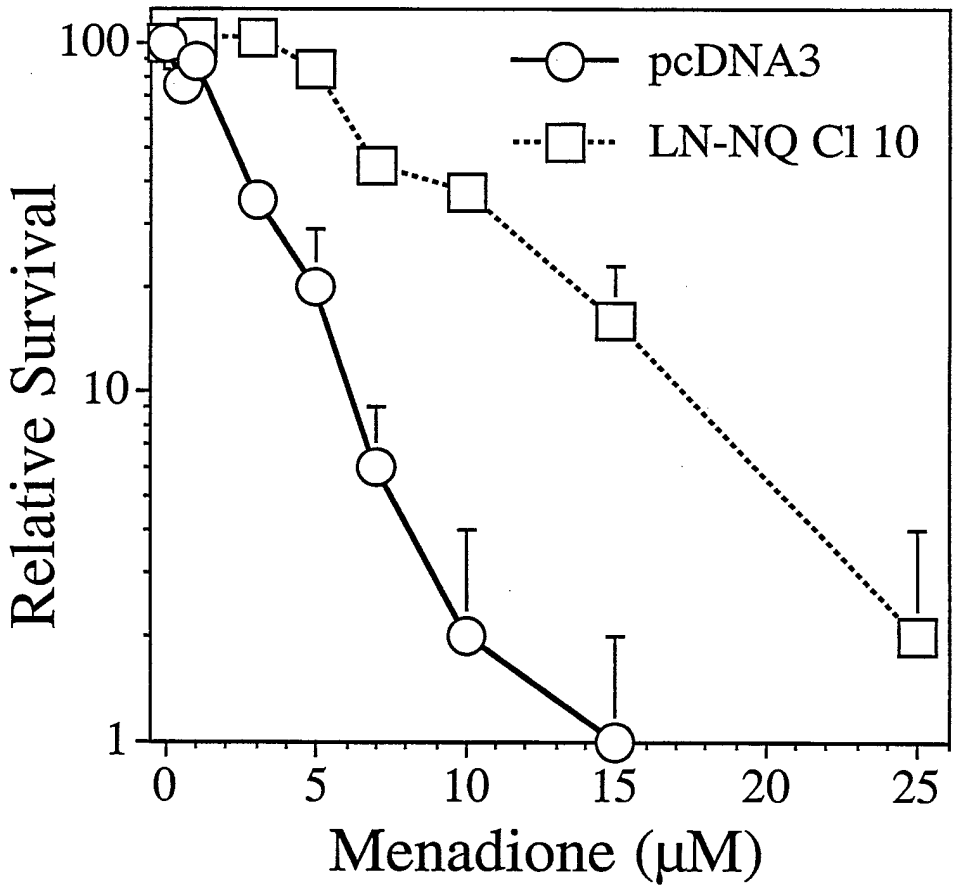
100
10
1
Relative Survival
pcDNA3
LN-NQ Cl 10
0
5
10
15
20
25
Menadione (μM)

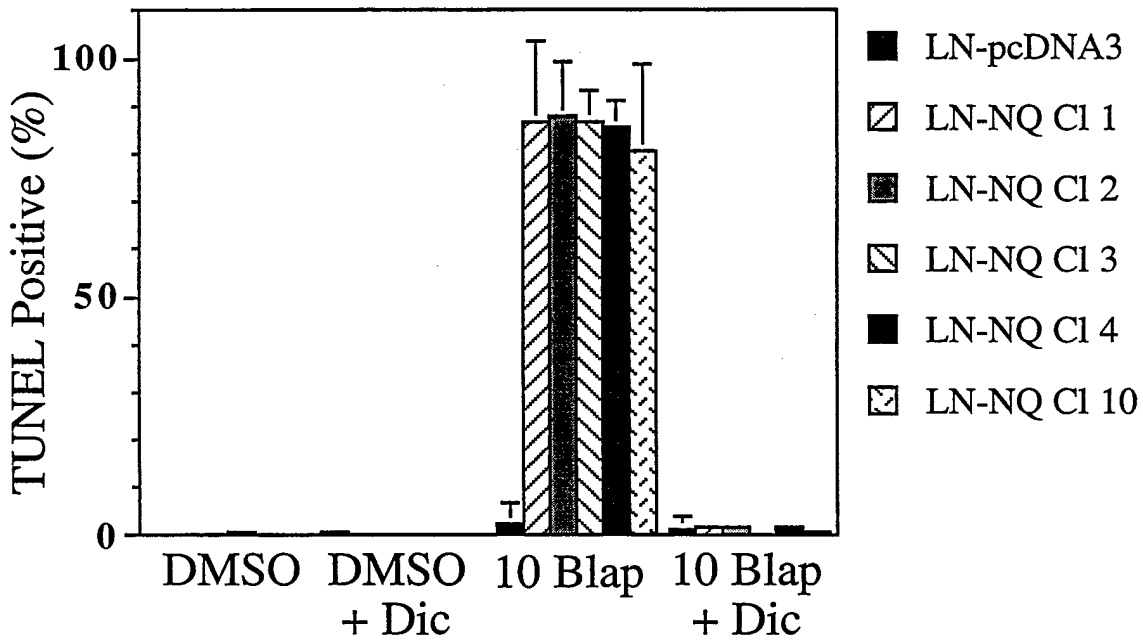
TUNEL Positive (%)
100
50
0
DMSO
DMSO + Dic
10 Blap
10 Blap + Dic
LN-pcDNA3
LN-NQ Cl 1
LN-NQ Cl 2
LN-NQ Cl 3
LN-NQ Cl 4
LN-NQ Cl 10

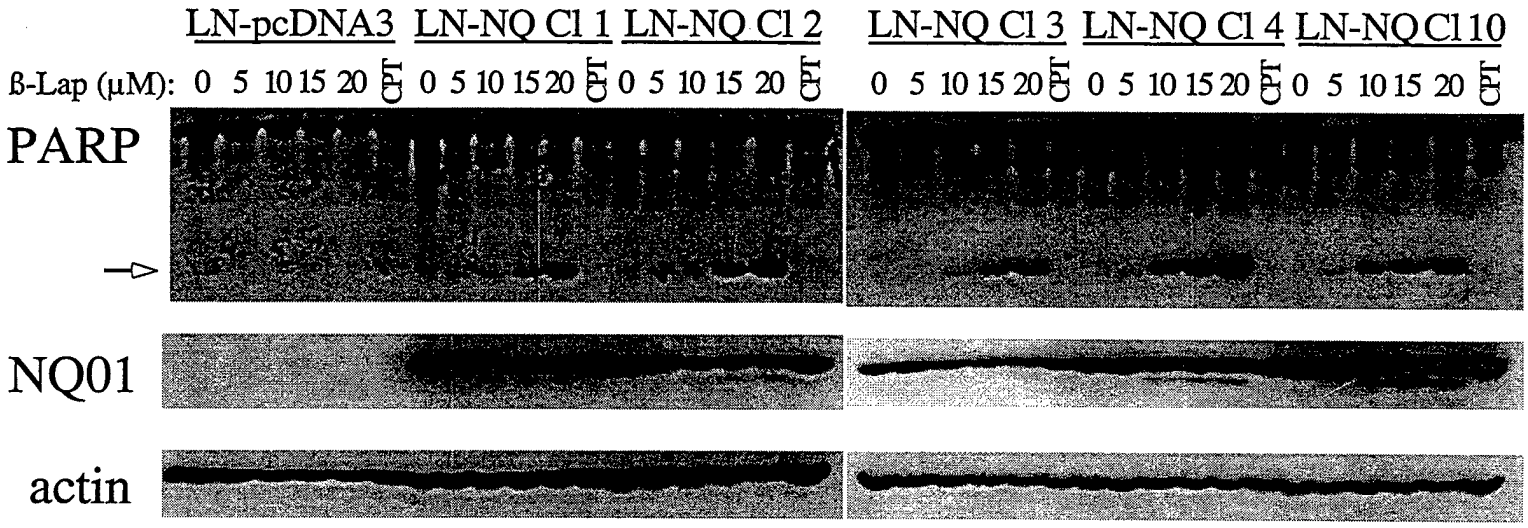
LN-pcDNA3
LN-NQ Cl 1
LN-NQ Cl 2
LN-NQ Cl 3
LN-NQ Cl 4
LN-NQ Cl 10
ß-Lap (µM): 0 5 10 15 20 CPT 0 5 10 15 20 CPT 0 5 10 15 20 CPT 0 5 10 15 20 CPT 0 5 10 15 20 CPT 0 5 10 15 20 CPT
PARP
NQ01
actin

THE JOURNAL OF BIOLOGICAL CHEMISTRY
Vol. 275, No. 13, Issue of March 31, pp. 9501–9509, 2000
Printed in U.S.A.

NF-κB Activation by Camptothecin

A LINKAGE BETWEEN NUCLEAR DNA DAMAGE AND CYTOPLASMIC SIGNALING EVENTS*

(Received for publication, November 17, 1999)

Tony T. Huang‡§, Shelly M. Wuerzberger-Davis¶, Bradley J. Seufzer§, Stuart D. Shumway§‖, Takeshi Kurama§, David A. Boothman¶, and Shigeki Miyamoto‡§¶‖‡‡**

*From the ‡Program in Molecular and Cellular Pharmacology, the ¶Human Cancer Biology Program, the ‖Program in Cellular and Molecular Biology, and the §Department of Pharmacology University of Wisconsin, Madison, Wisconsin 53792 and the **Departments of Radiation Oncology and Pharmacology, Laboratory of Molecular Stress Responses, Case Western Reserve University, Cleveland, Ohio 44106-4942*

Activation of the transcription factor NF-κB by extracellular signals involves its release from the inhibitor protein IκBα in the cytoplasm and subsequent nuclear translocation. NF-κB can also be activated by the anticancer agent camptothecin (CPT), which inhibits DNA topoisomerase (Topo) I activity and causes DNA double-strand breaks during DNA replication to induce S phase-dependent cytotoxicity. Here we show that CPT activates NF-κB by a mechanism that is dependent on initial nuclear DNA damage followed by cytoplasmic signaling events. NF-κB activation by CPT is dramatically diminished in cytoplasts and in CEM/C2 cells expressing a mutant Topo I protein that fails to bind CPT. This response is intensified in S phase cell populations and is prevented by the DNA polymerase inhibitor aphidicolin. In addition, CPT activation of NF-κB involves degradation of cytoplasmic IκBα by the ubiquitin-proteasome pathway in a manner that depends on the IκB kinase complex. Finally, inhibition of NF-κB activation augments CPT-induced apoptosis. These findings elucidate the progression of signaling events that initiates in the nucleus with CPT-Topo I interaction and continues in the cytoplasm resulting in degradation of IκBα and nuclear translocation of NF-κB to attenuate the apoptotic response.

The NF-κB/Rel family of transcription factors regulates expression of genes critical for multiple biological processes, including immune responses, inflammatory reactions, and apoptosis (1–3). In mammalian cells, NF-κB exists as dimeric complexes composed of p50, p65 (RelA), c-Rel, RelB, or p52. These proteins share a conserved Rel homology domain that encodes dimerization, DNA binding, and nuclear localization functions. NF-κB associates with members of the IκB family of proteins, most notably IκBα, which masks the nuclear localization sequence of NF-κB and retains it in the cytoplasm (4, 5). Dissociation from IκBα is essential for NF-κB to enter the nucleus and to activate gene expression. Several signaling cascades that control NF-κB activation converge at an IκB kinase (IKK)[1] complex, responsible for site-specific phosphorylation of IκBα at serines 32 and 36 (6–10). Phosphorylation of IκBα induces multiubiquitination of IκBα and its subsequent degradation by the ubiquitin-dependent 26 S proteasome (11, 12). This sequence of events can be induced without *de novo* protein synthesis by multiple extracellular stimuli, including tumor necrosis factor α (TNFα), interleukin-1, phorbol ester (PMA), bacterial lipopolysaccharide (LPS), and others. However, NF-κB activation can also be achieved through mechanisms that are distinct from the above IKK-dependent model. These include phosphorylation-independent yet proteasome-mediated IκBα degradation induced by ultraviolet irradiation (13, 14), calpain-dependent degradation of IκBα by silica and TNFα (15, 16), and tyrosine phosphorylation-induced dissociation of IκBα from NF-κB following hypoxia and reoxygenation (17). Thus, depending on the stimuli, NF-κB can be activated through multiple distinct regulatory pathways.

Activation pathways of NF-κB typically originate from ligand-receptor interactions on the cell membrane. However, NF-κB can also be activated by a group of agents that damage DNA in the nucleus. A paradox confounding our current understanding of the mechanism of NF-κB activation by agents that damage DNA is that the major source of damaged DNA is in the nucleus, whereas latent NF-κB complex is in the cytoplasm. It was previously hypothesized that a signal may transfer from the nucleus to the cytoplasm (18). In support of this model, a recent study by Piette and Piret (19) provides evidence that NF-κB activation by DNA-damaging agents correlates with their capacity to induce DNA breaks. However, the requirement of damaged DNA in the nucleus has not been directly demonstrated. In contrast, Devary *et al.* (20) showed that enucleated cells (*i.e.* cytoplasts) retained full capacity to activate NF-κB following UV irradiation, indicating that nuclear DNA damage is not necessary for NF-κB activation by UV irradiation. There is now substantial evidence to support the notion that UV activation of NF-κB involves activation of cell surface receptors by ligand-independent oligomerization (14,

* This work was supported by a Howard Hughes Medical Institute fund through the University of Wisconsin Medical School, the Shaw Scientist Award from the Milwaukee Foundation, and grants from the NIEHS, National Institutes of Health Center and the University of Wisconsin Comprehensive Cancer Center (to S. M.), Grant DAMD17-48-1-8260 from the United States Army Medical Research and Material Command Breast Cancer Initiative (to D. A. B.), a Cremer Scholar Award (to T. T. H.), and support from National Institutes of Health Training Grant T32GM07215 (to S. D. S.). The costs of publication of this article were defrayed in part by the payment of page charges. This article must therefore be hereby marked "*advertisement*" in accordance with 18 U.S.C. Section 1734 solely to indicate this fact.

‡‡ To whom correspondence should be addressed: Dept. of Pharmacology, University of Wisconsin, Medical School, K4/554 Clinical Science Center, 600 Highland Ave., Madison, WI 53792. E-mail: smiyamot@facstaff.wisc.edu.

[1] The abbreviations used are: IKK, IκB kinase; TNFα, tumor necrosis factor α; PMA, phorbol myristyl acetate; LPS, lipopolysaccharide; CPT, camptothecin; Topo I, DNA topoisomerase I; SSB, DNA single-strand break; DSB, DNA double-strand break; TPT, topotecan; ALLN, acetyl-leucinyl-leucinyl-norleucinal; EMSA, electrophoretic mobility shift assay; HA, hemagglutinin; GFP, green fluorescent protein; WT, wild type; FACS, fluorescence-activated cell sorter; X-gal, 5-bromo-4-chloro-3-indolyl β-D-galactopyranoside.

21–24) and/or oxidative stress-mediated inactivation of receptor tyrosine phosphatases, which ultimately leads to ligand-independent activation of receptor tyrosine kinases (25). Whether nuclear DNA damage can directly activate an intracellular NF-κB signaling pathway without involving cell surface receptors remains an important question yet to be resolved.

We and others have observed that an anti-cancer agent, camptothecin (CPT), can activate NF-κB in pre-B or T cell lines (19, 26). CPT inhibits the activity of DNA topoisomerase (Topo) I (27–29). Topo I changes the supercoiling of DNA and therefore plays critical roles in DNA replication, in RNA transcription, and, indirectly, in DNA damage repair (30). CPT selectively binds to and stabilizes a covalent Topo I-DNA reaction intermediate, referred to as the cleavable complex, which contains a single-strand DNA break (SSB) (31, 32). DNA double-strand breaks (DSBs) are then generated during DNA replication when the replication fork collides with the cleavable complex (33). In the present study, our objective was to determine whether or not nuclear events associated with the DNA-damaging action of CPT and a clinically utilized derivative of CPT, topotecan (TPT) (34, 35) were required for activation of cytoplasmically localized NF-κB complexes. We also examined whether CPT activation of NF-κB modulated an apoptotic response. Our findings elucidate a series of nuclear events induced by CPT/TPT that converge with cytoplasmic signaling events responsible for the activation of NF-κB, which can provide anti-apoptotic function.

EXPERIMENTAL PROCEDURES

Cell Culture—Culture conditions for 70Z/3 and 70Z/3-CD14 murine pre-B cells have been described (36). CEMp and CEM/C2 human T cell lines were kindly provided by Dr. Y. Pommier (National Institutes of Health) and maintained in RPMI 1640 medium (Cellgro, Mediatech) supplemented with 10% fetal bovine serum (HyClone Laboratory, Inc.), 1000 units of penicillin G (Sigma), and 0.5 mg/ml streptomycin sulfate (Sigma) in an humidified 5% CO_2-95% air incubator (Forma Scientific). HeLa human cervical carcinoma cells and PC-3 human prostate carcinoma cells were maintained in Dulbecco's modified Eagle's medium (Cellgro) supplemented with 10% fetal bovine serum and antibiotics as above in a 10% CO_2-90% air incubator. The human kidney embryonic fibroblast 293 (HEK293) was maintained in the latter medium on 0.1% (w/v) gelatin-coated plastic culture dishes.

Reagents—CPT, VP16, calpain inhibitor I (ALLN), Me_2SO, bacterial LPS, PMA, cycloheximide, aphidicolin, and cytochalasin B were purchased from Sigma. TPT was a gift from SmithKline Beecham. Lactacystin was generously provided by Dr. E. J. Corey (Harvard University). Stock solutions were prepared in Me_2SO at 10 mM (CPT), 10 mM (VP16), 30 mM (aphidicolin), cytochalsin B (10 mg/ml), and 25 mM (lactacystin, 25% Me_2SO-75% H_2O). TPT stock was made in water at 30 mM. LPS was prepared in RPMI growth medium at 1 or 10 mg/ml. Human recombinant TNFα was from CalBiochem and resuspended in phosphate-buffered saline containing 0.1% bovine serum albumin (fraction V, Sigma). A 50 μM PMA stock was made in 100% ethanol. A cycloheximide stock solution was made in water at 50 mg/ml. In each experiment, all samples received the same amounts of Me_2SO to control for potential Me_2SO effects. All stock solutions were stored in aliquots at either −70 °C or −20 °C. IgGs against IκBα (C21), c-Rel (C), p65 (A and C20), Rel-B (C-19), p52 (I-18), and p50 (NLS) were purchased from Santa Cruz Biotechnology. A monoclonal anti-FLAG antibody was purchased from Kodak, and horseradish peroxidase-conjugated anti-rabbit and anti-mouse antibodies and protein A were obtained from Amersham Pharmacia Biotech. Prestained protein molecular weight markers were purchased from Life Technologies, Inc. Cell preparation and Western immunoblots were performed as described (36) and developed using the ECL procedure according to the manufacturer (Amersham Pharmacia Biotech). Blots were then exposed to x-ray film (Kodak).

Electrophoretic Mobility Shift and Supershift Assays—The Igκ-κB oligonucleotide probe and conditions for EMSA were previously described (36). For supershift assays, 1 μg of IgG antibodies specific to members of the NF-κB proteins (Santa Cruz Biotechnology) were added to nuclear extracts for 20 min on ice prior to addition of radiolabeled probe. The AP-1 site used for control EMSA reactions was obtained from Promega.

Enucleation Procedure—Enucleation was performed as described (37) with the following modifications. PC3 or HeLa cells were seeded in 30-mm dishes, grown overnight, and exposed to cytochalasin B (10 μg/ml) for a total of 30 min at 37 °C. Plates were placed upside down in 400-ml centrifuge bottles and bathed in growth medium containing cytochalasin B at the same concentration. Plates were secured at the bottom of the centrifuge bottles by appropriately sized styrofoam. Samples were then centrifuged at 10,000 rpm for 15 min at 37 °C using a Beckman JA-14 rotor. The rotor and centrifuge chamber were prewarmed to ~37 °C by prior centrifugation without samples. Plates with enucleated cells (*i.e.* cytoplasts) were then removed from the centrifuge bottle, gently rinsed with phosphate-buffered saline, and incubated with prewarmed growth medium for 30 min at 37 °C. Samples of enucleated cells were fixed in 3:1 methanol/acetic acid, stained with Hoechst dye 33258, and photographed under a fluorescent microscope equipped with a 4′6,-diamidino-2-phenylindole-specific filter. The enucleation efficiency varied from ~75 to 95% for PC-3 and HeLa cells.

Transient Transfection Assay—Cells (HEK293, HeLa, or PC-3) were transiently transfected using a standard calcium phosphate precipitation method (38). CEMp and CEM/C2 cells were transfected with DEAE-Dextran method (39). An NF-κB-dependent luciferase reporter (3xκB-Luc) was constructed by inserting a *Hin*dIII-*Bgl*II fragment of 3xκB-CAT into the *Hin*dIII-*Bgl*II sites of the tk-Luc plasmid (kindly provided by Dr. R. Evans, Salk Institutite). 3xMκB-Luc was constructed using a similar cloning strategy starting with the 3xMκB-CAT (40). 24 h following transfection, cells were treated with TPT (30 μM) or CPT (10 μM) for 2 h, rinsed twice with growth medium, and further incubated without drugs for 6 h before termination of the cultures. Positive control samples were treated with TNFα (10 ng/ml) for a total of 8 h. Control samples were transfected with the LacZ cDNA under the control of the cytomegalovirus promoter in the pCMX vector (CMV-LacZ). For CEMp and CEM/C2 cells, total proteins were used for normalization.

Full-length human IKKα cDNA was provided by Dr. I. M. Verma (Salk Institute). Full-length human IKKβ cDNA was cloned by screening a human kidney cDNA library in λZAPII with a polymerase chain reaction-amplified DNA fragment using a HeLa cDNA library (CLONTECH) and TO237 (5-CTCAGCAGCTCAAGGCCAAG-3′) and TO240 (5′-CCAGAGCTCCTTCTGCCGC-3′) primers. IKKα and IKKβ with a Lys-to-Ala substitution at the conserved ATP binding site were generated by polymerase chain reaction mutagenesis and confirmed by DNA sequencing. The mutant genes were placed under the control of the cytomegalovirus promoter in the pcDNA3.1(+) expression vector (CLONTECH). HEK293 cells were transfected with these constructs by calcium phosphate precipitation and then treated with either TNFα (10 ng/ml) or TPT (30 μM) for 2 h. Nuclear extracts were analyzed by EMSA as described above. Cytoplasmic extracts were analyzed by Western blotting using the anti-FLAG monoclonal antibody (Kodak) to determine expression levels of respective dominant-negative mutants in each condition. An horseradish peroxidase-conjugated donkey anti-mouse antibody (Amersham Pharmacia Biotech) was used for secondary antibody followed by ECL development.

Retrovirus Construction and Infection—Production and infection of HA-tagged wild-type and HA-tagged S32A/S36A mutant IκBα expression constructs were described (36). Other IκBα deletion mutants were generated by polymerase chain reaction-mediated mutagenesis and confirmed by sequencing. Stable pools were selected with hygromycin (1 mg/ml, Roche Molecular Biochemicals), and the expression levels of the corresponding proteins were examined by either anti-IκBα (C21, a C-terminal epitope) or anti-HA antibodies. For experiments shown in Figs. 7*B* and 9, HA-S32A/S36A clone 5 that expressed a relatively high level of the mutant protein was used. Similar but less pronounced effects were also seen with pooled cultures and in five isolated clones expressing varying levels of mutant protein (not shown).

Generation of a Green Fluorescent Protein-IκBα Fusion Construct—N-terminally fused GFP-IκBα was generated by subcloning polymerase chain reaction amplified human IκBα (MAD3) into *Hin*dIII-*Bam*HI sites of the pEGFP vector (CLONTECH), such that the entire MAD3 coding sequence was in-frame with the GFP coding sequence. Stable HEK293 cell clones were generated by G418 selection and subsequent FACS sorting. Cells were photographed using a Zeiss Axioplan microscope equipped for fluorescence with the aid of a fluorescein-specific filter.

FACS Analyses—For FACS sorting of G_1, S, and total cell fractions for EMSA analyses, 70Z/3 cells untreated or treated with CPT, TPT, or LPS for appropriate durations were stained with Hoechst 33342 (stock at 10 mg/ml in water) at the final concentration of 10 μg/ml for 15 min

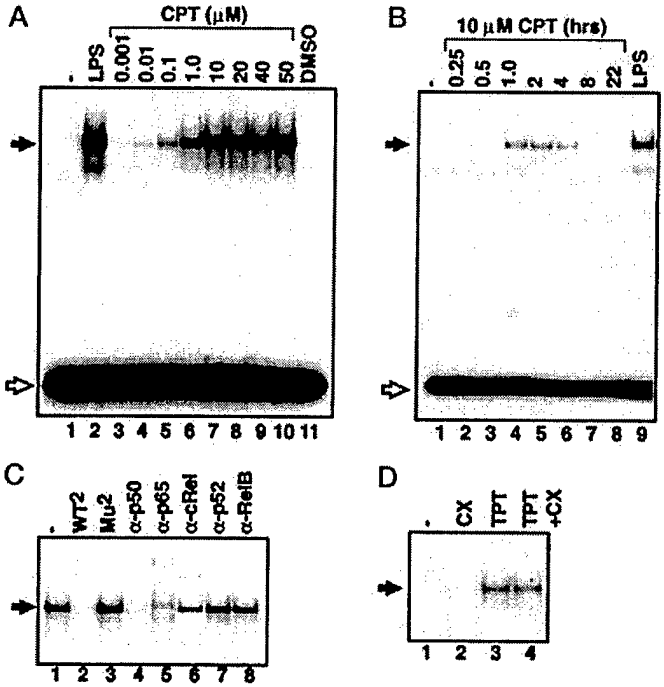

FIG. 1. **NF-κB activation by CPT is transient and does not require *de novo* protein synthesis.** *A*, dose response of CPT-induced NF-κB activation. Exponentially growing 70Z/3-CD14 murine pre-B cells were treated with various doses of CPT shown in μM for 2 h (*lanes 4–11*). Nuclear extracts (10 μg) were analyzed by EMSA using the Igκ-κB probe as in Ref. 36. Stimulation of NF-κB activation by LPS was for 15 min at 1 μg/ml final concentration. All samples, except for untreated cell extracts, were adjusted to 0.5% Me_2SO, a solvent for CPT. NF-κB complex and free probe were indicated by *closed* and *open arrows*, respectively. *B*, time course of CPT-induced NF-κB activation. 70Z/3-CD14 cells were treated with 10 μM CPT, terminated at various times and analyzed as described above. The LPS positive control (*lane 9*) was as described above. *C*, specificity of NF-κB complexes induced by CPT. A nuclear extract isolated from cells exposed to 10 μM CPT for 2 h was incubated with 50-fold excess wild-type or mutated oligonucleotides or with antibodies specific to p50 (NLS), p65/RelA (A), c-Rel (C), p52 (I-18), or RelB (C-19). Supershifted bands for anti-p65 and anti-c-Rel can be seen as slower migrating bands. Antibody against p50 causes reduced DNA binding. *D*, NF-κB activation by CPT occurs in the absence of *de novo* protein synthesis. Cells were treated with or without 20 μg/ml cycloheximide (*CX*) for 30 min to block *de novo* protein synthesis and treated with TPT (30 μM) for 1 h and analyzed as described above. The above data are representative of experiments performed at least three times.

at 37 °C in RPMI growth medium, followed by cell isolation using FACStar^{PLUS} (Becton Dickinson) at 4 °C. 10^6 cells each were purified, and total cell extracts were prepared for EMSA analyses. The status of the cell cycle of purified fractions was confirmed by propidium iodide staining followed by analysis with FACSCalibur (Becton Dickinson). Detailed protocols for apoptosis analyses using FACS have been published (41). Briefly, cells were fixed in ethanol, treated with a citric acid buffer to release fragmented DNA out of the cells, stained with propidium iodide, and analyzed using FACSCalibur.

RESULTS

CPT Induces Transient NF-κB Activation in the Absence of de Novo Protein Synthesis—NF-κB activity is dictated by its ability to bind cognate κB sites present in responsive genes. We utilized a κB site from the immunoglobulin κ intronic enhancer in EMSA analyses to evaluate NF-κB activation by CPT or TPT treatments. CPT induces dose-dependent (Fig. 1*A*, saturating at 10 μM) and transient (Fig. 1*B*, peaking at 1–2 h) NF-κB binding activity in 70Z/3-CD14 pre-B cells. Addition of 50-fold excess specific and nonspecific oligonucleotides (Fig. 1*C*, *lanes 1–3*) shows that the binding activity is specific to NF-κB. Specificity is further demonstrated by the interaction of binding complex with antibodies to p50, RelA, and c-Rel (Fig. 1*C*). Antibodies to other NF-κB family members, p52 and RelB, did not alter binding, indicating that these proteins are not components of the NF-κB complex induced by CPT in 70Z/3-CD14 cells. Pretreatment with cycloheximide (Fig. 1*D*, *lanes 3* and *4*) did not interfere with this pathway, which shows that CPT action does not require *de novo* protein synthesis. This activation is not limited to lymphoid cells because it was also induced

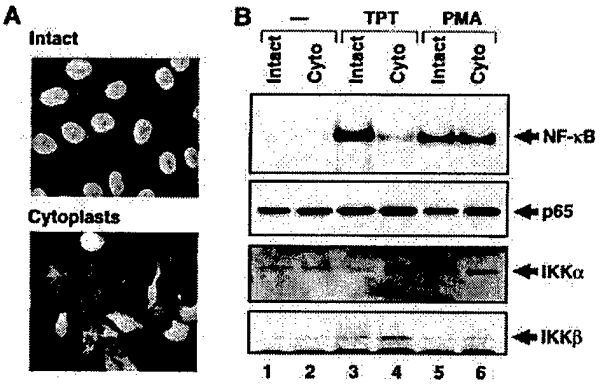

FIG. 2. **Intact nucleus is necessary for NF-κB activation by TPT.** *A*, Hoechst dye staining of intact and enucleated PC-3 cells. PC-3 cells were enucleated as described under "Experimental Procedures." Cells were fixed and stained with Hoechst DNA dye and visualized under a fluorescent microscope and photographed. The exposure time for the cytoplasts was longer than that for the intact cells to aid visualization of otherwise faint cytoplast staining. *B*, EMSA of intact cells and cytoplasts treated with TPT or PMA. Intact cells or cytoplasts were treated with TPT (30 μM) or PMA (50 nM) for 1 h, and equal amount of total cell extracts (2.5 μg) were analyzed by EMSA (NF-κB) or Western blots (p65, IKKα, and IKKβ). The data are representative of three independent experiments.

by both CPT and TPT in CEM T leukemic, PC-3 prostate cancer, HEK293 embryonic kidney fibroblast, and HeLa cervical cancer cell lines (see below, others not shown). Induction of

NF-κB DNA binding activity by CPT or TPT treatment resulted in increased NF-κB-dependent transcription of a luciferase reporter gene (see below). Thus, CPT or TPT activation of NF-κB occurs without *de novo* protein synthesis and may utilize preexisting regulatory component(s).

Interaction of CPT with Nuclear Topo I Is Necessary for NF-κB Activation—The primary molecular target of CPT or TPT is nuclear Topo I enzyme (27, 32). However, mitochondria also contain CPT-sensitive Topo I (42). It is also possible that CPT activation of NF-κB may involve molecular target(s) other than nuclear Topo I. To evaluate the requirement of a nuclear event in NF-κB activation by CPT, we enucleated PC-3 and HeLa cells by the cytochalasin B-mediated enucleation procedure (37). This protocol produced enucleated cells with approximately 90% efficiency as determined by nuclear staining with Hoechst dye (Fig. 2*A*). Consistent with a previous report (43), EMSA of total cell extracts prepared from intact and enucleated cells demonstrated that NF-κB activation by activators, such as PMA (Fig. 2*B*) or TNF (80), does not require an intact nucleus. By contrast, the NF-κB response by CPT and TPT was dramatically diminished in the enucleated cells (Fig. 2*B*). Modest activation by TPT in enucleated cells is likely due to low numbers of intact cells present in the enucleated cell population (Fig. 2*B*). NF-κB (p65), and upstream kinases in the signaling pathway, IKKα and IKKβ, are still present in the cytoplasts (Fig. 2*B*, *lanes 2*, *4*, and *6*), demonstrating that the lack of NF-κB activation response in certain enucleated samples (*lane 4*) is not due to potential leakage of these signaling components. Thus, these results are consistent with the hypothesis that a nuclear event is necessary for NF-κB activation by CPT-related compounds.

Although the above data are consistent with the notion that an intact nucleus is required for NF-κB activation by CPT, it is unknown whether Topo I-induced DNA damage is also required for this process. Its DNA-damaging function requires CPT to interact with Topo I-DNA cleavable complexes (33). To address whether direct interaction of CPT and a Topo I-DNA complex is necessary for activation of NF-κB, we examined human CEM/C2 cells, which exclusively express a mutant Topo I enzyme (44). This mutant Topo I enzyme contains two amino acid substitutions, Met^{370} to Thr and Asp^{722} to Ser. The latter mutation alone makes Topo I enzyme ~1000-fold more resistant to CPT (or TPT)-mediated inhibition of the religation of DNA nicks, making it incapable of efficiently inducing DNA damage by CPT treatment *in vivo* (45). We compared CPT-induced NF-κB activity in CEM/C2 and the parental CEMp cells by EMSA. Time course and dose response studies (Fig. 3, *A* and *B*, respectively), as well as κB-dependent luciferase reporter assay (Fig. 3*C*), clearly demonstrated that CEM/C2 cells could not mount the NF-κB response by CPT treatment, whereas the parental cell line retained the ability to activate NF-κB. Efficient activation of NF-κB in CEM/C2 cells by TNF (Fig. 3*B*) or other DNA-damaging agents, such as VP16 and ionizing radiation (Fig. 3*D*, others not shown), revealed that the lack of NF-κB activation was specific to CPT treatment. Thus, these results together provide strong evidence that Topo I-mediated nuclear DNA damage is necessary for NF-κB activation by CPT treatment.

NF-κB Activation by CPT Depends on DNA Replication and Is Concentrated in S phase of the Cell Cycle—CPT inhibition of the religation step during the Topo I reaction induces stabilization of the cleavable complexes, resulting in generation of SSB. These SSB are reversible but can be converted into lethal DSB during S phase, when the replication fork collides with the cleavable complex (33). It has been suggested that aphidicolin-induced inhibition of DNA polymerase activity prevents DSB

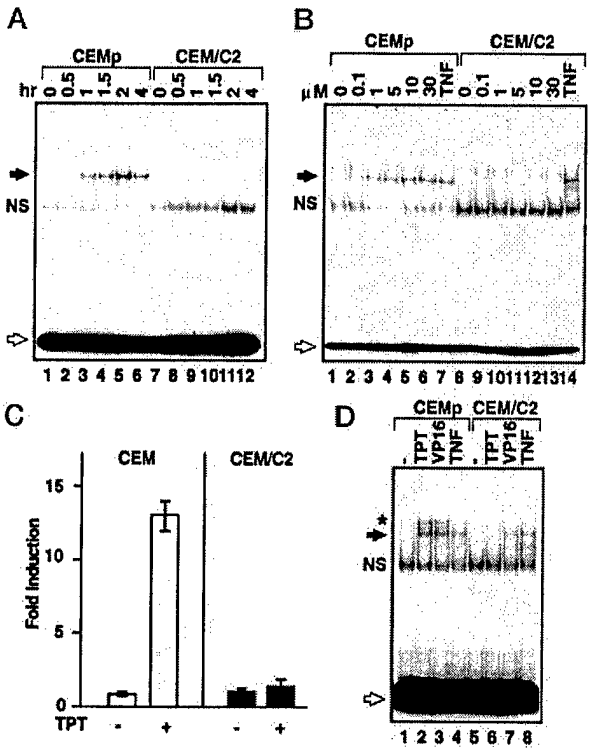

FIG. 3. **Interaction of CPT with Topo I is necessary for NF-κB activation.** *A*, time course of NF-κB activation by CPT treatment in CEMp and CEM/C2 cells. Asynchronous cultures of CEMp and CEM/C2 cells were treated with 10 μM CPT for the periods indicated, and nuclear extracts were analyzed by EMSA as in Fig. 1*A*. The *filled arrow* points to NF-κB, and the *open arrow* points to free probe. *NS* refers to nonspecific band. *B*, CPT dose response of NF-κB activation in CEMp and CEM/C2 cells. These cells were treated for 2 h with various doses of CPT in μM or TNFα (10 ng/ml) and analyzed as above. *C*, NF-κB-dependent luciferase activation in CEMp and CEM/C2 cells. These cells were transiently transfected with the 3xκB-Luc reporter construct treated with 30 μM TPT for 2 h at 24 h after transfection. After medium change, cells were further incubated in the absence of TPT for 6 additional hours before analysis for luciferase activity. Luciferase activity in untreated cells were set as an arbitrary unit of one. *Error bars* are standard deviation from three experiments. *D*, NF-κB activation by VP16 in CEMp and CEM/C2 cells. CEMp and CEM/C2 cells were treated with TPT (30 μM), VP16 (20 μM), or TNFα (20 ng/ml) for 2 h and analyzed by EMSA. The optimum dose of VP16 and exposure time was determined by dose response and time course experiments (not shown). The *asterisk* indicates an NF-κB complex whose appearance was not consistently seen. The above data are representative of three independent experiments.

liberation (34). Aphidicolin prevents S phase-specific toxicity of CPT (46). To evaluate whether a SSB or DSB is critical for NF-κB activation by CPT, we examined the influence of aphidicolin on CPT induction of NF-κB. FACS analysis confirmed that ~50% 70Z/3-CD14 cells were in S phase of the cell cycle at the time of CPT treatment (see below). The EMSA demonstrated that CPT activation of NF-κB was efficiently blocked by this treatment (Fig. 4*A*, *lanes 3–5*). Aphidicolin, however, did not block NF-κB activation by bacterial LPS (*lanes 10–12*). Aphidicolin also did not directly block NF-κB DNA binding activity (*lanes 6–8*). These results are consistent with the hypothesis that the generation of DSB, not SSB, is necessary for efficient NF-κB activation by CPT treatment (19). These data also imply that this activation pathway may occur only in the S phase of the cell cycle. We therefore enriched 70Z/3-CD14 cells in the S phase by FACS sorting after cells were stimulated with CPT or LPS for 2 h (Fig. 4*B*). Compared with a similarly obtained G_1 cell population, NF-κB activation was 2.8-fold higher in the S phase

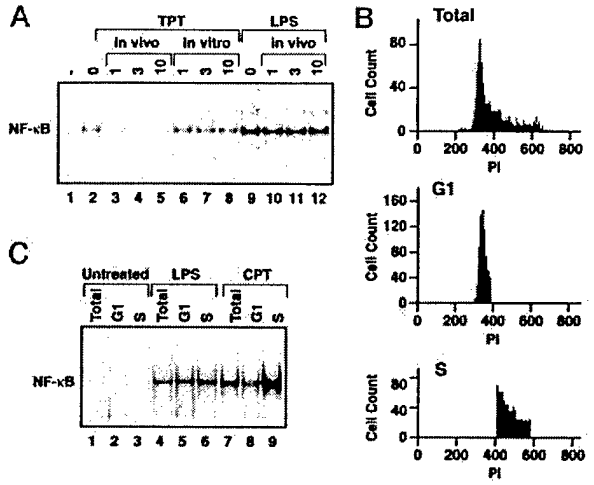

FIG. 4. **CPT activation of NF-κB requires S phase-dependent generation of DSB.** *A*, DNA replication is required for NF-κB activation by CPT treatment. 70Z/3-CD14 cells were treated with 30 μM TPT or 1 μg/ml LPS in the presence or absence of the indicated concentration of aphidicolin (*in vivo* treatments) and nuclear extracts were analyzed by EMSA. *In vitro* refers to addition of the drug direct to cell extracts as in *lane 2* prior to electrophoresis. *B*, FACS enrichment of G_1 and S phase cell population. Exponentially growing 70Z/3-CD14 cells were FACS purified based on DNA content as measured by Hoechst staining into total, G_1, and S populations. *C*, NF-κB activation by CPT treatment is concentrated in S phase of the cell cycle. NF-κB activation in cell fractions isolated as in *B* was analyzed by EMSA using equal protein loading. Phosphorimage analysis showed that CPT activation was 2.8-fold higher in S fraction than in G_1. The data are representative of at least two independent experiments.

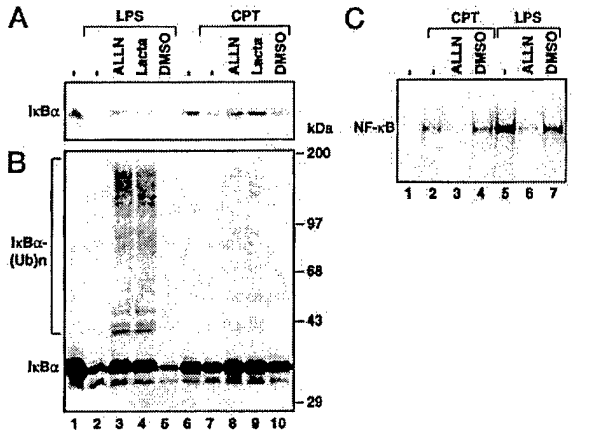

FIG. 5. **CPT induces degradation of IκBα by the ubiquitin-proteasome pathway.** *A*, IκBα degradation induced by CPT is blocked by proteasome inhibitors. 70Z/3-CD14 cells were pretreated for 30 min with ALLN (50 μg/ml), lactacystin (*Lacta*; 20 μM), or Me_2SO solvent (*DMSO*; 0.1%) and then treated with 1 μg/ml LPS (*lanes 2–6*) for 15 min or 10 μM CPT (*lanes 8–12*) for 1 h. Samples were analyzed by Western immunoblot using an IκBα-specific antibody (C21). *B*, inhibition of IκBα degradation by proteasome inhibitors induces accumulation of high molecular mass IκBα-ubiquitin ladders. A longer exposure of the blot in *A*. The positions of the IκBα band and multiubiquitinated IκBα ladders (IκBα-(Ub)n) are shown on the *left* of the figure. Relative molecular mass (in kDa) is shown on the *right*. *C*, NF-κB activation induced by CPT is blocked by proteasome inhibitors. Nuclear extracts prepared from cells that were treated as in *A* were analyzed by EMSA for NF-κB binding activity as in Fig. 1*A*. The data are representative of two or more independent experiments.

population when equivalent amounts of cell extracts were analyzed by EMSA (Fig. 4*C*). LPS stimulation did not show any significant differences between S and G_1 cells. These findings demonstrate that CPT activation of NF-κB is cell cycle coupled and predominantly takes place during the S phase of the cell cycle in a DNA-polymerase-dependent fashion. This also can explain why NF-κB activation by CPT or TPT is relatively lower in virtually all cell types examined when compared with LPS or TNFα. NF-κB activation by CPT or TPT is dependent on the percentage of replicating cells in S phase, whereas activation by either LPS or TNFα is not cell cycle coupled.

CPT Induces Degradation of IκBα by a Ubiquitin-Proteasome Pathway—The regulatory events governing NF-κB activity induced by cytokines and LPS are well characterized and involve activation of cytoplasmic signaling cascades (2). The primary regulator is the inhibitory protein, IκBα, which maintains NF-κB in the cytoplasm. Release of NF-κB to the nucleus depends on degradation of IκBα. To determine whether CPT activation of NF-κB is solely dependent on nuclear events or whether cytoplasmic events are also required, IκBα protein levels were monitored following treatment with CPT by Western immunoblot analyses. CPT treatment caused a reduction in IκBα protein levels (Fig. 5*A*, compare *lanes 6* and *7*), consistent with induction of IκBα degradation. This degradation was prevented by the proteasome inhibitors, ALLN and lactacystin (Fig. 5*A*, *lanes 8* and *9*). A longer exposure of the film (Fig. 5*B*, *lanes 8* and *9*) revealed an accumulation of characteristic high molecular mass multiubiquitinated IκBα ladders (11, 12). Proteasome inhibitors not only prevented IκBα degradation but also NF-κB activation by CPT treatment (Fig. 5*C*, compare *lanes 2* and *3*). TPT induced similar IκBα degradation (Fig. 6*A*). Inhibition of IκBα degradation by ALLN resulted in accumulation of IκBα in the cytoplasm, as visualized by an IκBα protein N-terminally tagged with the green fluorescent protein (GFP-IκBα) (Fig. 6*B*, *right panel*). Control coimmunoprecipitation experiments with RelA-specific antibodies confirmed that the addition of the GFP tag did not interfere with its association with NF-κB (80). The GFP tag also did not affect TPT-induced proteolysis (Fig. 6*A*, *lanes 2–5*). Thus, induction of IκBα degradation by CPT or TPT is similar to that induced by LPS in 70Z/3 cells or TNFα in multiple cell types (1, 2), which utilizes a ubiquitin-proteasome pathway. Moreover, we also found that IκBα degradation by TPT was markedly reduced in enucleated PC3 cells (not shown). These data demonstrate that the progression of events initiated in the nucleus by TPT or CPT treatment is continued in the cytoplasm.

IκBα Degradation Induced by CPT or TPT Is $Ser^{32/36}$-dependent—Although cytokines and LPS cause IκBα degradation by a ubiquitin-proteasome pathway that requires intact Ser^{32} and Ser^{36} residues, UV irradiation causes IκBα degradation by a ubiquitin-proteasome pathway independent of these Ser residues (13, 14). To evaluate whether CPT or TPT-induced IκBα degradation requires intact $Ser^{32/36}$ residues, the S32A/S36A mutant protein was N-terminally tagged with an HA epitope (HA-S32A/S36A) (36), stably introduced in 70Z/3-CD14 cells, and analyzed for sensitivity to degradation by TPT treatment. The S32A/S36A mutant protein was completely resistant to degradation induced by TPT treatment (Fig. 7*A*). This was not due to the presence of the HA tag because the control HA-WT IκBα protein was efficiently degraded. Moreover, a $Ser^{32/36}$ deletion mutant without the HA tag also failed to be efficiently degraded (Fig. 7*A*, Δ30–40). Stable expression of the HA-S32A/S36A mutant, but not HA-WT, selectively eliminated the appearance of NF-κB DNA binding in the nucleus after treatment with CPT or TPT (Fig. 7*B*, *lanes 9* and *10*). Consistent with the formation of multiubiquitinated IκBα ladders (Fig. 5*B*, *lanes 8* and *9*), substitution of the primary ubiquitination sites Lys^{21} and Lys^{22} (11, 50), with Arg resulted in retardation of degradation following TPT treatments (Fig. 7*A*, *HA-K21/22R*). These results are similar to those obtained with LPS (Fig. 7, *A*,

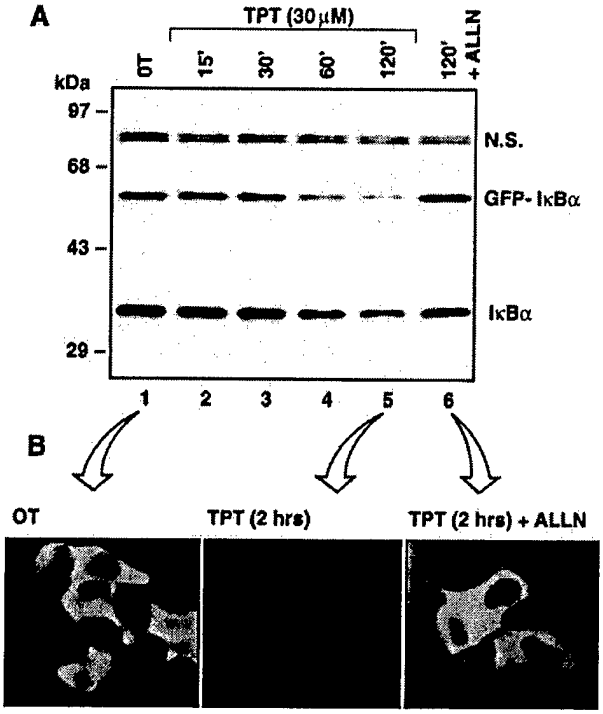

FIG. 6. **Inhibition of IκBα degradation induced by TPT results in accumulation of IκBα in the cytoplasm.** *A*, GFP-IκBα degraded in a similar manner to the endogenous IκBα protein following TPT treatment. Human IκBα (MAD-3), N-terminally fused to GFP, was stably transfected into the HEK293 cells and brighter GFP-IκBα expressing pools were isolated by fluorescent activated cell sorting. These cells were treated with TPT (30 μM) for the indicated times without (*lanes 2–5*) or with 100 μM ALLN (*lane 6*) and analyzed by Western blot using an anti-IκBα antibody (C21) as above. GFP-IκBα, but not IκBα, was also detected using GFP-specific antibody (CLONTECH; not shown). *B*, degradation of GFP-IκBα protein is largely cytoplasmic. *Left panel*, HEK293 stably expressing the GFP-IκBα protein was left untreated and visualized under fluorescein-aided fluorescent microscopy. *Middle panel*, parallel cultures as in the left panel were treated with TPT (30 μM) for 2 h as in A and visualized as above. There were decline of GFP signals in ~50% of the cell population (those showing reduced fluorescence are shown), potentially corresponding to replicating cells as suggested from results in Fig. 4. *Right panel*, parallel cultures were treated with 100 μM ALLN and 30 μM TPT and visualized as above. The exposure settings for all three panels were identical. The above data are representative of two independent experiments.

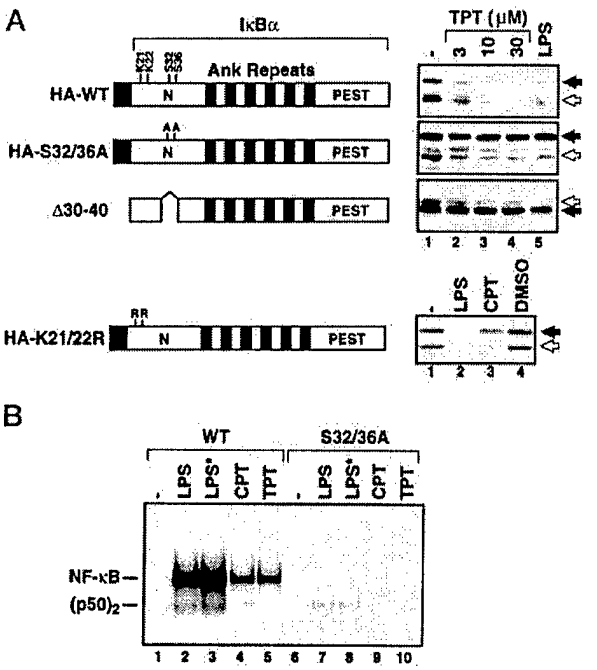

FIG. 7. **IκBα degradation induced by CPT or TPT requires intact $Ser^{32/36}$ and $Lys^{21/22}$ sites.** *A*, mutation or deletion of $Ser^{32/36}$ or $Lys^{21/22}$ abrogates IκBα degradation induced by TPT or CPT. *Left figures* show schematic presentation of IκBα mutants analyzed. Pools of 70Z/3-CD14 cells stably expressing HA-WT, HA-S32A/S36A, or Δ30–40 IκBα were treated with TPT (3, 10 or 30 μM) for 1 h (*lanes 2–4*). The cells were also treated with LPS (1 μg/ml) for 15 min (*lane 5*). Total cell extracts were analyzed by Western blot analysis using the C21 anti-IκBα antibody. A pool of 70Z/3-CD14 cells stably expressing HA-K21/22R IκBα mutant protein was treated with 1 μg/ml LPS for 15 min (*lane 2*), 10 μM CPT for 1 h (*lane 3*), or 0.1% Me_2SO for 1 h (*lane 4*) and analyzed as above. *Filled arrows* point to the exogenously introduced IκBα proteins, and *open arrows* point to the endogenous IκBα proteins. *B*, HA-S32A/S36A mutant prevents NF-κB activation. EMSA was performed as described in the legend to Fig. 1*A* using nuclear extracts from a 70Z/3-CD14 cell clone stably expressing either HA-WT (*lanes 1–5*) or HA-S32A/S36A (*lanes 6–10*) and treated with LPS (1 μg/ml for 15 min or 2 h—marked LPS*), CPT (10 μM for 2 h), or TPT (30 μM for 2 h). Positions of NF-κB and p50 homodimeric complexes are indicated on the *left*. The data are representative of two or more independent experiments.

lane 5, and *B*, *lanes 7* and *8*) or TNFα (1, 2) but distinct from data obtained with UV irradiation (13, 14). Of note, LPS caused efficient degradation of HA-K21/22R (Fig. 7*A*, *K21/22R*, *lane 2*), which is consistent with the observations that other Lys residue(s) can compensate for the lack of $Lys^{21/22}$ sites when cells are exposed to potent NF-κB inducers (50).

The IKK Complex Is Essential for NF-κB Activation by CPT—To further elucidate the events upstream of IκBα degradation that are involved in CPT activation of NF-κB, we evaluated the NF-κB response by EMSA in HEK293 cells transiently expressing dominant-negative IKKα and β proteins. The use of EMSA analysis to investigate potential inhibitory responses was possible because transfection efficiency was consistently >90% in this cell type (Fig. 8*A*), and thus almost all cells in the transfected population expressed the IKK mutant proteins. Both IKK mutants (N-terminally tagged with a FLAG epitope) reduced the level of NF-κB activation by TPT in a dose-dependent manner (Fig. 8*B*, *upper panel*). By contrast, these mutants did not appreciably alter the DNA binding levels of AP-1 complex (Fig. 8*B*, *lower panel*). Dose-dependent expression of IKK mutant proteins is shown by Western blot analysis of cell extracts using monoclonal anti-FLAG antibody (Fig. 8*C*).

To independently determine the requirement of IKKα and IKKβ in NF-κB activation by CPT, embryonic fibroblast lines derived from IKKα and IKKβ knockout mice (51, 52) were treated with TNFα or CPT. Consistent with published observations (51–55), TNF activation of NF-κB was much weaker in IKKβ knockout cells than in IKKα knockout cells (Fig. 8*D*). However, NF-κB activation by CPT treatment was undetectable in both IKKα- and IKKβ-deficient cells (Fig. 8*D*, *lanes 12* and *8*, respectively). In addition, CPT activation of NF-κB was also undetectable in IKKγ-deficient 1.3E2 cells (56) (Fig. 8*E*, *lane 6*). Thus, key components of the IKK complex (IKKα/β/γ) are essential for NF-κB activation by CPT.

NF-κB Activation by CPT or TPT Is an Anti-apoptotic Cell Survival Response—Recent studies demonstrated that NF-κB activation by certain death inducing agents can provide an anti-apoptotic function (57–59). To evaluate whether NF-κB activation affects CPT induced apoptotic responses, the levels of apoptosis were estimated by FACS analysis based on sub-G_0/G_1 DNA content in WT and S32A/S36A expressing 70Z/3-CD14 cells. Untreated cells showed an expected pattern of cell cycle distribution for these cells with more than half of the cell

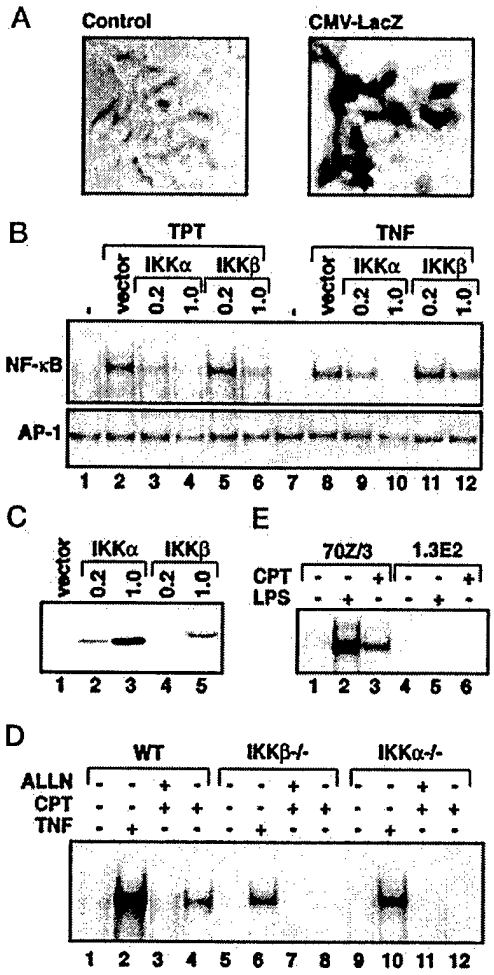

FIG. 8. **IKKα, β, and γ are essential for CPT activation of NF-κB.** *A*, X-gal staining of transiently transfected HEK293 cells. HEK293 cells were transfected with the empty vector (*left panel*) or the CMV-LacZ construct (*right panel*) and 36 h following transfection they were stained with X-gal. No X-gal-positive cells are visible in the *left panel*, whereas most cells are strongly X-gal-positive in the *right panel*. *B*, EMSA analysis of HEK293 cells transfected with dominant-negative IKKα and IKKβ constructs and treated with TPT. HEK293 cells were transfected with expression vectors (pcDNA, 0.2 or 1.0 μg/sample) for either a FLAG-tagged IKKα or IKKβ dominant-negative mutant (a Lys-to-Ala mutation at the putative ATP binding site as in Refs. 7–10 and 74) for 36 h and then treated with 30 μM TPT (2 h) or 10 ng/ml TNFα (20 min). Equivalent total cell extracts were analyzed by EMSA using Igκ-κB site (*upper panel*) or an AP-1 site (*lower panel*). Vector refers to empty pcDNA transfected cells. *C*, Western blot analysis of transfected dominant-negative IKKα and IKKβ proteins. Cell extracts prepared as above in *B* were analyzed by Western blot analysis using an anti-FLAG antibody. *D*, CPT activation of NF-κB requires IKKα and IKKβ. Mouse embryonic fibroblast lines generated from IKKα−/−, IKKβ−/−, or control mice were treated with 10 μM CPT in the presence or absence of 100 μM ALLN or 10 ng/ml TNFα for 1 h, and nuclear extracts were analyzed by EMSA. *E*, CPT activation of NF-κB requires IKKγ. 1.3E2 (IKKγ-deficient) or parental 70Z/3 cells were treated with 10 μM CPT or 10 μg/ml LPS for 1 h, and nuclear extracts were analyzed by EMSA. The above data are representative of two to three independent experiments.

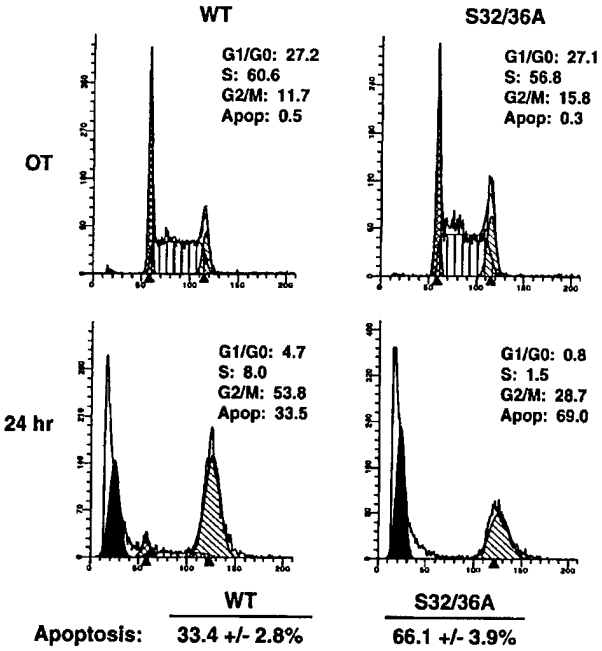

FIG. 9. **Inhibition of CPT activation of NF-κB results in an increased apoptotic response.** 70Z/3-CD14 cell clones expressing either WT or S32A/S36A IκBα were exposed to 1 μM CPT for 24 h. These cells were fixed, stained with propidium iodide, and analyzed by FACS for relative DNA content. Each panel shows the relative levels of cells in each of the cell cycle phases as well as in sub-G_1/G_0 apoptotic peaks. Average levels of apoptosis ± S.D. from three independent experiments are shown below the figure.

population in S phase of the cell cycle (Fig. 9, *OT*, *WT*). Expression of S32A/S36A mutant protein did not significantly affect the cell cycle status of untreated cells (OT, S32A/S36A). After treatment with 1 μM CPT for 24 h, however, most of the cells appeared in either a G_2/M or sub-G_0/G_1 apoptotic peak (Fig. 9, *24 h*, *WT*). The fraction of apoptotic peak was approximately twice as great in S32A/S36A expressing cells as WT expressing cells (24 h, S32A/S36A). Similar results were obtained with higher CPT doses or TPT treatments (not shown). Thus, these observations indicate that activation of NF-κB retards some cancer cells from undergoing apoptosis. These findings demonstrate that CPT activation of NF-κB can provide an anti-apoptotic activity.

DISCUSSION

The activity of NF-κB depends on a series of reactions that releases it from an inhibitory complex in the cytoplasm and allows it to migrate to the nucleus. The elucidation of the individual steps within NF-κB signaling cascades induced by a variety of structurally and functionally unrelated stimuli has revealed the use of both shared and unique components that may contribute to the diverse functions of this ubiquitous transcription factor (38, 60–68). DNA-damaging agents represent a unique group of NF-κB activators because their primary site of action is in the nucleus. In this study, we demonstrate that nuclear events arising from the DNA-damaging function of CPT and TPT are components of a NF-κB signaling pathway that converges in the cytoplasm with events associated with signaling pathways induced by cytokines or LPS stimulation.

The DNA-damaging function of CPT in replicating cells is a multi-step process that initiates with intercalation of CPT into a covalent Topo I-DNA reaction intermediate. CPT stabilizes this transient intermediate, forming the cleavable complex with a SSB. The cleavable complexes and associated SSBs are mostly reversible until the cell undergoes replication, during which the replication fork collides with the cleavable complex and yields a DSB. Our results obtained by utilizing mutant CEM/C2 cells, pharmacological agents, and FACS enrichment of S phase cells indicate that S phase-dependent generation of DSB is essential for NF-κB activation. Of note, however, is that

CPT or TPT activation of NF-κB is transient in all cell lines tested thus far. Similar dose-dependent and time course responses in lymphoid, fibroblastic, and epithelial cell lines suggest that a conserved activation mechanism may be involved. It has been demonstrated that CPT can induce degradation of Topo I enzyme by the ubiquitin-proteasome pathway causing marked reduction of Topo I enzyme within 2–4 h (69). Although this correlates well with the reduction of NF-κB activation in the continual presence of CPT in the present study, substantial levels of DSBs induced by CPT can persist for as long as 24 h in SV40-transformed human skin fibroblast cells (SV40MRC5VI) and EJ30/8D human bladder carcinoma cells (70). Because the critical DNA lesion (*i.e.* DSBs) may remain despite declining levels of Topo I enzyme, it is unlikely that the reduction of Topo I enzyme is solely responsible for transient NF-κB activation. It further implies that the mere presence of DSBs is insufficient to maintain NF-κB activation. It is thus possible that event(s) downstream of DSBs or those coupled to cell cycle may be responsible for transient NF-κB activation by CPT-related compounds. A recent study has implicated the involvement of the ataxia telangiectasia mutant protein in sustained activation of NF-κB by CPT (81).

Enucleation studies demonstrated that the process of NF-κB activation induced by CPT or TPT requires an intact nucleus. To our knowledge, this is the first demonstration of the lack of NF-κB activation in enucleated cells. Although this may be implied from the demonstration that events associated with DNA damage are required for NF-κB activation, mitochondria also contain DNA and CPT-sensitive Topo I enzyme (42). Studies utilizing L929 fibrosarcoma cells deficient for mitochondrial (DNA) and antimycin A, which increases the generation of reactive oxygen intermediates by inhibiting the electron transport chain, indicate that NF-κB activation by TNFα requires reactive oxygen intermediates derived from mitochondria (71). Because NF-κB is implicated as an important mammalian oxidative stress-responsive transcription factor (72), determination of the contribution of nuclear *versus* potential mitochondrial events was crucial for elucidating the NF-κB activation mechanism induced by CPT and TPT. Our findings provide direct evidence that CPT- or TPT-induced DNA damage in the nucleus is a primary component of the signaling events required for NF-κB activation. Although recent studies that utilized UV-C treatment of Xeroderma pigmentosa group A fibroblasts suggested the involvement of DNA damage in late stage NF-κB activation (14), whether or not an intact nucleus is required for this late activation was not investigated. Previous studies demonstrated that UV activation of NF-κB could efficiently take place in enucleated cells (20).

CPT induction of DNA damage translates into activation of a cytoplasmic signaling cascade that liberates active NF-κB from the inhibitor protein, IκBα. We utilized well characterized mutants of signaling components within the cytokine-inducible NF-κB signaling pathway to dissect the signaling cascade activated by CPT and TPT. Ser-to-Ala mutations at positions 32 and 36 of IκBα disrupt inducible phosphorylation and prevent subsequent ubiquitination and degradation by the proteasome pathway (47–49). We showed that these mutants also prevent IκBα degradation and activation of NF-κB induced by CPT and TPT. We additionally demonstrated that dominant-negative IKK mutants that inhibit phosphorylation of IκBα at these sites also prevent NF-κB activation by TPT. IKKα-, β-, or γ-deficient cells fail to activate NF-κB by CPT treatment. Mutation of Lys residues critical for the attachment of ubiquitin moieties further disrupts CPT-inducible IκBα degradation. Together with pharmacological evidence using proteasome inhibitors, our findings show that CPT and TPT induction of IκBα degradation is similar to that induced by cytokines, LPS, and several other signals (7, 8, 10, 11, 47–50, 73, 74). Our findings therefore demonstrate that nuclear DNA damage causes IKK-dependent degradation of IκBα in the cytoplasm. This activation may involve signal transfer from the nucleus to the cytoplasm. This type of nuclear-to-cytoplasmic signaling has also been suggested for the late stage NF-κB activation induced by UV irradiation, which involves the production of an autocrine/paracrine factor, interleukin-1α (14). A recent study has also implicated the involvment of the DNA-dependent protein kinase in NF-κB activation by certain DNA damaging agents (82). Further definition of signaling components and reactions will help to determine whether NF-κB activation by CPT indeed involves a nuclear-to-cytoplasmic signal transduction pathway.

CPT derivatives, including TPT, are utilized clinically as part of cancer therapy regimes (34, 35). Recently, several studies have reported that NF-κB may control expression of genes involved in the regulation of apoptosis (57–59, 75–78). In particular, Wang *et al.* (58) have shown that NF-κB activation by ionizing radiation and daunarubicin may have anti-apoptotic effects in HT1080 human fibrosarcoma cells. The same group recently showed that NF-κB activation by CPT-11 can display similar anti-apoptotic effects in the above cell line (79). We have also shown that CPT activation of NF-κB provides an anti-apoptotic function. NF-κB-dependent survival of even a fraction of cancer cells after treatment with DNA-damaging agents, such as TPT or ionizing radiation, will likely lead to increased mutation rates and accelerated manifestation of malignancy. Moreover, it may also contribute to transformation of normal cells during the therapy. Understanding the mechanism(s) of NF-κB activation, therefore, may help improve the current methods of cancer therapy by defining a resistance mechanism to Topo I inhibitors and potentially other clinically important DNA-damaging and NF-κB-activating agents, such as ionizing radiation and Topo II inhibitors.

Acknowledgments—We thank Dr. Y. Pommier for CEMp and CEM/C2 cells, Dr. I. M. Verma for IKKα and IKKβ knockout cell lines, Dr. A. Israel for IKKγ-deficient cells, Drs. R. Wisdom, J. Petrini, and E. T. Alarid for their critical reading of the manuscript, and B. True for help in the preparation of the figures.

REFERENCES

1. Baeuerle, P. A., and Baltimore, D. (1996) *Cell* **87,** 13–20
2. Verma, I. M., Stevenson, J. K., Schwarz, E. M., Van Antwerp, D., and Miyamoto, S. (1995) *Genes Dev.* **9,** 2723–2735
3. Sonenshein, G. E. (1997) *Semin. Cancer Biol.* **8,** 113–119
4. Beg, A. A., Ruben, S. M., Scheinman, R. I., Haskill, S., Rosen, C. A., and Baldwin, A. S. J. (1992) *Genes Dev.* **6,** 1899–1913
5. Ganchi, P. A., Sun, S. C., Greene, W. C., and Ballard, D. W. (1992) *Mol. Biol. Cell* **3,** 1339–1352
6. Chen, Z. J., Parent, L., and Maniatis, T. (1996) *Cell* **84,** 853–862
7. DiDonato, J. A., Hayakawa, M., Rothwarf, D. M., Zandi, E., and Karin, M. (1997) *Nature* **388,** 548–554
8. Mercurio, F., Zhu, H., Murray, B. W., Shevchenko, A., Bennett, B. L., Li, J. W., Young, D. B., Barbosa, M., Mann, M., Manning, A., and Rao, A. (1997) *Science* **278,** 860–866
9. Woronicz, J. D., Gao, X., Cao, Z., Rothe, M., and Goeddel, D. V. (1997) *Science* **278,** 866–869
10. Zandi, E., Rothwarf, D. M., Delhase, M., Hayakawa, M., and Karin, M. (1997) *Cell* **91,** 243–252
11. Alkalay, I., Yaron, A., Hatzubai, A., Orian, A., Ciechanover, A., and Ben-Neriah, Y. (1995) *Proc. Natl. Acad. Sci. U. S. A.* **92,** 10599–10603
12. Chen, Z., Hagler, J., Palombella, V. J., Melandri, F., Scherer, D., Ballard, D., and Maniatis, T. (1995) *Genes Dev.* **9,** 1586–1597
13. Li, N., and Karin, M. (1998) *Proc. Natl. Acad. Sci. U. S. A.* **95,** 13012–13017
14. Bender, K., Gottlicher, M., Whiteside, S., Rahmsdorf, H. J., and Herrlich, P. (1998) *EMBO J.* **17,** 5170–5181
15. Han, Y., Weinman, S., Boldogh, I., Walker, R. K., and Brasier, A. R. (1999) *J. Biol. Chem.* **274,** 787–794
16. Chen, F., Lu, Y., Kuhn, D. C., Maki, M., Shi, X., Sun, S. C., and Demers, L. M. (1997) *Arch. Biochem. Biophys.* **342,** 383–388
17. Imbert, V., Rupec, R. A., Livolsi, A., Pahl, H. L., Traenckner, E. B. M., Mueller-Dieckmann, C., Farahifar, D., Rossi, B., Auberger, P., Baeuerle, P. A., and Peyron, J. F. (1996) *Cell* **86,** 787–798
18. Stein, B., Kramer, M., Rahmsdorf, H. J., Ponta, H., and Herrlich, P. (1989) *J. Virol.* **63,** 4540–4544
19. Piret, B., and Piette, J. (1996) *Nucleic Acids Res.* **24,** 4242–4248

20. Devary, Y., Rosette, C., DiDonato, J. A., and Karin, M. (1993) *Science* **261,** 1442–1445
21. Coffer, P. J., Burgering, B. M., Peppelenbosch, M. P., Bos, J. L., and Kruijer, W. (1995) *Oncogene* **11,** 561–569
22. Herrlich, P., Blattner, C., Knebel, A., Bender, K., and Rahmsdorf, H. J. (1997) *Biol. Chem.* **378,** 1217–1229
23. Rosette, C., and Karin, M. (1996) *Science* **274,** 1194–1197
24. Tobin, D., van Hogerlindern, M., and Toftgard, R. (1998) *Proc. Natl. Acad. Sci. U. S. A.* **95,** 565–569
25. Knebel, A., Rahmsdorf, H. J., Ullrich, A., and Herrlich, P. (1996) *EMBO J.* **15,** 5314–5325
26. Miyamoto, S., Wuerzberger, S. M., Seufzer, B., and Boothman, D. A. (1997) *Proc. Am. Assoc. Cancer Res.* **38,** 624
27. Hsiang, Y. H., and Liu, L. F. (1988) *Cancer Res.* **48,** 1722–1726
28. Giovanella, B. C., Stehlin, J. S., Wall, M. E., Wani, M. C., Nicholas, A. W., Liu, L. F., Silber, R., and Potmesil, M. (1989) *Science* **246,** 1046–1048
29. Liu, L. F. (1989) *Annu. Rev. Biochem.* **58,** 351–375
30. Wang, J. C. (1996) *Annu. Rev. Biochem.* **65,** 635–692
31. Hsiang, Y. H., Hertzberg, R., Hecht, S., and Liu, L. F. (1985) *J. Biol. Chem.* **260,** 14873–14878
32. Covey, J. M., Jaxel, C., Kohn, K. W., and Pommier, Y. (1989) *Cancer Res.* **49,** 5016–5022
33. Hsiang, Y.-H., Lihou, M. G., and Liu, L. F. (1989) *Cancer Res.* **49,** 5077–5082
34. Slichenmyer, W. J., Rowinsky, E. K., Donehower, R. C., and Kaufmann, S. H. (1993) *J. Natl. Cancer Inst.* **85,** 271–291
35. Rothenberg, M. L. (1997) *Ann. Oncol.* **8,** 837–855
36. Miyamoto, S., Seufzer, B., and Shumway, S. (1998) *Mol. Cell. Biol.* **18,** 19–29
37. Poste, G. (1972) *Exp. Cell Res.* **73,** 273–286
38. Cao, Z. D., Xiong, J., Takeuchi, M., Kurama, T., and Goeddel, D. V. (1996) *Nature* **383,** 443–446
39. Chiao, P. J., Miyamoto, S., and Verma, I. M. (1994) *Proc. Natl. Acad. Sci. U. S. A.* **91,** 28–32
40. VanAntwerp, D. J., and Verma, I. M. (1996) *Mol. Cell. Biol.* **16,** 6037–6045
41. Wuerzberger, S. M., Pink, J. J., Planchon, S. M., Byers, K. L., Bornmann, W. G., and Boothman, D. A. (1998) *Cancer Res.* **58,** 1876–1885
42. Lin, J. H., and Castora, F. J. (1995) *Arch. Biochem. Biophys.* **324,** 293–299
43. Baeuerle, P. A., and Baltimore, D. (1988) *Science* **242,** 540–546
44. Fujimori, A., Hoki, Y., Popescu, N. C., and Pommier, Y. (1996) *Oncol. Res.* **8,** 295–301
45. Fujimori, A., Harker, W. G., Kohlhagen, G., Hoki, Y., and Pommier, Y. (1995) *Cancer Res.* **55,** 1339–1346
46. D'Arpa, P., Beardmore, C., and Liu, L. F. (1990) *Cancer Res.* **50,** 6919–6924
47. Brockman, J. A., Scherer, D. C., McKinsey, T. A., Hall, S. M., Qi, X., Lee, W. Y., and Ballard, D. W. (1995) *Mol. Cell. Biol.* **15,** 2809–2818
48. Brown, K., Gerstberger, S., Carlson, L., Franzoso, G., and Siebenlist, U. (1995) *Science* **267,** 1485–1488
49. Traenckner, E. B., Pahl, H. L., Henkel, T., Schmidt, K. N., Wilk, S., and Baeuerle, P. A. (1995) *EMBO J.* **14,** 2876–2883
50. Scherer, D. C., Brockman, J. A., Chen, Z., Maniatis, T., and Ballard, D. W. (1995) *Proc. Natl. Acad. Sci. U. S. A.* **92,** 11259–11263
51. Li, Q., Lu, Q., Hwang, J. Y., Buscher, D., Lee, K. F., Izpisua-Belmonte, J. C., and Verma, I. M. (1999) *Genes Dev.* **13,** 1322–1328
52. Li, Q., Van Antwerp, D., Mercurio, F., Lee, K. F., and Verma, I. M. (1999) *Science* **284,** 321–325
53. Li, Z. W., Chu, W., Hu, Y., Delhase, M., Deerinck, T., Ellisman, M., Johnson, R., and Karin, M. (1999) *J. Exp. Med.* **189,** 1839–1845
54. Tanaka, M., Fuentes, M. E., Yamaguchi, K., Durnin, M. H., Dalrymple, S. A., Hardy, K. L., and Goeddel, D. V. (1999) *Immunity* **10,** 421–429
55. Hu, Y., Baud, V., Delhase, M., Zhang, P., Deerinck, T., Ellisman, M., Johnson, R., and Karin, M. (1999) *Science* **284,** 316–320
56. Yamaoka, S., Courtois, G., Bessia, C., Whiteside, S. T., Weil, R., Agou, F., Kirk, H. E., Kay, R. J., and Israel, A. (1998) *Cell* **93,** 1231–1240
57. Beg, A. A., and Baltimore, D. (1996) *Science* **274,** 782–784
58. Wang, C. Y., Mayo, M. W., and Baldwin, A. S. (1996) *Science* **274,** 784–787
59. VanAntwerp, D. J., Martin, S. J., Kafri, T., Green, D. R., and Verma, I. M. (1996) *Science* **274,** 787–789
60. Hirano, M., Osada, S., Aoki, T., Hirai, S., Hosaka, M., Inoue, J., and Ohno, S. (1996) *J. Biol. Chem.* **271,** 13234–13238
61. Lee, F. S., Hagler, J., Chen, Z. J., and Maniatis, T. (1997) *Cell* **88,** 213–222
62. Yin, M. J., Christerson, L. B., Yamamoto, Y., Kwak, Y. T., Xu, S., Mercurio, F., Barbosa, M., Cobb, M. H., and Gaynor, R. B. (1998) *Cell* **93,** 875–884
63. Cheng, G., Cleary, A. M., Ye, Z. S., Hong, D. I., Lederman, S., and Baltimore, D. (1995) *Science* **267,** 1494–1498
64. Cheng, G., and Baltimore, D. (1996) *Genes Dev.* **10,** 963–973
65. Ishida, T., Mizushima, S., Azuma, S., Kobayashi, N., Tojo, T., Suzuki, K., Aizawa, S., Watanabe, T., Mosialos, G., Kieff, E., Yamamoto, T., and Inoue, J. (1996) *J. Biol. Chem.* **271,** 28745–28748
66. Rothe, M., Sarma, V., Dixit, V. M., and Goeddel, D. V. (1995) *Science* **269,** 1424–1427
67. Malinin, N. L., Boldin, M. P., Kovalenko, A. V., and Wallach, D. (1997) *Nature* **385,** 540–544
68. Tsukamoto, N., Kobayashi, N., Azuma, S., Yamamoto, T., and Inoue, J. (1999) *Proc. Natl. Acad. Sci. U. S. A.* **96,** 1234–1239
69. Desai, S. D., Liu, L. F., Vazquez-Abad, D., and D'Arpa, P. (1997) *J. Biol. Chem.* **272,** 24159–24164
70. Ryan, A. J., Squires, S., Strutt, H. L., Evans, A., and Johnson, R. T. (1994) *Carcinogenesis* **15,** 823–828
71. Schulze-Osthoff, K., Beyaert, R., Vandevoorde, V., Haegeman, G., and Fiers, W. (1993) *EMBO J.* **12,** 3095–3104
72. Schreck, R., Albermann, K., and Baeuerle, P. A. (1992) *Free Radical Res. Commun.* **17,** 221–237
73. Zandi, E., Chen, Y., and Karin, M. (1998) *Science* **281,** 1360–1363
74. Regnier, C. H., Song, H. Y., Gao, X., Goeddel, D. V., Cao, Z., and Rothe, M. (1997) *Cell* **90,** 373–383
75. Wu, M., Lee, H. Y., Bellas, R. E., Schauer, S. L., Arsura, M., Katz, D., Fitzgerald, M. J., Rothstein, T. L., Sherr, D. H., and Sonenshein, G. E. (1996) *EMBO J.* **15,** 4682–4690
76. Wu, M. X., Ao, S., Prasad, K. V. S., Wu, R., and Schlossman, S. F. (1998) *Science* **281,** 998–1001
77. Chu, Z.-L., McKinsey, T. A., Liu, L., Gentry, J. J., Halim, M. H., and Ballard, D. W. (1997) *Proc. Natl. Acad. Sci. U. S. A.* **94,** 10057–10062
78. Wang, C. Y., Mayo, M. W., Korneluk, R. G., Goeddel, D. V., and Baldwin, A. S. (1998) *Science* **281,** 1680–1683
79. Wang, C. Y., Cusack, J. C. J., Liu, R., and Baldwin, A. S. (1999) *Nat. Med.* **5,** 412–417
80. Huang, T. T., Kudo, N., Yoshida, M., and Miyamoto, S. (2000) *Proc. Natl. Acad. Sci. U. S. A.* **97,** 1014–1019
81. Piret, B., Schoonbroodt, S., and Piret, J. (1999) *Oncogene* **18,** 2261–2271
82. Basu, S., Rosenzweig, K. R., Youmell, M., and Price, B. D. (1998) *Biochem. Biophys. Res. Commun.* **247,** 79–83

Annals of New York Academy of Sciences, 092500
For meeting: ***"The Camptothecins", March 17-21,2000***

CELLULAR AND MOLECULAR RESPONSES TO TOPOISOMERASE I POISONS: EXPLOITING SYNERGY FOR IMPROVED RADIOTHERAPY*

Shigeki Miyamoto[1], Tony Huang[1], Shelly Wuerzberger-Davis[1], William G. Bornmann[2] John J. Pink[3], Colleen Tagliarino[3], , Timothy J. Kinsella[3], and David A. Boothman[3#]

[1]Department of Pharmacology, University of Wisconsin-Madison, Madison, WI 53792, 3Preparative Synthesis Core Facility, Memorial Sloan-Kettering Cancer Center, New YORK, NY 10021, and [2]Departments of Radiation Oncology & Pharmacology, Case Western Reserve University, Cleveland, OH 44106-4942.

[#]*To whom reprint requests should be addressed at:* 10900 Euclid Avenue (BRB-326 East), Laboratory of Molecular Stress Responses, Case Western Reserve University, Cleveland, Ohio 44106-4942. Tel: (216) 368-0840; Fax: (216) 368-1142; e-mail: dab30@po.cwru.edu.

*Support for this work was provided by grant #DAMD17-98-1-8260 to D.A.B from the U.S. Department of Defense (DOD) Breast Cancer Initiative; a post-doctoral research fellowship (DAMD17-97-1-7221) to J.J.P. from the DOD Breast Cancer Initiative; and a pre-doctoral fellowship (DAMD18-00-2354) to C.T. from the DOD Breast Cancer Initiative. This work was also funded by a Howard Hughes Medical Institute grant through the UW Medical School, a Shaw Scientist Award from the Milwaukee Foundation, and grants from the NIEHS Center and UW Comprehensive Cancer Center to S.M.

Abbreviations: 9-AC, 9-amino-camptothecin; ALLN, acetyl-leucinyl-leucinyl-norleucinal; beta(ß)-lapachone, (ß-lap, 3,4-dihydro-2,2-dimethyl-2H-naphtho[1,2-*b*] pyran-5,6-dione); CMV, cytomegalovirus; CPT, camptothecin; DMSO, dimethylsolfoxide; DSB, DNA double strand break; ECL, enhanced chemiluminescent; EMSA, electrophoretic mobility shift assay; GFP, green fluorescent protein; HA, hemagglutinin; HRP, horse raddish peroxidase; IL-1, interleukin-1; IR, ionizing radiation; MMC, mitomycin C; MTD, maximally tolerated dose; NQO1, NAD(P)H:quinone oxidoreductase (a.k.a., DT-diaphorase, xip-3, (E.C. 1.6.99.2)); PARP, poly (ADP)-ribose polymerase; PMA, phorbol myristyl acetate; LPS, lipopolysaccharide; SSB, DNA single strand break; TNFα, tumor necrosis factor alpha; Topo I, DNA topoisomerase I; TPT, topotecan; UV, ultraviolet irradiation.

Key Words: apoptosis; beta(ß)-lapachone; breast cancer; calpain; caspases; colon cancer; IκB; lung cancer; NF-κB; NQO1 (DT diaphorase); poisons; prostate cancer; radiosensitizers; signal transduction; Topoisomerase (Topo) I; Topo II-alpha; x-ray-inducible transcript leading to protein #3 (xip3).

ABSTRACT

The efficacy of topoisomerase (Topo) I-active drugs may be improved by better understanding the molecular and cellular responses of tumor compared to normal cells after genotoxic insults. Ionizing radiation (IR) + Topo I-active drugs (e.g., Topotecan) caused synergistic cell killing in various human cancer cells, even in cells from highly radioresistant tumors. Topo I poisons had to be added either during or immediately after IR. Synergy was caused by DNA lesion modification mechanisms, as well as by concomitant stimulation of two pathways of cell death: necrosis (IR) + apoptosis (Topo I poisons). Cumulative data favor a mechanism of synergistic cell killing caused by altered DNA lesion modification and enhanced

apoptosis. However, alterations in cell cycle regulation may also play a role in the synergy between these two agents in certain human cancers.

We recently showed that NF-κB, a known anti-apoptotic factor, was activated in various cancer cells after poisoning Topo I using clinically active drugs. NF-κB activation was dependent on initial nuclear DNA damage followed by cytoplasmic signaling events. Cytoplasmic signaling leading to NF-κB activation after Topo I poisons was diminished in cytoplasts (lacking nuclei), and in CEM/C2 cells that expressed a mutant Topo I protein that did not interact with Topo I-active drugs. NF-κB activation was intensified in S-phase and blocked by aphidicolin, suggesting that activation was a result of double strand break formation due to Topo I poisoning and DNA replication. Dominant-negative IκB expression augmented Topo I poison-mediated apoptosis. Elucidation of molecular signal transduction pathways after Topo I drug-IR combinations may lead to improved radiotherapy by blocking anti-apoptotic NF-κB responses.

Recent data also indicate that synergy caused by IR + Topo I poisons is different from radiosensitization by ß-lapachone (ß-lap), a "reported" Topo I and II-alpha poison *in vitro*. In fact, ß-lap does not kill cells by poisoning either Topo I or II-alpha *in vivo*. Instead, the compound is "activated" by an IR (damage)-inducible enzyme, NAD(P)H:quinone oxidoreductase (NQO1), a gene cloned as x-ray-inducible transcript #3, xip3. Unlike the lesion modification pathway induced by IR + Topo I drugs, ß-lap kills cells via NQO1 futile cycle metabolism. Downstream apoptosis caused by ß-lap appears to be non-caspase-mediated, involving calpain or a calpain-like protease. Thus, although Topo I poisons or ß-lap in combination with IR both synergistically kill cancer cells, the mechanisms are very different.

INTRODUCTION

Topoisomerase I Poisons. Topoisomerase I (Topo I) is a nuclear enzyme that unwinds genomic supercoiled DNA by nicking a single DNA strand, passing the intact strand through

the nick, and then ligating the break. Topo I activity, thereby, decreases the linking number of DNA by one. Thus, Topo I unwinds supercoiled DNA, functioning mainly during RNA transcription and DNA replication, as well as in viral encapsulation, HIV replication, genetic recombination, and chromosomal condensation/decondensation.[1]

Drugs active against Topo I can cause lethality through an enzyme-mediated nicking reaction. Camptothecin (CPT) and its analogues reversibly stabilize DNA-Topo I "cleavable" complexes.[2] Precisely how stabilization of cleavable complexes lead to cell responses and subsequent death is under intense investigation. Since CPT-mediated cell death is largely S-phase-specific in many but not all cells,[3] it was hypothesized that DNA replication forks collide with DNA-Topo I complexes. This collision then results in several potentially toxic problems for the cell, including replication fork arrest, topologically (or strain)-induced DNA double strand breaks, inhibition of transcription, stabilization of the p53 tumor-suppressor, and subsequent p53-mediated apoptosis. Concentration-dependent G_1 and/or G_2 cell cycle checkpoint arrests, as well as non-apoptotic cell death responses are also observed after Topo I poisons.[4-6] Most CPT-mediated cell death models predict that Topo I poisons would be clinically efficacious if continuously administered over long periods of time, similar to 5-fluorouracil (which inhibits thymidylate synthase), another S-phase specific drug.[6] Interestingly. however, most animal studies and clinical trials to date have not reported major differences in anti-tumor activity based on treatment schedules,[7] and many current clinical trials are re-testing the theory that CPT is S-phase specific *in vivo* and should be given under prolonged, continuous routes of administration. Recently, we discovered dramatic S phase-specific activation of NF-κB, a transcription factor, in various human cancer cells following brief (1-2 h) exposures to CPT analogs (e.g., topotecan, TPT). Since NF-κB is an anti-apoptotic factor that can induce downstream genes that protect against cell death, this cellular

response to Topo poisons (also found with Topo II-alpha poisons) may be a leading factor in mitigating the efficacy of these drugs. These recent findings will be discussed below.

ß-Lapachone (ß-lap). ß-Lap is a naturally occurring 1,2-naphthoquinone initially isolated from the bark of the Lapacho tree, native to South America. We showed that this drug was a radiosensitizing agent against radioresistant human cancer cells, including human laryngeal carcinoma (HEp-2) and malignant melanoma (U1-Mel) cell lines.[8, 9] Using cell-free assays, ß-lap inhibited Topo I by catalytic inhibition, a mechanism quite different from that of CPT, TPT, 9-AC or Irinotecan (CPT-11).[10-12] ß-Lap administration did not **(a)** stabilize Topo I-DNA cleavable complexes *in vivo* [12] or *in vitro*[10]; **(b)** result in formation of DNA single strand nicks *in vivo*[13]; or **(c)** lead to the damage-mediated stabilization (induction) of wild-type p53.[14] The fact that ß-lap did not produce DNA single strand nicks in human or hamster cancer cells[13] was indirectly confirmed by the absence of wild-type p53 induction in breast or prostate cancer cells.[11, 14] While assays *in vitro* indirectly suggested that Topo I and/or Topo II-alpha may be intracellular targets of ß-lap, it seemed likely that it was not the mechanism through which this compound killed cells.[14-16] We reported that the cytotoxicity caused by ß-lap in MCF-7 breast cancer cells could be solely accounted for by apoptotic responses.[14] Further investigation revealed that ß-lap probably does not act on Topo I or Topo II-alpha *in vivo*, but is instead activated to induce a novel noncaspase-mediated apoptotic response directed by the NQO1 damage-inducible enzyme, also refered to as xip3.[17, 18]

NF-κB Activation Responses. The NF-κB/Rel family of transcription factors regulates expression of genes critical for apoptosis, as well as many other genes.[19-21] NF-κB exists as dimeric complexes composed of p50, p65 (RelA), c-Rel, RelB, or p52. NF-κB associates with members of the IκB family of proteins, such as IκBα, which localizes NF-κB in the cytoplasm.[22, 23] Dissociation from IκBα is essential for NF-κB to enter the nucleus and

activate gene expression. Several signaling cascades that control NF-κB activation converge at an IκB kinase (IKK) complex, responsible for site-specific phosphorylation of IκBα.[24-27] Phosphorylation of IκBα causes multi-ubiquitination of IκBα and its subsequent degradation by the 26S proteasome.[28, 29] This sequence of events can be induced without *de novo* protein synthesis by multiple extracellular stimuli.

NF-κB activation pathways typically originate from ligand-receptor interactions at the cell membrane. However, NF-κB can also be activated by certain DNA damaging agents. We hypothesized that a signal may be transferred from the nucleus to the cytoplasm to activate NF-κB after DNA damage in the nucleus.[30] Devary *et al.*[31] showed that enucleated cells (i.e., cytoplasts) retained full capacity to activate NF-κB after UV irradiation, showing that nuclear DNA damage is not required for NF-κB activation after this cytotoxic stress. In contrast, NF-κB activation by certain DNA-damaging agents, including CPT, correlated with their capacity to induce DNA breaks.[32] The requirement of damaged DNA in the nucleus for activation was not examined. One of our objectives was to determine whether or not nuclear events associated with the DNA damaging action of CPT or topotecan (TPT) were required for activation of cytoplasmically located NF-κB complexes. We also examined the influence of NF-κB activation in CPT-mediated apoptosis. We discovered a series of nuclear events induced by CPT/TPT that converged with cytoplasmic signaling events responsible for the activation of NF-κB. These signal transduction responses provided an anti-apoptotic function.

MATERIALS AND METHODS

Chemicals and cell treatments. 9-Amino-20(RS)camptothecin (9-AC) was obtained from Monroe E. Wall (Research Triangle Park, N.C.) as previously described. Topotecan (TPT, MW: 421.4) was a gift from SmithKline Beecham (King of Prussia, PA) and was made fresh in DMSO. CPT, VP16, calpain inhibitor I (ALLN), DMSO, bacterial LPS, PMA, cycloheximide, aphidicolin, and cytochalasin B were purchased from Sigma Chem. Co.. Human recombinant

TNFα was from CalBiochem. IgGs against IκBα (C21), c-Rel (C), p65 (A and C20), Rel-B (C-19), p52 (I-18), and p50 (NLS) were purchased from Santa Cruz Biotechnology. A monoclonal anti-Flag antibody was purchased from Kodak, horse raddish peroxidase-conjugated anti-rabbit and anti-mouse antibodies and Protein A were obtained from Amersham. ß-Lap (M_r: 242.3, see top insert, Fig. #1) and camptothecin (M_r: 348.3) were obtained and prepared as described.[9, 11] Both drugs were dissolved in DMSO, concentrations determined, and stock aliquots stored at -20 °C.[3, 8, 14, 17] Exact concentrations of drugs were determined using spectrophotometric analyses.[14, 17] Stored vials were used only once.

Tissue culture techniques. Human malignant melanoma (U1-Mel) cells were generously provided by Dr. J. B. Little (Dept. Radiation Therapy, Harvard Medical School, Boston, MA). Their initial plating and growth to confluence-arrest were described.[8, 14, 33, 34] Cells were free of mycoplasma contamination and contaminated cells were found to be a major cause of artifacts in nearly all of the endpoint investigated in this study, as we recently described for cellular responses to IR.[35] Culture conditions for 70Z/3 and 70Z/3-CD14 murine pre-B cells were described.[36] CEMp and CEM/C2 human T cell lines were kindly provided by Dr. Y. Pommier (NIH) and maintained in RPMI-1640 medium (Cellgro, Mediatech) supplemented with 10% fetal bovine serum (FBS, HyClone Laboratory, Inc.), 1000 units of penicillin G (Sigma Chem. Co., St. Louis, MO), and 0.5 mg/ml streptomycin sulfate (Sigma) in an humidified 5% CO_2-95% air incubator. HeLa human cervical carcinoma cells and PC-3 human prostate carcinoma cells were maintained in DMEM (Cellgro) supplemented with 10% FBS and antibiotics as above in a 10% CO_2-90% air incubator. The human kidney embryonic fibroblast 293 (HEK293) was maintained in the latter media on 0.1% (W/V) gelatin-coated plastic culture dishes.

Survival determinations. Typically, 5.0 x 10^5 cells from subconfluent cultures were plated onto 25 cm^2 tissue culture flasks. All flasks were letter-coded and experiments performed

double-blind. Cells were fed every 2-3 days until growth arrest by confluency was achieved, usually in 5-7 days. Cells were then fed every other day for an additional 7-10 days. One day before each experiment, cells were shifted to DME containing 0.2% FCS to further arrest U1-Mel cells. Confluence-arrested U1-Mel cells demonstrated $\leq$6% [^{3}H]thymidine-labeled nuclei and ~85% G_0/G_1, 4% S-phase, and 11% G_2/M cells.[8, 9, 34] Following IR exposure and ß-lap or Topo I poison posttreatments (e.g., with 9-AC, CPT or TPT), colony forming assays were performed using 10-fold limiting dilution analyses. All colony forming assays were performed at least seven times in duplicate. Survival curves were normalized for toxicity due to IR or drug exposures alone, as well as variations in initial viable cells plated. A colony consisted of 100 or more normal-appearing cancer cells. Data were obtained, analyzed and graphed.[8, 9, 34]

Topo I Enzyme Assays. Purified calf thymus Topo I or Topo I crude extracts from isolated nuclei of U1-Mel cells were used in enzymatic assays.[9] Loss of Form I relative to total DNA loaded onto each lane of the agarose gels was quantitated.[9]

SDS-K$^+$ Topo I complex assays. A modification of the SDS-KCl assay was used to quantify DNA-Topo I complexes via glass fiber filter binding as described.[12, 13]

Flow Cytometry. Changes in cell cycle distribution were recorded and cell death measured.[14] Data were analyzed by ModFit LT (Verity Software House). Statistical evaluations (p values) were calculated using the student's "t" test. For FACS sorting of G_1, S and total cell fractions for EMSA analyses, 70Z/3 cells were first treated with agents, stained with Hoechst 33342 at the final concentration of 10 µg/ml for 15 min at 37 °C in RPMI growth media, and sorted using FACStar^{PLUS} (Becton Dickinson) at 4 °C. Cells (10^6) were purified and total cell extracts prepared for EMSA analyses.[14]

Northern blot analyses. Northern blot analyses on control or IR-treated cells were performed as described.[34] Equal loading of Northern blots was accomplished by ethidium-stained gels and by 36B4 transcript levels.[34]

Electrophoretic mobility shift (EMSA) and supershift assays- The Igκ-κB oligonucleotide probe and conditions for EMSA were described.[36] For supershift assays, 1 μg of IgG antibodies specific to NF-κB proteins (Santa Cruz Biotechnology) were added to nuclear extracts for 20 min on ice prior to addition of radiolabeled probe. The AP-1 site used for control EMSA reactions was obtained from Promega.

Enucleation. Cytochalsin B-mediated enucleation was performed as described.[37] Cytoplasts were incubated with prewarmed growth media for 30 min, 37 °C for recovery. Enucleation efficiency varied from ~75%-95% for PC-3 and HeLa cells.[14]

Transient transfections. Cells (HEK293, HeLa or PC-3) were transiently transfected using a standard calcium phosphate precipitation method.[38] CEMp and CEM/C2 cells were transfected with DEAD-Dextran method.[39] An NF-κB-dependent luciferase reporter construct (3xκB-Luc) and the negative control construct (3xMκB-Luc) have been recently described.[40] Twenty-four hr following transfection, cells were treated with TPT (30 μM) or CPT (10 μM) for 2 hr, rinsed twice with growth medium and further incubated without drugs for six hr before termination of the cultures. Positive control samples were treated with TNFα (10 ng/ml) for a total of 8 hr. Control samples were transfected with the LacZ cDNA under the control of the cytomegalovirus promoter in the pCMX vector (CMV-LacZ). For CEMp and CEM/C2 cells, total proteins were used for normalization. Full-length human IKKα cDNA was provided by Dr. I. M. Verma (Salk Institute). Full-length human IKKβ cDNA was cloned as described.[40] IKKα and IKKβ with a Lys-to-Ala substitution at the conserved ATP binding site were generated by PCR mutagenesis and confirmed by DNA sequencing. The mutant genes were placed under the control of the CMV promoter in the pcDNA3.1(+) expression vector (Clontech). HEK293 cells were transfected with these constructs by calcium phosphate precipitation.

Retrovirus construction and infection. Production and infection of HA-tagged wild-type and HA-tagged S32/36A mutant IκBα expression constructs were described.[36] Other IκBα deletion mutants were generated by PCR-mediated mutagenesis and confirmed by sequencing. Stable pools were selected with hygromycin (1 mg/ml, Boehringer Mannheim) and the expression levels of the corresponding proteins were examined by either anti-IκBα (C21, a C-terminal epitope) or anti-HA antibodies.

Generation of a green fluorescent protein (GFP)-IκBα fusion construct. N-terminally fused GFP-IκBα was generated by subcloning PCR amplified human IκBα (MAD3) into HindIII-BamHI sites of the pEGFP vector (Clontech), such that the entire MAD3 coding sequence was in-frame with the GFP coding sequence. Stable HEK293 cell clones were generated by G418 selection and subsequent FACS sorting.

RESULTS

Investigation of ß-lap radiosensitization led to studies using Topo I-active poisons. Our initial studies began with the observation that ß-lap could work effectively as a radiosensitizer, even against the most (in the literature) radioresistant human cancer cell lines (e.g., Hep-2 or U1-Mel cells).[8, 12] Figure 1 illustrates the ability of this drug to dramatically sensitize IR-exposed confluent U1-Mel cells. The data were similar to those previously published for various human cancer cells.[8, 9, 13] Confluent and low serum (0.2% fetal calf serum)-treated radioresistant U1-Mel cells were irradiated (3.5 Gy) or mock-irradiated (0 Gy), and then immediately exposed to DMSO (0.1%) or to various concentrations of ß-lap in 0.1% DMSO (Figure 1). Cells treated with DMSO alone showed no growth inhibition or lethality. As previously observed,[8, 9] IR-exposed U1-Mel cells treated with various concentrations of ß-lap for 4 h showed significant lethality, far more than mock-irradiated, ß-lap-treated cells. Confluent, low serum exposed U1-Mel cells were fairly resistant to ß-lap up to 9 μM. At

concentrations of ß-lap above 9 μM, however, significant lethality (90% lethality) was observed from exposure to the drug alone. Pharmacokinetic data showed, however, that levels of ß-lap above 8 μM were non-physiological, wherein only 5-8 μM ß-lap was achieved in the bloodstream, normal tissue or tumor tissue of mice at the MTD. [[41], unpublished data] Cells treated with 3.5 Gy and immediately assayed for survival (immediately re-seeded and not allowing for potentially lethal damage recovery, PLDR[8, 33] resulted in 30% survival, which dramatically increased to over 60% survival in the 4 h post-treatment period before re-dilution and sparse re-seeding of irradiated cells onto plates to promote log-phase growth in medium containing 10% fetal calf serum.

A few very important characteristics about the use of ß-lap as a radiosensitizer led us to the recent elucidation of this drug's mechanism of action *in vivo*. First and foremost, the drug had to be administered either during IR treatment with exposure for at least 4 h, or the drug had to be applied immediately after IR exposure for at least 4 h.[9] Pretreatment of cells for 4 h with various concentrations of ß-lap below 8 μM had little or no effect on the survival of IR-treated U1-Mel cells. Furthermore, the duration of drug exposure had to be at least 4-5 h, with logarithmic decreases in radiosensitization with decreasing time; e.g., a 2 h exposure of drugs had little radiosensitizing effects.[9]

We also investigated the intracellular mechanism of action of ß-lap using control or IR-treated cells in an attempt to better understand the reasons for radiosensitization. One important observation was made: when cells were treated with IR or UV, ß-lap exposure of confluent and low serum (arrested) U1-Mel or other cancer cells resulted in enhanced tritiated thymidine uptake, indicative of increased Unscheduled DNA Synthesis (UDS).[12, 42, 43] We reasoned that since only DNA ligase inhibitors were known to cause enhanced UDS,[42] this drug must prevent the final steps of DNA repair. We then tested the ability of ß-lap to inhibit DNA ligases using bacterial, yeast and eukaryotic sources of the enzyme. Interestingly and unexpectedly, the

compound did not inhibit DNA ligases using any of these enzyme sources. We noted, however, that ß-lap prevented alkaline phosphatase activity when mixed with cell extracts from irradiated, but not control U1-Mel cells (**unpublished data**). We suspect that this inhibition of kinases by S-lap exposure was the result of loss of energy (ATP) within the cell or extracts, caused by NQO1 activity (see below).

Since the final steps of Topos are to re-ligate the broken ends of DNA after their unwinding activities, and since ß-lap did not inhibit DNA ligases, we then tested the effects of ß-lap on purified Topo I or Topo II-alpha enzymes, as well as nuclear extracts from irradiated or nonirradiated cells. Addition of ß-lap did not affect Topo II-alpha activity, however, the compound inhibited Topo I from human extracts;[9, 11] we also noted an apparent activation of Topo I using chick erythrocyte Topo I, which was the result of an aberrant Topo I-mediated nicking reaction.[9, 11] Recently, inhibition of Topo II-alpha by pre-incubation of enzyme with ß-lap has been reported,[15] however, inhibitory effects were observed only *in vivo*, and other labs (including our own) have not reproduced these effects.[9] Collectively, our data prompted us to hypothesize that modulation of Topo I by any mechanism might result in enhanced cell killing follow IR.[9, 44] We, therefore, tested CPT (a prototype Topo I poison) for it's ability to radiosensitize various human cancer cells under conditions identical to those described above using ß-lap.

Topo I poisons also caused radiosensitization, in a similar fashion as ß-lap. Based on our results with ß-lap and discovering that this drug affected Topo I, we then tested CPT and TPT for their abilities to sensitize Hep-2 or U1-Mel cells to IR under conditions identical to those described above for ß-lap. We were the first to discover that camptothecin could synergistically kill cancer cells when combined with IR.[9] Later, we showed similar effects using 9-AC or TPT.[44-46] All Topo I poisons tested so far have similar radiosensitizing effects on radioresistant human cancer cells as described below for TPT or CPT.

We reasoned that if ß-lap worked as a radiosensitizer by influencing Topo I, then clinically relevant Topo I poisons should work in a similar manner with similar kinetics and chacteristics. Much to our surprise, we discovered that exposure of low serum-exposed, IR-treated, confluent U1-Mel or Hep-2 cells with CPT or TPT caused a significant enhancement of cell death beyond lethality caused by either IR or Topo I poison alone.[8] Furthermore, cell death responses were kinetically similar to those observed with ß-lap: (a) the drugs had to be administered immediately after IR exposure; (b) a 4 h posttreatment was optimal; (c) longer exposure of cells to Topo I poisons alone caused considerable toxicity, thereby, masking the abilities of these compounds to radiosensitize cells; and (d) pretreatment with Topo I poisons had little or no affect on cell killing following IR-the two drugs were additive and not synergistic under pre-treatment conditions.

Mechanistically, both ß-lap and CPT-related Topo I poisons (CPT, 9-AC or TPT) caused enhanced sensitization of IR-treated cells in very similar fashions.[44-46] Post-IR exposures of U1-Mel cells with either CPT or ß-lap led to increases in total DNA strand breaks (measured by alkaline elution) and in the formation of DSBs (measured by neutral elution).[13] Interestingly, post-IR exposures with either TPT or ß-lap caused the formation of new DSBs and SSBs that could not be explained by IR exposure alone.[12, 13] These lesions appeared to arise from lesion modification mechanisms and not from simple inhibition of DNA repair. Exposure of cells to ß-lap alone at any doses tested did not result in DNA breaks. Increased DNA break formation following IR + ß-lap or TPT + IR was also accompanied by a dramatic enhancement of Topo I-DNA complex formation, as measured using standard DNA filtration methods.[13] Taken together, these data not only suggested that ß-lap and Topo I poisons were good radiosensitizers, but that they worked by very similar mechanisms of action.[44-46] Since the intracellular targets of CPT, TPT, or 9-AC were already determined (i.e., all were Topo I poisons), these data appeared to confirm that ß-lap acted as a radiosensitizer via an identical

Topo I poison-mediated mechanism. Furthermore, we proposed that these Topo I poisons caused radiosensitization via a lesion modification mechanism, wherein Topo I binds to SSBs created by IR and cleaves the DNA forming DSBs that have Topo I enzyme linked to the DNA damage ends[9,12,45-47]. To date, all available data appear consistent with this mechanism of radiosensitization for classical Topo I poisons (TPT, CPT, and 9-AC). However, further research on elucidating this mechanism is needed.

Interestingly, other studies by Chen et al[47, 48] showed that pretreatments with Topo I posions prior to IR exposures resulted in synergistic cell killing, effects not observed in many other laboratories.[9, 44-46, 49-52] These data,[47, 48] using Chinese hamster DC3F or MCF-7 cells, are in contrast to the studies discussed above, and may be caused by increased apoptosis resulting from the combination treatment, or from altered cell cycle regulation. These data indicate that there are possibly multiple mechanisms in tumor cells for enhanced lethality due to Topo I poisons + IR, including altered cell cycle regulation effects. Furthermore, other studies[51, 53] have shown only additive effects of IR + Topo I poisons, underscoring the need for studies of the colecular factors that influence radiosensitization of human cancer cells.

Radiosensitization by ß-lap is not similar to other typical Topo I poisons. One difference between ß-lap and more typical Topo I poisons (i.e., CPT and its analogs) was that ß-lap did not cause DNA-Topo I complex formation as CPT or it's derivatives.[10, 12] The compound also catalytically inhibited DNA Topo I instead of forming DNA-Topo I-drug ternary complexes,[10, 11] as was the case with typical Topo I poisons.[2] Although we did find that SSBs and DSBs were enhanced by ß-lap in IR-treated cancer cells, DNA-Topo I complex formation increased only slightly above background; in cell extracts, this filtration method actually measures protein-DNA complexes and is not specific for DNA-Topo I protein complexes. Thus, although the kinetics of enhanced IR lethality appeared to be similar, the two drugs (ß-lap vs TPT or CPT) appeared to worked quite differently.

Other differences between CPT-related Topo I poisons and ß-lap were also apparent. Although both drugs caused apoptosis in various human cancer cells, ß-lap: **(a)** was far more efficient at inducing cell killing by apoptosis and, unlike CPT or other Topo I-active poisons, lethality caused by this drug was due entirely to apoptosis in various human cancer cells;[14] **(b)** caused an extremely steep dose-response cytotoxicity curve in confluent or log-phase cells, compared to CPT or TPT which exhibited some cell cycle dependency on overall cell killing; interestingly, the ability of CPT or TPT alone to induce apoptosis did not appear to be cell cycle-mediated;[14, 54] **(c)** caused little or no cell cycle checkpoint alterations and no induction (i.e., stabilization) of wild-type p53, whereas dramatic p53 stabilization responses were noted following CPT, 9-AC or TPT;[14] **(d)** treatment caused entirely different intracellular proteolysis during apoptosis (i.e., ß-lap induced atypical PARP cleavage producing an ~60 kDa polypeptide) in an apparent non-caspase-, calpain-or calpain-like-mediated pathway;[3, 14] CPT analogs caused classic caspase-mediated apoptosis;[3] and **(e)** killed cells independent of p53 status and was blocked by dicoumarol co-treatments, which had little or no affect on classical Topo I poisons, such as TPT, CPT or 9-AC;[3, 17] interestingly, CPT analogs also killed cells by p53-independent pathways.[3, 11, 18]

ß-Lap works through xip3, also known as NQO1. Recent data from our laboratory have elucidated the mechanism of action of ß-lap in human cancer cells when the drug was used without IR. Various assays *in vitro* implicated several DNA repair and metabolism enzymes as potential key targets (e.g., Topo I, Topo II-alpha, or DNA polymerase ß) for this drug (reviewed in[17]). Until recently, however, key intracellular enzymes required for the compound's cytotoxic activity have not been elucidated. The fact that dicoumarol (out of several inhibitors tested) could prevent ß-lap-mediated toxicity strongly suggested that NAD(P)H:quinone oxidoreductase (NQO1, also known as DT diaphorase or xip3) was a key intracellular determinant in lethality caused by this drug.[17] Dicoumarol is a fairly specific inhibitor of

NQO1 as discussed.[17] Furthermore, we discovered two cell lines, LNCaP human prostate cancer and MDA-MD-468 human breast cancer cells, that were inherently resistant to ß-lap-mediated apoptosis and cytotoxicity. In contrast, DU-145 human prostate and MCF-7 human breast cancer cells were sensitive to this drug.[3, 17, 18] Interestingly, these cell lines were not appreciably different in their sensitivities to CPT or Topo II-alpha poisons.[3, 18] Further studies demonstrated that LNCaP and MDA-MB-468 cells were deficient in NQO1 expression, whereas MCF-7 and DU-145 cells expressed high levels of the protein and enzyme. Thus, NQO1 levels correlated with sensitivity to ß-lap, and toxicity in DU-145 and MCF-7 cells after drug exposure was prevented by dicoumarol. However, unlike menadione which is detoxified by NQO1, ß-lap was "activiated" by this two-electron reductase.

As final proof that ß-lap exposure alone (without IR) killed cells through NQO1, LNCaP and MDA-MB-468 (NQO1-dificient) cells were transfected with CMV-controlled NQO1 and various expressing and non-expressing transfectants were analyzed for lethality to ß-lap compared to menadione, as well as to CPT-mediated lethality.[17, 18] These studies clearly demonstrate that NQO1 is a major determinant of cell sensitivity to ß-lap, since NQO1 transfected LNCaP or MDA-MB-468 cells became very sensitive to the drug and this sensitivity was blocked by dicoumarol. Once again, sensitivity to the drug correlated well with specific and atypical intracellular apoptotic proteolysis, namely atypical PARP cleavage and degradation of p53 and pRb, consistent with a noncaspase-mediated, calpain or calpain-like cysteine protease activation pathway.[3, 14]

NQO1 is a damage-inducible protein, possibly explaining ß-lap's ability to radiosensitize cells. Treatment of U1-Mel cells with IR (3.5 Gy) resulted in a dramatic increase in NQO1 transcript levels (Fig. 2). Peak levels of NQO1 were noted 4-8 h post-IR. In dose-response experiments, NQO1 levels were significantly induced by as little as 1.0 Gy,[34] a clinically relevant dose of IR. Interestingly, LNCaP cells, that lack NQO1 expression, were one of few

cancer cells that were not radiosensitized by ß-lap.[8, 9] Work is ongoing in our laboratory to demonstrate that ß-lap sensitizes cells via the IR induction of its intracellular activating enzyme, NQO1. Thus, although the kinetics of radiosensitization of ß-lap + IR compared to IR + CPT (or TPT or 9-AC) appear to be similar, the actual mechanism of cell killing is very different.

We recently demonstrated that when NQO1 expressing cells were exposed to ß-lap an NQO1-mediated futile cycling of the compound was apparent. ([17], and unpublished data) The rate limiting intracellular substrate of this NQO1-dependent reaction was apparently intracellular loss of NAD(P)H levels, and we theorize ultimate loss of energy balance in the cell. Thus, addition of ß-lap to cell extracts may lead to a complete loss of energy via NQO1-dependent futile cycling of the drug, thereby explaining the inhibition of alkaline phosphatase previously observed in ligase reaction assays (unpublished data). An NQO1-dependent mechanism of ß-lap-mediated radiosensitization also explains the temporal sequence of addition of ß-lap required during or immediately after IR exposures, since IR-induced NQO1 expression reached peak levels in 4 h. A two-hour exposure of ß-lap, which was shown to have little effect on radiosensitization,[9] may not have been sufficient time for NQO1 expression and/or for complete futile cycling of the drug. Short exposures thereby allow cell recovery. In contrast, a 4-h period of futile cycling of ß-lap would result in a critical (threshold) loss of energy leading to activation of calpain or calpain-like apoptosis.[3, 14] Research in our laboratory is currently directed towards elucidating the exact mechanism of ß-lap-mediated radiosensitization, a mechanism we theorize will involve NQO1 (or xip3) as a major factor in the response.

NF-κB Signaling after Topo I poisons. Since NF-κB is implicated in the control of apoptosis, we analyzed the mechanisms of NF-κB activation by DNA damaging agents. We were also interested in elucidating the potential nuclear-to-cytoplasmic signaling pathways activated by Topo I poisons, since inactive NF-κB is present in the cytoplasm and the majority of DNA damage is induced in the nucleus. Our rationale was that study of the NF-κB activation

mechanism by DNA damaging agents may provide novel targets for anti-cancer drug development, which may be used in combination with radiation or chemotherapy treatment to increase their efficacy. Since NF-κB can also be activated by oxidative stress in the cells (reviewed in[40]), we began our studies using CPT, a well characterized Topo I poison, which causes DNA strand breaks without simultaneous generation of oxidative stress in the cell.

Exposure of various murine or human cancer cell lines with CPT resulted in NF-κB activation, as measured by EMSA and κB-reporter gene assays.[40] We treated 70Z/3 murine pre-B cells, CEM T leukemic, PC-3 prostate cancer, HEK293 embryonic kidney fibroblast and HeLa cervical cancer cell lines. We found that in all cell lines tested, NF-κB activation by CPT was dose-dependent, detectable at 10 ng/ml, saturating at 10 μg/ml. The NF-κB activation profile was transient (peaking at 1-2 h, undetectable by 6-8 h) in treated cells despite continuous CPT exposure. Pretreatment with cycloheximide did not interfere with this pathway, indicating that this activity stimulated by CPT does not require *de novo* protein synthesis. A similar pattern of the NF-κB activation response was observed when these cells were treated with TPT. Induction of NF-κB DNA binding activity by CPT- or TPT treatment resulted in increased NF-κB-dependent transcription of a luciferase reporter gene. Thus, CPT or TPT activation of NF-κB occurs without *de novo* protein synthesis and may utilize pre-existing regulatory component(s).

The primary molecular target of CPT or TPT is Topo I enzyme, but CPT-sensitive Topo I is present both in the nucleus and mitochondria.[55] To determine the requirement of an intact nucleus for NF-κB activation by CPT, we enucleated PC-3 and HeLa cells by the cytochalasin B-mediated enucleation procedure.[37] While enucleation did not affect the activation of NF-κB by PMA or TNF, the NF-κB response after CPT or TPT was dramatically diminished in the cytoplasts. These observations indicated that the presence of intact nucleus

was essential for efficient NF-κB activation by CPT. To our knowledge, this is the first direct demonstration of the requirement of intact nucleus for any NF-κB activation pathways.

Next, we addressed whether direct interaction of CPT and a Topo I-DNA complex is necessary for activation of NF-κB by examining the human CEM/C2 cells, which express a CPT-resistant mutant Topo I enzyme.[56] This mutant Topo I enzyme contains two amino acid substitutions, Met370 to Thr and Asp722 to Ser. The latter mutation makes Topo I enzyme ~1000-fold resistant to CPT (or TPT)-mediated inhibition of the re-ligation of DNA nicks, making it incapable of efficiently inducing DNA damage after CPT treatment *in vivo*.[57] We compared CPT-induced NF-κB activity in CEM/C2 and the parental CEMp cells by EMSA. Time-course and dose-response studies, as well as κB-dependent luciferase reporter assays, clearly demonstrated that CEM/C2 cells could not mount an NF-κB response after CPT treatment. Activation of NF-κB in CEM/C2 cells by TNF-α or other DNA-damaging agents, such as VP16 and IR indicated that the lack of NF-κB activation was specific to CPT.

CPT inhibition of the re-ligation step during the Topo I reaction induces stabilization of the cleavable complexes, resulting in the generation of Topo I-associated SSBs. These SSBs were reversible, but could be converted into DSBs during S-phase, when the replication fork collides with the cleavable complex.[5] Therefore, we next evaluated whether SSBs or DSBs were critical for NF-κB activation by CPT. Cells were treated with aphidicolin for 30 min, then exposed to CPT for 2 h and cell extracts examined for NF-κB activation. EMSA analyses showed that amphidicolin selectively blocked activation of NF-κB by CPT, but not by other inducing agents, such as bacterial lipopolysaccharide (LPS) or TNF-α. These results suggested that DSBs, not SSBs, were critical for NF-κB activation after CPT. These data also implied that this activation pathway was coupled to S-phase. We, therefore, enriched 70Z/3-CD14 cells in S phase by FACS sorting after cells were stimulated with CPT or LPS for 2-h. Compared to similarly obtained G_1 cell populations, NF-κB activation was 2.8-fold higher in

the S-phase population, when equivalent amounts of cell extracts were analyzed by EMSA. LPS stimulation did not show any significant differences in NF-κB activation between S and G_1 cells. These findings demonstrated that CPT activation of NF-κB was cell cycle coupled, and predominantly took place during S-phase of the cell cycle in a DSB-dependent fashion.

Our data, thus far, are consistent with the onset of an NF-κB activation pathway initiated by DSBs in the nucleus (Figure 3). Even though inactive NF-κB/IκBα complexes are largely present in the cytoplasm in a pre-induction state, our recent studies demonstrated that these complexes continually shuttle between the nucleus and the cytoplasm.[58] These observations raised the possibility that the release of NF-κB from IκBα may take place within the nucleus after DNA damage, rather than in the cytoplasm. To evaluate this possibility, we first accumulated the inactive NF-κB complexes in the nucleus by treating cells with the nuclear export inhibitor, leptomycin B (LMB). Cells were then treated with CPT. Under these conditions, NF-κB activation was not induced.[58] Moreover, we found that NF-κB activation by CPT requires **(i)** degradation of IκBα by the ubiquitin-proteasome pathway; **(ii)** inhibition of CPT-induced IκBα degradation by proteasome inhibitors caused accumulation of IκBa in the cytoplasm; **(iii)** mutation of the IκB kinase phosphorylation sites on IκBα blocked NF-κB activation by CPT; **(iv)** dominant-negative mutants of IκB kinases, IKKα and IKKβ, blocked CPT activation of NF-κB; **(v)** CPT activation of NF-κB was deficient in $IKK\alpha^{-/-}$, $IKK\beta^{-/-}$ or $IKK\gamma^{-/-}$ cells; and **(vi)** IKKα and IKKβ are not shuttling between the nucleus and the cytoplasm.[40] While we cannot completely discount the possibility that some post-translational modification may be imposed on inactive NF-κB/IκBα complexes in the nucleus after DNA damage, our observations are consistent with the hypothesis that DSBs initiate a nuclear-to-cytoplasmic signaling pathway to activate the IKK complex in the cytoplasm to ultimately induce degradation of IκBα to release NF-κB in the cytoplasm. Once in the nucleus, NF-κB appears to regulate expression of anti-apoptotic genes (Figure 3), since inhibition of NF-κB

activation by expression of a dominant-negative IκBα mutant protein enhanced apoptotic responses in certain cancer cells after CPT treatment.[58]

DISCUSSION AND CONCLUSIONS

The studies summarized above highlight the need to better understand the cellular and molecular responses of normal compared to tumor tissues to cytotoxic agents (such as IR, Topo I poisons, ß-lap and combinations of these agents). The Topo I poison-mediated activation of NF-κB could be a very important anti-apoptotic response which affects efficacy of therapy using Topo I poisons, with or without other cytotoxic agents (e.g., IR). Our laboratories are currently working to better understand the unique S-phase-specific signal transduction pathways induced by CPT analogs that simultaneously activate apparently functionally opposing p53 and NF-κB transcriptional responses (Figure 3). These coordinate cellular responses presumably evolved in eukaryotic cells to halt the cell cycle in G_1 and/or G_2 (dependent on dose and timing) to allow time for repair and recovery (p53-dependent), but also possibly to stimulate transcriptional responses which lead to enhanced cell survival (NF-κB-mediated). Manipulating these pathways will presumably allow for enhanced cytotoxic affects and possibly methods for greatly improving therapy. We speculate that manipulating these pathways could be accomplished through the use of tissue- and tumor-specific expression of dominant-negative IκB, or through the use of proteasome inhibitors. Both of these methods should prevent NF-κB activation by sequestering NF-κB in the cytosol of tumor cells, thereby preventing nuclear translocation of this transcription factor. Alternatively, by dissecting the components and biochemical reactions involved in the putative nuclear-to-cytoplasmic signaling pathway, inhibitors specific to NF-κB activation induced by DSBs may be developed. Overall, these findings highlight the need for further investigation and elucidation of the molecular responses

occurring in normal compared to tumor cells following the combination of IR and Topo I poison exposures.

Interestingly, ß-lap exposure of human cancer cells does not lead to induction of NF-κB.[59] In fact, administration of this drug actually suppresses NF-κB activation responses,[59] that we theorize occurs via the futile cycling of this drug and loss of energy balance within exposed cells expressing NQO1.[17] Thus, ß-lap holds special interest as a radiosensitizer in that the overall enhanced IR-mediated cytotoxicity is equivalent to that of the Topo I poisons, but is not susceptible to the same downstream protective responses. In fact, not only are NF-κB responses suppressed, but p53 and pRb are specifically degraded.[3, 14] p53 and pRb are apparently substrates for the downstream activated calpain or calpain-like protease which is activated following ß-lap exposure.([3], Tagliarino etl al., unpublished data) Thus, apoptotic responses are stimulated following ß-lap exposure, simultaneously with suppression of anti-apoptotic responses (mediated by NF-κB down-regulation). Furthermore, identification of NQO1 as a principal target or activating enzyme within the cell is a major step towards improving specificity of radiosensitization with this drug.

FIGURE LEGENDS

Figure 1. **ß-Lap synergistically enhances the cytotoxicity of low serum-treated, confluent U1-Mel cells.** Radioresistant human malignant melanoma (U1-Mel) cells were grown to confluency and shifted to medium containing a low (0.2 %) percentage of fetal bovine serum, where >85% G_0/G_1 and fewer than 5% S-phase (incorporating [^{3}H]thymidine into their DNA) were noted.[8, 9, 33, 34] Arrested cells were then treated with 3.5 Gy IR or mock-irradiated. Immediately after IR exposure, cells were treated with or without various concentrations of ß-lap as described in "Materials and Methods". Control cells were treated with an equivalent percentage of DMSO for each dose of drug, and no dose of DMSO used in the experiment

caused growth inhibition or lethality. **Top insert,** structure of ß-lap. A number of R-substituted derivatives have been made and these do not affect the activity of this compound, however, many alter the solubility or other pharmacokinetic properties.[41, 60] ***Bottom insert,*** *open square,* non-irradiated U1-Mel cells treated with various concentrations of ß-lap alone for 4-h; *solid circle*, U1-Mel cells treated with IR followed immediately with various concentrations of ß-lap for 4-h. Colony forming ability assays were then performed and analyzed as described in "Materials and Methods". The vertical dashed line indicates the approximate cut-off between physiologically relevant doses of ß-lap found for mice.[41] Results are similar to those previously published.[9] Any concentration of ß-lap above ~8 μM would be non-physiological, achieved in tissue culture but not in mice at the mean tolerated dose (MTD) of the drug.

Figure 2. [From Boothman et. al.,[34]] **NQO1 is an IR-inducible transcript in low serum-exposed, confluent U1-Mel cells.** ***Left panel***, Confluent U1-Mel cells were treated with 3.5 Gy IR, total RNA was extracted 5 h later, and specific transcript levels were analyzed by Northern blot analyses using random-primed NQO1 or 36B4 cDNAs as probes. 36B4 transcript levels remain unaltered after IR exposure and were used as a loading standard. ***Right panel,*** the kinetics of NQO1 induction in U1-Mel cells after 4.5 Gy with respect to $ß_2$-microglobulin (or 36B4); the relative levels were multiplied by an arbitrary factor of 100 to graph the data. Similar responses were observed after 3.5 Gy. Peak NQO1 levels were observed between 4-5 h post-IR exposure. The induction kinetics of NQO1 in U1-Mel cells were consistent with cellular responses to ß-lap, which is activated by this IR (damage)-inducible enzyme (see Figure 1, text). Reprinted with permission from the *Proceedings of the National Academy of Science, USA.*[34]

Figure 3. **A model depicting a putative "nuclear-to-cytoplasmic" signal transduction pathway activated by Topo I poisons.** See discussion section and the paper by Huang et. al.,[40] for further detail.

REFERENCES

1. Wang, J. C. (1996) DNA topoisomerases. *Ann. Rev. Biochem. 65*, 635-692.
2. Hertzberg, Y.-H., Lihou, M. G., and Liu, L. F. (1989) Arrest of replication forks by drug-stabilized topoisomerase I-DNA cleavable complexes as a mechanism of cell killing by camptothecin *Cancer Research 49*, 5077-5082.
3. Pink, J. J., Wuerzberger-Davis, S., Tagliarino, C., Planchon, S. M., Yang, X., Froelich, C. J., and Boothman, D. A. (2000) Activation of a Cysteine Protease in MCF-7 and T47D Breast Cancer Cells during beta-Lapachone-Mediated Apoptosis *Exp Cell Res 255*, 144-155.
4. Avemann, K., Knippers, R., Koller, T., and Sogo, J. M. (1988) Camptothecin, a specific inhibitor of type I DNA topoisomerase, induces DNA breakage at replication forks *Mol Cell Biol 8*, 3026-34.
5. Hsiang, Y. H., Lihou, M. G., and Liu, L. F. (1989) Arrest of replication forks by drug-stabilized topoisomerase I-DNA cleavable complexes as a mechanism of cell killing by camptothecin *Cancer Res 49*, 5077-82.
6. Zhang, H., D'Arpa, P., and Liu, L. F. (1990) A model for tumor cell killing by topoisomerase poisons *Cancer Cells 2*, 23-7.
7. Grochow, L. B., Rowinsky, E. K., Johnson, R., Ludeman, S., Kaufmann, S. H., McCabe, F. L., Smith, B. R., Hurowitz, L., DeLisa, A., Donehower, R. C., and et al. (1992) Pharmacokinetics and pharmacodynamics of topotecan in patients with advanced cancer *Drug Metab Dispos 20*, 706-13.
8. Boothman, D. A., Greer, S., and Pardee, A. B. (1987) Potentiation of halogenated pyrimidine radiosensitizers in human carcinoma cells by beta-lapachone (3,4-dihydro-2,2-dimethyl-2H- naphtho[1,2-b]pyran- 5,6-dione), a novel DNA repair inhibitor *Cancer Res 47*, 5361-6.
9. Boothman, D. A., Trask, D. K., and Pardee, A. B. (1989) Inhibition of potentially lethal DNA damage repair in human tumor cells by beta-lapachone, an activator of topoisomerase I *Cancer Res 49*, 605-12.

10. Li, C. J., Averboukh, L., and Pardee, A. B. (1993) beta-Lapachone, a novel DNA topoisomerase I inhibitor with a mode of action different from camptothecin *J Biol Chem 268*, 22463-8.
11. Planchon, S. M., Wuerzberger, S., Frydman, B., Witiak, D. T., Hutson, P., Church, D. R., Wilding, G., and Boothman, D. A. (1995) Beta-lapachone-mediated apoptosis in human promyelocytic leukemia (HL- 60) and human prostate cancer cells: a p53-independent response *Cancer Res 55*, 3706-11.
12. Boothman, D. A., Wang, M., Schea, R. A., Burrows, H. L., Strickfaden, S., and Owens, J. K. (1992) Posttreatment exposure to camptothecin enhances the lethal effects of X-rays on radioresistant human malignant melanoma cells *Int. J. Radiation Oncology Biol. Phys. 24*, 939-948.
13. Boothman, D. A., and Pardee, A. B. (1989) Inhibition of radiation-induced neoplastic transformation by beta- lapachone *Proc Natl Acad Sci U S A 86*, 4963-7.
14. Wuerzberger, S. M., Pink, J. J., Planchon, S. M., Byers, K. L., Bornmann, W. G., and Boothman, D. A. (1998) Induction of apoptosis in MCF-7:WS8 breast cancer cells by beta- lapachone *Cancer Res 58*, 1876-85.
15. Frydman, B., Marton, L. J., Sun, J. S., Neder, K., Witiak, D. T., Liu, A. A., Wang, H. M., Mao, Y., Wu, H. Y., Sanders, M. M., and Liu, L. F. (1997) Induction of DNA topoisomerase II-mediated DNA cleavage by beta- lapachone and related naphthoquinones *Cancer Res 57*, 620-7.
16. Dolan, M. E., Frydman, B., Thompson, C. B., Diamond, A. M., Garbiras, B. J., Safa, A. R., Beck, W. T., and Marton, L. J. (1998) Effects of 1,2-naphthoquinones on human tumor cell growth and lack of cross-resistance with other anticancer agents *Anticancer Drugs 9*, 437-48.
17. Pink, J. J., Planchon, S.M.m Tagliarino, C., Wuerzberger-Davis, S.M., Varnes, M.E., Siegel, D., and Boothman, D.A. (2000) NAD(P)H:quinone oxidoreductase (NQO1) activity is the principal determinant of ß-lapachone cytotoxicity. *Journal of Biological Chemistry 275*, 5416-5424.
18. Planchon, S. M., Pink, J. J., Tagliarino, C., Bornmann, W. G., Varnes, M. E., and Boothman, D. A. (2000) ß-Lapachone-induced apoptosis in human prostate cancer cells: involvement of NQO1/xip3 *Experimental Cell Research Submitted.*
19. Baeuerle, P. A., and Baltimore, D. (1996) NF-κB - Ten years after. *Cell 87*, 13-20.
20. Verma, I. M., Stevenson, J. K., Schwarz, E. M., Van Antwerp, D., and Miyamoto, S. (1995) Rel/NF-κB/IκB family: intimate tales of association and dissociation. *Genes Dev. 9*, 2723-2735.
21. Sonenshein, G. E. (1997) Rel/NF-κB transcription factors and the control of apoptosis. *Sem. Cancer Biol. 8*, 113-119.

22. Beg, A. A., Ruben, S. M., Scheinman, R. I., Haskill, S., Rosen, C. A., and Baldwin, A. S. J. (1992) IκB interacts with the nuclear localization sequences of the subunits of NF-κB: a mechanism for cytoplasmic retention. *Genes Dev. 6*, 1899-1913.

23. Ganchi, P. A., Sun, S. C., Greene, W. C., and Ballard, D. W. (1992) IκB/MAD-3 masks the nuclear localization signal of NF-κB p65 and requires the transactivation domain to inhibit NF-κB p65 DNA binding. *Mol. Biol. Cell 3*, 1339-1352.

24. DiDonato, J. A., Hayakawa, M., Rothwarf, D. M., Zandi, E., and Karin, M. (1997) A cytokine-responsive IκB kinase that activates the transcription factor NF-κB. *Nature 388*, 548-554.

25. Mercurio, F., Zhu, H., Murray, B. W., Shevchenko, A., Bennett, B. L., Li, J. W., Young, D. B., Barbosa, M., Mann, M., Manning, A., and Rao, A. (1997) IKK-1 and IKK-2: Cytokine-activated IκB kinases essential for NF-κB activation. *Science 278*, 860-866.

26. Woronicz, J. D., Gao, X., Cao, Z., Rothe, M., and Goeddel, D. V. (1997) IκB kinase-β: NF-κB activation and complex formation with IκB kinase-a and NIK. *Science 278*, 866-869.

27. Zandi, E., Rothwarf, D. M., Delhase, M., Hayakawa, M., and Karin, M. (1997) The IκB kinase complex (IKK) contains two kinase subunits, IKKα and IKKβ, necessary for IκB phosphorylation and NF-κB activation. *Cell 91*, 243-252.

28. Alkalay, I., Yaron, A., Hatzubai, A., Orian, A., Ciechanover, A., and Ben-Neriah, Y. (1995) Stimulation-dependent IκBα phosphorylation marks the NF-κB inhibitor for degradation via the ubiquitin-proteasome pathway. *Proc. Natl. Acad. Sci. U. S. A. 92*, 10599-10603.

29. Chen, Z., Hagler, J., Palombella, V. J., Melandri, F., Scherer, D., Ballard, D., and Maniatis, T. (1995) Signal-induced site-specific phosphorylation targets IκBα to the ubiquitin-proteasome pathway. *Genes Dev. 9*, 1586-1597.

30. Stein, B., Kramer, M., Rahmsdorf, H. J., Ponta, H., and Herrlich, P. (1989) UV-induced transcription from the human immunodeficiency virus type 1 (HIV-1) long terminal repeat and UV-induced secretion of an extracellular factor that induces HIV-1 transcription in nonirradiated cells. *J. Virol. 63*, 4540-4544.

31. Devary, Y., Rosette, C., DiDonato, J. A., and Karin, M. (1993) NF-κB activation by ultraviolet light not dependent on a nuclear signal. *Science 261*, 1442-1445.

32. Piret, B., and Piette, J. (1996) Topoisomerase poisons activate the transcription factor NF-κB in ACH-2 and CEM cells. *Nuc. Acids Res. 24*, 4242-4248.

33. Boothman, D. A., Bouvard, I., and Hughes, E. N. (1989) Identification and characterization of X-ray-induced proteins in human cells *Cancer Res 49*, 2871-8.

34. Boothman, D. A., Meyers, M., Fukunaga, N., and Lee, S. W. (1993) Isolation of x-ray-inducible transcripts from radioresistant human melanoma cells *Proc Natl Acad Sci U S A 90*, 7200-4.

35. Yang, C. R., Wilson-Van Patten, C., Planchon, S. M., Wuerzberger-Davis, S. M., Davis, T. W., Cuthill, S., Miyamoto, S., and Boothman, D. A. (2000) Coordinate modulation of Sp1, NF-kappa B, and p53 in confluent human malignant melanoma cells after ionizing radiation *Faseb J 14*, 379-90.

36. Miyamoto, S., Seufzer, B., and Shumway, S. (1998) Novel IκBα degradation process in WEHI231 murine immature B cells. *Mol. Cell. Biol. 18*, 19-29.

37. Poste, G. (1972) Enucleation of mammalian cells by cytochalasin B. I. Characterization of anucleate cells. *Exp. Cell Res. 73*, 273-286.

38. Cao, Z. D., Xiong, J., Takeuchi, M., Kurama, T., and Goeddel, D. V. (1996) TARF6 is a signal transducer for interleukin-1. *Nature 383*, 443-446.

39. Chiao, P. J., Miyamoto, S., and Verma, I. M. (1994) Autoregulation of IκBα activity. *Proc. Natl. Acad. Sci. U. S. A. 91*, 28-32.

40. Huang, T. T., Wuerzberger-Davis, S. M., Seufzer, B. J., Shumway, S. D., Kurama, T., Boothman, D. A., and Miyamoto, S. (2000) NF-κB activation by camptothecin: A linkage between nuclear DNA damage and cytoplasmic signaling events. *J. Biol. Chem. 275*, 9501-9509.

41. Glen, V. L., Hutson, P. R., Kehrli, N. J., Boothman, D. A., and Wilding, G. (1997) Quantitation of beta-lapachone and 3-hydroxy-beta-lapachone in human plasma samples by reversed-phase high-performance liquid chromatography *J Chromatogr B Biomed Sci Appl 692*, 181-6.

42. Boorstein, R. J., and Pardee, A. B. (1984) Beta-lapachone greatly enhances MMS lethality to human fibroblasts *Biochem Biophys Res Commun 118*, 828-34.

43. Boorstein, R. J., and Pardee, A. B. (1983) Coordinate inhibition of DNA synthesis and thymidylate synthase activity following DNA damage and repair *Biochem Biophys Res Commun 117*, 30-6.

44. Lamond, J. P., Wang, M., Kinsella, T. J., and Boothman, D. A. (1996) Radiation lethality enhancement with 9-aminocamptothecin: comparison to other topoisomerase I inhibitors *Int J Radiat Oncol Biol Phys 36*, 369-76.

45. Lamond, J. P., Mehta, M. P., and Boothman, D. A. (1996) The potential of topoisomerase I inhibitors in the treatment of CNS malignancies: report of a synergistic effect between topotecan and radiation *J Neurooncol 30*, 1-6.

46. Lamond, J. P., Wang, M., Kinsella, T. J., and Boothman, D. A. (1996) Concentration and timing dependence of lethality enhancement between topotecan, a topoisomerase I inhibitor, and ionizing radiation *Int J Radiat Oncol Biol Phys 36*, 361-8.

47. Chen, A. Y., Okunieff, P., Pommier, Y., and Mitchell, J. B. (1997) Mammalian DNA topoisomerase I mediates the enhancement of radiation cytotoxicity by camptothecin derivatives *Cancer Res 57*, 1529-36.

48. Chen, A. Y., Choy, H., and Rothenberg, M. L. (1999) DNA topoisomerase I-targeting drugs as radiation sensitizers *Oncology (Huntingt) 13*, 39-46.
49. Sauer, R., and Heuser, A. (1997) [Topoisomerase I inhibitor with potential radiosensitizing effect] *Strahlenther Onkol 173*, 125-30.
50. Mattern, M. R., Hofmann, G. A., McCabe, F. L., and Johnson, R. K. (1991) Synergistic cell killing by ionizing radiation and topoisomerase I inhibitor topotecan (SKF 104864) *Cancer Res 51*, 5813-6.
51. Marchesini, R., Colombo, A., Caserini, C., Perego, P., Supino, R., Capranico, G., Tronconi, M., and Zunino, F. (1996) Interaction of ionizing radiation with topotecan in two human tumor cell lines *Int J Cancer 66*, 342-6.
52. Lanza, A., Tornaletti, S., Stefanini, M., Evans, H. H., Ricanati, M., Astaldi Ricotti, G. C., and Pedrini, A. M. (1993) The sensitivity to DNA topoisomerase inhibitors in L5178Y lymphoma strains is not related to a primary defect of DNA topoisomerases *Carcinogenesis 14*, 1759-63.
53. Balosso, J., Giocanti, N., and Favaudon, V. (1991) Additive and supraadditive interaction between ionizing radiation and pazelliptine, a DNA topoisomerase inhibitor, in Chinese hamster V-79 fibroblasts *Cancer Res 51*, 3204-11.
54. Pink, J. J., Planchon, S. M., Tagliarino, C., Varnes, M. E., Siegel, D., and Boothman, D. A. (2000) NAD(P)H:Quinone oxidoreductase activity is the principal determinant of beta-lapachone cytotoxicity [In Process Citation] *J Biol Chem 275*, 5416-24.
55. Lin, J. H., and Castora, F. J. (1995) Response of purified mitochondrial DNA topoisomerase I from bovine liver to camptothecin and m-AMSA. *Arch. Biochem. Biophys. 324*, 293-299.
56. Fujimori, A., Hoki, Y., Popescu, N. C., and Pommier, Y. (1996) Silencing and selective methylation of the normal topoisomerase I gene in camptothecin-resistant CEM/C2 human leukemia cells. *Onc. Res. 8*, 295-301.
57. Fujimori, A., Harker, W. G., Kohlhagen, G., Hoki, Y., and Pommier, Y. (1995) Mutation at the catalytic site of topoisomerase I in CEM/C2, a human leukemia cell line resistant to camptothecin. *Cancer Res. 55*, 1339-1346.
58. Huang, T. T., Kudo, N., Yoshida, M., and Miyamoto, S. (2000) A nuclear export signal in the N-terminal regulatory domain of IκBα controls cytoplasmic localization of inactive NF-κB/IκBα complexes. *Proc. Natl. Acad. Sci. U.S.A. 97*, 1014-1019.
59. Manna, S. K., Gad, Y. P., Mukhopadhyay, A., and Aggarwal, B. B. (1999) Suppression of tumor necrosis factor-activated nuclear transcription factor-kappaB, activator protein-1, c-Jun N-terminal kinase, and apoptosis by beta-lapachone *Biochem Pharmacol 57*, 763-74.
60. Planchon, S. M., Wuerzberger-Davis, S. M., Pink, J. J., Robertson, K. A., Bornmann, W. G., and Boothman, D. A. (1999) Bcl-2 protects against -lapachone-mediated caspase 3

activation and apoptosis in human myeloid leukemia (HL-60) cells [In Process Citation] *Oncol Rep 6*, 485-92.

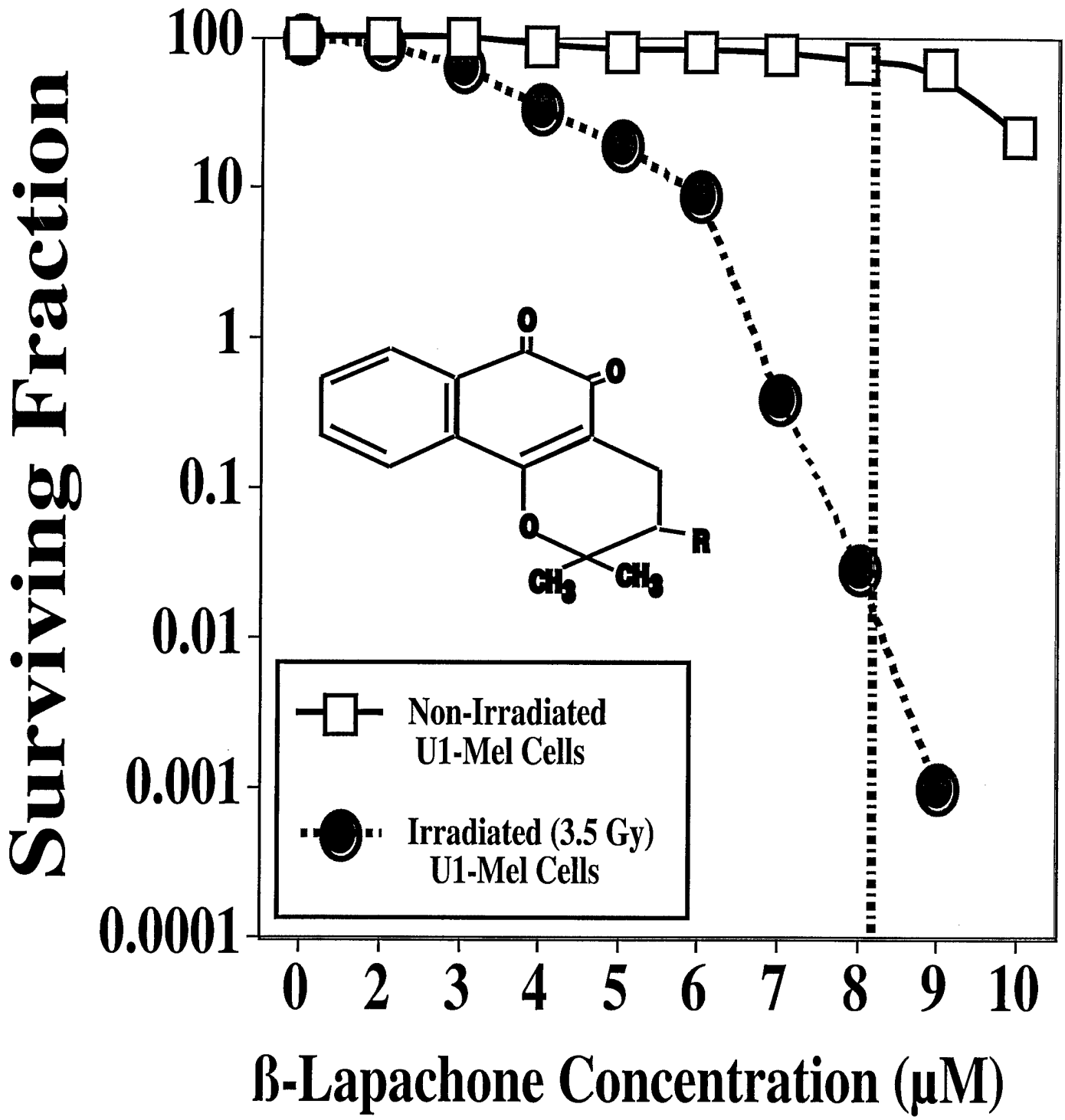
Surviving Fraction
100
10
1
0.1
0.01
0.001
0.0001
0
2
3
4
5
6
7
8
9
10
ß-Lapachone Concentration (µM)
O
O
O
R
CH3
CH3
Non-Irradiated
U1-Mel Cells
Irradiated (3.5 Gy)
U1-Mel Cells

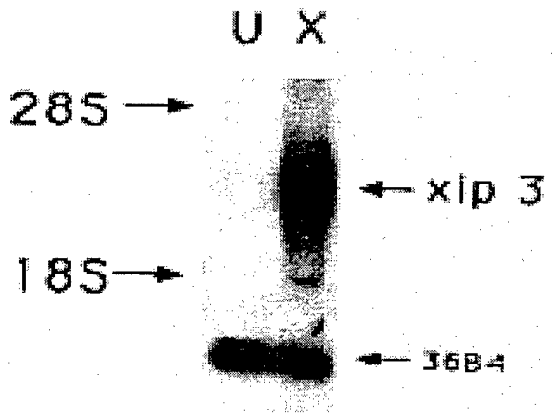
U X
28S
18S
xip 3
36B4

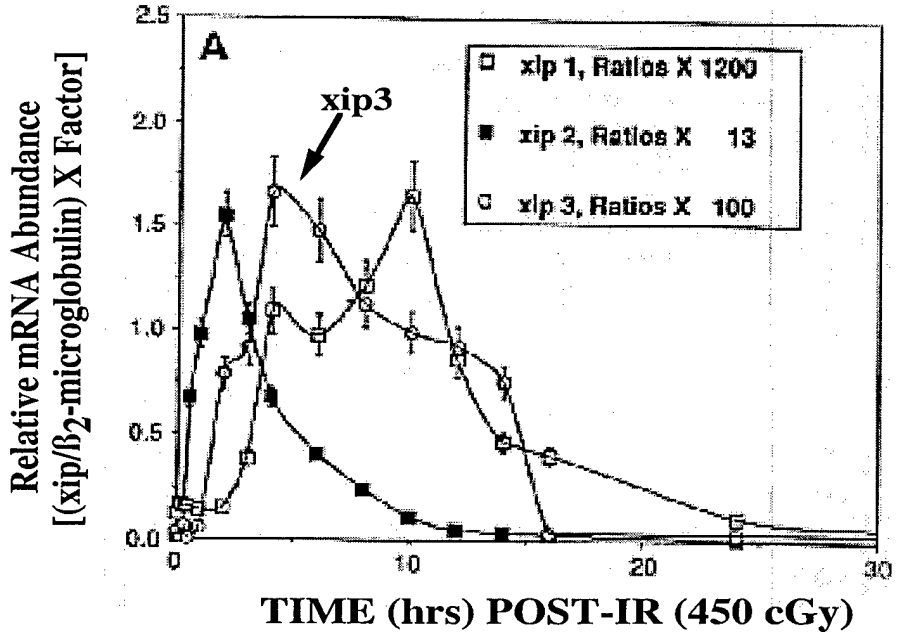
A
xip3
xip 1, Ratios X 1200
xip 2, Ratios X 13
xip 3, Ratios X 100
Relative mRNA Abundance
[(xip/β2-microglobulin) X Factor]
2.5
2.0
1.5
1.0
0.5
0.0
0
10
20
30
TIME (hrs) POST-IR (450 cGy)

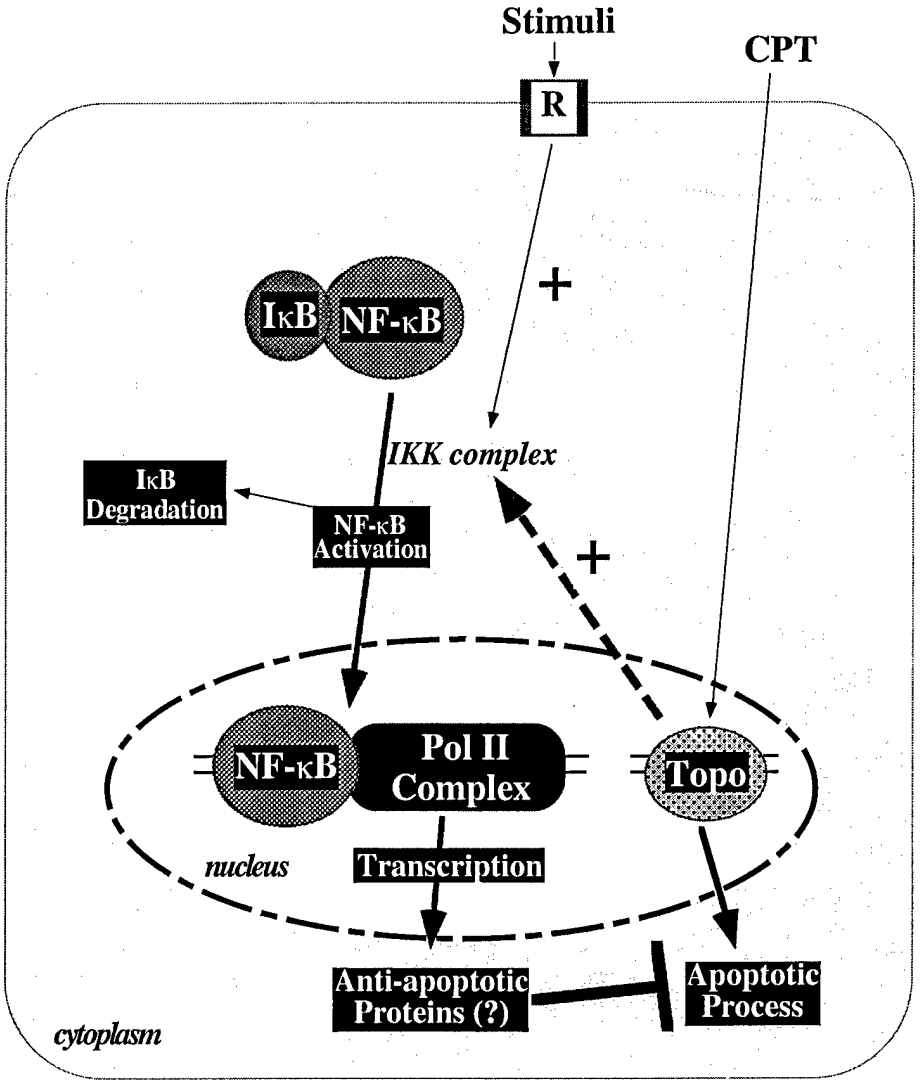
Stimuli
CPT
R
+
IκB
NF-κB
IKK complex
IκB
Degradation
NF-κB
Activation
+
NF-κB
Pol II
Complex
Topo
nucleus
Transcription
Anti-apoptotic
Proteins (?)
Apoptotic
Process
cytoplasm